TEMPORAL AND SPATIAL TRENDS OF ATMOSPHERIC TOXIC SUBSTANCES NEAR THE GREAT LAKES: IADN RESULTS THROUGH 2003

Ping Sun	School of Public and Environmental Affairs and Department of Chemistry, Indiana University
Ilora Basu	School of Public and Environmental Affairs and Department of Chemistry, Indiana University
Pierrette Blanchard	Environment Canada, 4905 Dufferin Street, Toronto, Ontario M3H 5T4, Canada
Sean M. Backus	Environment Canada, 4905 Dufferin Street, Toronto, Ontario M3H 5T4, Canada
Kenneth A. Brice	Air Quality Research Branch, Meteorological Service of Canada, Environment Canada
Melissa L. Hulting	Great Lakes National Program Office, U.S. Environmental Protection Agency
Ronald A. Hites	School of Public and Environmental Affairs and Department of Chemistry, Indiana University

Temporal and Spatial Trends of Atmospheric Toxic Substances near the Great Lakes: IADN Results through 2003

Published by
Environment Canada and the United States Environmental Protection Agency
ISBN: 978-0-662-45561-5

Public Works and Government Services Canada Catalogue Number: En164-13/2007E
US EPA Report Number: 905-R-07-001

Report available in printed form from

Air Quality Research Branch
Environment Canada
4905 Dufferin Street
Toronto ON
M3H 5T4
Canada

Great Lakes National Program Office
U.S. Environmental Protection Agency
77 West Jackson Boulevard (G17-J)
Chicago IL
60604
U.S.A.

and in electronic form at

www.msc.ec.gc.ca/IADN/

www.epa.gov/glnpo/iadn/

Table of Contents

1.0 Introduction ……..... 1
2.0 Method……..... ...1
2.1 Substances Considered……...1
2.2 Sampling Sites and Data Range……2
2.3 Trend Analysis……...3
3.0 Results and Discussion…….....3
3.1 ΣPAHs……....4
3.2 Total PCBs……7
3.3 Organochlorine Pesticides……8
3.3.1 α- and γ-HCHs……8
3.3.2 Total Endosulfans……10
3.3.3 Total Chlordanes……...13
3.3.4 Total DDTs……...14
3.3.5 Hexachlorobenzene (HCB)……...19
4.0 Conclusions……..... 19
Acknowledgements..... 21
References 22

Appendix A. Temporal and Spatial Trend Analysis Procedure ……..... 25
Appendix B. Annual Variation of Polycyclic Aromatic Hydrocarbon Concentrations in Precipitation Collected near the Great Lakes ……..... 29
Appendix C. Temporal Trends of Polychlorinated Biphenyls (PCBs) in Precipitation and Air at Chicago……48
Appendix D. Temporal and Spatial Trends of Organochlorine Pesticides in Great Lakes Precipitation.....64
Appendix E. Trends in Polycyclic Aromatic Hydrocarbon Concentrations in the Great Lakes Atmosphere…….....88
Appendix F. Atmospheric Organochlorine Pesticide Concentrations near the Great Lakes: Temporal and Spatial Trend…….....120
Appendix G. Temporal and Spatial Trends of Atmospheric Polychlorinated Biphenyl Concentrations near the Great Lakes…….....154

List of Tables

Table 1. Data availability at IADN sites for this report……..2
Table BS1. Fit parameters for PAH concentrations in precipitation at Brule River…….44
Table BS2. Fit parameters for PAH concentrations in precipitation at Eagle Harbor…...44
Table BS3. Fit parameters for PAH concentrations in precipitation at Sleeping Bear Dunes…….45
Table BS4. Fit parameters for PAH concentrations in precipitation at Sturgeon Point…45
Table BS5. Fit parameters for PAH concentrations in precipitation at Chicago.....46
Table BS6. Fit parameters for PAH concentrations in precipitation at Burnt Island.....46
Table BS7. Fit parameters for PAH concentrations in precipitation at Point Petre.....47
Table CS1. Student's *t*-test results for the comparison of PCB concentrations between Chicago and Sleeping Bear Dunes…….62
Table DS1. Chemical structures and properties of OC pesticides…….82
Table DS2. Fit parameters for pesticide concentrations in precipitation at Brule River...83
Table DS3. Fit parameters for pesticide concentrations in precipitation at Eagle Harbor……..83
Table DS4. Fit parameters for pesticide concentrations in precipitation at Sleeping Bear Dunes…….84
Table DS5. Fit parameters for pesticide concentrations in precipitation at Sturgeon Point……...84
Table DS6. Fit parameters for pesticide concentrations in precipitation at Chicago……85
Table DS7. Fit parameters for pesticide concentrations in precipitation at Burnt Island..85
Table DS8. Fit parameters for pesticide concentrations in precipitation at Point Petre…86
Table DS9. Range and Annual Mean Concentration (ng/L) of Selected Organochlorine Pesticides in Precipitation from Various Studies.....87
Table E1. Half-lives (in years) of PAH concentrations in the vapor and particle phases at seven sites near the Great Lakes…….....100
Table ES1. Fit parameters for PAHs in vapor phase at Brule River……....107
Table ES2. Fit parameters for PAHs in vapor phase at Eagle Harbor……107
Table ES3. Fit parameters for PAHs in vapor phase at Sleeping Bear Dunes……108
Table ES4. Fit parameters for PAHs in vapor phase at Sturgeon Point……..108
Table ES5. Fit parameters for PAHs in vapor phase at Chicago……109
Table ES6. Fit parameters for PAHs in vapor phase at Burnt Island……..109
Table ES7. Fit parameters for PAHs in vapor phase at Point Petre……110
Table ES8. Fit parameters for PAHs in particle phase at Brule River……110
Table ES9. Fit parameters for PAHs in particle phase at Eagle Harbor……..111
Table ES10. Fit parameters for PAHs in particle phase at Sleeping Bear Dunes……....111
Table ES11. Fit parameters for PAHs in particle phase at Sturgeon Point…….112
Table ES12. Fit parameters for PAHs in particle phase at Chicago……112
Table ES13. Fit parameters for PAHs in particle phase at Burnt Island…..……....113
Table ES14. Fit parameters for PAHs in particle phase at Point Petre……....113
Table F1. Half-lives (in years) of Selected OC Pesticides in the Gas and Particle Phases at Seven IADN Sites…….....132
Table FS1. Method comparison between U.S. and Canadian sites……138

Table FS2. Average Concentrations and Fit parameters for Pesticides in the Gas Phase at Brule River…….139
Table FS3. Average Concentrations and Fit parameters for Pesticides in the Gas Phase at Eagle Harbor……..139
Table FS4. Average Concentrations and Fit parameters for Pesticides in the Gas Phase at Sleeping Bear Dunes…….140
Table FS5. Average Concentrations and Fit parameters for Pesticides in the Gas Phase at Sturgeon Point……..…….140
Table FS6. Average Concentrations and Fit parameters for Pesticides in the Gas Phase at Chicago…….…….141
Table FS7. Average Concentrations and Fit parameters for Pesticides in the Gas Phase at Burnt Island……..…….141
Table FS8. Average Concentrations and Fit parameters for Pesticides in the Gas Phase at Point Petre……..……142
Table FS9. Average Concentrations and Fit Parameters for Pesticides in the Particle Phase at Brule River……..……...142
Table FS10. Average Concentrations and Fit Parameters for Pesticides in the Particle Phase at Eagle Harbor…..……..……..143
Table FS11. Average Concentrations and Fit Parameters for Pesticides in the Particle Phase at Sleeping Bear Dunes...……..143
Table FS12. Average Concentrations and Fit Parameters for Pesticides in the Particle Phase at Sturgeon Point..……..……...144
Table FS13. Average Concentrations and Fit Parameters for Pesticides in the Particle Phase at Chicago……..……..……..144
Table FS14. Range and Mean Concentration (pg/m^3) of Selected Organochlorine Pesticides in the Gas Phase from Various Studies……...145
Table G1. Average Total PCB Concentrations, half-lives, Clausius-Clapeyron slopes, and phase-transition energies at the seven IADN sites……165
Table GS1. Selected PCB congener concentrations, half-lives, Clausius-Clapeyron slopes, and phase-transition energies at the seven IADN sites…...170

List of Figures

Figure 1. Maps of the Great Lakes indicating the seven IADN sites…..... 2
Figure 2. Spatial and temporal trends of ΣPAHs…….....5
Figure 3. Average ΣPAH and suite PCB concentration at the seven IADN sampling sites as a function of the population lining within a 25-km radius of the sampling site.....6
Figure 4. Spatial and temporal trends of suite PCBs …….....9
Figure 5. Spatial and temporal trends of α-HCH….. …….....11
Figure 6. Spatial and temporal trends of γ-HCH….. …….....12
Figure 7. Spatial and temporal trends of total endosulfans…….....15
Figure 8. Spatial and temporal trends of total chlordane…….....16
Figure 9. Spatial and temporal trends of total DDTs..…….....17
Figure 10. Spatial and temporal trends of hexachlorobenzene 18
Figure A1. Example of a temporal trend analysis for vapor phase concentration.....27
Figure A2. Example of a temporal trend analysis for particle phase concentration.....27
Figure A3. Example of a temporal trend analysis for precipitation phase concentrations……28
Figure B1. Phenanthrene, pyrene, retene, benzo[*a*]pyrene, and total PAH concentrations in precipitation collected at seven IADN sites near the Great Lakes…...41
Figure B2.Total PAH concentrations in precipitation at the seven IADN sites……....42
Figure B3. Retene concentrations and the ratio between retene and total PAH concentrations in precipitation collected at the five U.S. IADN sites……...42
Figure C1. ΣPCB concentrations in precipitation and in the gas phase in Chicago and at Sleeping Bear Dunes, Michigan…….59
Figure C2. Long-term trend of ΣPCB concentrations in precipitation and in the gas phase at Chicago……60
Figure C3. PCB congener profiles measured in the gas phase at Chicago and at Sleeping Bear Dunes, in precipitation at Chicago and at Sleeping Bear Dunes……61
Figure CS1. Temporal trends of wet deposition flux of PCBs in Chicago and Sleeping Bear Dune……...63
Figure D1. Map of the Great Lakes indicating the sampling sites……75
Figure D2. Concentrations of α-HCH (top), β-HCH (middle), and γ-HCH (bottom) in precipitation collected from 1997 to 2003 at the seven IADN sites……..76
Figure D3. Concentrations of endosulfans (α- plus β-endosulfan) in precipitation at the seven IADN sites……77
Figure D4. Organochlorine pesticide concentrations in precipitation collected at seven IADN sites near the Great Lakes……...78
Figure E1. Total PAH concentrations (ΣPAH) in air (vapor plus particle), vapor and particle phases at seven IADN sites sequenced by the population living within a 25 km radius of the sampling site……101
Figure E2. Average ΣPAH concentration at the seven IADN sampling sites as a function of the population living within a 25-km radius of the sampling site……102
Figure E3. Average PAH profiles for the vapor and particle phases at Chicago and at Point Petre.…….....103
Figure E4. Temporal trends of vapor and particle phase ΣPAH concentrations at Chicago and at Sleeping Bear Dunes.…….....104

Figure ES1. Temporal trends of vapor-phase PAH concentrations at seven IADN sites……...114
Figure ES2. Temporal trends of particle-phase PAH concentrations at seven IADN sites……...116
Figure F1. Concentrations of γ-HCH and α-endosulfan in the gas-phase and particle-phase at the seven IADN sites……..……...133
Figure F2. Concentrations of α-HCH, β-HCH, and γ-HCH in the gas-phase at the five U.S. IADN sites……134
Figure F3. Concentrations of chlordanes (sum of α-, β-chlordane, and *trans*-nonachlor) and endosulfans (α- plus β-endosulfan) in the gas-phase at the seven IADN sites…….135
Figure FS1. Temporal trends of gas-phase OC pesticide concentrations at seven IADN sites……...147
Figure FS2. Temporal trends of particle-phase OC pesticide concentrations at five U.S. IADN sites……...151
Figure G1. Map of the Great Lakes indicating the six regionally representative IADN sampling sites……166
Figure G2. Long-term trend of temperature corrected total PCB partial pressures in the gas phase at the six regionally representative IADN sites…….167
Figure G3. Correlation between average total PCB concentration and the local population within a 25 km radius of the sampling site……168
Figure GS1. Long-term trends of PCB congener partial pressures in the gas phase at seven IADN sites…….....172

TEMPORAL AND SPATIAL TRENDS OF ATMOSPHERIC TOXIC SUBSTANCES NEAR THE GREAT LAKES: IADN RESULTS THROUGH 2003

1. Introduction

The Integrated Atmospheric Deposition Network (IADN) was established in 1990 to monitor the persistent organic pollutants in air and precipitation in the Great Lakes region (Hoff et al., 1996; Buehler and Hites, 2002). The objectives of this network are to acquire quality-assured air and precipitation concentration measurements; determine atmospheric loadings and trends of toxic organic chemicals to the Great Lakes; and determine the sources of continuing input of toxic chemicals.

By maintaining a master station on each of the five Great Lakes and several satellite stations near the Great Lakes, IADN is able to monitor regionally-representative concentrations of toxic substances in gas, particle, and precipitation samples. Biennial loading estimates have been produced for data from 1992 through 2000 to determine the atmospheric deposition of toxic substances to the Great Lakes (Hoff et al., 1996; Galarneau et al., 2000; Buehler, et al., 2002; Blanchard, et al., 2004). Technical summaries, produced prior to past peer-reviews of the network, have presented temporal and spatial trends of selected chemicals (U.S. EPA and Environmental Canada, 1997 and 2002). For the first time, this report presents comprehensive long-term temporal and spatial trends of atmospheric toxic substances collected in the Great Lakes basin. This report covers data from the early 1990s through 2003.

2. Method

2.1. Substances Considered

A subset of the substances measured at the IADN sites were used for temporal and spatial trend analysis. These substances include individual polycyclic aromatic hydrocarbons (PAHs): fluorene, phenanthrene, anthracene, fluoranthene, pyrene, retene, benz[*a*]anthracene, triphenylene and chrysene (not resolved chromatographically, counted as one compound), benzo[*b*]fluoranthene, benzo[*k*]fluoranthene, benzo[*e*]pyrene, benzo[*a*]pyrene, indeno[*1,2,3-cd*]pyrene, benzo[*ghi*]perylene, dibenz[*a,h*]anthracene, and coronene as well as the total of sixteen of these PAHs expressed as ΣPAH; a sum of 56 polychlorinated biphenyl (PCB) congeners and coeluting congener groups expressed as "total PCB"; and the organochlorine pesticides aldrin, α-chlordane, γ-chlordane, *p,p'*-DDT, *p,p'*-DDD, *p,p'*-DDE, *o,p'*-DDT, dieldrin, α-endosulfan, β-endosulfan, endrin, heptachlor epoxide, hexachlorobenzene (HCB), α-, β-and γ-hexachlorocyclohexane (HCH), methoxychlor, and *trans*-nonachlor. The detailed temporal and spatial trends of these substances can be found in the Appendix B to G. In this report, the temporal and

spatial trends of ΣPAH, total PCB, and severl organochlrine pesticides including α-, γ-HCH, total endosulfans, total chlordanes, total DDTs, and HCB are presented.

2.2. Sampling Sites and Data Availability

As shown in Figure 1, data considered in this report were obtained at the five IADN master stations (Eagle Harbor, near Lake Superior; Sleeping Bear Dunes, near Lake Michigan; Burnt Island, near Lake Huron; Sturgeon Point, near Lake Erie; and Point Petre, near Lake Ontario) and two satellite stations (Brule River, near Lake Superior; and Chicago, near Lake Michigan). The IADN website (www.msc.ec.gc.ca/iadn) provides detailed information on these sites.

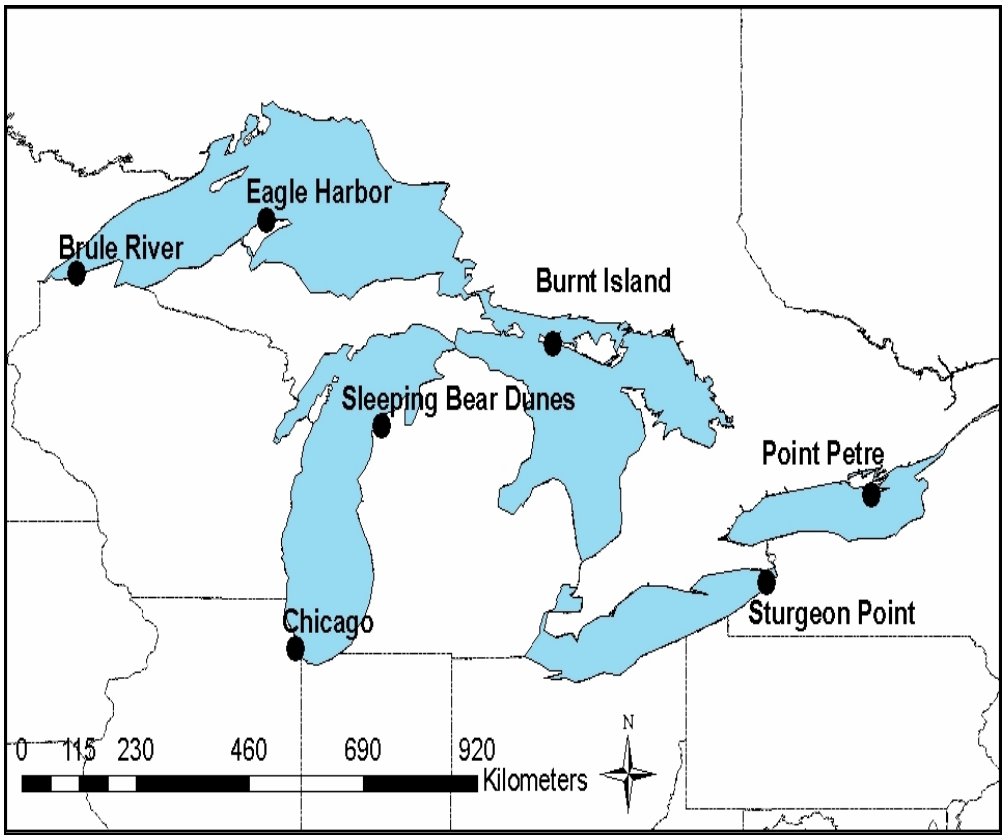

Figure 1. Map of the Great Lakes indicating the seven Atmospheric Integrated Deposition Network (IADN) sampling sites.

The air samples have been collected for both vapor and particle phases. Measurements of organic toxic substances in the vapor phase started at different time at these sites as shown in Table 1. Because measurements of vapor phase PAHs at Burnt Island and Point Petre were stopped in 1992 and resumed in 1997, only vapor phase data from January 1997 onward are reported for PAHs at these two sites.

Table 1. Data availability at seven IADN sites for this report.

IADN site	*Vapor phase*	*Particle phase*	Precipitation
Brule River	Jan.1996—Aug.2002	Oct. 1996—Dec. 2003	Mar. 1997—Dec. 2003
Eagle Harbor	Nov.1990—Dec.2003		
Sleeping Bear	Jan.1992—Dec.2003		
Sturgeon Point	Dec.2001—Dec.2003		
Chicago	Jan.1996—Dec.2003		
Burnt Island	Jan.1997—Dec.2003		
Point Petre	Jan.1997—Dec.2003		

For the particle-phase samples, data from October 1996 to December 2003 were used because U.S. particle phase samples collected before October 1996 were combined monthly. No data are available for organochlorine pesticide concentrations in the particle phase at the two Canadian sites. As for PCBs, the preliminary results from 1993 to 1995 showed that, although higher molecular weight PCB congeners tended to partition onto the particle phase, the total PCB concentrations in the particle phase were about 5-10% of the total PCBs in atmosphere; therefore measurements of particle-bound PCB concentrations were stopped in 1997. Thus, no trend analysis was conducted for PCB concentrations in particle phase.

Precipitation samples have been collected at several sites (e.g. Eagle Harbor, Sturgeon Point) since 1991. However, the analytical method changed (Carlson et al., 2004) in March of 1997 for the U.S. sites. To ensure data consistency, only data from March 1997 to December 2003 are used to conduct the temporal trend analysis for precipitation samples at all seven IADN sites.

2.3. Trend Analysis

For vapor phase concentrations, a temporal trend analysis procedure adopted by Cortes et al. (1998) was used. Details are provided in Appendix A but will be summarized briefly here. The vapor phase concentrations of the organic substances (in pg/m^3) were first converted to partial pressures using the ideal gas law. These partial pressures were then adjusted to a reference temperature (15°C). This procedure effectively "temperature-corrects" the data so that temporal trends can be detected. The pressures are regressed with time to ultimately determine the rate of increase or decrease of the air concentrations. When the rate is statistically significant, they are converted to half-lives ($t_{1/2,}$ in years) which indicate the time when concentrations in the air will have dropped by half. For concentrations in particle and precipitation, another procedure was used (Carlson and Hites, 2005), whereby the concentrations are used directly to determine the temporal trends.

3. Results and Discussion

The spatial and temporal trends of ΣPAHs, total PCB, and organochlorine pesticides are explained in detail in the papers listed in Appendix B to G. In the summary here, for

selected chemicals, six-panel figures were produced where the top three box plots show the spatial difference of the pollutant concentration in the vapor (in yellow), particle (in gray), and precipitation phases (in blue) among seven IADN sites (see Figure 2 as example). The boxes represent the 25th to 75th percentiles, the black lines in the boxes are the medians and the red lines are the means. The two vertical lines outside each box extend to the outliers representing the 10th and 90th percentiles; and outliers are shown as the 5th and 95th percentiles. The small letter "a, b, c, d, e, f" on the top of each box indicates the spatial trends of concentration. The site marked with "a" has the lowest average concentration and increases with 'b", "c", "d" and so on. The sites with the same letter have statistically the same concentrations on average. Half-lives, representing the period of time necessary for the atmosperhic concentration to decrease by half, are plotted in the bottom left panel. The maximum to minimum concentration ratio which provides an indication of the seasonal variation is plotted in the bottom middle panel while the dates at which concentrations peaked are plotted in the bottom right panel. The horizontal lines in the bottom three figures represent the average (e.g. average half-life, average ratio of maximum to minimum concentration, and the average date with maximum concentration). The bar color codes are the same as in the top three panels.

3.1. ΣPAHs

PAHs are a class of organic compounds that have attracted environmental and health concerns. They are ubiquitous, persisting in the environment for months to years (Beak, et al., 1991). Many PAHs are carcinogenic and/or mutagenic (Denissenko, et al., 1996). PAHs can be formed from both natural and anthropogenic sources. Natural sources include combustion in nature such as volcanic eruptions and forest and prairie fires (Ebert, 1988). Major anthropogenic sources include incomplete combustion of fossil fuels and other organic matter, oil refining, and many other industrial activities (Junk and Ford, 1980).

Spatial and temporal trends of ΣPAHs are shown in Figure 2. The highest PAH concentrations in the vapor, particle, and precipitation phases were all observed in Chicago followed by the semi-urban site at Sturgeon Point. In the vapor phase, the spatial trend of PAH concentrations is: Burnt Island < Eagle Harbor ≈ Brule River ≈ Point Petre < Sleeping Bear Dunes < Sturgeon Point << Chicago. In the particle phase, the spatial trend of PAH concentrations is: Eagle Harbor < Burnt Island ≈ Brule River ≈ Sleeping Bear Dunes < Point Petre <Sturgeon Point << Chicago. The ΣPAH concentrations in the particle phase were generally much lower compared to those in the vapor phase, an observation which agrees with other studies (Poor et al., 2004; Gigliotti et al., 2005), which is mainly due to higher concentrations of the lighter PAHs (e.g. phenanthrene and fluorene) in vapor phase. The spatial trend of ΣPAH concentration in precipitation is: Eagle Harbor ≈ Brule River < Sleeping Bear Dunes < Burnt Island ≈ Point Petre < Sturgeon Point << Chicago.

The atmospheric PAH concentrations at seven IADN sites showed a strong correlation with local population (r^2 = 0.91) (see Figure 3). As Chicago is a large urban center, the very high ΣPAH concentrations are not surprising. The major sources of

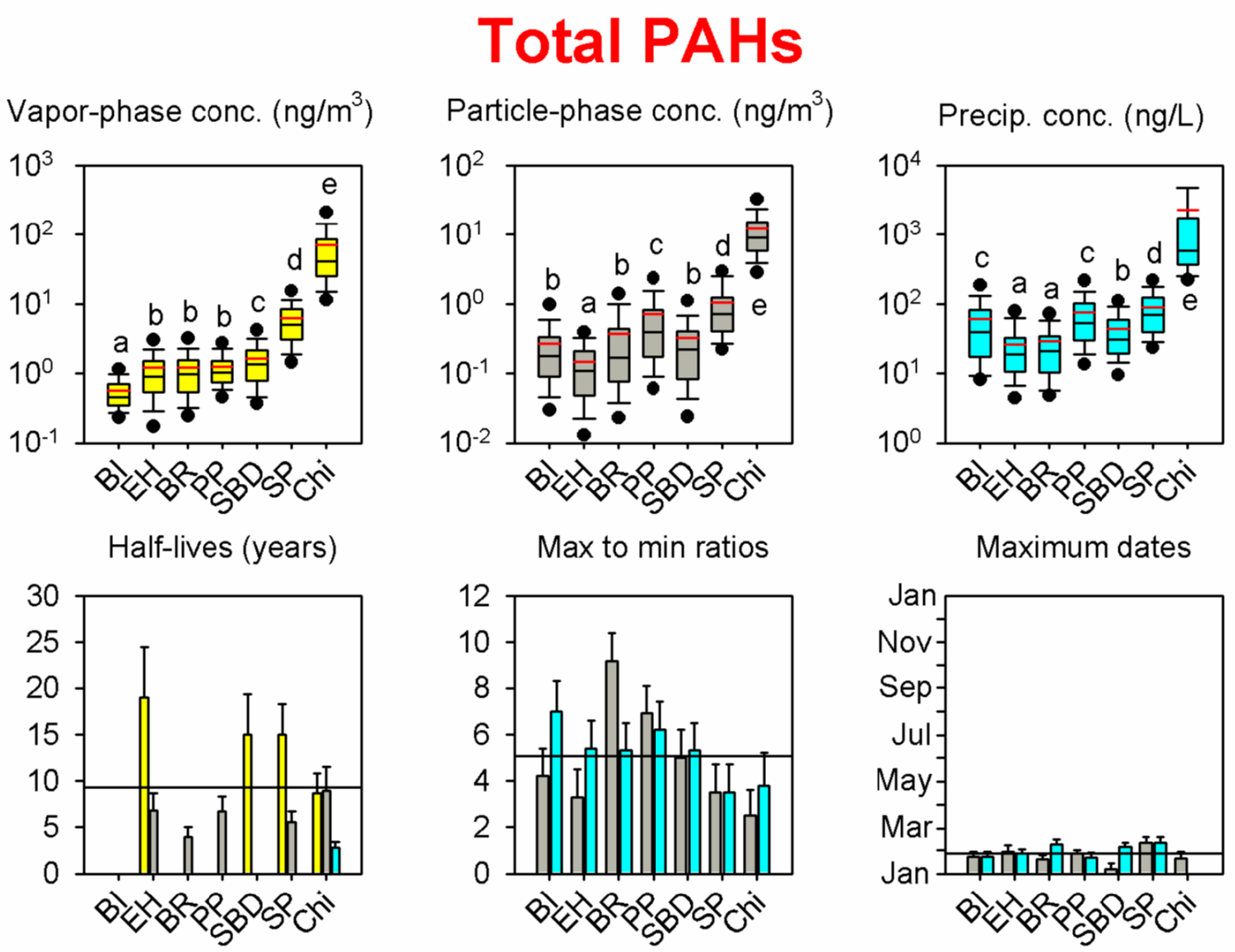

Figure 2. Spatial and temporal trends of ΣPAHs. Yellow bars are the vapor phase, gray bars are the particle phase, and blue bars are the precipitation phase. "a,b,c,d,e" in the box plots means the increasing trends of concentrations with "a" has the lowest concentration. BI: Burnt Island; EH: Eagle Harbor; BR: Brule River; PP: Point Petre; SBD: Sleeping Bear Dunes; SP: Sturgeon Point: Chi: Chicago.

PAHs in and around Chicago are vehicle emissions, coal and natural gas combustion, and coke production (Simcik et al., 1999). The second highest PAH concentrations we observed were at Sturgeon Point, which is located 25 km south of the city of Buffalo, NY, and about 110,000 people live within a 25-km radius of this sampling site. At the other five sites, the lower atmospheric PAH concentrations likely represent a background level in the Great Lakes basin.

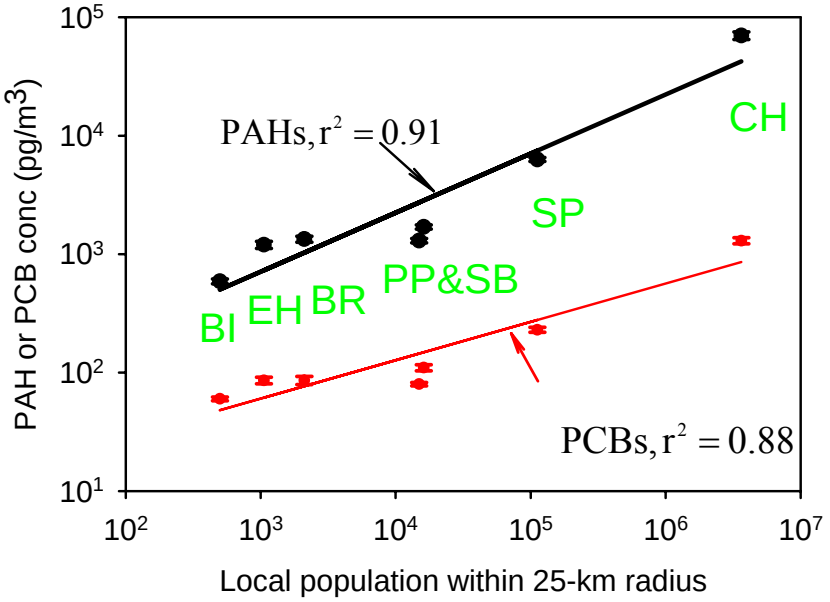

Figure 3. Average ΣPAH and total PCB concentration at seven IADN sampling sites as a function of the population living within a 25-km radius of the sampling site. The error bars are standard errors. See Figure 2 for the description of the site abbreviation.

Long-term decreasing trends of ΣPAH concentrations were observed at Chicago in all three phases (Figure 2, bottom left panel). The half-lives were about 9 years in both vapor and particle phases, about 3 years in the precipitation phase. At the other IADN sites, vapor phase ΣPAH concentrations showed significant, but slower long-term decreasing trends (>15 years). Particle-phase ΣPAH concentrations also declined slowly at the sites that were impacted by nearby cities e.g. Sturgeon Point (near Buffalo) and Point Petre (near Toronto). Much of the decline of ΣPAH concentrations in Chicago could be the result of a commitment to cleaner air, including improved petroleum fuels, automobile engines, and industrial pollution control technology. Regulations on coke ovens in steel mills in the area (as well as steel facility shutdowns), mobile source diesel regulations, and efforts to retrofit and replace bus fleets in the region could all have contributed to decreasing PAH concentrations at this site. For example, the Clean Cities Program has promoted the use of alternative fuels and alternative fuel vehicles to reduce air pollution from motor vehicles since 1998. The diesel retrofit portion of the program involves installing devices that lower emissions by over 90% on Chicago's bus fleet. These efforts on improving air quality in Chicago may explain the continuous decrease of ΣPAH concentrations in vapor, particle, and precipitation phases.

Seasonal variations of ΣPAH concentrations were observed in the particle and precipitation phases (Figure 2, bottom middle panel). The ratios between the highest concentrations in the winter and the lowest concentrations in the summer are usually about 5, indicating the ΣPAH concentrations in the winter were much higher than those in the summer. There are many reasons that may lead to increased particle and precipitation phase PAH concentrations in the winter; these include lower atmospheric mixing heights (Bidleman et al., 1986), decreased photolytic reactions in the atmosphere (Baek et al., 1991), and more emissions from domestic space heating. This seasonal trend of ΣPAH concentrations was further proved by the calculated date when the concentration peaked, which is around the end of January for both particle and precipitation samples at the IADN sites.

3.2. Total PCBs

PCBs are mixtures of up to 209 individual chlorinated compounds (known as congeners), which have been used as coolants and lubricants in transformers, capacitors, and other electrical equipment due to their good stablility. PCBs have been banned in the late seventies in the U.S. because of their bio-accumlation and harmful health effects (U.S. EPA, 2006). In this report, total PCB represents a suite of 56 PCB congeners monitored by IADN. Each congener contributes more than 1% to the total PCB mass for at least one site monitored by IADN. The toxicologically important congeners (PCB 77, 105, 108, 126, 128, 138, 156, 169, and 170) are also included. The detailed list of congeners is available in the supporting information of Appendix G.

Total PCB concentrations in the vapor phase samples collected at six regionally representative IADN sites (e.g. average concentration of 60-230 pg/m^3) near the Great Lakes were much lower compared to Chicago (e.g. average 1300 pg/m^3) as shown in Figure 4. The spatial difference of total PCB concentration among these sites showed the industrial and urban influence on PCB concentrations at Chicago and Sturgeon Point similarly to that observed for PAHs (see Figure 3). For the total PCB concentrations in precipitation phase, our results showed that the total PCB levels in precipitation at the remote sites in U.S. are close to the field blank levels. Therefore, we only focused on total PCB concentrations in Chicago and used Sleeping Bear Dunes as a background site. Much higher total PCB concentrations in the vapor phase and precipitation (7.1 ± 0.9 ng/L) at Chicago compared to Sleeping Bear Dunes (1.1 ± 0.1 ng/L) re-iterates the fact that Chicago is a source of PCB to the atmosphere.

The long-term temporal trends of selected PCB congeners at these IADN sites are given in Appendix G. As for the long-term temporal trends of total PCB, Brule River had a negative half-life indicating an increase as a function of time. Given that the data for the Brule River site covered only 6 years, we do not consider these trends reliable. For all remaining IADN sites, the overall slower decline or no significant trend of total PCB concentrations near Lakes Superior and Huron may be due to the colder water temperatures and larger volumes of these lakes. For total PCBs at Sturgeon Point near Lake Erie, half-life was on the order of ~20 years. This slower rate of decrease for PCB concentrations in recent years at Sturgeon Point may indicate that atmospheric PCB concentrations are now approaching a steady state in Lake Erie after a more rapid decline from 1975 to 1995 (Buehler et al., 2004). On the other hand, the relatively faster decline of gas-phase PCB concentrations around Lakes Michigan and Ontario (half-lives of 7

years) may be due to effective reduction efforts, aimed at eliminating PCB point sources that have occurred in the areas surrounding these two lakes. In precipitation, a long-term decreasing trend of PCB concentrations was observed at Chicago with a half-life of 6.8 ± 3.1 years, which agrees with the half-life in the vapor phase (8.0 ± 1.1 years), suggesting that regulatory efforts are working in this city

In the precipitation regression (Appendix A, Equation 4), the terms b_2, b_3, and b_4 were not significant ($p > 0.05$) for total PCB concentration, indicating the seasonal effects were not statistically significant. Therefore, the ratio between maximum and minimum concentration of PCB in precipitation and the date at which the concentration peaked were not available.

3.3. Organochlorine Pesticides

Temporal and spatial trends of selected organochlorine pesticides including α-, and γ-hexachlorocyclohexane (HCH), total endosulfan (sum of α-endosulfan and β-endosulfan), total chlordane (sum of α-chlordane, γ-chlordane, and *trans*-nonachlor), total DDT (sum of *p,p'*-DDT, *p,p'*-DDD, and *p,p'*-DDE), and hexachlorobenzene (HCB) are presented here. The detailed information on the other organochlorine pesticides is in Appendices D and F.

3.3.1 α-, and γ- HCH

Technical HCH contains 60-70% of α-HCH, 2-12% of β-HCH, and 10-15% of γ-HCH (Iwata, et al., 1993). The technical HCH mixture was banned in North America in 1970s and replaced by purified γ-HCH (lindane). For the study period, γ-HCH was still a current-use pesticide with continuous input. For α-HCH, its source is mainly from the previously usage of technical HCH.

α-HCH is more volatile than γ-HCH, and slower to react with atmospheric hydroxyl radicals (Willett et al., 1998); therefore, α-HCH is more readily transported through the atmosphere and will tend to have a relatively uniform global atmospheric concentration. As shown in Figure 5, α-HCH concentrations were slightly higher at Eagle Harbor (average 100 ± 5.3 pg/m^3) compared to the other sites. The concentrations were similar (average 82 ± 1.8 pg/m^3) at Sleeping Bear Dunes and Sturgeon Point. Chicago and Brule River showed similar but lower α-HCH concentrations (average 54 ± 2.2 pg/m^3). It has been established that a loss of α-HCH of the order of 10-20% results from the method of collection at the Canadian sites. Taking this into account, α-HCH concentrations are still generally smaller at Point Petre and Burnt Island relative to the other sites. In precipitation, α-HCH concentrations were about the same at all sites except for Eagle Harbor, which had slightly higher concentrations.

For the current-use pesticide γ-HCH, Chicago, Sleeping Bear Dunes and Sturgeon Point had similar vapor-phase concentrations (Figure 6), but these were significantly higher than γ-HCH vapor-phase concentrations at Brule River, Eagle Harbor, Point Petre and Burnt Island. The γ-HCH concentrations in precipitation at the two Canadian sites (Burnt Island and Point Petre) were similar and significantly higher than the other five U.S. sites, which were all about the same. The technical HCH mixture was banned in North America in 1970s and replaced by purified γ-HCH (lindane). Although the National Center for Food and Agricultural Pesticides showed that the U.S. usage of lindane for all crops during the period of 1992 and 1997

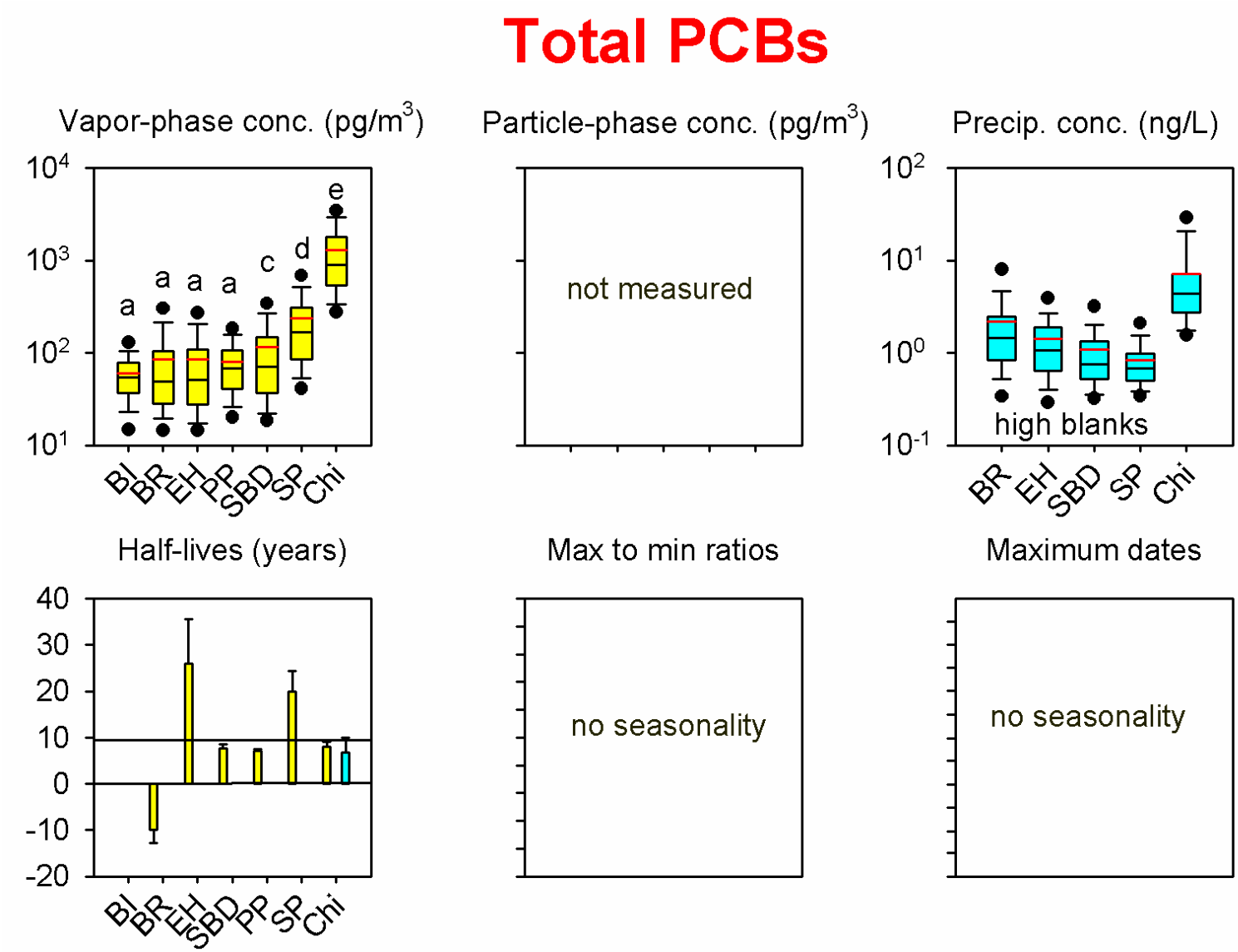

Figure 4. Spatial and temporal trends of total PCBs. The color code and site abbreviation are same as in Figure 2.

in the Great Lakes area was limited, the Canadian lindane usage inventories showed that ~410 t of lindane had been applied during the period 1970 to 2000 in the provinces of Quebec and Ontario close to Lakes Ontario and Huron (Li et al., 2004).

Although γ-HCH was still in-use in Canada until 2004 and in the U.S. through the present time, long-term decreasing trends were observed in both the gas and particle phases at all seven IADN sites except for the particle phase at Brule River (Figure 6). Our results showed that γ-HCH had a half-life of 5 to 10 years around the Great Lakes, which were longer compared to a 4-year half-life for α-HCH in all phases at most IADN sites. The slower decline of γ-HCH measured by IADN in the Great Lakes region is likely due to the continuing usage of lindane in the U.S. and Canada.

Most of the α-HCH concentrations did not have a significant seasonal trend except in the precipitation at Sleeping Bear Dunes and Point Petre. At these two sites, the maximum concentrations of α-HCH in precipitation occurred in winter time, in January at Sleeping Bear Dunes and late December at Point Petre. In contrast, the concentrations of γ-HCH in the particle and precipitation phases showed significant seasonal trends. The ratio between the highest and the lowest γ-HCH ranged between about 2-9, indicating that the seasonal variations can be substantial. Interestingly, the concentrations peaked in the summer for γ- HCH, which agrees well with their maximum agricultural usage.

It has been suggested that competing processes could explain the winter concentration peak for the banned pesticides such as α-HCH in precipitation (Carlson et al., 2004). These pesticides enter the atmosphere due to re-volatilization from lake and terrestrial surfaces, and these sources tend to maximize during the warmer summer months (Buehler et al., 2001). However, the concentrations of these pesticides in the atmospheric particle phase tend to increase during the winter due to enhanced partitioning to the particles. In addition, snow is a better scavenger for both particle-associated and vapor-phase pesticides than rain (Franz and Eisenreich, 1998). The lower intensity of sunlight in the winter lowers the atmospheric OH radical concentration, which in turn increases the atmospheric lifetime of the pesticides, favoring their accumulation in the winter-time air and precipitation. All these mechanisms could contribute to higher winter concentrations in precipitation for α-HCH.

3.3.2 Total Endosulfans

Endosulfan is used to control insects on food and non-food crops and also as a wood preservative. Endosulfan is a current-use pesticide. For example, endosulfan is widely used in Michigan and New York State (Hafner and Hites, 2003) and in Ontario (Harris, et al., 2002), particularly in the southern and western portions of the province.

The endosulfan concentrations (shown as the sum of α- and γ-endosulfan) in vapor phase showed a clear increasing trend from the west to east (Figure 7), except for the remote site of Burnt Island. At each site, the average concentration was affected by high concentration outliers that usually occurred in the summer and were likely due to the

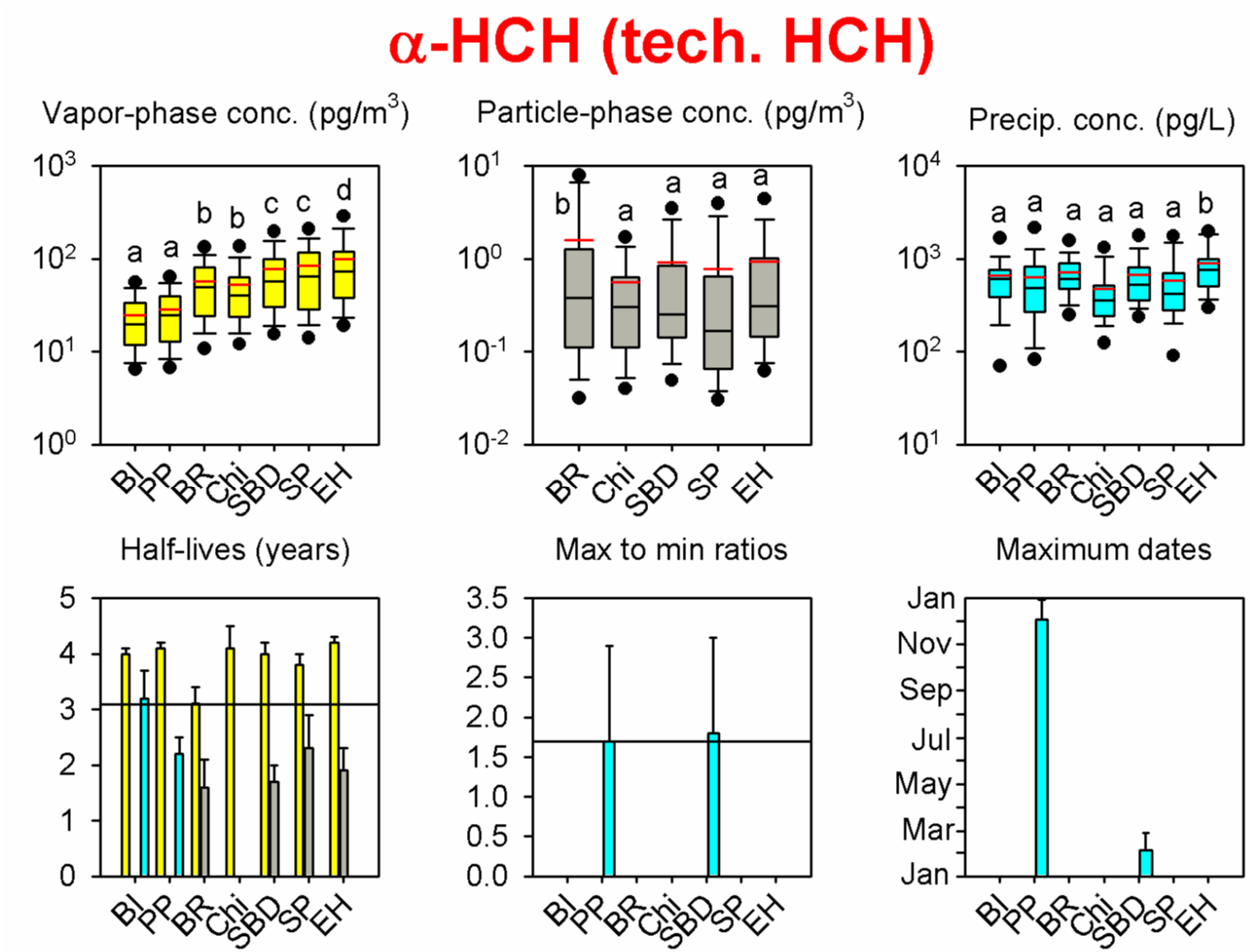

Figure 5. Spatial and temporal trends of α-HCH. The color code and site abbreviation are same as in Figure 2.

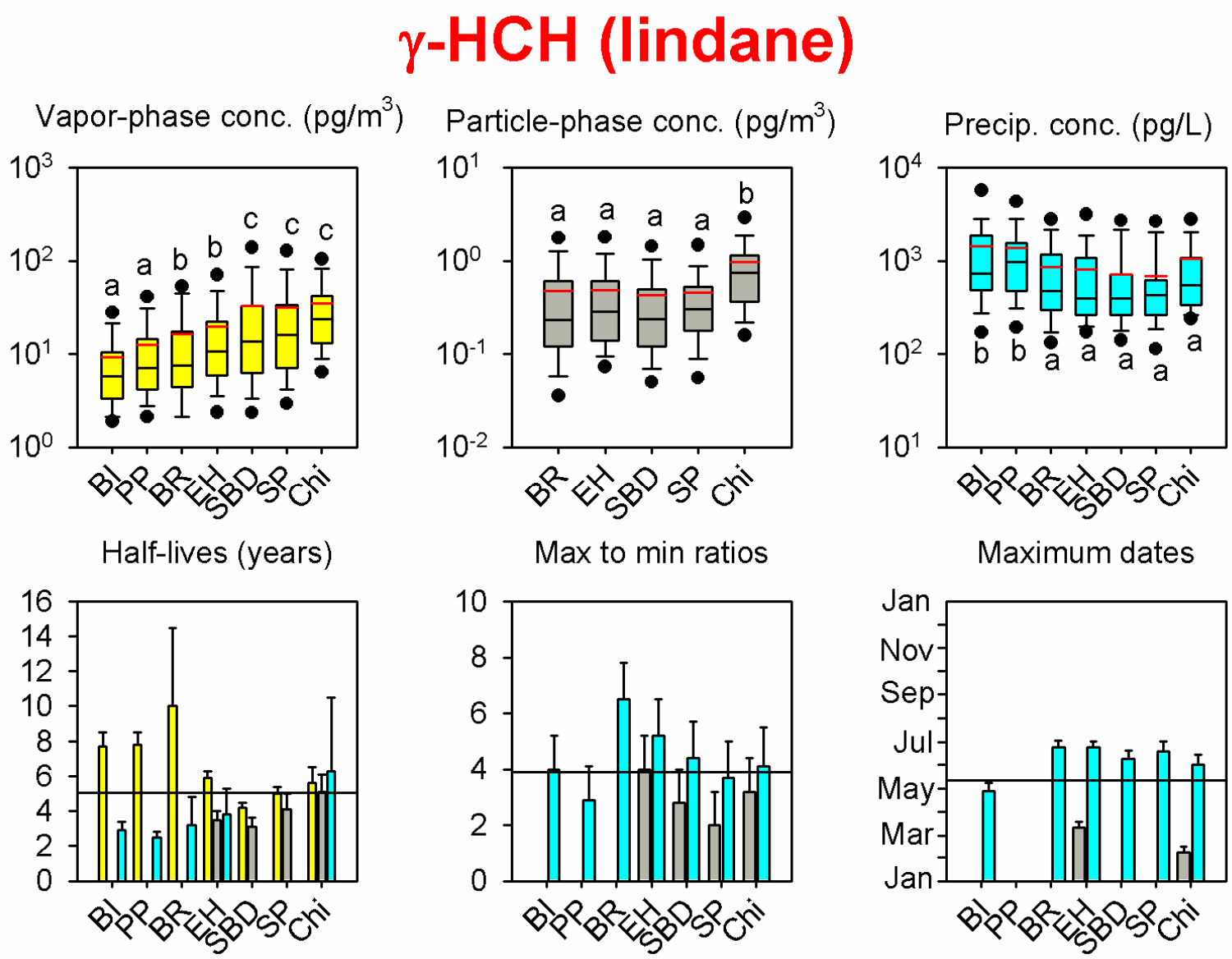

Figure 6. Spatial and temporal trends of γ-HCH. The color code and site abbreviation are same as in Figure 2.

current agricultural use of endosulfan. Higher endosulfan concentrations were observed at Point Petre, Sturgeon Point, and Sleeping Bear in vapor, particle, and precipitation phases, which could be explained by its heavy usage in the surrounding areas (Hoh and Hites, 2004). For example, endosulfan is widely used in Michigan and New York State (Hafner and Hites, 2003) and in Ontario (Harris, et al., 2001), particularly in the southern and western portions of the province.

Total endosulfan concentrations showed no long-term decreasing trends in the vapor phase at Eagle Harbor, Sleeping Bear Dunes, or Sturgeon Point (Figure 7). However, total endosulfan concentrations in the particle phase declined at all five U.S. sites. In the precipitation phase, total endosulfan concentrations only decreased at Point Petre, while at the other six sites, these concentrations did not change from 1997 to 2003. The National Center for Food and Agriculture Policy provides an endosulfan usage database for the period 1992-97 in the U.S. Although endosulfan usage in Michigan significantly decreased from 29 tons to 19 tons between 1992 and 1997, increasing usage was also observed in the surrounding states, including New York, Indiana, Kentucky, and Minnesota. Because of the lack of updated usage data, correlation between the decreasing particle-bound endosulfan concentrations and its usage pattern is difficult.

Similar to γ-HCH, total endosulfan concentrations also showed a strong seasonal variation in precipitation. The ratio between the highest and the lowest total endosulfan concentration ranged between about 2-10. In particular, this ratio is as high as 10 at Point Petre, suggesting a heavy usage in the surrounding area. At all sites, the total endosulfan concentrations peaked in early July in precipitation, a time which corresponds well with its maximum agricultural usage.

3.3.3 Total Chlordanes

Technical chlordane was introduced in 1947 to control termite and phased out in the United States and Canada in 1988 and 1990, respectively. Technical chlordane was a mixture containing γ-chlordane (13%), α-chlordane (11%), *trans*-nonachlor (5%), and more than 140 other compounds with six to nine chlorine atoms (Dearth and Hites, 1991). Here total chlordane is presented as the sum of α-, γ-chlordane, and *trans*-nonachlor concentrations.

As shown in Figure 8, the spatial trend of the total chlordane gas-phase concentrations is: Brule River≈ Eagle Harbor ≈ Burnt Island < Point Petre < Sleeping Bear Dunes < Sturgeon Point < Chicago. Precipitation concentrations of total chlordane were also the highest in Chicago followed by Sturgeon Point and Sleeping Bear Dunes. Brule River, Eagle Harbor, Burnt Island, and Point Petre had similar but lower total chlordane concentrations. Chlordane's most common use in the U.S. was for termite control near homes, suggesting that urban areas could be emission sources (Harner et al., 2004). It has been suggested that volatilization of old chlordane residues from soil in the southern United States was the predominant source of chlordane to the Great Lakes (Hafner and Hites, 2003). Thus, both historical local applications used to control termites and the influence of long-range transport from areas of historical high chlordane use could contribute to the relatively high chlordane concentrations at Chicago. Long-range transport of chlordane would impact all of the sites, not just Chicago. The relative difference between Chicago and the other sites is likely due to historical local use in Chicago.

Total chlordane concentrations in the gas phase declined at all seven IADN sites (Figure 8, bottom left panel). Overall, chlordane concentrations in the gas phase had half-lives around 8 years at most sites except Brule River. The decline of total chlordane in the particle and precipitation phases was not as notable compared to the vapor phase. The particle-phase chlordane only decreased in Eagle Harbor, Sturgeon Point, and Chicago, two of these three sites (e.g. Eagle Harbor and Sturgeon Point) had a half-life longer than 10 years. A faster decline of total chlordane concentration in precipitation was observed at Sturgeon Point and Chicago, while no temporal trends were observed at the other five sites for total chlordane concentrations in precipitation.

Strong seasonal concentration variations were observed for total chlordane at most IADN sites in both particle and precipitation phases. The ratio between the highest and the lowest total chlordane concentrations ranged between 2 to 9. As a banned pesticide, the concentrations of total chlordane in the particle and precipitation phases usually peaked in late January, which is similar as α-HCH but different from γ-HCH and total endosulfan, both current-use pesticides during the data period.

3.3.4 Total DDTs

Technical DDT is consisted of *p,p´*-DDT (65-80%), *o,p´*-DDT (15-21%), *p,p´*-DDD (<4%), and small amounts of other compounds. *p,p´*-DDT can dehydrochlorinate in the environment to form *p,p'*-DDE (Ranson, et al., 2000). Although technical DDT was deregistered in the U.S. in 1972 and in Canada in 1973, it was used extensively in urban aerial sprays to control mosquitoes and other insects in the 1940s and 1950s. Due to its high persistence, these residuals may still act as a source of DDTs to the atmosphere. IADN measures the gas phase concentrations of several DDT-related compounds, including *p,p'*-DDT, *p,p'*-DDD, *p,p'*-DDE, *o,p'*-DDT, and *o,p'*-DDD in gas phase, but in the particle phase, *p,p'*-DDE and *o,p'*-DDT are not measured. Here, the total DDT is reported as the sum of *p,p'*-DDT, *p,p'*-DDE, and *p,p'*-DDD.

The highest concentrations of total DDT were also observed in Chicago in all three phases suggesting urban sources (Figure 9). Total DDT concentrations in the vapor phase showed decreasing trends at most sites with half-lives ranging from 5 to 15 years except at Brule River. No long-term trends were observed for total DDT in the particle phase except in Chicago. In the precipitation phase, decline of total DDT was only shown at Chicago and Burnt Island.

Seasonal concentration variations of total DDT were observed at most IADN sites in both particle and precipitation phases. The ratio between the highest and the lowest total DDT concentrations ranged between 1.5 and 4.5. The concentrations of total DDT in the particle phases usually peaked in late January, which is similar to other banned organochlorine pesticides (discussed above).

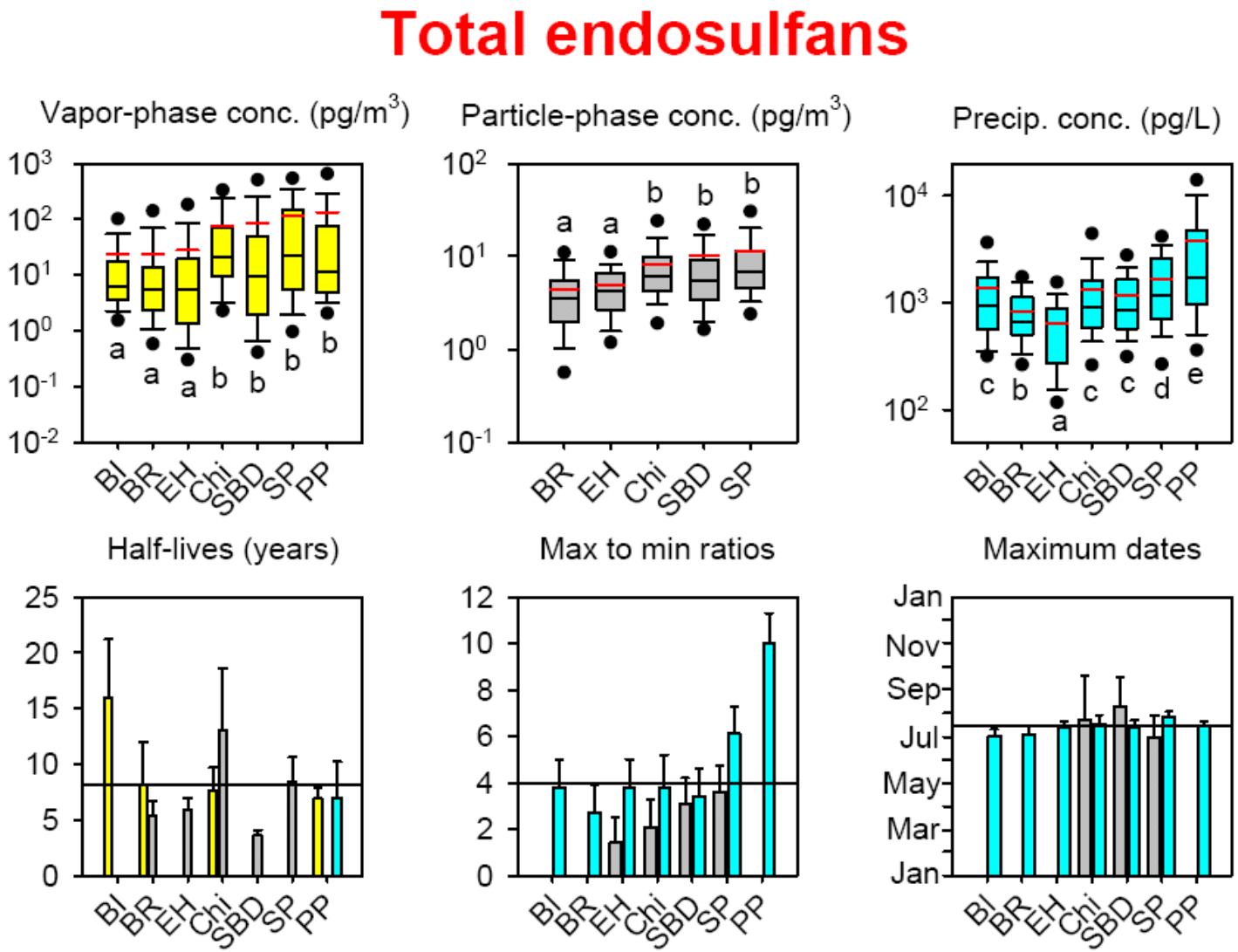

Figure 7. Spatial and temporal trends of total endosulfans (sum of α- and γ-endosulfan). The color code and site abbreviation are same as in Figure 2.

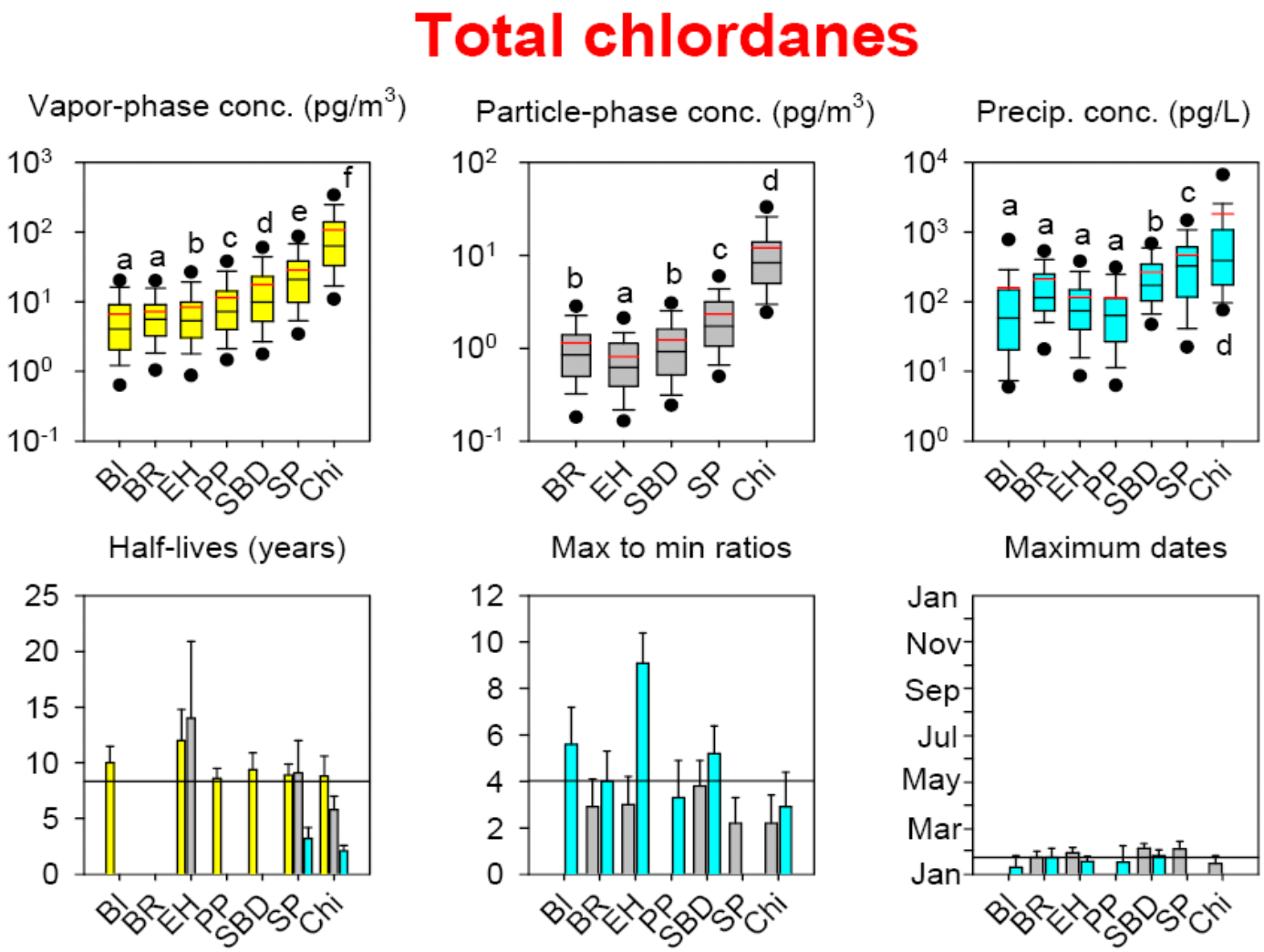

Figure 8. Spatial and temporal trends of total chlordane (sum of α- and γ-chlordane, and *trans*-nonachlor). The color code and site abbreviation are same as in Figure 2.

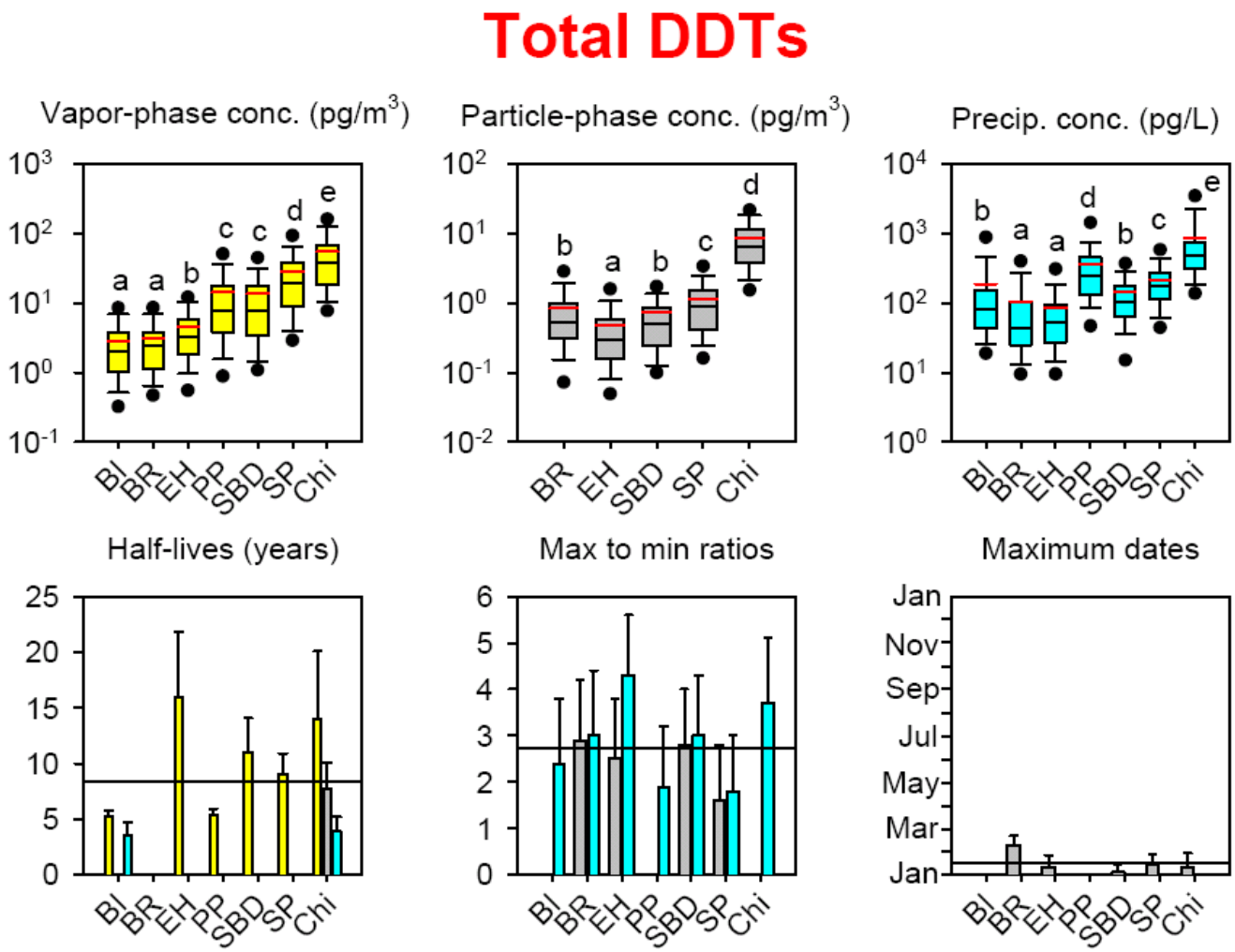

Figure 9. Spatial and temporal trends of total DDT (sum of *p,p'*-DDT, *p,p'*-DDE and *p,p'*-DDD). The color code and site abbreviation are same as in Figure 2.

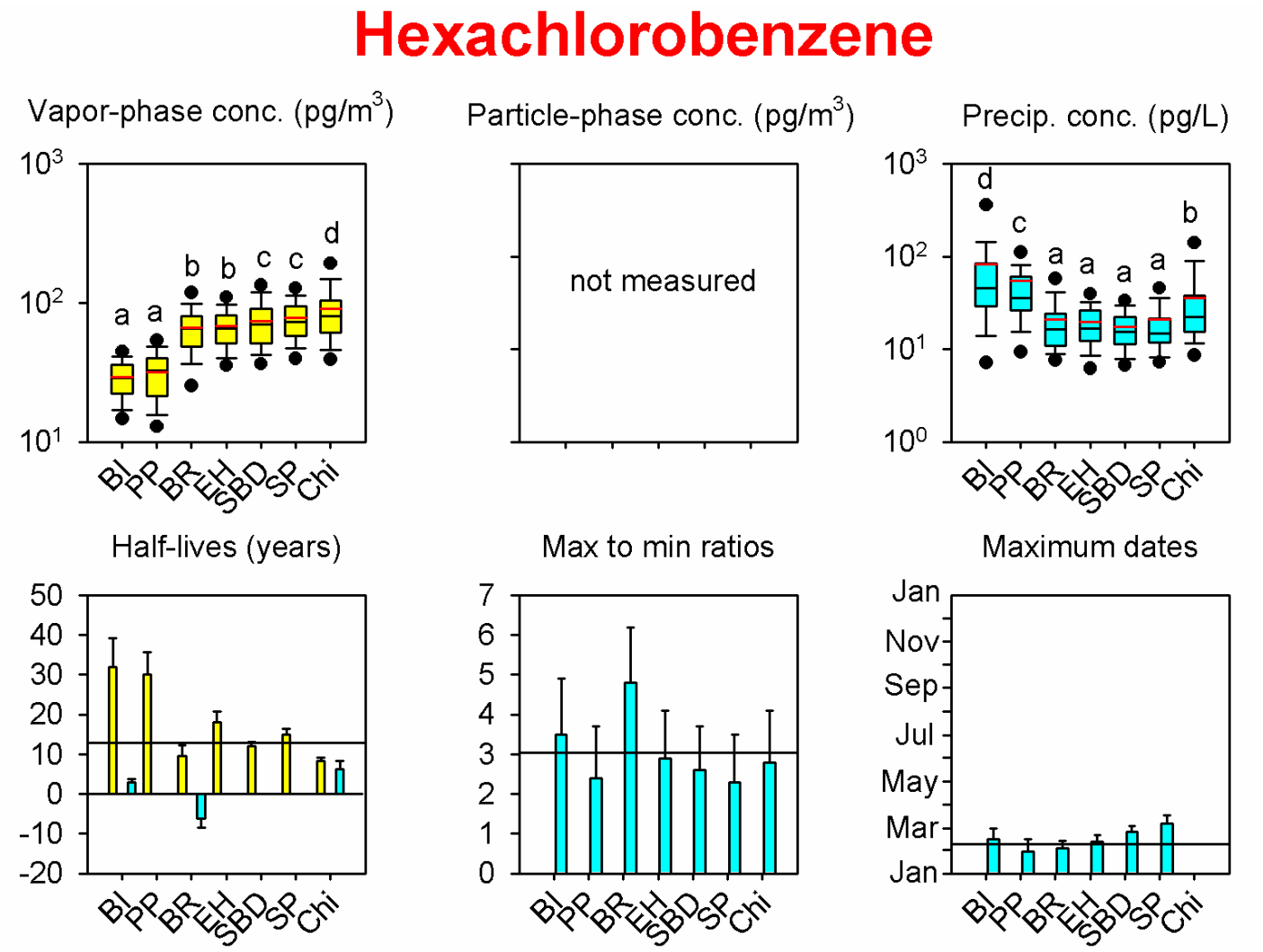

Figure 10. Spatial and temporal trends of hexachlorobenzene. The color code and site abbreviation are same as in Figure 2.

3.3.5 Hexachlorobenzene (HCB)

HCB has been used for protecting the seeds of onions and sorghum, wheat, and other grains against fungus until 1965. It was also used to make fireworks, ammunition, and synthetic rubber. HCB is a by-product in the production of making other chemicals, in the waste streams of chloralkali and wood-preserving plants, and when burning municipal waste.

Relatively high concentrations of HCB were observed in the vapor phase at Chicago (Figure 10). There is evidence of significant loss of vapour phase HCB during summer sample collection at the Canadian sites (Fowlie, 2002), hence the smaller concentrations seen in Figure 10. In precipitation, higher HCB concentrations were observed at the two Canadian sites, perhaps because HCB was used as an anti-fungal seed dressing for several crops in Canada until 1972, while it has been banned in the U.S. since 1965. In addition, the re-volatilization of HCB from Lake Ontario may also contribute to its higher level at Point Petre (Buehler, et al., 1998).

Vapor phase HCB concentrations showed decreasing trends at all these seven IADN sites, much longer half-lives (around 30 years) were observed at the two Canadian sites compared to the five U.S. sites (around 10 years) perhaps driven by wintertime concentrations which are not affected by sample loss. Interestingly, a significant *increasing* trend of HCB was observed at Brule River, which could be attributed to the short monitoring period at this site. The monitoring at Brule River started in January 1996 and ended in August 2002, which is about half of the sampling length at Eagle Harbor (e.g. from January 1992 to present). It is possible that the observed increasing trend of HCB concentrations at Brule River is just a short-term aberration.

The average ratio between the highest and the lowest HCB concentrations in precipitation was around 3 at seven IADN sites. The HCB concentration in the precipitation phase peaked around early February, which again is similar to other banned organochlorine pesticides.

4. Conclusions

Overall, the Chicago site has the highest concentrations of ΣPAHs, total PCBs, and most organochlorine pesticides, suggesting a strong urban atmospheric source of these persistent organic pollutants. This urban effect could also be observed at Sturgeon Point, a semi-urban site close to Lake Erie. The concentrations of ΣPAHs, total PCBs, and organochlorine pesticides at the other five IADN sites usually represent atmospheric background levels of these pollutants in the Great Lakes basin.

Fast decreasing trends of ΣPAH concentrations were observed at Chicago. The half-lives were about 9 years in both the vapor and particle phases, about 3 years in the precipitation phase. At other sites, vapor phase ΣPAH concentrations showed significant, but slower long-term decreasing trends (>15 years). The decline of ΣPAH concentrations

in Chicago could be the result of a basinwide commitment to cleaner air, including improved petroleum fuels, automobile engines, and industrial pollution control technology.

Significant long-term decreases of total PCB concentrations in the vapor phase, with the half-life of 7-14 years, were observed at Chicago, Sleeping Bear Dunes, Sturgeon Point, and Point Petre, suggesting reduction efforts are working in the surrounding areas. A much slower decline of vapor-phase PCB concentrations at Eagle Harbor (half-life of 18 years) and Burnt Island (half-life of 27 years) potentially due to the remoteness of the sites. In precipitation, a long-term decreasing trend of PCB concentrations was observed at Chicago with a half-life of 7 years, which agrees with the half-life of 8 years in the vapor phase.

Declines of organochlorine pesticide concentrations were observed at most IADN sites. For example, our results showed that γ-HCH had a half-life of 5-10 years around the Great Lakes, which is longer than a 4-year half-life for α-HCH at most IADN sites. The slower decline of γ-HCH measured by IADN in the Great Lakes region is likely due to the continuing usage of lindane during the study period. Since Canada withdrew agricultural uses of γ-HCH in January 2005 and the U.S. recently agreed to do likewise, future data should reveal whether levels of γ-HCH start to decline more quickly as a result. Another example is the total chlordane concentrations in the gas phase, which had half-lives around 8 years at most sites except Brule River.

Seasonal variations were observed for ΣPAH concentration and organochlorine pesticide concentrations in the particle and precipitation phases. Generally ΣPAH concentration showed higher concentrations in the winter time and lower concentration in the summer. The ratios between the highest concentration and the lowest concentration are usually larger than 2 indicating seasonal variations are substantial. The ΣPAH concentrations in the particle phase and precipitation usually peaked in late January, which could be due to commercial and home heating. Among all the organochlorine pesticides measured by IADN, two different seasonal trends could be observed. In the first, the concentrations peaked in the summer for pesticides that were in-use during our sampling period such as γ-HCH and endosulfan. In the second, the concentrations peaked in the winter for banned pesticides including α-HCH, chlordane, DDT, and HCB. Unlike PAHs and organochlorine pesticides, the PCBs in the precipitation phase did not show significant seasonal variations, apart from seasonality due to changes in temperature.

With more than a decade of data, IADN has successfully determined the atmospheric temporal and spatial trends of toxic substances including PAHs, PCBs, and several organochlorine pesticides around the Great Lakes. This report completely documented the trends of toxic substances in the Great Lakes region. Together with previous biennial loading reports prepared by IADN, this information will be helpful to better understand the cycling of persistent organic pollutants in the Great Lakes environment.

Acknowledgements

The authors would like to thank many people whose work supported the production of the IADN trend report.

Site operators at each sampling stations

Ed Sverko and staff at the National Laboratory, Environment Canada

Frank Froude and staff at the Centre for Atmospheric Research and Experiments, Environment Canada.

Staff at the Organic Analysis Laboratory, Environment Canada.

Karen Arnold, Jennifer Kelly, and James Bays at Indiana University

Ronald Piva at the North Central Research Stations of the USDA Forest Survey

Daniel Carlson at University of Minnesota

The U. S. Environmental Protection Agency's Great Lakes National Program Office for funding (Grant GL995656)

References

Baek, S. O.; Field, R. A.; Goldstone, M. E.; Kirk, P. W.; Lester, J. N.; Perry, R. A review of atmospheric polycyclic aromatic hydrocarbons: sources, fate and behavior. *Water, Air, Soil Poll*. **1991**, *60*, 279-300.

Bidleman, T.; Billings, W. N.; Foreman, W. T. Vapor-particle partitioning of semi-volatile organic compounds: estimates from field collections. *Environ. Sci. Technol.* **1986**, *20*, 1038-1043.

Blanchard, P.; Audette, C. V.; Hulting, M.L; Basu, I.; Brice, K. A.; Chan, C. H.; Dryfhout-Clark, H.; Froude, F.; Hites, R. A.; Neilson, M. *Atmospheric Deposition of Toxic Substances to the Great Lakes: IADN Results through 2000, Environmental Canada and The U.S. Environmental Protection Agency,* 2002.

Buehler, S. S.; Basu, I.; Hites, R. A. A comparison of PAH, PCB, and pesticide concentrations in air at two rural sites on Lake Superior. *Environ. Sci. Technol.* **2001**, *35*, 2417-2422.

Buehler, S. S.; Hites, R. A. The Great Lakes' integrated atmospheric deposition network. *Environ. Sci. Technol.* **2002**, *36*, 354A-359A.

Buehler, S.; Hafner, W.; Basu, I.; Audette, C. V.; Brice, K. A.; Chan, C. H.; Froude, F.; Galarneau, E.; Hulting, M. L.; Jantunen, L.; Neilson, M.; Puckett, K.; Hites, R. A. *Atmospheric Deposition of Toxic Substances to the Great Lakes: IADN Results through 1998, Environmental Canada and The U.S. Environmental Protection Agency,* 2002

Buehler, S. S.; Basu, I.; Hites, R. A. Causes of variability in pesticide and PCB concentrations in air near the Great Lakes. *Environ. Sci. Technol.* **2004**, *38*, 414-422.

Carlson, D. L.; Basu, I.; Hites, R. A. Annual variation of pesticide concentrations in Great Lakes precipitation. *Environ. Sci. Technol.* **2004**, *38*, 5290-5296.

Cortes, D. R.; Basu, I.; Sweet, C. W.; Brice, K. A.; Hoff, R. M.; Hites, R. A. Temporal trends in gas-phase concentrations of chlorinated pesticides measured at the shores of the Great Lakes. *Environ. Sci. Technol.* **1998**, *32*, 1920-1927.

Dearth, M. A.; Hites, R. A. Complete analysis of technical chlordane using negative ionization mass spectrometry. *Environ. Sci. Technol.* **1991**, *25*, 245-254.

Denissenko, M. F.; Pao, A.; Tang, M.-S.; Pfeifer, G. P. Preferential formation of benzo[a]pyrene adducts at lung cancer mutational hotspots in P53. *Science* **1996**, *274*, 430-432.

Ebert, L. B. *Polynuclear aromatic compounds*. American Chemical Society, Washington, D.C., 1988.

Franz, T. P.; Eisenreich, S. J. Snow scavenging of polychlorinated biphenyls and polycyclic aromatic hydrocarbons in Minnesota. *Environ. Sci. Technol.* **1998**, *32*, 1771-1778.

Fowlie, P. *Integrated Atmospheric Deposition Network (IADN) Interlaboratory Comparison for Pesticides, Polychlorinated Biphenyls and Polynuclear Aromatic Hydrocarbons in air and particulate samples, revision 2*; Cornerstone Science: Burlington, Ontario, 2002.

Galarneau, E.; Audette, C. V.; Bandemehr, A.; Basu, I.; Bidleman, T. F.; Brice, K. A.; Burniston, D. A.; Chan, C. H.; Froude, F.; Hites, R. A.; Hulting, M.L; Neilson, M.; Orr, D.; Simcik, M. F.; Strachan, W. M. J.; Hoff, R. M. *Atmospheric Deposition of Toxic Substances to the Great Lakes: IADN Results through 1996, Environmental Canada and The U.S. Environmental Protection Agency,* 2000.

Gigliotti, C. L.; Totten, L. A.; Offenberg, J. H.; Dachs, J.; Reinfelder, J. R.; Nelson, E. D.; Glenn IV, T. R.; Eisenreich, S. J. Atmospheric concentrations and deposition of polycyclic aromatic hydrocarbons to the Mid-Atlantic east coast region *Environ. Sci. Technol.* **2005**, *39*, 5550-5559.

Hafner, W. D.; Hites, R. A. Potential sources of pesticides, PCBs, and PAHs to the atmosphere of the Great Lakes. *Environ. Sci. Technol.* **2003**, *37*, 3764-3773.

Harner, T.; Shoeib, M.; Diamond, M.; Stern, G.; Rosenberg, B. Using passive air samplers to assess urban-rural trends for persistent organic pollutants. 1. polychlorinated biphenyls and Organochlorine pesticides. *Environ. Sci. Technol.* **2004**, *38*, 4474-4483.

Harris, M.L.; Van den Heuvel, M.R.; Rouse, J.; Martin, P.A.; Struger, J.; Bishop, C.A.; Takacs, P. *Pesticides in Ontario: A Critical Assessment of Potential Toxicity of Agricultural Products to Wildlife, with Consideration for Endocrine Disruption. Volume 1: Endosulfan, EBDC fungicides, Dinitroaniline herbicides, 1,3-Dichloropropene, Azinphos-methyl, and pesticide mixtures*. Technical Report Series No.340. Canadian Wildlife Service, Ontario Region. 2000.

Hoff, R. M.; Strachan, W. M. J.; Sweet, C. W.; Chan, C. H.; Shackleton, M.; Bidleman, T. F.; Brice, K. A.; Burniston, D. A.; Cussion, S.; Gatz, D. F.; Harlin, K.; Schroeder, W. H. Atmospheric deposition of toxic chemicals to the Great Lakes: a review of data through 1994, *Atmos. Environ*. **1996**, *30*, 3505-3527

Hoh, E.; Hites, R. A. Sources of toxaphene and other organochlorine pesticides in North America as determined by air measurements and potential source contribution function analyses. *Environ. Sci. Technol.* **2004**, *38*, 4187-4194.

Iwata, H.; Tanabe, S.; Sakai, N.; Tatsukawa, R. Distribution of persistent organochlorines in the oceanic air and surface seawater and the role of ocean on their global transport and fate. *Environ. Sci. Technol.* **1993**, *27*, 1080-1098.

Junk, G. A.; Ford, C. S. A review of organic emissions from selected combustion process. *Chemospere* **1980**, *9*, 187-230.

Li, Y.-F.; Struger, J.; Waite, D.; Ma, J. Gridded Canadian lindane usage inventories with 1/6 º × 1/4 º latitude and longitude resolution. *Atmos. Environ*. **2004**, *38*, 1117-1121.

Poor, N.; Tremblay, R.; Kay, H.; Bhethanabotla, V.; Swartz, E.; Luther, M.; Campbell, S. Atmospheric concentrations and dry deposition rates of polycyclic aromatic hydrocarbons (PAHs) for Tampa Bay, Florida, U.S.A. *Atmos. Environ*. **2004**, *38*, 6005-6015.

Ranson, H.; Jensen, B.; Wang, X.; Prapanthadara, L.; Hemingway, J.; Collins, F. H. Genetic mapping of two loci affecting DDT resistance in the malaria vector anopheles gambiae. *Insect Mole. Biol*. **2000**, *9*, 499–507.

Simcik, M. F.; Eisenreich, S. J.; Lioy, P. J. Source apportionment and source/sink relationships of PAHs in the coastal atmosphere of Chicago and Lake Michigan. *Atmos. Environ*. **1999**, *33*, 5071-5079.

Technical Summary of Progress under the Integrated Atmospheric Deposition Program 1990-1996; U.S./Canada IADN Steering Committee, 1997.

Technical Summary of Progress of Integrated Atmospheric Deposition Network (IADN) 1997-2002; U.S./Canada IADN Steering Committee, 2002.

http://www.epa.gov/pcb/, accessed on April 13, 2006.

Willett, K. L.; Ulrich, E. M.; Hites, R. A. Differential toxicity and environmental fates of hexachlorocyclohexane isomers. *Environ. Sci. Technol.* **1998**, *32*, 2197-2207.

Appendix A. Temporal and Spatial Trend Analysis Procedure

The vapor phase concentrations of the organic substances (in pg/m^3) were first converted to partial pressures (P, in atm) using the ideal gas law. These partial pressures were then adjusted to the reference temperature of 288 K using equation 1, where ΔH is a characteristic phase-transition energy of the compound (in kJ/mol), R is the gas constant, and T is the daily average atmospheric temperature at the sampling site (in Kelvin). This procedure effectively "temperature-corrects" the data so that temporal trends can be detected. Concentrations of many semivolatile organic compounds such as those measured by IADN are often higher in the summer due to increased volatilization from soils. The value of ΔH was determined by a preliminary regression of ln(P) vs. 1/T, which is the Clausius-Clapeyron equation (equation 2). An example of the correlation between ln(P) and 1/T is given in Figure A1a. The values of ln(P_{288}) were then regressed vs. time (t, in Julian days relative to January 1, 1990) using equation 3 to determine the rate (a_1, in days^{-1}) of exponential increase ($a_1 > 0$) or decrease ($a_1 < 0$) of these partial pressures. If this rate was statistically significant ($p < 0.05$), these rates were then converted to half-lives ($t_{1/2,}$ in years) by dividing the values into the ln(2)/365 for each compound at each site. Figure A1b shows an example of a decreasing trend based on the above analysis.

$$\ln P_{288} = \ln P - \frac{\Delta H}{R}\left(\frac{1}{288} - \frac{1}{T}\right) \tag{1}$$

$$\ln P = -\frac{\Delta H}{R}\left(\frac{1}{T}\right) + const \tag{2}$$

$$\ln P_{288} = a_0 + a_1 t \tag{3}$$

Equation 4 was used to fit the concentrations (C) in the particle phase:

$$\ln C = b_0 + b_1 t + b_2 \sin\left(\frac{t}{b_3} + b_4\right) \tag{4}$$

where t is the time in Julian Days relative to January 1 1990, b_0 is the intercept (unitless), b_1 is a first-order rate constant (in days^{-1}) describing the rate of exponential decrease or increase over time, b_2 is the periodic amplitude (unitless), b_3 is the length of the period (in days), and b_4 is the periodic offset (in days). An example of particle-phase concentration temporal trend analysis is shown in Figure A2.

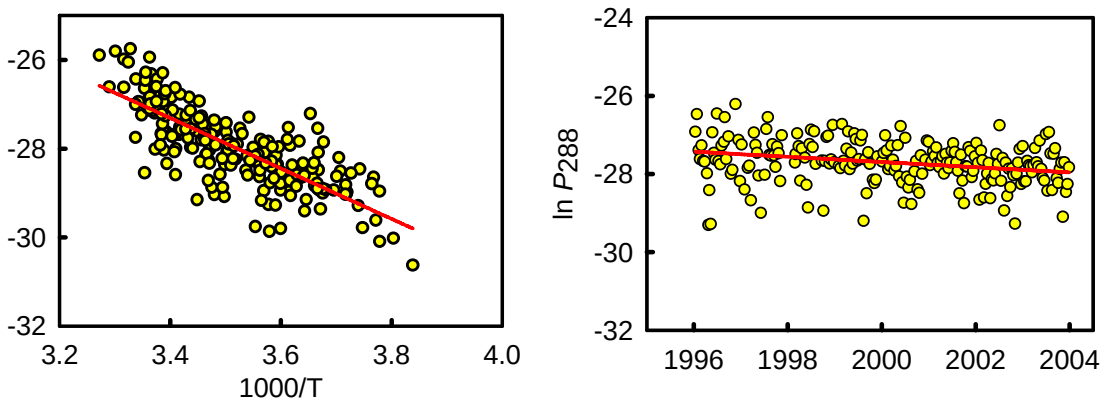

Figure A1a Figure A1b

Figure A1. Example of a temporal trend analysis for vapor phase concentration. Figure A1a, correlation between ln*P* and 1/*T*; Figure A1b, correlation between $\ln P_{288}$ and time (*t)*. Each yellow dot is the partial pressure of a vapor phase sample; the red line indicates the linear correlation (example is fluoranthene at Chicago, r^2=0.64).

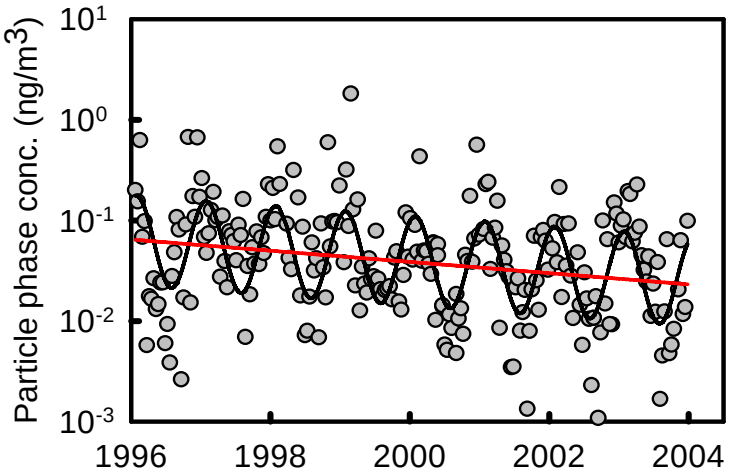

Figure A2. Example of temporal trend analysis for particle phase concentration. Each gray dot is the concentration in the particle phase; the red line indicates long-term significant decreasing trend; the black curve is the fitted line of the sinusoidal model with the period length (b_3) set to one year (example is chrysene at Point Petre, r^2=0.40).

To establish the dates of maximum concentrations, the ratio between the highest concentration and the lowest concentration in the particle or precipitation samples can be calculated from the fitted b_2 parameter (equation 4) by taking its anti-logarithm (e^{2b_2}, the factor of 2 in the exponent is needed to calculate the peak-to-valley amplitude). The sine wave would have a maximum at day 91 in a year. Therefore, the dates of the maximum of concentrations were calculated by first

converting the fitted b_4 values from radians to days (multiplying by $365/2\pi$) and then subtracting these values from 91.

Similarly, equation (4) was also used to explain the temporal trend of the concentrations in precipitation samples, where C is the concentration of organic compounds in precipitation phase. Figure A3 gives an example of a temporal trend analysis in precipitation. Obviously, the fitting parameters will be different for the particle and precipitation phases.

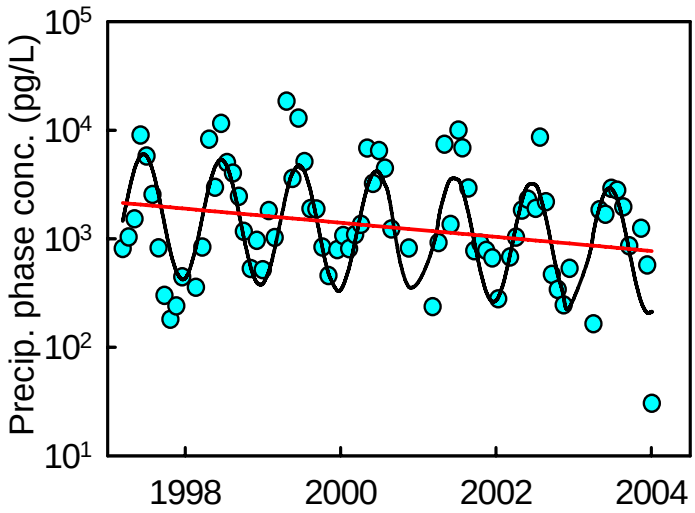

Figure A3. Example of a temporal trend analysis for precipitation phase concentration. Each blue dot is the concentration in precipitation samples, the red line indicates the long-term significant decreasing trend; the black curve is the fitted line of the sinusoidal model with the period length (b_3) set to one year (example is β-endosulfan at Point Petre r^2=0.52).

A one-way analysis of variance (ANOVA) was conducted to compare the average concentrations of each organic compound in each phase among the seven sites to explore spatial trend. A significance level of 0.05 was chosen for all the ANOVA analysis.

Appendix B. Annual Variation of Polycyclic Aromatic Hydrocarbon Concentrations in Precipitation Collected near the Great Lakes

Published in *Environmental Science & Technology*, **2006**, *40*, 696-701.

Annual Variation of Polycyclic Aromatic Hydrocarbon Concentrations in Precipitation Collected near the Great Lakes

Ping Sun,[1] Sean Backus,[2] Pierrette Blanchard,[2] and Ronald A Hites∗[1]

[1]School of Public and Environmental Affairs
Indiana University
Bloomington, Indiana, 47405 USA

and
[2]Environment Canada
4905 Dufferin Street
Toronto, ON M3H 5T4 Canada

∗Corresponding Author Email: hitesr@indiana.edu

Brief

At seven sites around the Great Lakes, concentrations of polycyclic aromatic hydrocarbons in precipitation from 1997 to 2003 were analyzed for temporal and spatial trends.

Abstract

Polycyclic aromatic hydrocarbon (PAH) concentrations were measured in precipitation samples collected from 1997 to 2003 at seven sites near the Great Lakes as a part of the Integrated Atmospheric Deposition Network (IADN). The 28-day integrated concentrations of most PAHs showed significant seasonal trends with higher concentrations in the winter and lower concentrations in the summer. Long-term decreasing trends were observed for all PAHs measured in precipitation at Chicago. At the sites on Lakes Superior, Michigan, and Erie, most PAHs did not show significant long-term trends. At the two Canadian sites on Lakes Huron and Ontario, lower molecular weight PAHs (e.g. fluorene to pyrene) showed long-term decreasing trends; however, no long-term trends were observed for higher molecular weight PAHs at these sites. Interestingly, retene, a marker for wood burning, showed increasing trends at the sites on Lakes Superior and Michigan. For all the other PAHs, precipitation collected at Chicago had by far the highest PAH concentrations followed by the site on Lake Erie. Generally, the Lake Superior sites had the lowest PAH concentrations. However, retene concentrations in precipitation collected at the Lake Superior site were higher compared to Lakes Michigan and Erie, which indicate more residential wood burning in the far north of the Great Lakes basin.

Introduction

Established in 1990, the Integrated Atmospheric Deposition Network (IADN) is a joint project operated by the United States and Canada. IADN operates five master sampling sites on the shores of the five Great Lakes to study the atmospheric input of toxic organic compounds to this important ecosystem (*1*). The concentrations of polychlorinated biphenyls (PCBs), organochlorine (OC) pesticides, and polycyclic aromatic hydrocarbons (PAHs) have been measured in the air and precipitation collected at these sites since 1990. Several previous publications have focused on the long-term trends of PCB, pesticide and PAH concentrations in

the gas phase at the IADN sites (*2-5*), and these results indicate that most of these concentrations are decreasing with half-lives on the order of 3-8 years.

Analysis of the concentration trends of these pollutants in the precipitation phase collected at the IADN sites has been more limited. Chan and co-workers studied OC pesticides and PCBs in rain and snow collected in Ontario, Canada, and reported decreasing concentrations of lindane and dieldrin over the period of 1986-1991 (*6*). Chan and co-workers also investigated spatial and temporal trends in the concentrations of selected OC pesticides and PAHs in precipitation collected at several Canadian sites from 1986 to 1999 (*7*). OC pesticide concentrations decreased over this time period; however, there were few changes in the concentrations of four PAHs (phenanthrene, fluoranthene, pyrene, and 2-methylnaphthalene). Simcik and co-workers reported on the temporal trends of PCBs, PAHs, and several OC pesticides in precipitation samples collected from the IADN sites from 1991 to 1997 (*8*). Their results showed that the concentrations of many OC pesticides decreased during this sampling period; however, there was no significant decrease in the concentrations of PAHs. The annual variations of OC pesticide concentrations at the U.S. IADN sites collected from 1997 to 2002 were studied by Carlson and co-workers (*9*). In this case, the concentrations of most OC pesticides did not decrease over time but showed clear seasonality. Higher concentrations were observed in the late spring or early summer for current-use pesticides, a phenomenon related to their agricultural use at this time of year. On the contrary, higher concentrations were observed in the winter for most of the banned pesticides, which is likely the result of the increased scavenging efficiency of snow compared to rain, and for some pesticides such as dieldrin, higher concentrations in the particulate phase during winter (*9*).

PAHs, however, are byproducts of incomplete combustion and thus come from vehicle emissions, space heating, and industrial activity (*10*). Some of these sources are more or less constant throughout the year (vehicle emissions, for example), but others tend to maximize during the winter months (space heating, for example). Therefore, the annual variations in PAH atmospheric concentrations will likely be different from those of pesticides and PCBs.

In this paper, the temporal and spatial trends of PAH concentrations in precipitation at the five U.S. IADN sites and at the two Canadian IADN sites will be presented. Although samples had been collected at several sites since 1991, the analytical method changed in March of 1997 for the U.S. sites (*9*). To ensure data consistency, only data from March 1997 to December 2003 are presented here.

Experimental

Samples were collected at the five U.S. IADN sites (Brule River and Eagle Harbor, near Lake Superior; Chicago and Sleeping Bear Dunes, near Lake Michigan; and Sturgeon Point, near Lake Erie) and at two the Canadian sites (Burnt Island, near Lake Huron; and Point Petre, near Lake Ontario). The IADN website (www.smc-msc.ec.gc.ca/iadn) and a previous publication (*1*) provide detailed information on these sites.

MIC automated wet-only samplers (MIC Co., Thornhill, ON) are used to collect precipitation samples at the five U.S. sites. Detail information on the performance of this sampler was given by Carlson and co-workers (*9*). Each sampler consists a 46 × 46 cm shallow stainless steel funnel connected to a 30 cm long by 1.5 cm i.d. glass column (ACE Glass, Vineland, NJ) packed with XAD-2 resin. The sampler is normally covered; the start of a precipitation event is sensed by a conductivity grid located outside the sampler, which signals the cover to open. The grid is heated to prevent condensation, ice build-up, and prolonged sampling

after the end of the precipitation event. Precipitation flows from the funnel through the XAD-2 column and into a large carboy used to measure the total precipitation volume. Since there is no filter in the system, both particulate and dissolved phase organic compounds are collected on the XAD column. The funnel and the interior of the sampler are kept at 15 ± 5 ºC to melt snow that falls into the sampler and to prevent the XAD resin column from freezing. Precipitation events are integrated for 28 days regardless of the amount of precipitation occurring during that time. This strategy results in 13 samples per year, but for simplicity, these samples are referred to as monthly samples. In addition, gas and particle phase samples are also collected at the IADN sites for 24 h every 12 days using modified Anderson high-volume air samplers. Detailed information on the sampling procedures for the gas and particle phases is given by Basu and co-workers (*11*).

For the U.S. sites, the wet XAD-2 cartridges were sent to Indiana University for analysis of the pesticides, PAHs, and PCBs. The analytical procedures are described in detail elsewhere (*12, 13*). Briefly, the XAD-2 resin was Soxhlet extracted for 24 h using a 1:1 (v/v) mixture of hexane and acetone. The extract was then concentrated by rotary evaporation and fractionated on 3.5% (w/w) water-deactivated silica gel. Hexane was first used to elute PCBs and some pesticides. PAHs were then eluted with 1:1 hexane and dichloromethane. The extracts were further concentrated by nitrogen blow-down to ~1 mL and spiked with d_{10}-anthracene, d_{12}-perylene, and d_{12}-benz[*a*]anthracene as internal standards.

The PAHs were quantitated on one of three instruments: a Hewlett-Packard (HP) 5890 gas chromatograph (GC) with a 5970A mass spectrometer (MSD); a HP 5890 GC with a 5895 MSD; or an Agilent 6890 GC with a 5973 MSD. In all cases, selected ion monitoring was used. Sixteen PAHs were measured: fluorene, phenanthrene, anthracene, fluoranthene, pyrene, retene, benz[*a*]anthracene, triphenylene and chrysene (not resolved chromatographically, counted as one compound), benzo[*b*]fluoranthene, benzo[*k*]fluoranthene, benzo[*e*]pyrene, benzo[*a*]pyrene, indeno[*1,2,3-cd*]pyrene, benzo[*ghi*]perylene, dibenz[*a,h*]anthracene, and coronene. In all cases, DB-5 columns (J & W Scientific; 30 m × 250 μm i.d.; film thickness, 0.25 μm) were used to separate the PAHs.

The detailed sampling and analytical procedure at the two Canadian sites is given by Chan and coworkers (*7*). Briefly, a 4-L amber glass bottle, pre-filled with 250 mL dichloromethane, was used for precipitation sampling in a MIC automated wet-only sampler. In this case, an XAD-filled column was not used. The liquid samples, consisting of the rain or snow-melt water and the dichloromethane, were sent to the National Laboratory for Environmental Testing (NLET) in Burlington for analysis. The samples were kept at 4 °C until analyzed. The aqueous phase was separated from the dichloromethane using a separatory funnel, and the precipitation volume was measured. The residual aqueous sample was then extracted twice with fresh dichloromethane. The combined extracts were then concentrated by rotary evaporation and fractionated on 3% (w/w) water-deactivated silica gel. Hexane was first used to elute PCBs, some pesticides, and some PAHs. The remaining pesticides and PAHs were then eluted with 1:1 hexane and dichloromethane. The extracts were further concentrated by nitrogen blow-down to ~1 mL. Equal amounts of the two fractions were combined and spiked with d_{10}-anthracene, d_{12}-perylene, and d_{12}-benz[*a*]anthracene as internal standards.

The PAHs were quantitated on one of two instruments: a HP 5890 GC with a 5971 MSD; or an Agilent 6890 GC with a 5973 MSD. In all cases, selected ion monitoring was used. The same list of PAHs described above was measured with the exception of retene and coronene. Perylene was also measured at these two sites. HP5-MS columns (Agilent; 25 m × 250 μm i.d.;

film thickness, 0.25 μm) were used to separate the PAHs. In this paper, the so-called "total PAH" concentration is the sum of the 14 PAHs measured by both laboratories. Prior to 2001, precipitation samples at the Canadian sites were collected every 14 days; this frequency was switched to 28 days at that time. Thus, the Canadian data before 2001 were combined into 28-day averages to make these data consistent with the U.S. data.

Strict quality assurance procedures were followed by both laboratories to ensure high data quality (*14*). Field blanks account for 10% and laboratory blanks account for 5% of the number of collected samples. At Indiana University, PAH standards prepared in the laboratory were spiked on XAD-2 resin as matrix spikes to monitor extraction efficiency. One matrix spike experiment was performed with every other batch of samples (about 10-12 samples per batch). The average matrix spike recovery rates ranged from 60-103% for 14 PAHs. Surrogate standards (d_{10}-phenanthrene and d_{10}-pyrene) were used in each sample to monitor recovery. The average percent recoveries for the surrogates were 83-89% (*14*). Surrogate spikes of 1,3-dibromobenzene and endrin-ketone were added to determine recovery efficiencies at NLET. In this case, the surrogate spike recoveries were 82-92% (*7*). Due to the very low PAH concentrations in the field and laboratory blanks (*14*), usually less than the instrumental detection limit, the concentrations reported here have not been blank corrected. A split-sample inter-laboratory comparison was conducted in early 2001 to evaluate the results from the two participating laboratories (*15*). The results showed that there was no bias between the Indiana University and NLET laboratories for PAHs concentrations.

Results and Discussion

Temporal trends. Our previous experience with IADN data suggested that a sinusoidal model would provide a good fit to the log-transformed data for PAH concentrations in precipitation (*9*). Therefore, the monthly concentrations (C_p) of a given PAH in precipitation collected at a given site were fitted by the following time-dependent function:

$$\ln C_p = a_0 + a_1 t + a_2 \sin\left(\frac{t}{a_3} + a_4\right) \quad (1)$$

where t is the time in Julian Days relative to January 1 1990, a_0 is the intercept (unitless), a_1 is a first-order rate constant (in days^{-1}) describing the rate of exponential decrease or increase over time, a_2 is the periodic amplitude (unitless), a_3 is the length of the period (in days), and a_4 is the periodic offset (in days).

Of the overall 117 datasets (16 PAH measured at five U.S. sites, 15 PAH measured at two Canadian sites, and total PAHs at each site), 105 had significant periodicity, indicated by both a_2 and a_3 being statistically significant at $P < 0.05$. The lack of significant periodicity of the other 12 data sets was due to insufficient data for certain PAH (e.g. anthracene and dibenz[*a,h*]anthracene) at remote sites. If a_1 was significant ($P < 0.05$), either a decreasing ($a_1 < 0$) or increasing ($a_1 > 0$) trend in the PAH concentrations could be determined for this sampling period. Because 74 of the 105 datasets had a period length (a_3) of 368 ± 12 days, the period length for all datasets was forced to be 365 days; this simplified the calculation of the date during the year when the PAH concentrations reached their maximum.

Figure B1 shows the temporal trends of phenanthrene, pyrene, retene, benzo[*a*]pyrene, and total PAH concentrations at the seven sites. For most PAHs, no significant long-term trends were observed at the U.S. rural sites: Brule River, Eagle Harbor, and Sleeping Bear Dunes. In contrast, all measured PAHs showed significant decreasing trends at the urban site in Chicago. Among the individual PAHs, phenanthrene, pyrene, and benzo[*a*]pyrene showed the same trends

as the total PAH at the U.S. sites. Retene, however, showed significantly increasing trends at Brule River, Eagle Harbor, and Sleeping Bear Dunes, and a significant decreasing trend at Chicago. At the two Canadian sites, Burnt Island and Point Petre, lower molecular weight PAHs (e.g. fluorene, phenanthrene, fluoranthrene and pyrene) showed long-term decreasing trends. However, the high molecular weight PAHs (e.g. larger than pyrene) did not show long-term trends (see Table BS6-BS7). For the other PAH concentrations not plotted in Figure B1, two datasets at the U.S. sites showed statistically significant trends: fluorene increased at Brule River, and coronene decreased at Sleeping Bear Dunes (see Tables BS1-BS5). The calculated half-lives of PAH concentrations in precipitation at Chicago ranged from 2-5 years (see Table BS5), while the half-lives ranged from 4-7 years at Burnt Island and Point Petre for the lower molecular weight PAHs (see Tables BS6-BS7).

Previous work by Simcik and coworkers showed that there were no apparent long-term trends for total PAH concentrations in precipitation at Eagle Harbor, Sleeping Bear Dunes, or Sturgeon Point from 1991 to 1997 (*8*). The data reported here cover the period 1997-2003, and no trends in the total PAH concentrations were observed over this period at these sites. Long-term trends of PAH concentrations in precipitation at Brule River and Chicago have not been reported before. Brule River is located on the south shore of Lake Superior, ~230 km west of Eagle Harbor. Because concentrations of almost all of the IADN analytes in the gas, particle, and precipitation phases were similar at Eagle Harbor and Brule River (*16*), the Brule River site was closed in 2002. Given the observed similarity of PAH concentrations at Brule River and Eagle Harbor, we would expect to see a similar long-term trend in these concentrations. In fact, we observe no change in the concentrations of any of the PAH except retene at these two sites (see Figure B1).

Another study on PAH concentrations in precipitation at rural sites was conducted by Brun and coworkers, who measured the concentrations of 16 PAHs at five sites close to the Gulf of St. Lawrence (*17*). Over the period 1980-2001, these authors reported an apparent long-term decreasing trend at one of their sampling sites; in this case, the concentrations decreased with a half-life of 4-6 years. Interestingly, long-term decreasing trends were also observed at two Canadian IADN sites for lower molecular weight PAHs (MW ≤ 202) with half-lives of 4-7 years (see Figure B1). The differences in trends observed by Brun and coworkers compared to our study are likely due to geographical and source differences. Also, the longer database covering a 20 year period in the work by Brun and co-workers compared to our seven year period may contribute to the differences in the long-term trend analyses.

The concentrations of all PAHs decreased significantly over the period 1997-2003 at Chicago; see Table BS5. According to the Illinois EPA (*18*), air quality (e.g. ozone and particulate matter) in Chicago has been improving ever since the passage of the 1970 Clean Air Act. Much of the progress to date is the result of a nationwide commitment to cleaner air, including improved petroleum fuels, automobile engines, and industrial pollution control technology. For example, the Clean Cities Program has promoted the use of alternative fuels and alternative fuel vehicles to reduce air pollution from motor vehicles since 1998. The diesel retrofit portion of the program involves installing devices that lower emissions by over 90% on Chicago's bus fleet. These efforts on improving air quality in Chicago may explain the continuous decrease of PAH concentrations in precipitation and a faster decline (i.e. shorter half-life) compared to the two rural sites in Canada: Burnt Island and Point Petre.

Higher PAH concentrations in precipitation during the winter have been observed by many researchers (*7, 19-21*). Brun and coworkers suggested that anthropogenic activities, such

as thermal power generation, home heating, and industrial activities, could explain the high PAH concentration in the winter close to the Gulf of St. Lawrence (*19*). Chan and co-workers suggested that the increased use of wood and gas fireplaces during the colder months may lead to higher PAH concentrations in the Canadian Great Lakes region (*7*). In addition, snow has been reported to be 25-900 times better than rain at scavenging particle associated PAHs (*22*). This higher scavenging efficiency may result in higher PAH concentrations in precipitation during the winter. The lower intensity of sunlight, the consequently lower concentration of OH radicals, and less efficient photochemical decomposition favors the accumulation of PAHs in the atmosphere, and these factors may also contribute to the higher PAH concentrations observed in precipitation in the winter (*10*).

The calculated dates on which the PAH concentrations in precipitation maximize at each of the IADN sites are listed in the supplementary information (see Tables BS1-BS7). PAH concentrations usually peaked in mid to late January at Eagle Harbor, Burnt Island, and Point Petre and in early to late February at Brule River, Sleeping Bear Dunes, and Sturgeon Point. In Chicago, the PAH concentrations usually peaked in early March, although eight of the results were not significant at $P < 0.05$. The time of peak PAH concentration at the IADN sites showed a slight north to south gradient. Presumably, this is the result of earlier seasonal use of fuel (and hence PAH production) for domestic and industrial heating in cooler climates.

The ratio between the highest PAH concentration during winter time and the lowest concentration during summer time can be calculated from the fitted a_2 parameter by taking its anti-logarithm (e^{2a_2}, the factor of 2 in the exponent is needed to calculate the peak-to-valley amplitude). These values are presented in Tables aS1-AS7. These ratios range between about 3-9, agreed well with other studies (*17, 23*), indicating that these seasonal variations are substantial.

Spatial trends of PAH concentrations in precipitation. Figure B2 shows the distribution of total PAH concentrations at the seven IADN sites. The concentration of total PAHs was the highest at Chicago followed by Sturgeon Point. The concentrations of PAHs were significantly higher at Sturgeon Point than at Sleeping Bear Dunes [$F = 34.01$, $P < 0.0001$, and df = (1, 166)]. As expected, Brule River and Eagle Harbor showed statistically indistinguishable PAH concentrations [$F = 0.11$, $P = 0.74$, and df = (1, 148)], but these concentrations were significantly lower than the PAH concentrations measured at Sleeping Bear Dunes [$F = 7.12$, $P = 0.001$, and df = (2, 230)]. The two Canadian sites, Burnt Island and Point Petre had similar PAH concentrations [$F = 2.02$, $P = 0.15$, and df = (1, 159)], but these concentrations were lower than at Sturgeon Point [$F = 3.95$, $P = 0.02$, and df = (2, 243)] and higher than at Sleeping Bear Dunes [$F = 6.23$, $P = 0.002$, and df = (2, 241)]. Thus, the spatial trend of total PAH concentration in precipitation is: Eagle Harbor ≈ Brule River < Sleeping Bear Dunes < Burnt Island ≈ Point Petre < Sturgeon Point << Chicago. Each individual PAH had the same spatial trend as the total PAHs with a few exceptions. For example, for fluorene, Eagle Harbor > Brule River and Burnt Island ≈ Point Petre ≈ Sturgeon Point; for anthracene, Eagle Harbor ≈ Sleeping Bear Dunes; and for retene, Sleeping Bear Dunes ≈ Sturgeon Point < Eagle Harbor ≈ Brule River < Chicago.

The average total PAH concentrations at the six rural IADN sites ranged from 26 to 90 ng/L, which are similar to PAH concentrations in precipitation collected at rural locations as reported in other studies (*17, 21*). The high total PAH concentration at Chicago (a mean concentration of 2300 ± 620 ng/L) is not surprising given that Chicago is a highly industrialized city with approximately 8 million inhabitants.

Among the individual PAHs, fluoranthene and phenanthrene are the most abundant, each making up about 15-25% of the total PAH concentration. The other abundant PAHs include pyrene and benzo[*b*]fluoranthene; these observations agree with other studies (*20, 21*). Generally, the relative abundances of the individual PAH are similar at the remote sites (Brule River, Eagle Harbor, Sleeping Bear, Burnt Island, and Point Petre) and at the more urban or urban-influenced sites (Chicago and Sturgeon Point). These differences in the relative abundances at the rural vs. the more urbanized sites suggest that different sources of PAHs affect these sites. For example, the major sources of PAHs in and around Chicago are vehicle emissions, coal and natural gas combustion, and coke production (*24*). The major PAH sources at Sturgeon Point are similar to Chicago, but they are located 25 km away in the city of Buffalo, New York (*25, 26*).

Temporal and spatial trends of retene concentrations in precipitation. Retene is formed from abietic acid, which is a natural product mainly found in coniferous trees. Abietic acid can be decarboxylated and aromatized to form retene by the combustion of coniferous wood (*27, 28*) or by slower, low-temperature degradation processes (*29*) (see below). Franz and Eisenreich reported retene concentrations in precipitation ranged from 1.4 to 50 ng/L in the winter in Minnesota in 1991-1992 (*22*). However, temporal and spatial trends of retene concentrations in precipitation have not been reported.

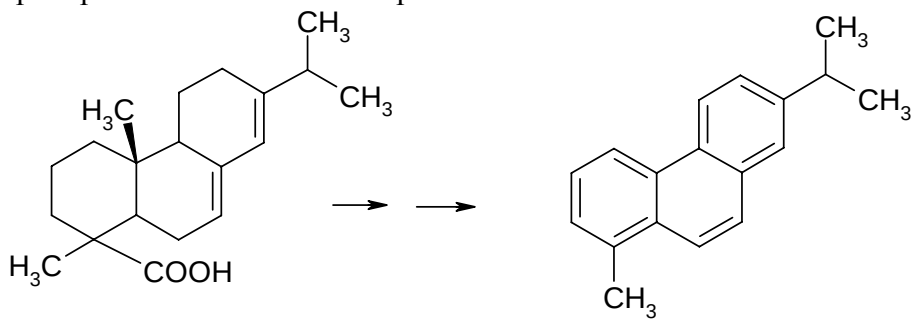

Abietic acid Retene

In this study, retene concentrations in precipitation measured at the five U.S. sites showed similar concentrations as reported by Franz and Eisenreich (*22*). In addition, these data showed some interesting trends compared to other PAHs. As discussed previously, the concentrations of retene increased significantly over time at Brule River, Eagle Harbor, and Sleeping Bear Dunes (see Figure B1), while the concentrations of most other PAH in precipitation at these sites did not show any long-term changes. The increase in retene concentrations suggests that biomass burning, particularly of wood from coniferous trees or synthetic logs (*30*), is increasing perhaps due to an increase of residential fuel wood burning in these rural areas. At Chicago, retene's concentration in precipitation has significantly decreased over time, suggesting that biomass burning in this city has decreased during the last seven years. For example, Chicago's Department of Environment has advocated against the open burning of leaves and other yard waste and against the burning wood in fireplaces (*31*).

As mentioned earlier, retene showed a different spatial trend (Sleeping Bear Dunes ≈ Sturgeon Point < Eagle Harbor ≈ Brule River < Chicago) compared to the other PAHs detected at the five U.S. IADN sites (see Figure B3, top). For the other PAHs, Sturgeon Point had the second highest concentration, but interestingly, the retene concentration at Sturgeon Point is even lower than at Eagle Harbor and Brule River. The average retene concentration at Chicago is

about 5.5 times higher than that at Sturgeon Point, which is a much lower ratio compared to the other PAHs (14-34 times).

These spatial differences in retene concentrations may be due to the different amounts of wood burned in these areas. Based on renewable energy annual reports from the electric power industry, more wood and wood waste are burned in Michigan, Wisconsin, and Minnesota compared to New York and Illinois (*32*). Most residential wood burning occurred in lower southern Michigan and in mid to northern Wisconsin (*33, 34*). Also, forest species composition is different in different regions. More softwood grows in Michigan, Minnesota, and Wisconsin (*35*). Thus, the relatively high retene concentrations at Brule River and Eagle Harbor are reasonable. In Chicago, although wood burning is not advocated by Chicago's Department of Environment, the large population of this region may explain the elevated retene concentration. Retene is also emitted from municipal waste incinerators (*36*), and this may contribute to retene's high concentration in Chicago. In addition, high concentrations of dehydroabietic acid (the partially aromatized product of abietic acid) and abietic acid itself have been found in tire debris (*37*) and in varnishes used for finishing wood in homes and furniture (*38*), which suggests that tire burning and incineration of building wastes may be other retene sources in Chicago.

The fraction of the retene concentration compared to the total PAH concentration at the five U.S. sites is shown in Figure B3, bottom. Here, total PAH is the sum of the 16 PAHs measured by Indiana University. A much lower proportion of retene (relative to total PAH concentration) was observed at Chicago. Sturgeon Point had the second lowest retene proportion, while at the other rural sites (Brule River, Sleeping Bear Dunes, and Eagle Harbor), the retene proportion was higher. These results suggest that biomass burning is less important in urban than in rural locations. This is consistent with a U.S. Department of Agriculture survey on residential wood consumption in the states of Michigan and Wisconsin, which found that most of each state's residential wood consumption took place in the more rural areas (*33, 34*). On average, each rural household consumed about three times more wood than its urban counterpart.

Occasionally, very high retene concentrations were observed at all U.S. sites, and we suspected that these high levels may have been related to forest fires. In order to address this hypothesis, data on wildfire occurrence near the Great Lakes were obtained from the National Interagency Fire Management Integrated Database, which covers fires in the U.S. during the period from 1970 to the present, and from the Canadian Forest Service, which covers fires in Canada during the period of 1959 to the present. These historical records showed that more wildfires occurred from April to September in each year, with most fires occurring in June. This timing does not agree with our observation that most samples with high retene concentrations were collected in either March or November. This difference suggests that wildfires are less of a source of retene than anthropogenic wood or waste burning in the winter.

Acknowledgments

We thank Ilora Basu and Team IADN and Ed Sverko and staff at the National Laboratory for Environmental Testing, Environment Canada for data acquisition; the U. S. Environmental Protection Agency's Great Lakes National Program Office for funding (Grant GL995656, Melissa Hulting, project monitor); Ronald Piva at the North Central Research Stations of the USDA Forest Survey for information on softwood consumption; and Daniel Carlson for suggestions and discussions on the analysis of these data.

Supporting Information Available

The supporting Information contains seven tables of values derived from modeled parameters for PAHs at seven IADN sites. This material is available free of charge via the Internet at http://pubs.acs.org.

Literature Cited

1 Buehler, S. S.; Hites, R. A. The Great Lakes' integrated atmospheric deposition network. *Environ. Sci. Technol.* **2002**, *36*, 354A-359A.

2 Simcik, M. F.; Basu, I.; Sweet, C. W.; Hites, R. A. Temperature dependence and temporal trends of polychlorinated biphenyl congeners in the Great Lakes atmosphere. *Environ. Sci. Technol.* **1999**, *33*, 1991-1995.

3 Strandberg, B.; Dodder, N. G.; Basu, I.; Hites, R. A. Concentrations and spatial variations of polybrominated diphenyl ethers and other organohalogen compounds in Great Lakes air. *Environ. Sci. Technol.* **2001**, *35*, 1078-1083.

4 Buehler, S. S.; Basu, I.; Hites, R. A. Gas-phase polychlorinated biphenyl and hexachlorocyclohexane concentrations near the Great Lakes: An historical perspective. *Environ. Sci. Technol.* **2002**, *36*, 5051-5056.

5 Buehler, S. S.; Basu, I.; Hites, R. A. Causes of variability in pesticides and PCB concentrations in air near the Great Lakes. *Environ. Sci. Technol.* **2004**, *38*, 414-422.

6 Chan, C. H.; Bruce, G.; Harrison, B. Wet deposition of organochlorine pesticides and polychlorinated biphenyls to the Great Lakes. *J. Great Lakes Res.* **1994**, *20*, 546-560.

7 Chan, C. H.; Williams, D. J.; Neilson, M. A.; Harrison, B.; Archer, M. L. J. Spatial and temporal trends in the concentrations of selected organochlorine pesticides (OCs) and polynuclear aromatic hydrocarbons (PAHs) in Great Lakes basin precipitation, 1986 to 1999. *J. Great Lakes Res.* **2003**, *29*, 448-459.

8 Simcik, M. F.; Hoff, R. M.; Strachan, W. M.; Sweet, C. W.; Basu, I.; Hites, R. A. Temporal trends of semi-volatile organic contaminants in Great Lakes precipitation. *Environ. Sci. Technol.* **2000**, *34*, 361-367.

9 Carlson, D. L.; Basu, I.; Hites, R. A. Annual variation of pesticide concentrations in great lakes precipitation. *Environ. Sci. Technol.* **2004**, *38*, 5290-5296.

10 Baek, S. O.; Field, R. A.; Goldstone, M. E.; Kirk, P. W.; Lester, J. N.; Perry, R. A review of atmospheric polycyclic aromatic hydrocarbons: sources, fate and behavior. *Water, Air, Soil Poll*. **1991**, *60*, 279-300.

11 Basu, I.; O'Dell, J. M.; Arnold, K.; Hites, R. A. A source of PCB contamination in modified high-volume air samplers. *Environ. Sci. Technol.* **2000**, *34*, 527-529.

12 Basu, I. *Analysis of PCBs, Pesticides, and PAHs in Air and Precipitation Samples, IADN Project Sample Preparation Procedure; Indiana University*: Bloomington, IN, 1999.

13 Sweet, C.; Harlin, K.; Gatz, D. F.; Bauer, S. *Great Lakes Integrated Atmospheric Deposition Network (IADN) Data Report 1993-1994*; Illinois State Water Survey: Champaign, IL, 1996.

14 Basu, I.; Arnold, K. *Quality Control Report 2003*; Indiana University: Bloomington, IN, 2003.

15 Fowlie, P. *Integrated Atmospheric Deposition Network (IADN) Interlaboratory Comparison for Pesticides, Polychlorinated Biphenyls and Polynuclear Aromatic Hydrocarbons in air and particulate samples, revision 2*; Cornerstone Science: Burlington, Ontario, 2002.

16 Buehler, S. S.; Basu, I.; Hites, R. A. A comparison of PAH, PCB, and pesticide concentrations in air at two rural sites on Lake Superior. *Environ. Sci. Technol.* **2001**, *35*, 2417-2422.
17 Brun, G. L.; Vaidya, O. C.; Leger, M. G**.** Atmospheric deposition of polycyclic aromatic hydrocarbons to Atlantic Canada: geographic and temporal distributions and trends 1980-2001. *Environ. Sci. Technol.* **2004**, *38,* 1941-1948.
18 *Illinois Annual Air Quality Report 2003,* Bureau of Air, Illinois Environmental Protection Agency, Springfield, IL 2004.
19 Brun, G. L.; Howell, G. D.; O'Neill, H. J. Spatial and temporal patterns of organic contaminants in wet precipitation in Atlantic Canada. *Environ. Sci. Technol.* **1991**, *25*, 1249-1261.
20 Kiss, G.; Varga-Puchony, Z.; Tolnai, B.; Varga, B.; Gelencser, A.; Krivacsy, Z.; Hlavay, J. The seasonal changes in the concentration of polycyclic aromatic hydrocarbons in precipitation and aerosol near Lake Balaton, Hungary. *Environ. Pollut.* **2001**, *114*, 55-61.
21 Motelay-Massei, A.; Ollivon, D.; Garban, B.; Chevreuil, M. Polycyclic aromatic hydrocarbons in bulk deposition at a suburban site: assessment by principal component analysis of the influence of meteorological parameters. *Atmos. Environ*. **2003**, *37*, 3135-3146.
22 Franz, T. P.; Eisenreich, S. J. Snow scavenging of polychlorinated biphenyls and polycyclic aromatic hydrocarbons in Minnesota. *Environ. Sci. Technol.* **1998**, *32*, 1771-1778.
23 Hart, K. M.; Tremp, J.; Molnar, E.; Giger, W. The occurrence and the fate of organic pollutants in the atmosphere. *Wat. Air Soil Pollut.* **1993**, *68*, 91-112.
24 Simcik, M. F.; Eisenreich, S. J.; Lioy, P. J. Source apportionment and source/sink relationships of PAHs in the coastal atmosphere of Chicago and Lake Michigan. *Atmos. Environ*. **1999**, *33*, 5071-5079.
25 Cortes, D. R.; Basu, I.; Sweet, C.; Hites, R. A. Temporal trends in and influence of wind on PAH concentrations measured near the Great Lakes. *Environ. Sci. Technol.* **2000**, *34*, 356-360.
26 Hafner, W. D.; Hites, R. A. Potential sources of pesticides, PCBs, and PAHs to the atmosphere of the Great Lakes. *Environ. Sci. Technol.* **2003**, *37*, 3764-3773.
27 Ramdahl, T. Retene-a molecular marker of wood combustion in ambient air. *Nature* **1983**, *306*, 580-582.
28 Schauer, J. J.; Kleeman, M. J.; Cass, G. R.; Simoneit, B. R. T. Measurement of emissions from air pollution sources. 3. C_1-C_{29} organic compounds from fireplace combustion of wood. *Environ. Sci. Technol.* **2001**, *35*, 1716-1728.
29 Laflamme, R. E.; Hites, R. A. The global distribution of polycyclic aromatic hydrocarbons in recent sediments. *Geochim. Cosmochim. Acta* **1978**, *42*, 289-303.
30 Rogge, W. F.; Hlldemann, L. M.; Mazurek, M. A.; Cass, G. R.; Simoneit, B. R. T. Sources of fine organic aerosol. 9. Pine, oak, and synthetic log combustion in residential fireplaces. *Environ. Sci. Technol.* **1998**, *32*, 13-22.
31 Partner for Clean Air program, The Chicago Department of Environment, http://www.cleantheair.org/
32 *Renewable Energy Annual*, Energy Information Administration, U.S. Department of Energy, Washington, DC, 1997-2003.

33 May, D. M.; Weatherspoon, A. K.; Hackett, R. L. *Residential Fuel wood Consumption and Production in Michigan, 1992*, U.S. Department of Agriculture, St. Paul, MN, 1993.
34 May, D. M.; Mace, T. *Residential Fuel wood Consumption and Production in Wisconsin, 1994*, U.S. Department of Agriculture, St. Paul, MN, 1996.
35 Smith, W. B.; Miles, P. D.; Vissage, J. S.; Pugh, S. A. *Forest Resources of the United States, 2002,* U.S. Department of Agriculture, Forest Service, St. Paul, MN, 2004.
36 Besombes, J.-L. M., A.; Patissier, O.; Marchard, N.; Chevron, N.; Stoklov, M.; Masclet, P. Particulate PAHs observed in the surrounding of a municipal incinerator. A*tmos. Environ.* **2001**, *35*, 6093-6104.
37 Rogge, W. F.; Hildemann, L. M.; Mazurek, M. A.; Cass, G. R.; Simoneit, B. R. T. Sources of fine organic aerosol. 3. Road dust, tire debris, and organometallic brake lining dust: roads as sources and sinks. *Environ. Sci. Technol.* **1993**, *27*, 1892-1904.
38 Osete-Cortina, L.; Dom´enech-Carb´, M. T. Analytical characterization of diterpenoid resins present in pictorial varnishes using pyrolysis–gas chromatography–mass spectrometry with on line trimethylsilylation. *J. Chromatog. A* **2005**, *1065*, 265–278.

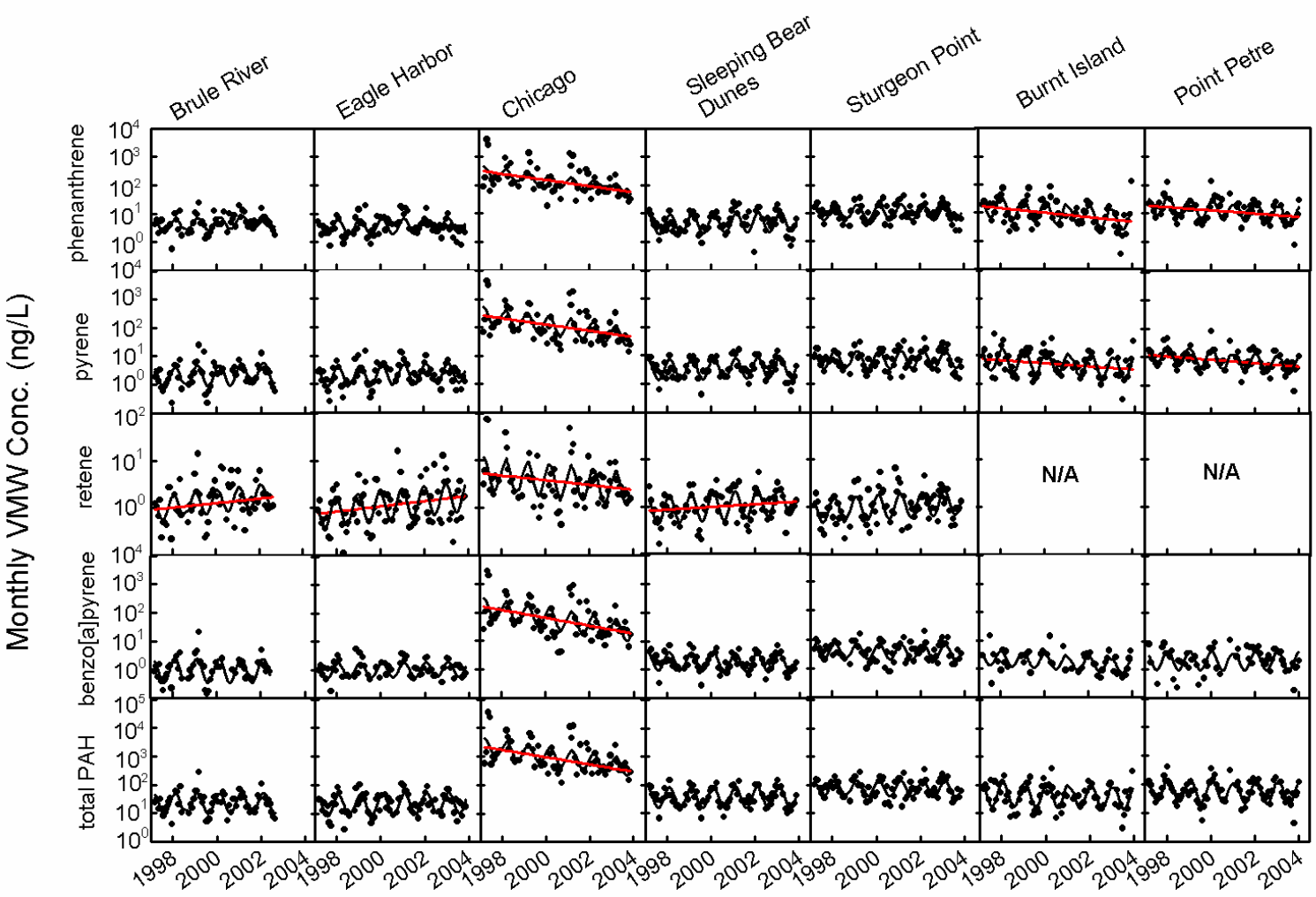

Figure B1. Phenanthrene, pyrene, retene, benzo[*a*]pyrene, and total PAH concentrations in precipitation collected at seven IADN sites near the Great Lakes. The black curve is the fitting line of the sinusoidal model with the period length (a_3) set to one year. The red lines indicate long-term significant decreasing or increasing trends. Detailed information on fitting parameters is in supporting information.

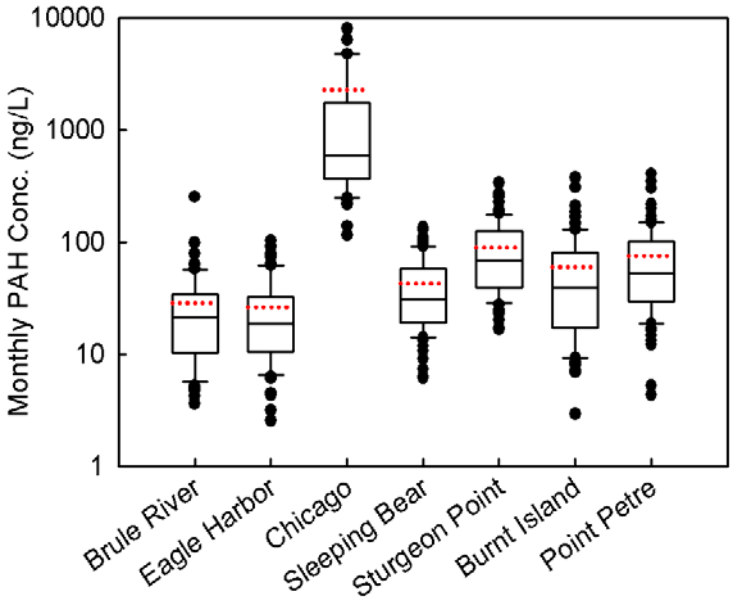

Figure B2. Total PAH concentrations in precipitation at the seven IADN sites. The horizontal lines represent the 10th, 50th, and 90th percentiles; the dotted red line is the mean; the boxes represent the 25th to 75th percentiles; and outliers are shown individually.

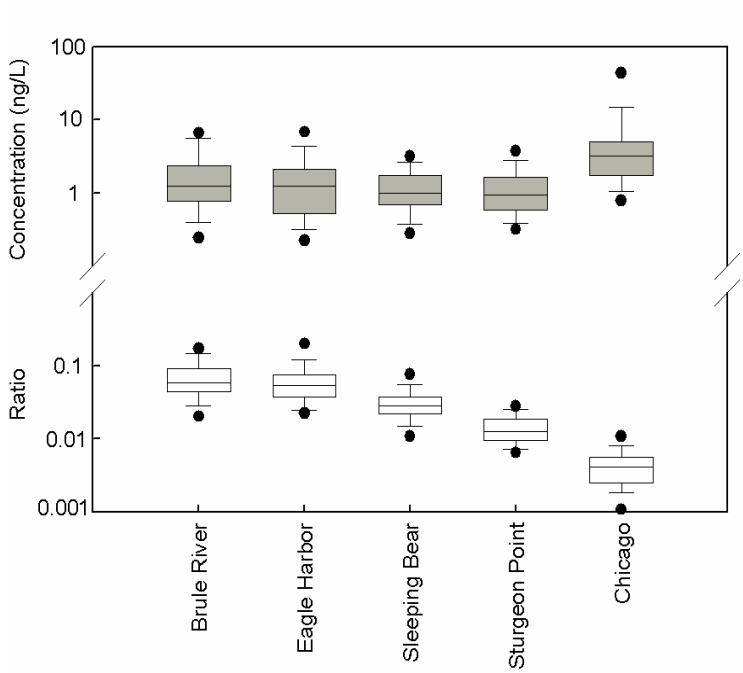

Figure B3. Retene concentrations (top set of boxes) and the ratio between retene and total PAH concentrations (bottom set of boxes) in precipitation collected at the five U.S. IADN sites. Note the logarithmic scales. The horizontal lines represent the 10th, 50th, and 90th percentiles; the boxes represent the 25th to 75th percentiles; and outliers are shown as the 5th and 95th percentiles.

Supporting Information for:

Annual Variations of PAH Concentrations in Precipitation Collected Near the Great Lakes

Ping Sun, Sean Backus, Pierrette Blanchard, and Ronald A Hites

This supporting Information contains seven tables of values derived from modeled parameters for PAHs at seven IADN sites. ΣPAH is the sum of 14 PAHs measured by both Indiana University and National Laboratory for Environmental Testing (NLET) in Burlington. These PAH are fluorene, phenanthrene, anthracene, fluoranthene, pyrene, benz[*a*]anthracene, triphenylene + chrysene (count as one compound), benzo[*b*]fluoranthrene, benzo[*k*]fluoranthrene, benzo[*e*]-pyrene, benzo[*a*]pyrene, indeno[1,2,3-*cd*]pyrene, benzo[*ghi*]perylene, and dibenz[*a,h*]-anthracene.

The following equation was used to fit the data:

$$\ln C_p = a_0 + a_1 t + a_2 \sin\left(\frac{t}{a_3} + a_4\right)$$

where t is the time in Julian Days relative to January 1 1990, a_0 is the intercept (unitless), a_1 is a first-order rate constant (in days^{-1}) describing the rate of exponential decrease or increase over time, a_2 is the periodic amplitude (unitless), a_3 is the length of the period (in days), and a_4 is the periodic offset (in days).

Because 74 of the 105 datasets had a period length (a_3) of 368 ±12 days, the period length for all 105 of these datasets was forced to be one year, which simplified the calculation of the date during the year when the PAH concentrations reached their maximum.

The tables show results of the fit to this sinusoidal model with a_3 of 365 days. The results are listed as mean ± standard error. Normal font numbers are significant for $0.01 < P < 0.05$; italic font numbers are significant for $0.001 < P < 0.01$, bold font numbers are significant at level of $P < 0.001$. "NS" means "not significant at $P > 0.05$. A negative half-life is actually a doubling time.

Table BS1. Fit parameters for PAH concentrations in precipitation at Brule River

PAHs	Half-life (years), (ln2)/365*a_1	Peak-to-valley ratio, e^{2a_2}	Maximum date (± days)	No. of detects	Average conc. (ng/L)	r^2
Fluorene	–6.3 ± 2.1*	**3.1 ± 1.2**	**Feb 11 ± 10**	63	1.0 ± 0.1	0.37
Phenanthrene	NS	**2.8 ± 1.2**	*Feb 14 ± 12*	64	5.7 ± 0.5	0.29
Anthracene	Limited data			23	0.3 ± 0.1	
Fluoranthene	NS	**5.8 ± 1.3**	**Feb 13 ± 7**	64	5.3 ± 0.9	0.51
Pyrene	NS	**5.6 ± 1.3**	**Feb 8 ± 9**	59	3.3 ± 0.5	0.42
Retene	–5.1 ± 2.4*	*3.0 ± 1.4*	**Jan 21 ± 15**	63	2.0 ± 0.3	0.21
Benz[*a*]anthracene	NS	NS	NS	46	0.9 ± 0.2	NS
Triphenylene + chrysene	NS	**7.7 ± 1.3**	**Feb 7 ± 6**	64	2.3 ± 0.3	0.58
Benzo[*b*]fluoranthrene	NS	**9.3 ± 1.3**	**Feb 7 ± 6**	63	3.3 ± 0.6	0.60
Benzo[*k*]fluoranthrene	NS	**4.8 ± 1.4**	**Feb 3 ± 10**	40	1.2 ± 0.1	0.40
Benzo[*e*]pyrene	NS	**6.5 ± 1.3**	**Feb 7 ± 7**	58	1.6 ± 0.2	0.50
Benzo[*a*]pyrene	NS	**7.0 ± 1.4**	**Feb 7 ± 8**	50	1.7 ± 0.4	0.48
Indeno[1,2,3-*cd*]pyrene	NS	**7.4 ± 1.3**	**Feb 5 ± 7**	57	2.3 ± 0.5	0.52
Benzo[*ghi*]perylene	NS	**6.7 ± 1.3**	**Feb 6 ± 7**	58	1.9 ± 0.3	0.52
Dibenz[*a,h*]anthracene	Limited data			10	0.3 ± 0.1	
Coronene	NS	**8.0 ± 1.4**	**Jan 31 ± 8**	35	1.2 ± 0.2	0.53
ΣPAH	NS	**5.3 ± 1.2**	**Feb 8 ± 7**	64	29 ± 4.3	0.39

*A negative half-life indicates that the concentrations are increasing and the listed value is the doubling time.

Table BS2. Fit parameters for PAH concentrations in precipitation at Eagle Harbor

PAHs	Half-life (years), (ln2)/365*a_1	Peak-to-valley ratio, e^{2a_2}	Maximum date (± days)	No. of detects	Average conc. (ng/L)	r^2
Fluorene	NS	**3.3 ± 1.2**	**Jan 30 ± 8**	80	0.8 ± 0.1	0.38
Phenanthrene	NS	**3.5 ± 1.2**	**Jan 31 ± 8**	82	4.7 ± 0.4	0.35
Anthracene	Limited data			20	0.3 ± 0.1	
Fluoranthene	NS	**5.6 ± 1.2**	**Feb 4 ± 6**	82	5.1 ± 0.5	0.51
Pyrene	NS	**5.1 ± 1.2**	**Feb 3 ± 8**	77	3.0 ± 0.3	0.43
Retene	*–5.4 ± 2.0**	**4.3 ± 1.3**	**Dec 28 ± 11**	82	2.0 ± 0.3	0.33
Benz[*a*]anthracene	NS	**5.9 ± 1.3**	**Jan 24 ± 7**	61	0.9 ± 0.1	0.50
Triphenylene + chrysene	NS	**6.0 ± 1.2**	**Jan 24 ± 6**	82	2.2 ± 0.2	0.50
Benzo[*b*]fluoranthrene	NS	**6.4 ± 1.2**	**Jan 29 ± 6**	79	3.1 ± 0.3	0.55
Benzo[*k*]fluoranthrene	NS	**3.8 ± 1.3**	**Jan 20 ± 10**	50	1.4 ± 0.1	0.39
Benzo[*e*]pyrene	NS	**4.2 ± 1.2**	**Jan 26 ± 8**	72	1.6 ± 0.1	0.39
Benzo[*a*]pyrene	NS	**3.3 ± 1.3**	**Jan 21 ± 11**	65	1.4 ± 0.1	0.31
Indeno[1,2,3-*cd*]pyrene	NS	**6.4 ± 1.2**	**Jan 30 ± 6**	74	2.3 ± 2.6	0.54
Benzo[*ghi*]perylene	NS	**4.9 ± 1.2**	**Jan 30 ± 7**	76	1.8 ± 0.2	0.49
Dibenz[*a,h*]anthracene	Limited data			6	0.3 ± 0.1	
Coronene	NS	**5.5 ± 1.3**	**Jan 23 ± 9**	39	1.1 ± 0.1	0.54
ΣPAH	NS	**5.4 ± 1.2**	**Jan 27± 6**	82	26 ± 2.5	0.51

*A negative half-life indicates that the concentrations are increasing and the listed value is the doubling time.

Table BS3. Fit parameters for PAH concentrations in precipitation at Sleeping Bear Dunes

PAHs	Half-life (years), (ln2)/365*a_1	Peak-to-valley ratio, e^{2a_2}	Maximum date (± days)	No. of detects	Average conc. (ng/L)	r^2
Fluorene	NS	**3.4 ± 1.2**	**Feb 11 ± 8**	80	1.3 ± 0.1	0.39
Phenanthrene	NS	**4.9 ± 1.3**	**Feb 17 ± 8**	82	6.3 ± 0.6	0.38
Anthracene	NS	**4.6 ± 1.5**	**Feb 3 ± 7**	45	0.3 ± 0.0	0.52
Fluoranthene	NS	**5.6 ± 1.2**	**Feb 20 ± 7**	83	8.1 ± 0.7	0.46
Pyrene	NS	**5.3 ± 1.2**	**Feb 11 ± 6**	81	4.6 ± 0.4	0.55
Retene	–9.5 ± 4.7*	**3.9 ± 1.2**	**Feb 1 ± 7**	82	1.3 ± 0.1	0.46
Benz[*a*]anthracene	NS	**4.9 ± 1.2**	**Feb 5 ± 6**	76	1.6 ± 0.1	0.59
Triphenylene + chrysene	NS	**4.0 ± 1.2**	**Feb 5 ± 5**	83	3.5 ± 0.3	0.64
Benzo[*b*]fluoranthrene	NS	**6.0 ± 1.2**	**Feb 5 ± 5**	83	5.3 ± 0.5	0.68
Benzo[*k*]fluoranthrene	NS	**4.5 ± 1.2**	**Feb 6 ± 7**	73	1.9 ± 0.2	0.53
Benzo[*e*]pyrene	NS	**4.9 ± 1.2**	**Feb 5 ± 5**	80	2.5 ± 0.2	0.58
Benzo[*a*]pyrene	NS	**4.4 ± 1.2**	**Feb 4 ± 6**	80	2.3 ± 0.2	0.54
Indeno[1,2,3-*cd*]pyrene	NS	**5.1 ± 1.2**	**Feb 1 ± 5**	80	3.6 ± 0.3	0.61
Benzo[*ghi*]perylene	NS	**4.7 ± 1.1**	**Jan 31 ± 5**	81	3.0 ± 0.2	0.62
Dibenz[*a*,*h*]anthracene	Limited data			29	0.5 ± 0.1	
Coronene	*8.2 ± 2.8*	**5.2 ± 1.2**	**Jan 30 ± 6**	65	1.5 ± 0.1	0.64
ΣPAH	NS	**5.3 ± 1.2**	**Feb 5 ± 5**	83	43 ± 3.5	0.64

*A negative half-life indicates that the concentrations are increasing and the listed value is the doubling time.

Table BS4. Fit parameters for PAH concentrations in precipitation at Sturgeon Point

PAHs	Half-life (years) (ln2)/365*a_1	Peak-to-valley ratio, e^{2a_2}	Maximum date (± days)	No. of detects	Average Conc. (ng/L)	r^2
Fluorene	NS	**2.6 ± 1.1**	**Feb 18 ± 7**	85	2.3 ± 1.4	0.43
Phenanthrene	NS	**3.6 ± 1.2**	**Feb 20 ± 7**	85	13 ± 1.0	0.45
Anthracene	NS	**4.3 ± 1.3**	**Feb 10 ± 7**	73	0.7 ± 0.1	0.47
Fluoranthene	NS	**4.0 ± 1.2**	**Feb 12 ± 7**	85	19 ± 1.5	0.45
Pyrene	NS	**4.0 ± 1.2**	**Feb 13 ± 8**	85	9.4 ± 0.8	0.39
Retene	NS	**3.2 ± 1.2**	**Feb 1 ± 9**	83	1.3 ± 0.1	0.34
Benz[*a*]anthracene	NS	**4.0 ± 1.2**	**Feb 16 ± 7**	81	3.4 ± 0.3	0.47
Triphenylene + chrysene	NS	**4.0 ± 1.2**	**Feb 6 ± 8**	85	6.8 ± 0.6	0.43
Benzo[*b*]fluoranthrene	NS	**3.6 ± 1.2**	**Feb 11 ± 8**	85	10 ±0.9	0.36
Benzo[*k*]fluoranthrene	NS	**3.2 ± 1.2**	**Feb 14 ± 8**	82	3.5 ± 0.3	0.37
Benzo[*e*]pyrene	NS	**3.6 ± 1.2**	**Feb 13 ± 7**	84	4.5 ± 0.3	0.41
Benzo[*a*]pyrene	NS	**3.3 ± 1.2**	**Feb 14 ± 8**	84	4.6 ± 0.4	0.35
Indeno[1,2,3-*cd*]pyrene	NS	**3.2 ± 1.2**	**Feb 8 ± 10**	84	6.7 ± 0.6	0.30
Benzo[*ghi*]perylene	NS	**3.5 ± 1.2**	**Feb 8 ± 8**	83	5.3 ± 0.4	0.40
Dibenz[*a*,*h*]anthracene	NS	**2.4 ± 1.2**	*Feb 24 ±11*	65	1.0 ± 0.1	0.27
Coronene	NS	**3.8 ± 1.2**	**Jan 31 ± 7**	81	2.0 ± 0.2	0.46
ΣPAH	NS	**3.5 ± 1.2**	**Feb 10 ± 8**	85	90 ±6.9	0.40

Table BS5. Fit parameters for PAH concentrations in precipitation s at Chicago

PAHs	Half-life (years), (ln2)/365*a_1	Peak-to-valley ratio, e^{2a_2}	Maximum date (± days)	No. of detects	Average conc. (ng/L)	r^2
Fluorene	**3.4 ± 0.8**	**2.0 ± 1.3**	NS	70	36 ± 8.6	0.29
Phenanthrene	**3.0 ± 0.7**	*2.4 ± 1.4*	NS	70	290 ± 72	0.45
Anthracene	**2.0 ± 0.4**	**4.0 ± 1.7**	NS	70	34 ± 8.3	0.38
Fluoranthene	**2.9 ± 0.7**	**3.9 ± 1.1**	**Mar 4 ± 3**	70	480 ± 130	0.49
Pyrene	**2.7 ± 0.6**	**4.2 ± 1.4**	NS	70	290 ± 82	0.37
Retene	4.7 ± 2.3	**4.8 ± 1.3**	Mar 7 ± 12	69	7.3 ± 1.7	0.35
Benz[*a*]anthracene	**2.3 ± 0.5**	**5.4 ± 1.5**	NS	70	140 ± 41	0.41
Triphenylene + chrysene	**2.3 ± 0.5**	**5.1 ± 1.4**	Mar 1 ± 13	70	160 ± 46	0.44
Benzo[*b*]fluoranthrene	**3.0 ± 0.8**	**3.6 ± 1.2**	Mar 5 ± 14	70	230 ± 63	0.37
Benzo[*k*]fluoranthrene	**2.4 ± 0.5**	**5.1 ± 1.4**	Mar 1 ± 13	70	79 ± 22	0.42
Benzo[*e*]pyrene	*2.8 ± 0.7*	**4.9 ± 1.4**	Mar 3 ± 13	70	93 ± 27	0.38
Benzo[*a*]pyrene	**2.4 ± 0.6**	**4.9 ± 1.5**	NS	70	170 ± 51	0.37
Indeno[1,2,3-*cd*]pyrene	**3.1 ± 0.9**	**4.6 ± 1.4**	NS	70	150 ± 40	0.33
Benzo[*ghi*]perylene	**3.1 ± 0.9**	**4.4 ± 1.4**	Mar 3 ± 14	70	100 ± 27	0.34
Dibenz[*a,h*]anthracene	*2.6 ± 0.7*	**4.9 ± 1.5**	NS	69	28 ± 8.2	0.36
Coronene	**2.7 ± 0.6**	*3.8 ± 1.4*	Feb 25 ± 16	70	26 ± 7.2	0.35
ΣPAH	**2.8 ± 0.6**	**3.8 ± 1.4**	NS	70	2300 ± 620	0.38

Table BS6. Fit parameters for PAH concentrations in precipitation at Burnt Island

PAHs	Half-life (years), (ln2)/365*a_1	Peak-to-valley ratio, e^{2a_2}	Maximum date (± days)	No. of detects	Average conc. (ng/L)	r^2
Fluorene	*4.7 ± 1.2*	**4.7 ± 1.3**	**Jan 23 ± 10**	76	2.2 ± 0.3	0.38
Phenanthrene	*3.8 ± 0.8*	**5.5 ± 1.3**	**Jan 18 ± 8**	79	16 ± 2.3	0.43
Anthracene	Limited data			20	2.0 ± 0.9	
Fluoranthene	*6.3 ± 2.1*	**7.8 ± 1.2**	**Jan 17 ± 6**	79	13 ± 1.4	0.58
Pyrene	6.3 ± 2.1	**6.4 ± 1.3**	**Jan 19 ± 7**	80	8.0 ± 1.0	0.47
Retene	Not available					
Benz[*a*]anthracene	NS	**4.6 ± 1.4**	**Jan 2 ± 12**	39	1.6 ± 0.3	0.44
Chrysene	NS	**6.2 ± 1.3**	**Jan 10 ± 9**	39	4.8 ± 0.8	0.53
Benzo[*b*]fluoranthrene	NS	**7.9 ± 1.4**	**Jan 23 ± 9**	64	6.7 ± 0.9	0.38
Benzo[*k*]fluoranthrene	NS	**7.8 ± 1.4**	**Jan 16 ± 9**	62	4.4 ± 0.6	0.41
Benzo[*e*]pyrene	NS	**6.3 ± 1.4**	**Jan 4 ± 10**	34	3.2 ± 0.6	0.56
Benzo[*a*]pyrene	NS	*3.3 ± 1.4*	**Jan 10 ±14**	52	1.7 ± 0.4	0.48
Indeno[1,2,3-*cd*]pyrene	NS	**7.5 ± 1.4**	**Jan 25 ± 8**	57	3.8 ± 0.5	0.40
Benzo[*ghi*]perylene	NS	**5.1 ± 1.4**	**Jan 11 ± 11**	59	3.9 ± 0.5	0.34
Dibenz[*a,h*]anthracene	Limited data			16	0.8 ± 0.1	
Perylene	Limited data			16	0.8 ± 0.1	
Coronene	Not available					
ΣPAH	NS	**7.0 ± 1.3**	**Jan 23 ± 7**	80	60 ± 7.2	0.46

Table BS7. Fit parameters for PAH concentrations in precipitation at Point Petre

PAHs	Half-life (years), (ln2)/365*a_1	Peak-to-valley ratio, e^{2a_2}	Maximum date (± days)	No. of detects	Average conc. (ng/L)	r^2
Fluorene	*6.3 ± 2.1*	**4.0 ± 1.2**	**Jan 23 ± 8**	72	2.3 ± 0.3	0.43
Phenanthrene	*4.7 ± 1.1*	**4.6 ± 1.2**	**Jan 23 ± 7**	81	17 ± 2.3	0.49
Anthracene	Limited data			18	1.9 ± 0.8	
Fluoranthene	**6.3 ± 1.7**	**5.5 ± 1.2**	**Jan 23 ± 6**	80	18 ± 2.2	0.60
Pyrene	**4.7 ± 1.0**	**4.6 ± 1.2**	**Jan 13 ± 7**	81	10 ± 1.2	0.55
Retene	Not available					
Benz[*a*]anthracene	NS	**4.0 ± 1.4**	**Jan 11 ± 12**	38	2.2 ± 0.3	0.42
Chrysene	NS	**4.2 ± 1.4**	**Jan 18 ± 12**	38	7.5 ± 1.0	0.38
Benzo[*b*]fluoranthrene	NS	**7.2 ± 1.3**	**Jan 10 ± 7**	55	10 ± 1.5	0.52
Benzo[*k*]fluoranthrene	NS	**9.0 ± 1.3**	**Jan 13 ± 7**	54	5.9 ± 0.8	0.56
Benzo[*e*]pyrene	NS	**4.6 ± 1.4**	**Jan 18 ± 11**	37	4.9 ± 0.6	0.46
Benzo[*a*]pyrene	NS	**4.5 ± 1.4**	**Jan 12 ±11**	59	3.1 ± 0.3	0.28
Indeno[1,2,3-*cd*]pyrene	NS	**4.7 ± 1.3**	**Jan 24 ± 8**	69	4.6 ± 0.4	0.41
Benzo[*ghi*]perylene	NS	**4.3 ± 1.3**	**Jan 26 ± 9**	61	4.4 ± 0.4	0.36
Dibenz[*a*,*h*]anthracene	Limited data			24	0.6 ± 0.1	
Perylene	Limited data			17	0.6 ± 0.1	
Coronene	Not available					
ΣPAH	NS	**6.2 ± 1.2**	**Jan 22 ± 6**	81	76 ± 8.0	0.55

Appendix C. Temporal Trends of Polychlorinated Biphenyls (PCBs) in Precipitation and Air at Chicago

Published in *Environmental Science & Technology*, **2006**, *40*, 1178-1183.

Temporal Trends of Polychlorinated Biphenyls (PCBs) in Precipitation and Air at Chicago

Ping Sun, Ilora Basu, and Ronald A Hites*
School of Public and Environmental Affairs
Indiana University
Bloomington, Indiana, 47405 USA

*Corresponding Author Email: hitesr@indiana.edu

Brief

Concentrations of PCBs in precipitation and air in Chicago declined from 1997 to 2003 with half-lives of about 7 years.

Abstract

Polychlorinated biphenyl (PCBs) concentrations in precipitation (1997 to 2003) and in the atmospheric gas phase (1996 to 2003) collected in Chicago are reported. These data were obtained as part of the Integrated Atmospheric Deposition Network (IADN). For comparison, PCB concentrations at a remote site, Sleeping Bear Dunes on the northeastern shore of Lake Michigan, are also reported. Much higher PCB concentrations in both precipitation (7.1 ± 0.9 ng/L) and the gas phase (1.4 ± 0.1 ng/m^3) at Chicago compared to Sleeping Bear Dunes (1.1 ± 0.1 ng/L and 0.1 ± 0.08 ng/m^3, respectively) indicate that Chicago is a source of PCBs to the Great Lakes. A long-term decreasing trend of PCB concentrations in precipitation was observed at Chicago with a half-life of 6.8 ± 3.1 years. The corresponding half-life for PCB concentrations in the gas phase was 7.7 ± 1.1 years. The significant long-term decrease of PCB concentrations in precipitation and the gas phase in Chicago suggests that regulatory efforts are working, at least in this city.

Introduction

Production and sales of polychlorinated biphenyls (PCBs) were banned in the United States in 1976. However, PCBs are still being emitted into the atmosphere through primary (e.g. vaporization from products containing PCBs) or open burning of products containing PCBs or secondary (e.g. water-air exchange) processes (*1*). In addition, PCBs are transported from sources to background areas through advective and deposition processes (*2-4*).

The Integrated Atmospheric Deposition Network (IADN) was established in 1990 to monitor PCBs (and many other contaminants) in the air and precipitation around the Great Lakes (*5*). IADN has published several studies on PCBs in air (*6-9*) and precipitation (*10,11*) at remote sites near the lakes; these include Eagle Harbor, near Lake Superior; Sleeping Bear Dunes, near Lake Michigan; Sturgeon Point, near Lake Erie; and Point Petre, near Lake Ontario. In these studies, long-term decreasing concentrations of PCBs have been observed in both air and precipitation. For example, Buehler and co-workers reported that atmospheric PCB concentrations decreased with a half-life of 10 years at Sleeping Bear Dunes and 6 years at Eagle Harbor. These conclusions were based on IADN data up to the year 2000 and supplemental historical data going back to 1977 (*7*). Simcik and co-workers reported on temporal trends of PCBs in precipitation samples collected from the IADN sites during the period 1991 to 1997

(*11*). Their results showed that these PCB concentrations decreased during this time period at Sleeping Bear Dunes and at Point Petre with half-lives of 7 and 4 years, respectively. However, no significant decreases in the precipitation PCB concentrations were observed in samples collected near Lakes Superior or Erie. In general, these reported declines of PCBs in air and precipitation agreed well with the data reported for aquatic biota (*12,13*).

Previous studies have shown that industrial or urban centers are PCB sources (*14,15*). For example, high concentrations of PCBs in air and precipitation in Chicago have been reported previously (*16-18*). Most of these measurements were on a short term basis (*16,17*) or over a single year (*19,20)*. Detailed temporal trends of PCB concentrations in Chicago, particularly in precipitation, have not yet been reported. In this paper, we report on the temporal trends of PCB concentrations in precipitation collected in Chicago over the period 1997 to 2003 and in air collected in Chicago over the period 1996 to 2003. For comparison, PCB concentrations at Sleeping Bear Dunes, a remote site located approximately 400 km north-northeast of Chicago are also reported.

Experimental

Sampling methodology. Samples in Chicago were collected at the Illinois Institute of Technology, approximately 1.6 km from the shore of Lake Michigan. The sampling site is located on the roof of the Environmental Engineering Building, which is a four-story building built in 1948. Samples at Sleeping Bear Dunes were collected at the Sleeping Bear Dunes National Lakeshore approximately 1.5 km from the shore of Lake Michigan. This is a background site located near the northeastern shore of the lake. The IADN website (www.msc.ec.gc.ca/iadn/) provides detailed information on these two sites.

MIC automated wet-only samplers (MIC Co., Thornhill, ON) were used to collect precipitation samples. The detailed sampling procedure has been reported before by Carlson and co-workers (*21*). Briefly, each sampler consists a 46 × 46 cm shallow stainless steel funnel connected to a 30 cm long by 1.5 cm i.d. glass column (ACE Glass, Vineland, NJ) packed with XAD-2 resin. The sampler is normally covered; the start of a precipitation event is sensed by a conductivity grid located outside the sampler, which signals the cover to open. Precipitation flows through the XAD-2 column, which collects both particle and dissolved organic compounds. Precipitation samples were integrated over 28 days. The precipitation volume that passed through the resin column was recorded to calculate the concentrations. Breakthrough of PCBs was studied by analyzing the effluent rain water from the XAD column. No PCBs were detected. Recovery of PCBs was studied by spiking the columns with PCB surrogate standards before sampling. About 75% of the PCBs were recovered.

Modified Anderson Hi-Vol air samplers (General Metal Works, model GS 2310) were used to collect air samples for a 24 hour duration at a frequency of once every 12 days. Air was pulled into the sampler through Whatman quartz micro-fiber filters (QM-A, 20.3 × 25.4 cm) at a flow rate of 34 m^3/hr and passed through dry Amberlite XAD-2 resin (Supelco, Bellefonte, PA; 20-60 mesh, 330 m^2/g surface area) in a stainless steel cartridge. Particles in the air were retained on the quartz filters, and gas-phase components were adsorbed on the XAD resin. Our preliminary results from 1993 to 1995 showed that although higher molecular weight PCB congeners tended to partition onto the particle phase, the total PCB concentrations in the particle phase were about 5-10% of the total PCBs in atmosphere. Therefore, measurements of particle-bound PCB concentrations were stopped in 1997.

Analytical methodology. The wet XAD-2 cartridges containing PCBs in precipitation and the dry cartridges containing gas phase PCBs were sent to Indiana University for analysis. The XAD-2 resin was Soxhlet extracted for 24 h using a 1:1 (v/v) mixture of hexane and acetone. The extract was then concentrated by rotary evaporation. For the precipitation extracts, the water layer was separated, back extracted with hexane, and added to the original extract. The concentrated extract was then fractionated on a 3.5% (w/w) water-deactivated, silica gel column. Hexane was used to elute the PCBs. The extracts were further concentrated by N_2 blow-down to ~1 mL and spiked with PCB congeners 30 and 204 as internal standards for quantitation. The PCBs were analyzed on a Hewlett-Packard (HP) 6890 gas chromatograph with a ^{63}Ni electron capture detector. A DB-5 column (J & W Scientific; 60 m × 250 μm i.d.; film thickness, 0.10 μm) was used for PCB analysis.

Quality control and quality assurance procedures were followed to ensure data accuracy. The detailed procedures are described in the IADN Quality Assurance Program Plan and in the IADN Quality Control Project Plan (*22*). Surrogate standards (PCB congeners 14, 65, and 166) were spiked into each sample prior to extraction to monitor recovery. The average percent recoveries for the surrogates were 83-100% for the gas phase samples and 73-87% for the precipitation samples (*23*). One matrix spike experiment was performed with every 20 samples to assure high extraction efficiency; average ΣPCB recoveries for the gas phase and precipitation samples were 85 ± 5% and 77 ± 6%, respectively. Laboratory blanks were also checked regularly. Generally, laboratory blank values were less then 5% of actual sample values. Precipitation field blanks were not collected at Chicago. However, the levels of PCBs in the gas phase field blanks in Chicago were less than 5% of the levels measured in the actual samples. Assuming 100% capture efficiency at Chicago, the field blank values in precipitation should be, on average, less than 5% of the sample values; therefore, none of the PCB concentrations reported here have been blank corrected.

In this paper, ΣPCB represents a suite of 84 PCB congeners monitored by the IADN. Each congener contributes more than 1% to the total PCB mass for at least one site monitored by IADN. The toxicologically important congeners (77, 105, 108, 126, 128, 138, 156, 169, and 170) are also included. The detailed list of congeners is available in the Technical Summary of Progress of the IADN project, 1997-2002 (*24*).

Data analysis. The monthly concentrations (C_p) of ΣPCB in precipitation were fitted by the following time-dependent function to study the temporal trend

$$\ln C_p = a_0 + a_1 t + a_2 \sin\left(\frac{t}{a_3} + a_4\right) \quad (1)$$

where t is the time in Julian days relative to January 1 1990, a_0 is an intercept (unitless), a_1 is a first-order rate constant (in days^{-1}) describing the rate of exponential decrease or increase over time, a_2 is a periodic amplitude (unitless), a_3 is the length of the period (in days), and a_4 is the periodic offset (in days). If a_1 was significant ($p < 0.05$), either a decreasing ($a_1 < 0$) or increasing ($a_1 > 0$) trend in the ΣPCB concentrations could be determined over this sampling period.

Atmospheric temperature variations affect the gas phase PCB concentrations, and these variations must be removed before a valid trend can be determined. The temperature correction procedure was given by Cortes and co-workers in detail (*25*). Briefly, the gas phase concentration of each PCB congener are first converted to a partial pressure (P) using the ideal

gas law. These partial pressures are then corrected to a reference temperature of 288 K by application of the Clausius-Clapeyron equation:

$$P_{288} = P \exp\left[\frac{\Delta H}{R}\left(\frac{1}{T} - \frac{1}{288}\right)\right] \tag{2}$$

where *exp* is the exponential function, ΔH is a characteristic phase-transition energy (in kJ/mol), R is the gas constant, and T is the mean temperature during the 24-hour sampling period (in K). The value of ΔH was determined by a linear regression of the natural logarithm of the partial pressure (P) vs. the reciprocal of T. The natural logarithms of the corrected partial pressures at 288 K (called here P_{288}) of ΣPCB were then regressed vs. t to determine a temporal trend, if any.

Results and Discussion

Concentrations of PCBs in precipitation and air at Chicago. Concentrations of ΣPCB in precipitation and in the gas phase at Chicago are shown annually in Figure C1 as a function of sampling year. ΣPCB concentrations at Sleeping Bear Dunes measured over the same time period are also shown in Figure B1 for comparison. Note the concentration scale is logarithmic. The ΣPCB concentrations in precipitation ranged from 1.5 to 35 ng/L at Chicago and 0.1 to 6.1 ng/L at Sleeping Bear Dunes. In the gas phase, ΣPCB concentrations were from 0.1 to 9.5 ng/m^3 at Chicago and from 0.04 to 0.76 ng/m^3 at Sleeping Bear Dunes. Clearly, ΣPCB concentrations in both precipitation and in the gas phase are consistently higher in Chicago than at Sleeping Bear Dunes. Student's *t*-tests were conducted to compare the ΣPCB concentrations at these two sites year by year, and the detailed statistical results are given in Table BS1. These results show that, in each year, the ΣPCB concentrations at Chicago are significantly higher than those that at Sleeping Bear Dunes ($p < 0.05$). On average, precipitation concentrations are 7 times higher in Chicago, and gas phase concentrations are 12 times higher in Chicago, compared to Sleeping Bear Dunes.

The high concentrations of ΣPCB in Chicago indicate a strong source of PCBs in this urban area. PCBs were used heavily in urban areas from 1931 until their production and sales were banned in the U.S. in 1976. However, the continuing use of PCBs in exempt applications (e.g. transformers and capacitors) is still allowed. Thus, there are still many potential PCB sources in urban areas, such as Chicago, even 30 years after domestic production ceased. Hsu and co-workers used receptor modeling and field sampling to locate PCB sources in Chicago (*26*), and their results showed that there are potentially major PCB sources to the south and southwest of Chicago that could contribute to PCB concentrations at the Chicago site. These potential PCB sources include transformers, capacitors, municipal sludge drying beds, and landfills.

Due to their volatilization and stability, PCBs emitted from source areas can be transported to remote areas such as Sleeping Bear Dunes. The average concentration of ΣPCB in precipitation at Sleeping Bear Dunes is 1.1 ± 0.1 ng/L. However, the calculated concentration ratio between the field blanks and the precipitation samples was 0.72 ± 0.06 at this site suggesting the concentrations reported above may not be accurate but should be considered upper bounds. Similarly low concentrations of PCBs have been reported at other remote sites. For example, Franz and Eisenreich sampled precipitation at three remote sites along the eastern shore of Green Bay, Lake Michigan, from April 18, 1989 through May 15, 1990 and measured 86 PCB congeners (*4*). Their reported mean ΣPCB concentration was 2.2 ng/L (*4*). In another study, a concentration of 1.3 ng/L for precipitation phase PCBs (the sum of 53 congeners) was

measured in southeastern Sweden from 1993 to 1995 (*27*). In New Jersey, ΣPCB concentrations at rural sites were in the range of 0.30-0.50 ng/L from 1998 to 1999 (*28*).

The average concentration of ΣPCB in precipitation in Chicago is 7.1 ± 0.9 ng/L, which is similar to concentrations reported for other cities. For example, Offenberg and Baker reported ΣPCB concentrations in Chicago precipitation ranging from 4.1 ng/L (on January 19, 1995) to 189 ng/L (on July 21, 1994) (*16*). Since these samples were event-based samples, the high concentration on July 21, 1994 is likely an exceptional case. PCB concentrations in precipitation have also been measured in New Jersey by the New Jersey Atmospheric Deposition Network (NJADN) (*28*). The highest PCB concentrations were observed at the urban-industrial sites (13 ± 2.8 ng/L and 3.9 ± 0.72 ng/L at Camden and Jersey City, NJ, respectively) from 1998 to 1999. Thus, our results for Chicago are similar to those measured at other urban sites in North America.

The wet deposition fluxes ($ng \cdot m^{-2} d^{-1}$) of suite PCB at Chicago and Sleeping Bear Dunes were calculated by multiplying the 28-day integrated concentration (ng/L) by the precipitation volume (L) and dividing by the sampling time (28 days) and the surface area (0.212 m^2) of the collection funnel. In Chicago, the average wet deposition flux was 8.4 $ng \cdot m^{-2} d^{-1}$, which is about 6 times higher than 1.4 $ng \cdot m^{-2} d^{-1}$ at Sleeping Bear Dunes. These calculated values are similar to those reported by other studies (*1*,*28*). For example, NJADN reported a wet flux of approximately 0.8 $ng \cdot m^{-2} d^{-1}$ at Pinelands, a background site, and 11 $ng \cdot m^{-2} d^{-1}$ at Jersey City, an urban site (*28*).

The average concentration of ΣPCB in the gas phase at Sleeping Bear Dunes is 0.1 ± 0.08 ng/m^3 over our study period. Similar concentrations have been reported at other remote sites. Sampled in July 1997, an average concentration of 0.55 ng/m^3 for ΣPCB was observed near the Chesapeake Bay (*3*). Motelay-Massei and coworkers sampled air in Egbert, a rural site located north of Toronto from June 2000 to July 2001. Their results showed a range of 0.06 to 0.27 ng/m^3 for ΣPCB (sum of 13 PCB congeners) concentrations (*29*).

From 1996 to 2003, the concentration of ΣPCB in the gas phase in Chicago ranged from 0.1 to 9.5 ng/m^3 with a mean of 1.4 ± 0.1 ng/m^3, which was similar to concentrations previously reported for Chicago. For example, Pirrone and co-workers reported an average PCB concentration of 2.1 ± 1.2 ng/m^3 from July 8 to August 9, 1991 without providing information on the congener profile (*20*). Tasdemir and co-workers observed an average ΣPCB (sum of 50 congeners) concentration of 1.9 ± 1.7 ng/m^3 from June to October, 1995 (*30*). Simcik et al. reported a range of 0.27 to 14 ng/m^3 for ΣPCBs (sum of 87 congeners) during May and July 1994 and January 1995 (*17*). In addition, a range of 2.4 to 4.1 ng/m^3 for annual average ΣPCB concentrations in the gas phase in Chicago from 1997 to 1999 was also reported (*8*).

The ΣPCB gas phase concentrations at Chicago measured in this study are similar to those observed at other urban sites including New Jersey, Milwaukee, and Baltimore. For example, the concentration of ΣPCB ranged from 0.02 to 3.4 ng/m^3 in June, 1996, for samples collected in Baltimore, MD (*31*). Measurements by the NJADN, gave PCB concentrations in the gas phase at Camden and Jersey City from October 1997 to May 2001 of 3.2 and 1.3 ng/m^3, respectively (*32*). Most recently, Wethington and Hornbuckle demonstrated that Milwaukee, WI was a potential source of atmospheric PCBs to Lake Michigan (*33*). The average ΣPCB (sum of 88 congeners) gas phase concentration here was 1.9 ± 0.78 ng/m^3 during June of 2001. The range of PCB concentrations measured in Chicago falls in the range observed in these other cities in North America.

Temporal trends. Figure C2 shows the long-term trends of Chicago ΣPCB concentrations in both precipitation (top) and in the gas phase (bottom). The scatter of ΣPCB concentrations in the precipitation phase may indicate the effects of storm type, wind direction of the prevailing storm track, and other complex interactions between the atmospheric gas phase and precipitation (*1,4*). In the precipitation regression (see equation 1), the terms a_2, a_3, and a_4 were not significant ($p > 0.05$), indicating the seasonal effects were not statistically significant. The a_1 term indicated that ΣPCB concentrations significantly decreased from 1997 to 2003 with a half-life of 6.8 ± 3.1 years. In the gas phase, ΣPCB concentrations also significantly decreased from 1996 to 2003 with a half-life of 7.7 ± 1.1 years. Note the half-lives in precipitation and in the gas phase are statistically the same.

Previous studies have shown that PCBs concentrations in Chicago had been declining faster. For example, over the period 1993-1997, gas phase PCBs concentrations declined with a half-life of 2.7 ± 1.3 years (*34*). Offenberg and Baker reported a 3 year half-life for PCB concentrations in Chicago based on air samples collected from 1994-1995 (*35*). These reported half-lives are somewhat faster than reported here (~7 years) for the time period from 1997 to 2003. A slower rate of decrease for PCB concentrations in recent years may indicate that atmospheric PCB concentrations are now approaching a steady state after a rapid decline from 1970 to 1995 (*7,36*). This suggestion is supported by the observation that PCB concentrations in Great Lakes lake trout declined rapidly between 1974 and 1986 but have not changed much since then (*37*). On the other hand, other studies reported PCB concentration half-lives (in water and biota) on the order of 8 ± 2 years (*11,35*). Buehler and co-workers reported a half-life of 8.3 ± 1.5 years for PCBs in the atmospheric gas phase at Sleeping Bear Dunes for IADN samples collected up to 2001 (*6*). No newer data are available on trends of PCBs, particularly around Chicago.

Long-term decreasing trends for PCB concentrations in precipitation have been observed at some locations around the Great Lakes (*10,11*); however, this is the first time that a decreasing trend in Chicago precipitation has been reported. Simcik and co-workers reported on the temporal trends of ΣPCB (sum of 98 congeners) in precipitation collected from the IADN sites from 1991 to 1997. These concentrations showed significant decreases at Sleeping Bear Dunes with a half-life of 6.9 ± 3.5 years (*11*). In our study, if we ignore the relatively high blank levels, a similar decreasing trend for PCB concentrations in precipitation was also observed at this remote site from 1997 to 2003. However, as mentioned above, the concentrations we measured in these precipitation samples were close to those in the field blanks, and thus, a numerical trend for ΣPCB concentrations in Sleeping Bear Dunes precipitation is not reported here.

The decrease of PCB concentrations in both the gas phase and precipitation at Chicago may be due to efforts aimed at PCB reduction in the Great Lakes area. On April 7, 1997, the "Canada-United States Strategy for the Virtual Elimination of Persistent Toxic Substances in the Great Lakes Basin" (the so-called Binational Toxics Strategy) was signed by the environmental administrators of the U.S. and Canada. This strategy targets many toxic substances for virtual elimination, including PCBs. Under this Strategy, the U.S. EPA seeks a 90% reduction of PCBs used in electrical equipment by 2006 and assurance that all PCBs retired from use are properly managed and disposed (*38*). Numerous successful reduction activities have been reported in the 2004 Great Lakes Binational Toxics Strategy Report. For example, the International Steel Group has removed from service and destroyed PCB-containing equipment from several facilities including ones in Burns Harbor, Indiana, which is close to Chicago. ComEd, a subsidiary of Exelon Energy, operating in northern Illinois close to Chicago, has removed 95% of all PCB-

containing capacitors at its substations (*38*). In Chicago, the U.S. EPA and local partners established a PCB Clean Sweep program in 1999 to collect PCB-containing articles then in use. This program collects a wide range of PCB-containing articles, including old light ballasts, switches, transformers, and small capacitors, and disposes of these items properly (*39*). All of these efforts may have caused the decline of PCB concentrations in the gas phase and in precipitation that we have observed in Chicago.

Previous work has shown that there were no significant temporal trends of PCB wet deposition fluxes at Chicago or Sleeping Bear Dunes from 1996 to 2000 (*40*). Currently, IADN is working on expanding this loading analysis up to 2003. Preliminary calculations based on the data presented here indicate that there is no temporal trend for PCB wet fluxes at either Chicago or Sleeping Bear Dunes (see Figure BS1), but these results will be confirmed by a more complete study that will be available soon.

Congener profile. A PCB congener profile is the concentration of each measured congener (or chromatographically un-resolvable group of congeners) divided by the total concentration of all PCBs in the sample. These profiles are usually expressed in percent. Figure C3 shows the average congener profile for PCBs in the gas phase and in precipitation from Chicago and from Sleeping Bear Dunes. The small standard errors (and other statistical tests) suggest that none of these profiles have changed much over the years.

The PCB profiles for the gas phase in Chicago and in Sleeping Bear Dunes are virtually identical (r^2 = 0.91), suggesting that the composition of PCB congeners in the atmosphere is uniform even though the absolute concentrations vary dramatically. On the other hand, the PCB profiles in precipitation from Chicago and Sleeping Bear Dunes differ somewhat (r^2 = 0.67), suggesting that the composition of PCB congeners in precipitation can be quite variable. These differences mat be due to spatial PCB concentration gradients, different heights of rain clouds, or differences in total suspended particulate levels, all of which can alter the atmospheric gas/particle distribution and influence the PCB congener profiles in precipitation (*4*,*41*,*42*).

Comparing the PCB profiles on a site specific basis, we notice that the PCB composition in precipitation is enriched by more highly chlorinated congeners in both cases. For example, the more highly chlorinated congeners 110, 132+153+105, and 163+138 are dominant in the Chicago precipitation samples, while less chlorinated congeners 18, 33, and 52 are more dominant in the Chicago gas phase samples. This indicates that, compared with less chlorinated congeners, the more highly-chlorinated PCB congeners are more efficiently removed from the atmosphere by wet deposition (*41*).

The PCB congener distributions in our study are similar to profiles observed in rain samples collected by NJADN: Van Ry and co-workers extensively sampled gas, particle, and precipitation samples from August 7-11, 2000 and found a dominance of heavy PCB congeners in rain samples (*28*). By comparing PCB profiles in rain, particle, and gas phases, they concluded that wet washout of particle-bound PCBs is the dominant removal mechanism (*16*,*28*). We did not analyze for PCBs in particle-phase samples in our study; thus, the distribution of PCB congeners in the particle phase could not be measured.

Although more highly chlorinated congeners were also present in the precipitation samples at Sleeping Bear Dunes, their contribution to ΣPCB was lower compared to that in Chicago: The contribution of congeners heavier than penta-chlorinated PCB to ΣPCB is 42 ± 5% at Sleeping Bear Dunes and 57 ± 6% at Chicago. A study by Mandalakis and Stephanou on wet deposition of PCBs in the eastern Mediterranean showed higher contributions of lower molecular weight congeners (e.g tri- and tetra- chlorinated congeners) to ΣPCB in rain samples

(*1*). According to Van Ry et al. (*28*), the relative importance of higher chlorinated PCBs in environmental samples decreases with the increasing distance away from sources because heavier congeners tend to be associated with particles and have correspondingly lower residence times. This suggestion is compatible with our findings.

Acknowledgments

We thank Team IADN (including Karen Arnold and Jennifer Hamilton) for data acquisition and the U.S. Environmental Protection Agency's Great Lakes National Program Office for funding (Grant GL995656, Melissa Hulting, project monitor).

Supporting Information Available

The supporting Information contains a table of Student's *t*-test results from comparison of gas and precipitation phase PCB concentrations between Chicago and Sleeping Bear Dunes, a figure of temporal trends of wet deposition fluxes at Chicago and Sleeping Bear Dunes. These materials are available free of charge via the Internet at http://pubs.acs.org.

Literature cited

1. Mandalakis, M.; Stephanou, E. G. Wet deposition of polychlorinated biphenyls in the eastern Mediterranean. *Environ. Sci. Technol.* **2004**, *38*, 3011-3018.
2. Swackhamer, D. L.; McVeety, B. D.; Hites, R. A. Deposition and Evaporation of Polychlorobiphenyl Congeners to and from Siskiwit Lake, Isle Royale, Lake Superior. *Environ. Sci. Technol.* **1988**, *22*, 664-672.
3. Brunciak, P. A.; Dachs, J.; Franz, T. P.; Gigliotti, C. L; Nelson, E. D.; Turpin, B. J.; Eisenreich, S. J. Polychlorinated biphenyls and particulate organic/element carbon in the atmosphere of Chesapeake Bay, USA. *Atmos. Environ*. **2001**, *35*, 5663-5677.
4. Franz, T. P.; Eisenreich, S. J. Wet deposition of polychlorinated biphenyls to Green Bay, Lake Michigan. *Chemosphere* **1993**, *26*, 1767-1788.
5. Buehler, S. S.; Hites, R. A. The Great Lakes' Integrated Atmospheric Deposition Network. *Environ. Sci. Technol.* **2002**, *36*, 355A-359A.
6. Buehler, S. S.; Basu, I.; Hites, R. A. Causes of variability in pesticide and PCB concentrations in air near the Great Lakes. *Environ. Sci. Technol.* **2004**, *38*, 414-422.
7. Buehler, S. S.; Basu, I.; Hites, R. A. Gas-phase polychlorinated biphenyl and hexachlorocyclohexane concentrations near the Great Lakes: a historical perspective. *Environ. Sci. Technol.* **2002**, *36*, 5051-5056.
8. Strandberg, B.; Dodder, N. G.; Basu, I.; Hites, R. A. Concentrations and spatial variations of polybrominated diphenyl ethers and other organohalogen compounds in Great Lakes air. *Environ. Sci. Technol.* **2001**, *35*, 1078-1083.
9. Hillery, B. R.; Basu, I.; Sweet, C. W.; Hites, R. A. Temporal and spatial trends in a long-term study of gas-phase PCB concentrations near the Great Lakes. *Environ. Sci. Technol.* **1997**, *31*, 1811-1816.
10. Chan, C. H.; Bruce, G.; Harrison, B. Wet deposition of organochlorine pesticides and polychlorinated biphenyls to the Great Lakes. *J. Great Lakes Res.* **1994**, *20*, 546-560.
11. Simcik, M. F.; Hoff, R. M.; Strachan, W. M.; Sweet, C. W.; Basu, I.; Hites, R. A. Temporal trends of semi-volatile organic contaminants in Great Lakes precipitation. *Environ. Sci. Technol.* **2000**, *34*, 361-367.

12. Ryckman, D. P.; Weseloh, D. V.; Hamr, P.; Fox, G. A.; Collins, B.; Ewins, P. J.; Norstrom, R. J. Spatial and temporal trends in organochlorine contamination and bill deformities in double-crested cormorants (Phalacrocoraxauritus) from the Canadian Great Lakes. *Environ. Monit. Assess*. **1998**, *53,* 169-195.
13. Ashpole, S. L.; Bishop, C. A.; Brooks, R. J. Contaminant residues in snapping turtle (Chelydra s. serpentine) eggs from the Great Lakes-St. Lawrence River basin (1999 to 2000). *Arch. Environ. Con. Tox*. **2004**, *47*, 240-252.
14. Breivik, K.; Sweetman, A.; Pacyna, J. M.; Jones, K. C. Sci. Towards a global historical emission inventory for selected PCB congeners . a mass balance approach 2. Emissions. *Sci. Total Environ.* **2002**, *290*, 199-224.
15. Hafner, W. D.; Hites, R. A. Potential sources of pesticides, PCBs, and PAHs to the atmosphere of the Great Lakes. *Environ. Sci. Technol.* **2003**, *37*, 3764-3773.
16. Offenberg, J. H.; Baker, J. E. Polychlorinated biphenyls in Chicago precipitation: enhanced wet deposition to near-shore Lake Michigan. *Environ. Sci. Technol.* **1997**, *31*, 1534-1538.
17. Simcik, M. F.; Zhang, H.-X.; Eisenreich, S. J.; Franz, T. P. Urban contamination of Chicago/coastal Lake Michigan atmosphere by PCBs and PAHs during AEOLOS. *Environ. Sci. Technol.* **1997**, *31*, 2141-2147.
18. Basu, I.; Hafner, W. D.; Mills, W. J.; Hites, R. A. Differences in atmospheric persistent organic pollutant concentrations at two locations in Chicago. *J. Great Lakes Res*. **2004**, *30*, 310-315.
19. Cotham, W. E.; Bidleman, T. F. Polycyclic aromatic hydrocarbons and polychlorinated biphenyls in air at urban and a rural site near Lake Michigan. *Environ. Sci. Technol.* **1995**, *29*, 2782-2789.
20. Pirrone N.; Keeler, G. J.; Holsen, T. M. Dry deposition of semi-volatile organic compounds to Lake Michigan. *Environ. Sci. Technol.* **1995**, *29*, 2123-2132.
21. Carlson, D. L.; Basu, I.; Hites, R. A. Annual variation of pesticide concentrations in great lakes precipitation. *Environ. Sci. Technol.* **2004**, *38*, 5290-5296.
22. Basu, I. *Quality Assurance Project Plan (Revision 4)*; Indiana University: Bloomington, IN, 2000.
23. Basu, I.; Arnold, K. *Quality Control Report 2003*; Indiana University: Bloomington, IN, 2004.
24. *Technical Summary of Progress of Integrated Atmospheric Deposition Network (IADN) 1997-2002.*
25. Cortes, D. R.; Basu, I.; Sweet, C. W.; Brice, K. A.; Hoff, R. Am.; Hites, R. A. Temporal trends in gas-phase concentrations of chlorinated pesticides measured at the shores of the Great Lakes. *Environ. Sci. Technol.* **1998**, *32*, 1920-1927.
26. Hsu, Y.-K.; Holsen, T. M.; Hopke, P. K. Locating and quantifying PCB sources in Chicago: receptor modeling and field sampling. *Environ. Sci. Technol.* **2003**, *37*, 681-690.
27. Bremle G.; Larsson, P. Long-term variations of PCB in the water of a river in relation to precipitation and internal sources. *Environ. Sci. Technol.* **1997**, *31*, 3232-3237.
28. Van Ry, D. A.; Gigliotti, C. L.; Glenn, T. R.; Nelson, E. D.; Totten, L. A.; Eisenreich, S. J. Wet deposition of polychlorinated biphenyls in urban and background areas of the Mid-Atlantic States. *Environ. Sci. Technol.* **2002**, *36*, 3201-3208.
29. Motelay-Massei, A.; Harner, T.; Shoeib, M.; Diamond, M.; Stern, G.; Rosenberg, B. Use passive air-sampler to assess urban-rural trends for persistent organic pollutants and

polycyclic aromatic hydrocarbons. 2 Seasonal trends of PAHs, PCBs, and Organochlorine pesticides. *Environ. Sci. Technol.* **2005**, *39*, 5763-5773.
30. Tasdemir, Y.; Vardar, N.; Odabasi, M.; Holsen, T. M. Concentrations and gas/particle partitioning of PCBs in Chicago. *Environ. Pollut.* **2004**, *131*, 35-44.
31. Offenberg, J. H.; Baker, J. E. Influence of Baltimore's urban atmosphere on organic contaminants over the northern Chesapeake Bay. *J. Air Waste Manage. Assoc.* **1999**, *49*, 959-965.
32. Totten, L. A.; Gigliotti, C. L.; Vanry, D. A.; Offenberg, J. H.; Nelson, E. D.; Dachs, J.; Reinfelder, J. R.; Eisenreich, S. J. Atmospheric concentrations and deposition of polychlorinated biphenyls to the Hudson River Estuary. *Environ. Sci. Technol.* **2004**, *38*, 2568-2573.
33. Wethington, D. M.; Hornbuckle, K. C. Milwaukee, WI, as a source of atmospheric PCBs to Lake Michigan. *Environ. Sci. Technol.* **2005**, *39*, 57-63.
34. Simcik, M. F.; Basu, I.; Sweet, C. W.; Hites, R. A. Temperature dependence and temporal trends of polychlorinated biphenyl congeners in the Great lakes atmosphere. *Environ. Sci. Technol.* **1999**, *33*, 1991-1995.
35. Offenberg, J. H.; Baker, J. E. PCBs and PAH in southern Lake Michigan in 1994 and 1995: Urban atmospheric influences and long-term declines. *J. Great Lakes Res.* **2000**, *26*, 196-208.
36. Schneider, A. R.; Stapleton, H. M.; Cornwell, J.; Baker J. E. Recent declines in PAH, PCB, and toxaphene levels in the northern Great Lakes as determined from high resolution sediment cores. *Environ. Sci. Technol.* **2001**, *35*, 3809-3815.
37. De Vault, D. S.; Hesselberg, R.; Rodgers, P. W.; Feist, T. J. Contaminant trends in lake trout and walleye from the Laurentian Great Lakes. *J. Great Lakes Res.* **1996**, *22*, 881-895.
38. *Great Lakes Binational Toxic Strategy 2004 Progress Report*, http://www.binational.net
39. Cook County PCB and Mercury Clean Sweep Program. *PCB & Mercury Fact Sheet*. http://www.erc.uic.edu/cleansweep/
40. Atmospheric Deposition of Toxic Substances to the Great Lakes: IADN Results Through 2000, www.epa.gov/glnpo/monitoring/air/iadn/iadn.html
41. Bidleman, T. F. Atmospheric processes: wet and dry deposition of organic compounds are controlled by their vapor-particle partitioning. *Environ. Sci. Technol.* **1988**, *22*, 361-367.
42. Ligocki, M. P.; Leuenberger, C. Pankow, J. F. Trace organic compounds in rain-III. Particle scavenging of neutral organic compounds. *Atmos. Environ*. **1985**, *19*, 1619-1626.

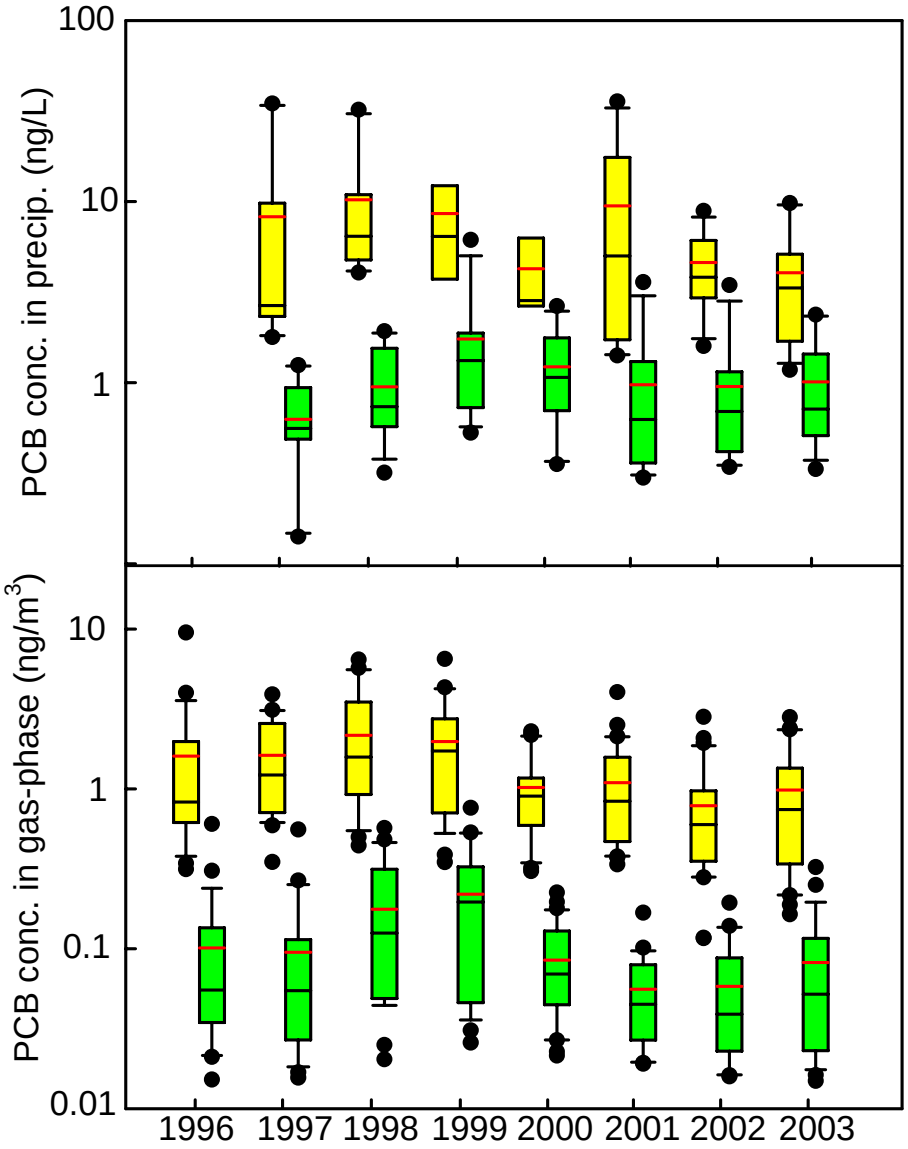

Figure C1. ΣPCB concentrations in precipitation (top) and in the gas phase (bottom) in Chicago (yellow) and at Sleeping Bear Dunes, Michigan (green). The horizontal lines represent the 10th, 50th, and 90th percentiles; the red line is the mean; the boxes represent the 25th to 75th percentiles; and outliers are shown individually.

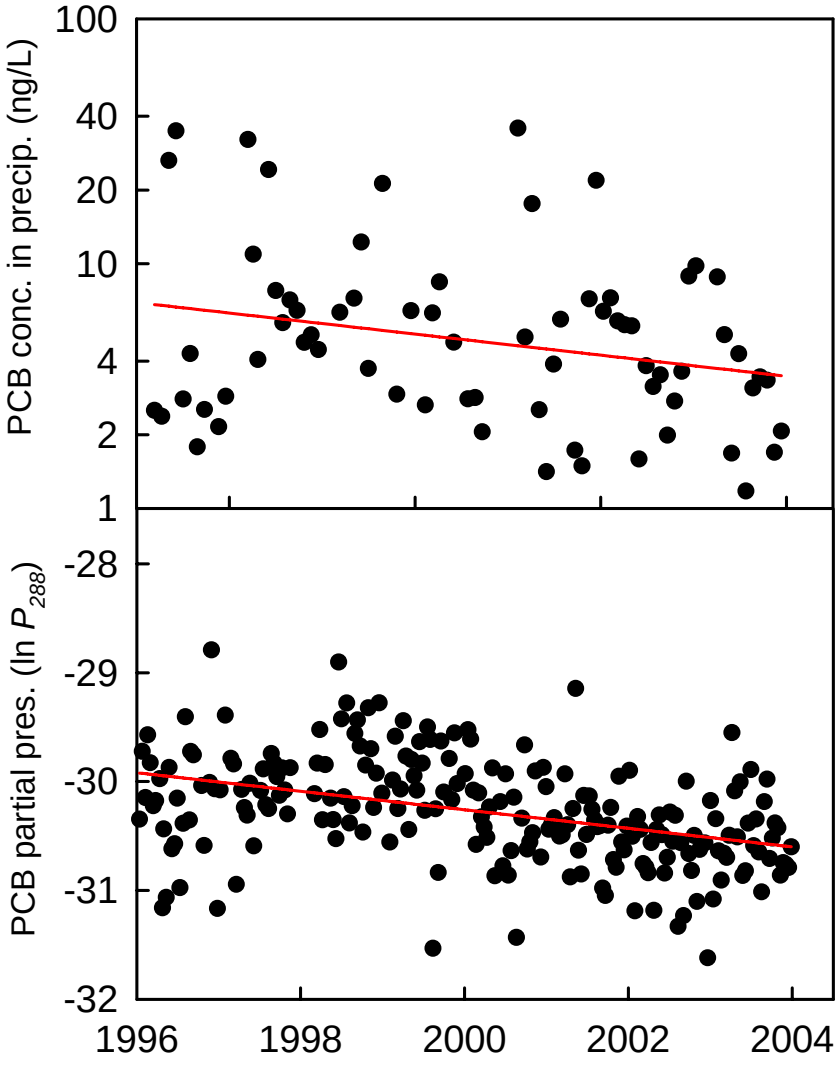

Figure C2. Long-term trend of ΣPCB concentrations in precipitation (top) and in the gas phase (bottom) at Chicago. Red lines indicate regressions of the data as shown. A statistically significant long-term decrease is observed in both cases; the half-lives for PCB concentrations in precipitation and the gas phase are 6.8 ± 3.1 and 7.7 ± 1.1 years, respectively.

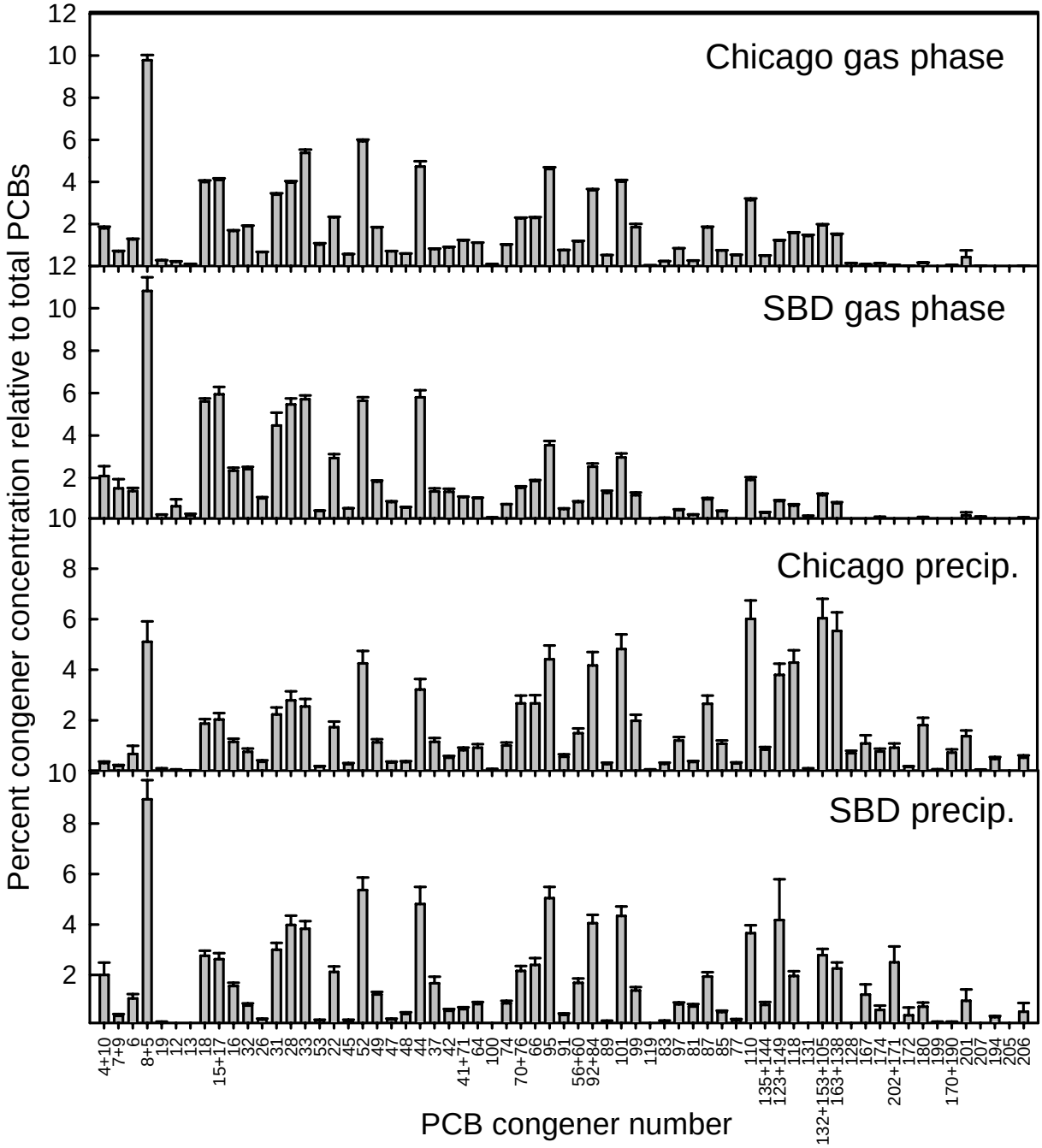

Figure C3. PCB congener profiles measured in the gas phase at Chicago (top), in the gas phase at Sleeping Bear Dunes (SBD), in precipitation at Chicago, and in precipitation at Sleeping Bear Dunes (bottom). The error bars represent one standard error.

Supporting Information
Temporal Trends of Polychlorinated Biphenyls (PCBs) in Precipitation and Air at Chicago

Ping Sun, Ilora Basu, and Ronald A Hites∗
School of Public and Environmental Affairs
Indiana University
Bloomington, Indiana, 47405 USA

∗Corresponding Author Email: hitesr@indiana.edu

Table CS1. Student's *t*-test results for the comparison of PCB concentrations between Chicago and Sleeping Bear Dunes

Year	***Gas phase***			***Precipitation***		
	t	**P**	**df***	**t**	**P**	**df**
1996	4.20	0.0001	53			
1997	7.21	<0.0001	43	2.12	0.048	19
1998	6.15	<0.0001	52	3.49	0.002	21
1999	6.28	<0.0001	52	3.78	0.001	18
2000	9.03	<0.0001	56	4.22	0.0006	17
2001	6.78	<0.0001	57	2.67	0.01	21
2002	6.26	<0.0001	58	5.47	<0.0001	23
2003	6.02	<0.0001	55	3.57	0.002	21

*df: degree of freedom

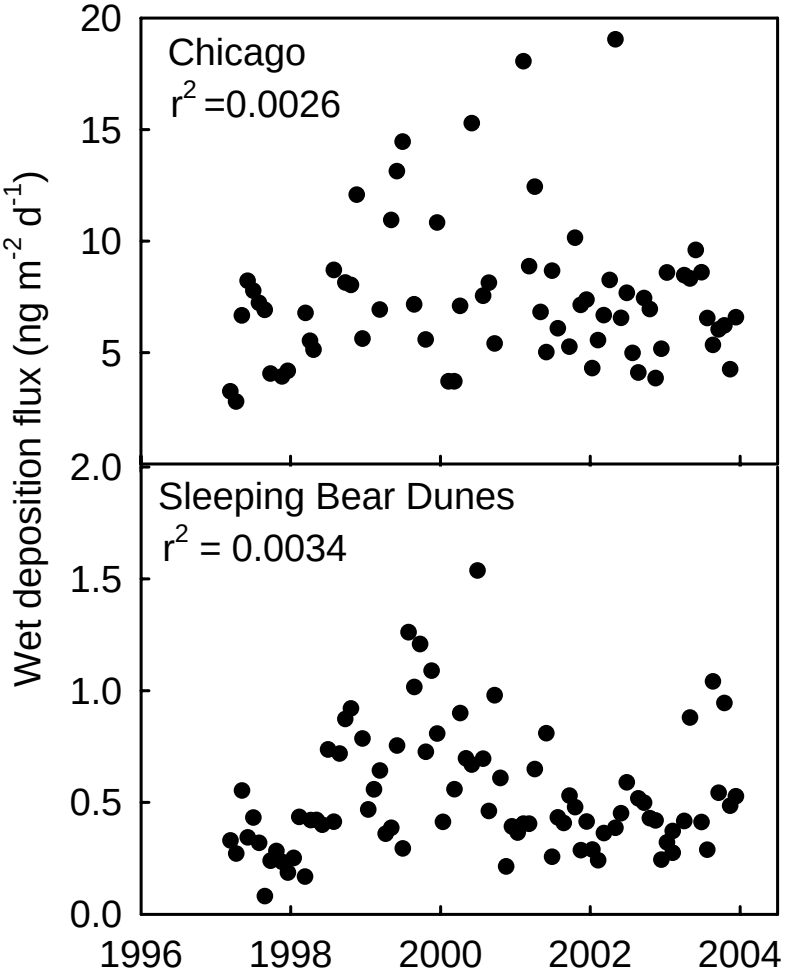

Figure CS1. Temporal trends of wet deposition flux of PCBs in Chicago and Sleeping Bear Dune (bottom).

Appendix D. Temporal and Spatial Trends of Organochlorine Pesticides in Great Lakes Precipitation

Published in *Environmental Science & Technology*, **2006**, *40*, 2135-2141.

Temporal and Spatial Trends of Organochlorine Pesticides in Great Lakes Precipitation

Ping Sun,[1] Sean Backus,[2] Pierrette Blanchard,[2] and Ronald A Hites∗[1]

[1]School of Public and Environmental Affairs
Indiana University
Bloomington, Indiana, 47405 USA

and
[2]Environment Canada
4905 Dufferin Street
Toronto, ON M3H 5T4 Canada

∗Corresponding Author Email: hitesr@indiana.edu

Brief

Concentrations of organochlorine pesticides in Great Lakes precipitation were analyzed for temporal and spatial trends from 1997 to 2003.

Abstract

Organochlorine pesticide concentrations in precipitation samples collected from 1997 to 2003 at seven Integrated Atmospheric Deposition Network sites around the Great Lakes are reported. The 28-day volume weighted mean concentrations of several pesticides, including γ-hexachlorocyclohexane (HCH), endosulfan, hexachlorobenzene, chlordane, and DDE, showed significant seasonal trends. For current-use pesticides (endosulfan and γ-HCH), their concentrations peaked in late spring to summer just after their agricultural application. For the banned pesticides, higher concentrations were observed in the winter due to their enhanced partitioning to particles and scavenging by snow. Long-term decreasing trends were observed for several pesticides such as γ-HCH and DDE. On the other hand, β-HCH showed significant *increasing* concentrations as a function of time at Brule River, Eagle Harbor, and Sleeping Bear Dunes. Generally, Chicago had the highest concentrations for chlordanes, dieldrin, and DDT, indicating that urban areas could be a source for these compounds to precipitation. For γ-HCH and endosulfans, Point Petre had the highest concentrations due to the application of these pesticides in the surrounding areas.

Introduction

Founded in 1990, the objectives of the Integrated Atmospheric Deposition Network (IADN) were to measure the concentrations of persistent organic pollutants, including polychlorinated biphenyls (PCBs), organochlorine (OC) pesticides, and polycyclic aromatic hydrocarbons (PAHs) in air and precipitation around the Great Lakes. One special focus of IADN has been the OC pesticides, many of which were banned in the 1970s in North America due to their toxicity, environmental persistence, and tendency of bioaccumulate. More than 20 years after their phase-out, these compounds are still present in the environment (*1,2*).

Long-term monitoring of OC pesticide concentrations has shown decreasing trends in Great Lakes air (*3,4*), biota (*5,6*), water, and sediment (*7*). Precipitation (both as rain and snow) is an important pathway for the transport and deposition of OC pesticides. However, long-term measurements of OC pesticides in precipitation are limited. One study conducted by Chan and co-workers reported decreasing trends of OC pesticide concentrations in rain and snow collected in southern Ontario, Canada, over the period of 1986-1991 (*8*). The concentrations of several OC pesticides, such as the hexachlorocyclohexanes (HCHs) at some Canadian Great Lakes sites (e.g. Burlington and Point Petre), decreased over the time period 1986 to 1999 based on another study by Chan and co-workers (*9*). Simcik and co-workers reported on the temporal trends of several organochlorine pesticides (including the HCHs, dieldrin, chlordane, and DDTs) in precipitation samples collected at three U.S. and two Canadian IADN sites from 1991 to 1997 (*10*). Their results showed that the concentrations of many pesticides decreased during this sampling period, which agreed with the results of Chan and coworkers. Most recently, Carlson and co-workers reported the annual variations of OC pesticide concentrations in precipitation collected from 1997 to 2002 at five U.S. IADN sites (*11*). In this case, the concentrations of most pesticides did not decrease over time but showed clear seasonality: Higher concentrations were observed in the summer for current-use pesticides, and higher concentrations were observed in the winter for most of the banned pesticides.

In this paper, the temporal and spatial trends of OC pesticide concentrations in precipitation at seven IADN sites (five American and two Canadian), covering the Great Lakes basin, from 1997 to 2003 will be presented to provide information on the long-term transport and fate of OC pesticides. This is the fist time that the concentration trends of these organochlorine pesticides in precipitation have been compared between U.S. and Canadian sites.

Experimental

Precipitation samples were collected at the five U.S. IADN sites (Brule River and Eagle Harbor, near Lake Superior; Chicago and Sleeping Bear Dunes, near Lake Michigan; and Sturgeon Point, near Lake Erie) and at two Canadian sites (Burnt Island, near Lake Huron and Point Petre, near Lake Ontario). The sampling site locations are shown in Figure D1. The IADN website (www.smc-msc.ec.gc.ca/iadn) provides detailed information on these sites.

At the five U.S. sites, MIC automated wet-only samplers (MIC Co., Thornhill, ON) were used to collected precipitation samples. The detailed sampling procedure can be found in Carlson and co-workers (*11*). Briefly, a XAD-2 resin column is used to collect both particle and dissolved organic compounds from precipitation during a given 28-day period. Because all of the precipitation during this time passes through the XAD-2 column, the concentrations measured in this study can be considered to be volume weighted mean (VWM) concentrations, minimizing the bias of high concentrations observed from storm and other events during the 28-day sampling period. Therefore, the concentrations reported in this paper are monthly VWM concentrations unless stated otherwise, although the sampling period is a little shorter than one month.

After sampling, the wet XAD-2 cartridges were returned to Indiana University for the analysis of the pesticides. The XAD-2 resin was Soxhlet extracted for 24 h using a 1:1 (v/v) mixture of hexane and acetone. The extract was then concentrated by rotary evaporation and fractionated on 3.5% (w/w) water-deactivated silica gel. Hexane was first used to elute PCBs, HCB, *p,p'*-DDE, and *o,p'*-DDT. The other pesticides were then eluted with 1:1 hexane in dichloromethane. The extracts were further concentrated by nitrogen blowdown to ~1 mL and

spiked with PCB-155 as the internal standard. The OC pesticides were analyzed on a Hewlett-Packard 5890 gas chromatograph with a ^{63}Ni electron capture detector. A DB-5 column (J & W Scientific; 60 m × 250 μm i.d.; film thickness, 0.10 μm) was used.

The detailed sampling and analysis procedure at the two Canadian sites were given by Chan and co-workers (*8*). A 4-L amber glass bottle was pre-filled with 250 mL dichloromethane for precipitation sampling in a MIC automated wet-only sampler. Liquid samples were returned to the National Laboratory for Environmental Testing (NLET) in Burlington, Ontario for analysis. The samples were kept at 4 °C until analyzed. The aqueous phase was separated from the dichloromethane solvent in a separatory funnel, and the precipitation volume was measured. The aqueous phase was then extracted twice with fresh dichloromethane. The combined extracts were concentrated by rotary evaporation to 3.0 mL, and the solvent was exchanged to isooctane. The extract was then fractionated on 3.5% (w/w) water-deactivated silica gel. Hexane was first used to elute PCBs, HCB, *p,p'*-DDE, and *o,p'*-DDT. The other pesticides were then eluted with 1:1 hexane in dichloromethane. The extracts were concentrated by nitrogen blowdown to 1.0 mL. The two fractions were analyzed for pesticides by dual-capillary gas chromatography with electron capture detection on an Agilent 6890 gas chromatograph. A HP-5 MS (30 m x 250 μm i.d.; film thickness, 0.25 μm) column was used as the primary column, and detections were verified on a HP1-MS (30 m x 250 μm i.d.; film thickness, 0.25 μm) column.

Quality control and assurance procedures were followed by both laboratories to ensure data quality. Selected XAD columns were spiked with dibutylchlorendate prior to sampling to measure the stability of OC pesticides during the 28-day sampling period. The average recovery was ~87%. Assuming a 5% loss of these compounds during extraction and sample preparation, the loss of OC pesticides during the sampling procedure was less than 10%. At Indiana University, laboratory mixed pesticide standards were used for matrix spikes. One matrix spike experiment was performed per two batches of samples to assure extraction efficiency. Surrogate standards of dibutylchlorendate and δ-HCH were used in each sample to monitor recovery. The average percent recoveries for the surrogates were 67-117% (*12*). Surrogate spikes of 1,3-dibromobenzene and endrin-ketone were added to determine recovery efficiencies at NLET. The surrogate spike recoveries varied between 82% and 92% (*9*). Field and laboratory blanks were also collected regularly. Generally, laboratory blank values were less then 5% of the actual sample values, while field blank values were on average less than 10% of the sample values; therefore, the pesticide concentrations reported here have not been blank corrected. In early 2001, a split-sample interlaboratory comparison was conducted to evaluate possible systematic biases between the participating laboratories (*13*). No biases were found.

Eighteen pesticides were measured by both Indiana University and NLET. These pesticides are aldrin, α-chlordane, γ-chlordane, *p,p'*-DDT, *p,p'*-DDD, *p,p'*-DDE, *o,p'*-DDT, dieldrin, α-endosulfan, β-endosulfan, endrin, heptachlor epoxide, HCB, α-HCH, β-HCH, γ-HCH, methoxychlor, and *trans*-nonachlor. The structures and major properties (including octanol-water partition coefficients, vapor pressures, and Henry's law constants) of these pesticides are given in Table DS1 of the Supporting Information.

Results and Discussion

The average concentrations of the OC pesticides in precipitation measured by IADN from 1997 to 2003 are listed in Tables DS2-DS8 of the Supporting Information. The comparison of selected OC pesticide concentrations between IADN and other studies over the same time period is given in Table DS9. Overall, pesticide concentrations measured by IADN are within the same

range as those monitored by the New Jersey Atmospheric Deposition Network (NJADN) (*14*). For example, the concentrations of *p,p'*-DDT at Jersey City, NJ were 0.18 to 0.55 ng/L, which falls in the range of the concentrations measured at Chicago (0.007-18 ng/L). Chlordanes also showed similar concentrations between the rural sites at Pineland, NJ and at Sleeping Bear Dunes, MI.

Generally, HCH concentrations were higher in Europe than in the U.S. and Canada, which may be due to heavier applications of technical HCH and γ-HCH in Europe (*15*). One study in Brazil showed higher endosulfan concentrations in rainwater compared to IADN, but this result could be attributed to the heavy use of endosulfan on cotton fields near the collection site (*16*). Pesticides measured in precipitation at Senga Bay, Africa, showed lower concentrations compared to IADN, NJADN, and France, indicating less pesticide usage in this economically developing region (*17*).

Spatial trends. The spatially resolved concentrations of the three major technical HCH isomers for 1997 to 2003 are shown in Figure D2. A one-way analysis of variance was conducted to compare the average concentrations among these sites. α-HCH concentrations were about the same at all sites [$F = 1.60$, $P = 0.16$ and df = (5, 355), except for Eagle Harbor, which had slightly higher concentrations [$F = 3.51$, $P = 0.002$ and df = (6, 410)]. β-HCH concentrations were highest in Chicago, followed by similar concentrations at Sleeping Bear Dunes, Sturgeon Point, Burnt Island, and Point Petre [$F = 1.0$, $P = 0.39$ and df = (3, 159)]. Brule River and Eagle Harbor had the lowest β-HCH concentrations [$F = 0.14$, $P = 0.71$ and df = (1, 80)]. Concentrations of γ-HCH at Burnt Island and Point Petre were similar [$F = 0.04$, $P = 0.84$ and df = (1, 156)] and significantly higher than at Brule River, Eagle Harbor, Chicago, Sleeping Bear Dunes, and Sturgeon Point, which were all about the same [$F = 3.91$, $P = 0.002$ and df = (5, 413)].

The uniformity of α-HCH concentrations in precipitation agrees well with other spatial studies of this compound (*9,18-20*). Due to its higher volatility (*21*) and its slower atmospheric reaction rate with hydroxyl radicals (*22*), relative to β-HCH and γ-HCH, α-HCH is easily transported into the atmosphere and has a relatively uniform atmospheric concentration on a global scale. Unlike α-HCH, β-HCH mostly stays near its source due to its relatively low volatility and high stability (*23*). Therefore, the relatively high concentration of β-HCH in Chicago suggests heavier past usage of technical HCH, which contains 60-70% of α-HCH, 2-12% of β-HCH, and 10-15% of γ-HCH (*24*), around this urban area before its phase-out in the 1970s.

The relatively high concentrations of γ-HCH at the two Canadian sites (Burnt Island and Point Petre) is not surprising. The technical HCH mixture was banned in North America in 1970s and replaced by purified γ-HCH (lindane). Li and co-workers modeled Canadian lindane usage inventories with high spatial resolution (*25*). Their results showed that ~410 t of lindane had been applied during the period 1970 to 2000 in the provinces of Quebec and Ontario close to Lakes Ontario and Huron. In the U.S., lindane was mainly used on fruits and vegetables and as a seed treatment for grains, legumes, and oilseed crops (*15*). However, the National Center for Food and Agricultural Pesticides showed that the U.S. usage of lindane for all crops during the period of 1992 and 1997 in the Great Lakes area was limited.

The average ratio between α-HCH and γ-HCH in precipitation ranged from 0.7 to 0.9 at the two Canadian sites and at the Chicago site. Given that α-HCH was the major component in technical HCH, the relatively high concentration of γ-HCH may be due to the replacement of technical HCH with lindane or to the higher water solubility of γ-HCH compared to α-HCH (*26*),

which would cause γ-HCH to preferentially partition into precipitation. At the other four U.S. rural sites, this ratio is between 1.4 and 2.4, indicating an aged HCH source.

The concentrations of endosulfan (α- plus β-endosulfan) showed a clear increasing trend from the west to east (see Figure D3). Higher concentrations were observed at Point Petre, Burnt Island, and Sturgeon Point. These higher levels could be explained by the agricultural application of endosulfan in this area. For example, endosulfan is widely used in Michigan and New York State (*27*) and in Ontario (*28*), particularly in the southern and western portions of the province.

Precipitation concentrations of chlordane (expressed as the sum of α- and γ-chlordane and *trans*-nonachlor) were the highest in Chicago followed by Sturgeon Point and Sleeping Bear Dunes. Brule River, Eagle Harbor, Burnt Island, and Point Petre had similar but lower chlordane concentrations [F = 1.44, P = 0.23 and df = (3, 277)]. Technical chlordane was introduced in 1947 and phased out in the United Sates in 1988. Before then, chlordane was used in approximately 20 million U.S. structures, usually as a termiticide, and it has been detected in the home environment as long as 35 years after its agricultural application (*29,30*). Although most abundant in the south and southeastern United States, subterranean termites are found in every state except Alaska, with moderate to heavy structural infestations in Chicago. Hafner and Hites suggested that the volatilization from soil in the southern United States was the predominant source of chlordane to the Great lakes (*27*). Thus, the higher chlordane concentration in Chicago is likely due to *both* historical local applications used to control termites *and* the influence of long range transport from areas of high chlordane usage. In fact, Harner and co-workers have suggested urban areas act as emission sources of chlordane (*31*). Moreover, the chlordane concentrations in precipitation monitored by NJADN also showed that the concentrations at urban sites were higher than at rural sites (*14*).

The highest precipitation concentrations of DDT (the sum of *p,p'*-DDT, *p,p'*-DDE and *p,p'*-DDD) were also observed in Chicago, suggesting urban sources. Although technical DDT (containing >85% *p,p'*-DDT) was deregistered in the U.S. in 1972 and in Canada in 1973, it was used extensively in urban aerial sprays to control mosquitoes and other insects in the 1940s and 1950s. Due to its high persistence, these residuals may still act as a source of DDTs to the atmosphere. One previous study showed higher DDT concentrations in window films collected in urban areas, with a clear urban to rural trend (*32*). Similarly, DDT concentrations in precipitation measured by NJADN also showed higher concentrations at the urban sites compared to rural sites (*14*).

The concentrations of *p,p'*-DDT relative to its degradation products, *p,p'*-DDE and *p,p'*-DDD, showed some interesting relations. On average, the concentrations were *p,p'*-DDT > *p,p'*-DDE > *p,p'*-DDD (see Tables CS2-CS8). The higher *p,p'*-DDT concentrations in precipitation do not necessary mean that there are "fresh" DDT sources around the Great Lakes; rather, the higher *p,p'*-DDT levels could be the result of the different properties of these compounds (*11*). For example, *p,p'*-DDE has a higher vapor pressure and a higher Henry's law constant compared to *p,p'*-DDT and *p,p'*-DDD (Table DS1). Therefore, more *p,p'*-DDE tends to partition into the gas phase. A study of pesticides in Quebec by Aulagnier and Poissant showed higher DDT precipitation concentrations compared to DDE despite higher DDE concentrations in the air (*26*). We observed the same effect at the IADN sites.

Results for the other pesticides are varied (Tables DS2-DS8). Dieldrin had the highest concentration in precipitation collected in Chicago. HCB had higher concentrations at the two Canadian sites, perhaps because HCB was used as an anti-fungal seed dressing for several crops

in Canada until 1972, while it has been banned in the U.S. since 1965. In addition, the re-volatilization of HCB from Lake Ontario may also contribute to its higher level at Point Petre (*33*). The highest concentrations of heptachlor epoxide in precipitation were also observed in Chicago, which may due to the application of this pesticide for termite control.

Temporal trends. The monthly VWM concentrations (C_p) of a given pesticide in precipitation collected at a given site were fitted by the following time-dependent function:

$$\ln C_p = a_0 + a_1 t + a_2 \sin\left(\frac{t}{a_3} + a_4\right) \quad (1)$$

where t is the time in Julian days relative to January 1 1990, a_0 is an intercept (unitless), a_1 is a first-order rate constant (in days^{-1}) describing the rate of exponential decrease or increase over time, a_2 is a periodic amplitude (unitless), a_3 is the length of the period (in days), and a_4 is the periodic offset (in days). Although samples have been collected from several sites since 1991, the analytical method changed in March of 1997 for the U.S. sites (*11*); thus, only data from March 1997 to December 2003 have been used for trend analysis.

Seventy-six datasets among the total of 126 datasets (18 pesticides × 7 IADN sites) had significant periodicity as indicating by both a_2 and a_3 being statistically significant at $P < 0.05$. Since 52 of those 76 datasets had a period length (a_3) of 366 ± 10 days, the period length for all 76 datasets with significant periodicity was forced to be one year; this simplified the calculation of the date during the year when the pesticide concentrations reached their maximum.

Among the 126 datasets, 36 of them showed significant long-term decreasing trends and six of them showed significant increasing trends (Figure D4). In particular, the concentrations of γ-HCH showed decreasing trends at five of the seven sites (the exceptions were Sleeping Bear Dunes and Sturgeon Point). *p,p'*-DDD concentrations decreased at Chicago, Sleeping Bear Dunes, Sturgeon Point, Burnt Island, and Point Petre. *p,p'*-DDE is the only pesticide decreasing at all seven IADN sites. α-Endosulfan concentrations only decreased at Point Petre, while at the other six sites, these concentrations did not change from 1997 to 2003. Interestingly, significant *increasing* trends were also observed for several pesticides. For example, β-HCH concentrations in precipitation significantly increased at Brule River, Eagle Harbor, and Sleeping Bear Dunes; β-endosulfan increased at Sturgeon Point; and *trans*-nonachlor increased at the two Canadian sites, Burnt Island and Point Petre.

Long-term decreasing trends of organochlorine pesticides in precipitation have been observed by other researchers (*9,10,34*). Simcik and co-workers reported on the temporal trends of several pesticides (e.g. γ-HCH, HCB, dieldrin, and γ-chlordane) in precipitation samples collected from the IADN sites from 1991 to 1997, with the half-lives ranging between 1 to 5 years (*10*). Comparing our results with those of Simcik and co-workers shows that most of the pesticides they reported stopped decreasing during the time period from 1997 to 2003. For example, between 1991 and 1997, α-HCH decreased with a half-life of 2-4 years at Eagle Harbor, Sleeping Bear Dunes, and Sturgeon Point; however, no decreasing trend of α-HCH was observed in the present study from 1997 onward. Similar situations were also observed for HCB, dieldrin, γ-chlordane, and *p,p'*-DDT. The lack of decreasing temporal trends for these pesticides indicates that a much slower decline (e.g. longer half-life than the sampling period in our study) is taking place after 1997.

A significant increase in β-HCH concentrations at Brule River, Eagle Harbor, and Sleeping Bear Dunes, Chicago, and Sturgeon Point from 1997 to 2002 has also been reported by Carlson and co-workers (*11*). β-HCH has the highest physical and metabolic stability among all

the isomers in technical HCH due to its relatively planar structure (*21*). Thus, β-HCH's environmental concentrations decrease more slowly than those of α-HCH and γ-HCH. As a result, it would be difficult to observe a significant decreasing trend over the seven-year time frame of this study for a pesticide with a longer atmospheric half-life. Carlson and co-workers suggested the observed increase in the precipitation concentrations of β-HCH is a brief exception to a general decrease that would be evident over a longer period of time (*11*). Indeed, by adding 2003 data into the dataset used by Carlson et al., the significant long-term increasing trends of β-HCH at Chicago and Sturgeon Point that they observed, disappeared.

Among all the pesticides measured by IADN, two different seasonal trends could be observed. In the first, the concentrations peaked in the summer for in-use pesticides, and in the second, the concentrations peaked in the winter for banned pesticides. The calculated dates on which the pesticide concentrations in precipitation maximize at each of the IADN sites are listed in Tables DS2-DS8. Concentrations of endosulfan and γ-HCH, which are still in-use, usually peaked in June or July, a time which corresponds well with their maximum agricultural usage (*35,36)*. The use of all the other pesticides is restricted in the U.S., with the exception of methoxychlor, which is still being used in agriculture and on livestock. The concentrations of these banned pesticides usually peaked in January or February. Higher concentration of γ-HCH and endosulfan in precipitation in the late spring to summer have been observed by other researchers (*17,26,37,38*). Incidentally, lindane was used mainly in central Canada on canola (*3*) and in the U.S. as a seed treatment (*39*) during the time of our sampling, but these uses in Canada were abandoned at the end of 2004 (*40*).

It has been suggested that competing processes could explain the winter concentration peak for the banned pesticides (*11*). These pesticides enter the atmosphere due to re-volatilization from lake and terrestrial surfaces, and these sources tend to maximize during the warmer summer months (*41*). However, the concentrations of these pesticides in the atmospheric particle phase tend to increase during the winter due to enhanced partitioning to the particles. In addition, snow is a better scavenger for both particle-associated and vapor-phase pesticides than is rain. The lower intensity of sunlight in the winter lowers the atmospheric OH radical concentration, which in turn increases the atmospheric lifetime of the pesticides, favoring their accumulation in the winter-time atmosphere and precipitation. All these mechanisms could contribute to higher winter concentrations in precipitation for banned OC pesticides.

The ratio between the highest and the lowest pesticide concentration can be calculated from the fitted a_2 parameter by taking its anti-logarithm (e^{2a_2}, the factor of 2 in the exponent is needed to calculate the peak-to-valley amplitude). These values are presented in Tables S2-S8. These ratios range between about 2-9, indicating that the seasonal variations can be substantial.

Acknowledgments

We thank Ilora Basu and Team IADN at Indiana University and Ed Sverko and the staff at the National Laboratory for Environmental Testing, Environment Canada for data acquisition; the U. S. Environmental Protection Agency's Great Lakes National Program Office for funding (Grant GL995656, Melissa Hulting, project monitor); and Bruce Harrison and Mary Lou Archer for managing the field collection at the Canadian sites.

Supporting Information

One table showing chemical structures and major properties of the OC pesticides discussed in this paper, seven tables showing values derived from modeled parameters for OC pesticides at

seven IADN sites, and one table showing the comparison between our data and other previous studies. These material are available free of charge via the Internet at http://pubs.acs.org.

Literature cited

1 Shen, L.; Wania, F.; Lei, Y. D.; Teixeira, C.; Muir, D. C. G.; Bidleman, G. F. Atmospheric distribution and long-range transport behavior of organochlorine pesticides in North America. *Environ. Sci. Technol.* **2005**, *39*, 409-420.

2 Dickhut, R. M.; Cincinelli, A.; Cochran, M.; Ducklow, H. W. Atmospheric concentrations and air-water flux of organochlorine pesticides along the Western Antarctic Peninsula. *Environ. Sci. Technol.* **2005**, *39*, 465-470.

3 Cortes, D. R.; Basu, I.; Sweet, C. W.; Brice, K. A.; Hoff, R. Am.; Hites, R. A. Temporal trends in gas-phase concentrations of chlorinated pesticides measured at the shores of the Great Lakes. *Environ. Sci. Technol.* **1998**, *32*, 1920-1927.

4 Buehler, S. S.; Basu, I.; Hites, R. A. Gas-phase polychlorinated biphenyl and hexachlorocyclohexane concentrations near the Great Lakes: a historical perspective. *Environ. Sci. Technol.* **2002**, *36*, 5051-5056.

5 Ryckman, D. P.; Weseloh, D. V.; Hamr, P.; Fox, G. A.; Collins, B.; Ewins, P. J.; Norstrom, R. J. Spatial and temporal trends in organochlorine contamination and bill deformities in double-crested cormorants (Phalacrocoraxauritus) from the Canadian Great Lakes. *Environ. Monit. Assess*. **1998**, *53,* 169-195.

6 Ashpole, S. L.; Bishop, C. A.; Brooks, R. J. Contaminant residues in snapping turtle (Chelydra s. serpentine) eggs from the Great Lakes-St. Lawrence River basin (1999 to 2000). *Arch. Environ. Con. Tox*. **2004**, *47*, 240-252.

7 Marvin, C.; Scott, P.; Williams, D.; Richardson, V.; Rossmann, R.; Van Hoof, P. Spatial and temporal trends in surface water and sediment contamination in the Laurentian Great Lakes. *Environ. Pollut.* **2001**, *129*, 131-144.

8 Chan, C. H.; Bruce, G.; Harrison, B. Wet deposition of organochlorine pesticides and polychlorinated biphenyls to the Great Lakes. *J. Great Lakes Res.* **1994**, *20*, 546-560.

9 Chan, C. H.; Williams, D. J.; Neilson, M. A.; Harrison, B.; Archer, M. L. J. Spatial and temporal trends in the concentrations of selected organochlorine pesticides (OCs) and polynuclear aromatic hydrocarbons (PAHs) in Great Lakes basin precipitation, 1986 to 1999. *Great Lakes Res.* **2003**, *29*, 448-459.

10 Simcik, M. F.; Hoff, R. M.; Strachan, W. M.; Sweet, C. W.; Basu, I.; Hites, R. A. Temporal trends of semi-volatile organic contaminants in Great Lakes precipitation. *Environ. Sci. Technol.* **2000**, *34*, 361-367.

11 Carlson, D. L.; Basu, I.; Hites, R. A. Annual variation of pesticide concentrations in Great Lakes precipitation. *Environ. Sci. Technol.* **2004**, *38*, 5290-5296.

12 Basu, I.; Arnold, K. *Quality Control Report 2002*; Indiana University: Bloomington, IN, 2003.

13 Fowlie, P. *Integrated Atmospheric Deposition Network (IADN) Interlaboratory Comparison for Pesticides, Polychlorinated Biphenyls and Polynuclear Aromatic Hydrocarbons in air and particulate samples, revision 2*; Cornerstone Science: Burlington, Ontario, 2002.

14 Gioia, R.; Offenberg, J. H.; Gigliotti, C. L.; Totten, L. A.; Du, S.-Y.; Eisenreich, S. J. Atmospheric concentrations and deposition of Organochlorine pesticides in the US Mid-Atlantic region. *Atmos. Environ*. **2005**, *39*, 2309-2322.
15 Sang, S.; Petrovic, S.; Cuddeford, V. *Lindane A Review of Toxicity and Environmental Fate*; World Wildlife Fund Canada: Toronto, ON, 1999.
16 Laabs, V.; Amelung, W.; Pinto, A. A.; Wantzen, M.; Silva, C. J.; Zech, W. Pesticides in surface water, sediment, and rainfall of the northeastern Pantanal Basin, Brazil. *J. Environ. Qual*. **2002**, *31*, 1636-1648.
17 Karlsson, H.; Muir, D. C. G.; Teixiera, C. F.; Burniston, D. A.; Strachan, W. M. J.; Hecky, R. E.; Mwita, J.; Bootsma, H. A.; Grift, N. P.; Kidd, K. A.; Rosenberg, B. Persistent chlorinated pesticides in air, water and precipitation form the Lake Malawi Area, Southern Africa. *Environ. Sci. Technol.* **2000**, *34*, 4490-4495.
18 Motelay-Massei, A.; Harner, T.; Shoeib, M.; Diamond, M.; Stern, G.; Rosenberg, B. Using passive air sampler to assess urban-rural trends for persistent organic pollutants and polycyclic aromatic hydrocarbons. 2. Seasonal trends for PAHs, PCBs, and organochlorine pesticides. *Environ. Sci. Technol.* **2005**, *39*, 5763-5773.
19 Buehler, S. S.; Hites, R. A. The Great Lakes' Integrated Atmospheric Deposition Network. *Environ. Sci. Technol.* **2002**, *36*, 355A-359A.
20 Wania, F.; Haugen, J.-E. Long term measurements of wet deposition and precipitation scavenging of hexachlorocyclohexanes in Southern Norway. *Environ. Pollut*. **1999**, *105*, 381-386.
21 Willett, K. L.; Ulrich, E. M.; Hites, R. A. Differential toxicity and environmental fates of hexachlorocyclohexane isomers. *Environ. Sci. Technol.* **1998**, *32*, 2197-2207.
22 Brubaker, W. W.; Hites, R. A. OH reaction kinetics of gas-phase α- and γ-hexachlorocyclohexane and hexachlorobenzene. *Environ. Sci. Technol.* **1998**, *32*, 766-769.
23 Li, Y.-F.; Scholtz, M. T.; Van Heyst, B. J. Global gridded emission inventories of β-hexachlorocyclohexane. *Environ. Sci. Technol.* **2003**, *37*, 3493-3498.
24 Iwata, H.; Tanabe, S.; Sakai, N.; Tatsukawa, R. Distribution of persistent organochlorines in the oceanic air and surface seawater and the role of ocean on their global transport and fate. *Environ. Sci. Technol.* **1993**, *27*, 1080-1098.
25 Li, Y.-F.; Struger, J.; Waite, D.; Ma, J. Gridded Canadian lindane usage inventories with 1/6 º × 1/4 º latitude and longitude resolution. *Atmos. Environ*. **2004**, *38*, 1117-1121.
26 Aulagnier, F.; and Poissant, L. Some pesticides occurrence in air and precipitation in Quebec, Canada. *Environ. Sci. Technol.* **2005**, *39*, 2960-2967.
27 Hafner, W. D.; Hites, R. A. Potential sources of pesticides, PCBs, and PAHs to the atmosphere of the Great Lakes. *Environ. Sci. Technol.* **2003**, *37*, 3764-3773.
28 Harris, M.L.; Van den Heuvel, M.R.; Rouse, J.; Martin, P.A.; Struger, J.; Bishop, C.A.; Takacs, P. *Pesticides in Ontario: A Critical Assessment of Potential Toxicity of Agricultural Products to Wildlife, with Consideration for Endocrine Disruption. Volume 1: Endosulfan, EBDC fungicides, Dinitroaniline herbicides, 1,3-Dichloropropene, Azinphos-methyl, and pesticide mixtures*. Technical Report Series No.340. Canadian Wildlife Service, Ontario Region. 2000.

29 Savage, E. P. Termiticide use and indoor air quality in the United States. *Rev. Environ. Contam. Toxicol.* **1989**, *110*, 117-130.
30 Persistent Bioaccumulative and Toxic (PBT) Chemical Program: Chlordane; U. S. Environmental Protection Agency: Washington, DC, 2002; http://www.epa.gov/opptintr/pbt/chlordane.htm
31 Harner, T.; Shoeib, M.; Diamond, M.; Stern, G.; Rosenberg, B. Using passive air samplers to assess urban-rural trends for persistent organic pollutants. 1. polychlorinated biphenyls and Organochlorine pesticides. *Environ. Sci. Technol.* **2004**, *38*, 4474-4483.
32 Gingrich, S. E.; Diamond, M. L.; Stern, G. A,; McCarry, B. E. Atmospherically derived organic surface films along an urban-rural gradient. *Environ. Sci. Technol.* **2001**, *35*, 4031-4037.
33 Buehler, S.; Hafner, W.; Basu, I.; Audette, C. V.; Brice, K. A.; Chan, C. H.; Froude, F.; Galarneau, E.; Hulting, M. L.; Jantunen, L.; Neilson, M.; Puckett, K.; Hites, R. A. *Atmospheric Deposition of Toxic Substances to the Great Lakes: IADN Results through 1998, Environmental Canada and The U.S. Environmental Protection Agency.*
34 Buijsman, E.; Van Pul W. A. J. Long-term measurements of γ-HCH in precipitation in the Netherlands. *Water, Air, Soil Pollut.* **2003**, *150*, 59-71.
35 Buehler, S. S.; Basu, I.; Hites, R. A. Causes of variability in pesticide and PCB concentrations in air near the Great Lakes. *Environ. Sci. Technol.* **2004**, *38*, 414-422.
36 Waite, D. T.; Gurprasad, N. P.; Sproull, J. F.; Quiring, D. V.; Kotylak, M. W. Atmospheric movements of Lindane (γ-hexachlorocyclohexane) from canola fields planted with treated seeds. *J. Environ. Qual*. **2001**, *30*, 768-775.
37 Teil, M.J.; Blanchard, M.; Chevreuil, M. Atmospheric deposition of organochlorines (PCBs and pesticides) in northern France. *Chemosphere* **2004**, *55*, 501-514.
38 Brun, G. L.; Howell, G. D.; O'Neill, H. J. Spatial and temporal patterns of organic contaminants in wet precipitation in Atlantic Canada. *Environ. Sci. Technol.* **1991**, *25*, 1249-1261.
39 Walker, K.; Vallero, D. A.; and Lewis, R. G. Factors influencing the distribution of lindane and other hexachlorocyclohexanes in the environment. *Environ. Sci. Technol.* **1999**, *33*, 4373-4378.
40 http://panna.org/resources/documents/lindaneRelease.pdf, accessed on August 12, 2005.
41 Buehler, S. S.; Basu, I.; Hites, R. A. A comparison of PAH, PCB, and pesticide concentrations in air at two rural sites on Lake Superior. *Environ. Sci. Technol.* **2001**, *35*, 2417-2422.
42. Grynkiewicz, M.; Polkowska, Z.; Gorecki, T.; Namiesnik, J. Pesticides in precipitation from an urban region in Poland (Gdansk-Sopot-Gdynia Tricity) between 1998 and 2000. *Water, Air, Soil Pollut.* **2003**, *149*, 3-16.

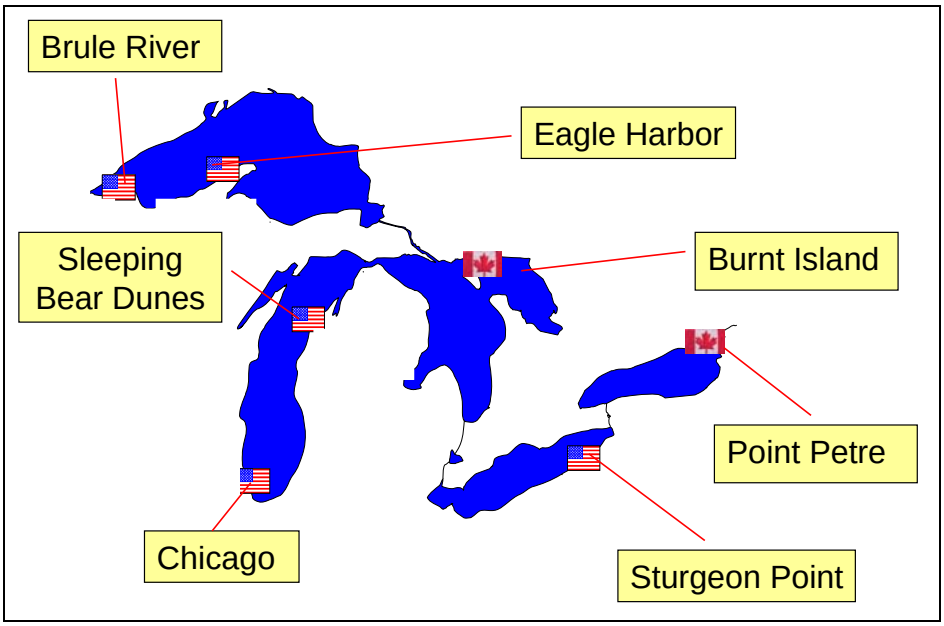

Figure D1. Map of the Great Lakes indicating the sampling sites at Brule River and Eagle Harbor, near Lake Superior; Chicago and Sleeping Bear Dunes, near Lake Michigan; Sturgeon Point, near Lake Erie; Burnt Island, near Lake Huron; and Point Petre, near Lake Ontario. Chicago is an urban site, Sturgeon Point is semi-urban site and the other sites are remote sites.

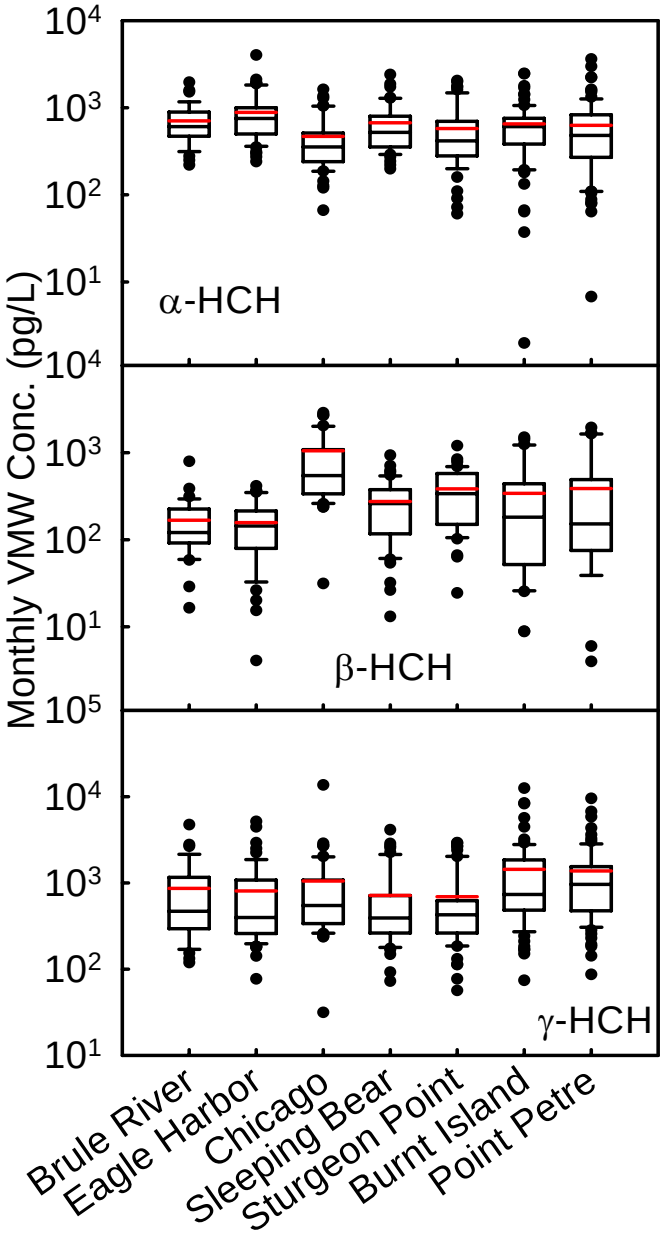

Figure D2. Concentrations of α-HCH (top), β-HCH (middle), and γ-HCH (bottom) in precipitation collected from 1997 to 2003 at the seven IADN sites. The boxes represent the 25th to 75th percentiles, the black lines in the boxes are the medians and the red lines are the means. The two vertical lines outside each box extend to the outliers representing the 10th and 90th percentiles; and outliers are shown individually.

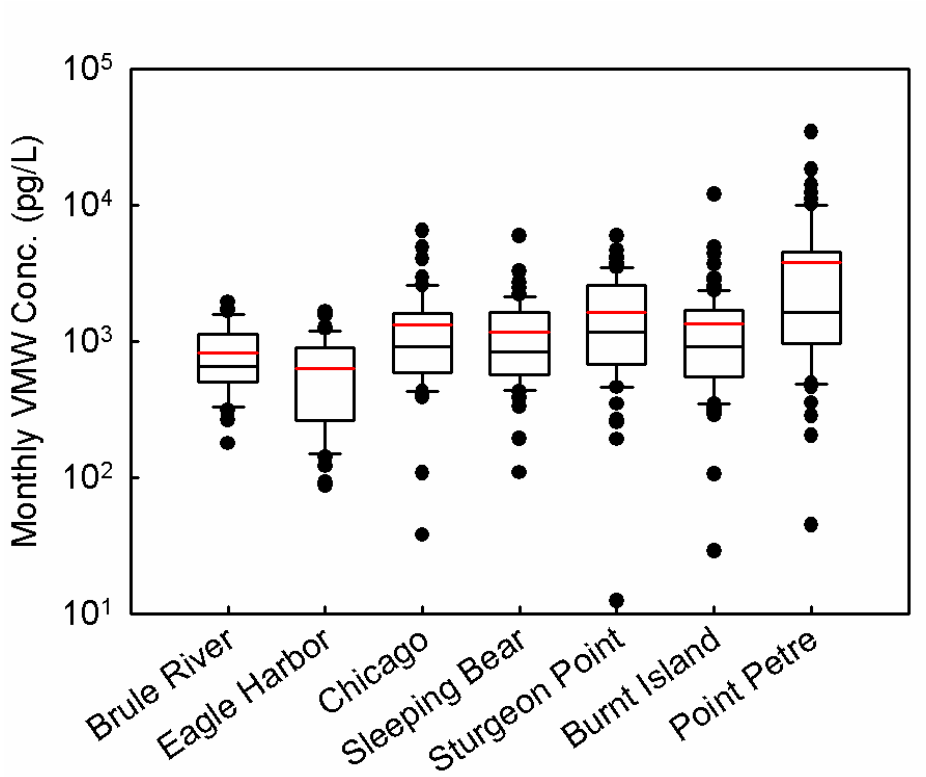

Figure D3. Concentrations of endosulfans (α- plus β-endosulfan) in precipitation at the seven IADN sites. See Figure D2 for the description of the box-plots.

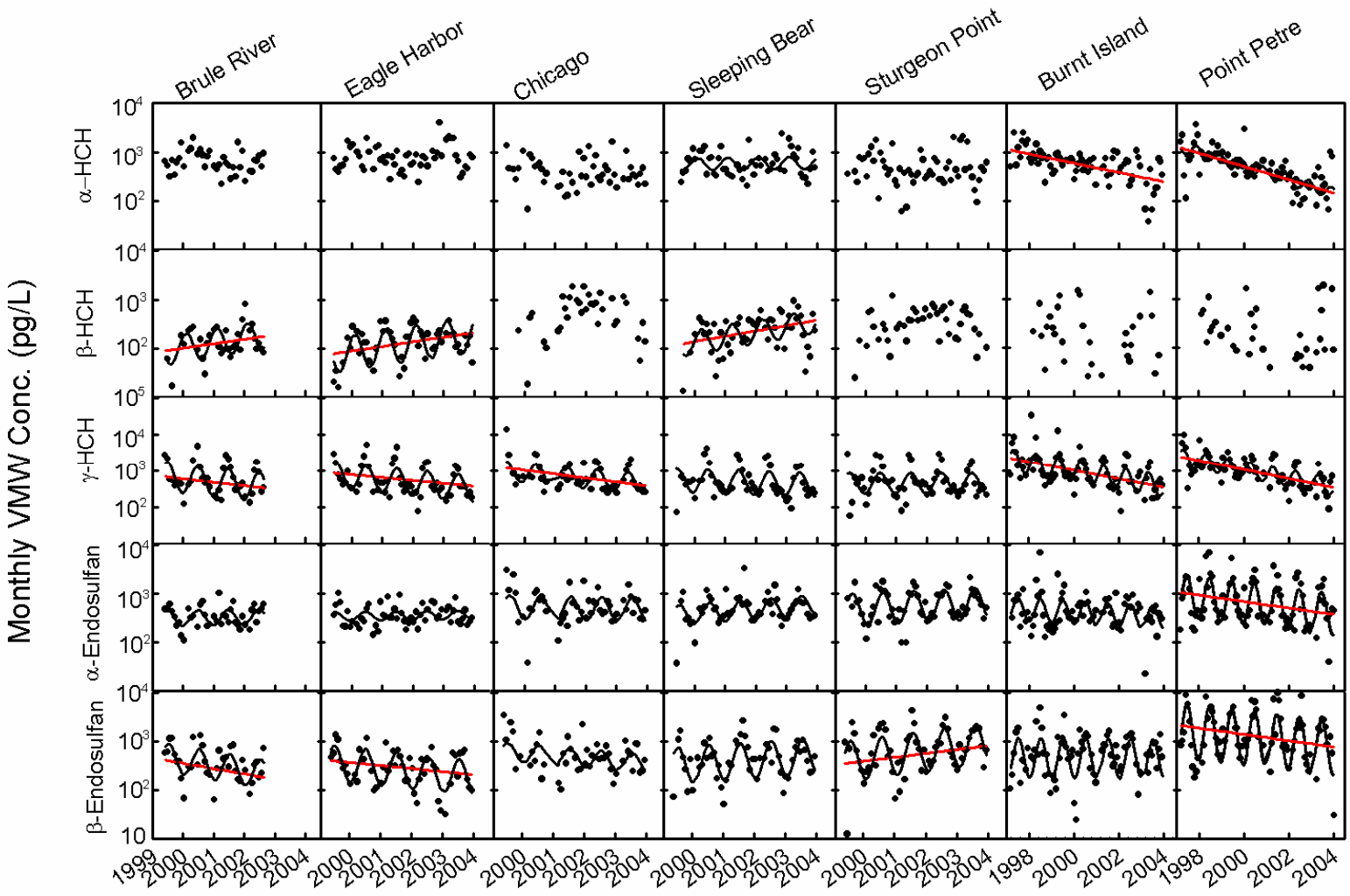

Figure D4. Organochlorine pesticide concentrations in precipitation collected at seven IADN sites near the Great Lakes. The black curve is the fitting line of the sinusoidal model with the period length (a_3) set to one year. The red lines indicate long-term significant decreasing or increasing trends. Detailed information on the fitting parameters is in the Supporting Information.

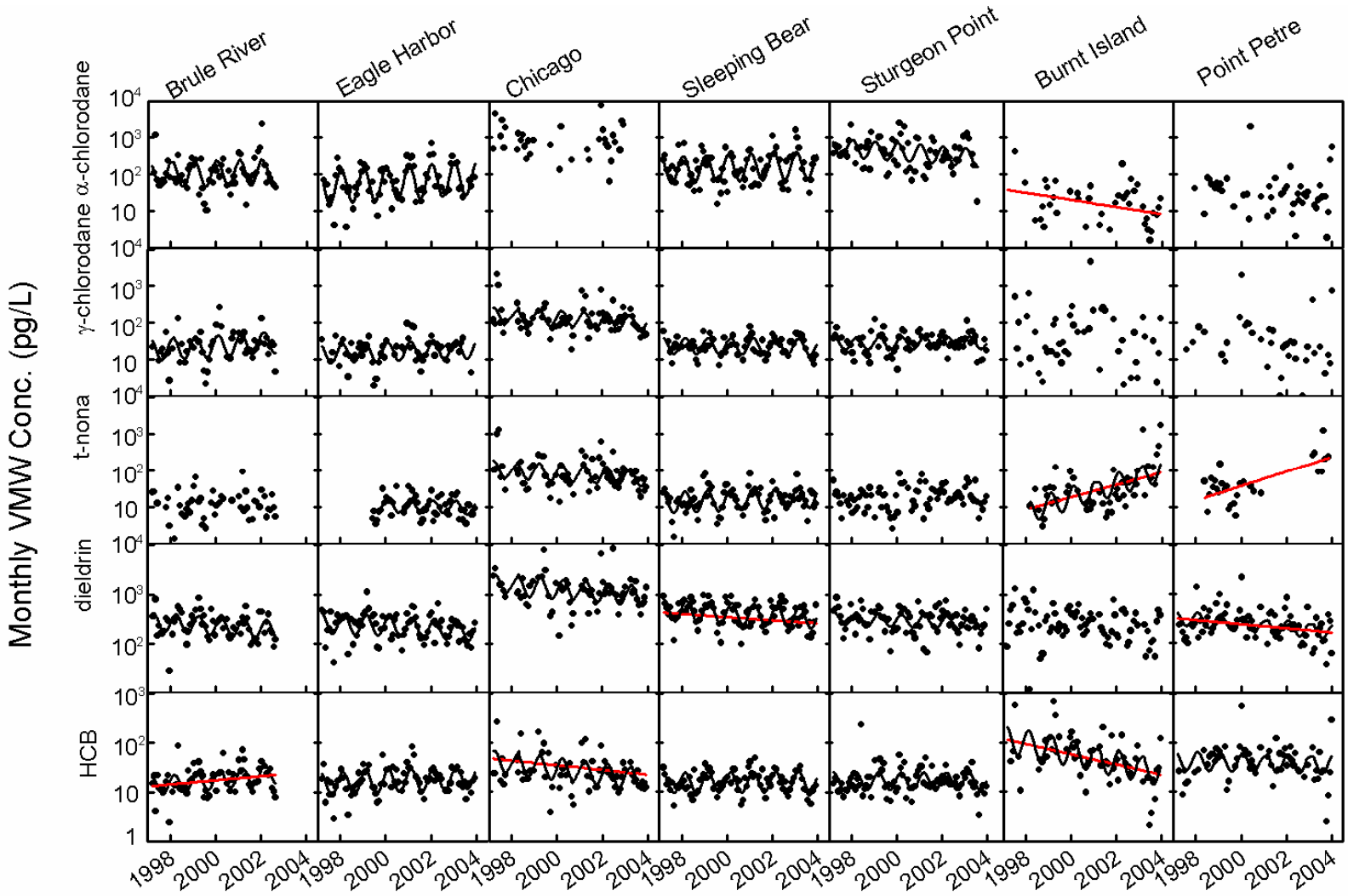

Figure D4 (continued).

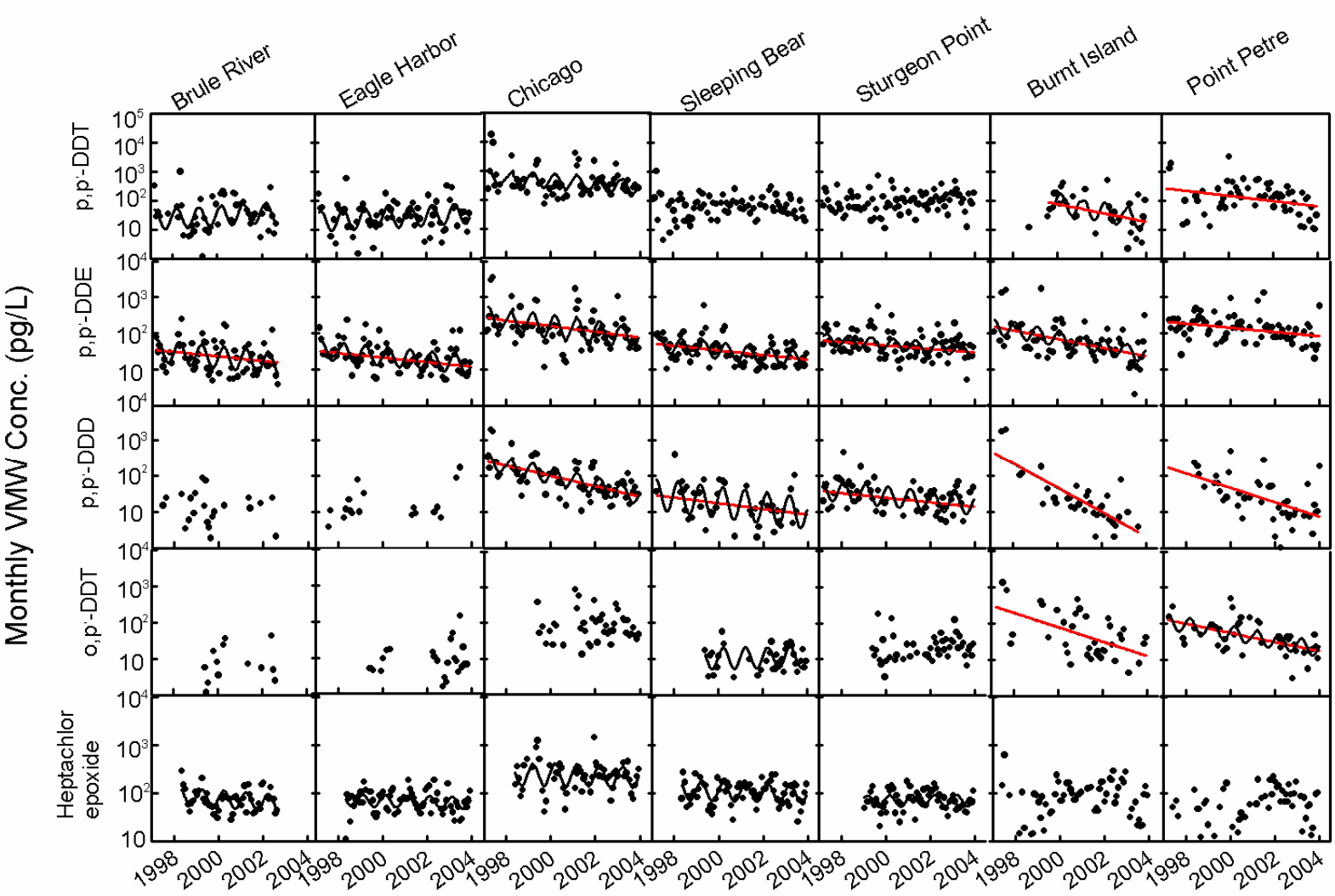

Figure D4 (continued).

Supporting Information for:

Temporal and Spatial Trends of Organochlorine Pesticides in Great Lakes Precipitation

Ping Sun,[1] Sean Backus,[2] Pierrette Blanchard,[2] and Ronald A Hites*[1]

[1]School of Public and Environmental Affairs
Indiana University
Bloomington, Indiana, 47405 USA

and
[2]Environment Canada
4905 Dufferin Street
Toronto, ON M3H 5T4 Canada

*Corresponding Author Email: hitesr@indiana.edu

This Supporting Information contains nine tables. Table DS1 shows the chemical structure and properties of the organochlorine pesticides discussed in this paper. Tables DS2-DS8 show the values derived from modeled parameters for pesticides at seven IADN sites. Table DS9 is a comparison between the results in this study with previous studies conducted by other researchers.

The following equation was used to fit the data:

$$\ln C_p = a_0 + a_1 t + a_2 \sin\left(\frac{t}{a_3} + a_4\right)$$

where t is the time in Julian days relative to January 1 1990, a_0 is an intercept (unitless), a_1 is a first-order rate constant (in days^{-1}) describing the rate of exponential decrease or increase over time, a_2 is a periodic amplitude (unitless), a_3 is the length of the period (in days), and a_4 is the periodic offset (in days).

Among 126 data sets, 76 datasets showed significant periodicity as indicating by both a_2 and a_3 being statistically significant at $P < 0.05$, and 52 of the 76 data sets had a period length (a_3) of 366 ± 10 days. Thus, the period length for all 76 datasets with significant periodicity was forced to be one year, which simplified the calculation of the date during the year when the concentrations reached their maximum.

The tables show results of the fit to this sinusoidal model. The results are listed as mean ± standard error. Normal font numbers are significant for $0.01 < P < 0.05$; italic font numbers are significant for $0.001 < P < 0.01$, bold font numbers are significant at $P < 0.001$. "NS" means "not significant" at $P > 0.05$. A negative half-life is actually a doubling time.

Table DS1. Chemical structures and properties of OC pesticides[1]

OC pesticide	Structure	MW	Vapor pressure (mm Hg)	Henry's Law constant (atm-m^3/mol, at 25°C)	log K_{ow}
α-HCH	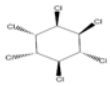	290.83	4.5×10^{-5} at 25°C	1×10^{-5}	3.8
β-HCH	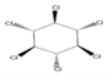	290.83	3.6×10^{-7} at 20°C	7.44×10^{-7}	3.78
γ-HCH	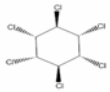	290.83	4.2×10^{-5} at 20°C	1.40×10^{-5}	3.72
α-Endosulfan	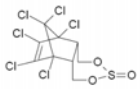	406.93	1×10^{-5} at 25°C	1×10^{-5}	3.83
β-Endosulfan	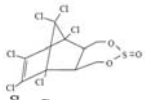	406.93	1×10^{-5} at 25°C	1.91×10^{-5}	3.52
α-Chlordane	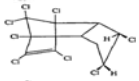	409.76	2.2×10^{-5} at 20°C	1.91×10^{-5}	6.0
γ-Chlordane	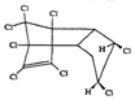	409.76	2.9×10^{-5} at 20°C	8.31×10^{-5}	6.0
Hexachlorobenzene		284.78	1.09×10^{-5} at 20°C	5.8×10^{-4}	5.73
p, p'-DDT	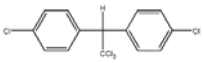	354.49	1.6×10^{-7} at 20°C	8.3×10^{-6}	6.91
p, p'-DDD	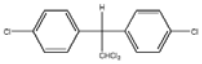	320.05	1.35×10^{-6} at 25°C	4.0×10^{-6}	6.02
p, p'-DDE	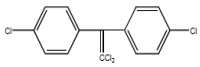	318.03	6.0×10^{-6} at 25°C	2.1×10^{-5}	6.51
o, p'-DDT	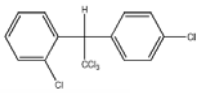	354.49	1.1×10^{-7} at 20°C	5.9×10^{-7}	6.79
Heptachlor epoxide	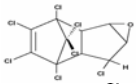	389.40	2.6×10^{-6} at 20°C	3.2×10^{-5}	5.40
Aldrin	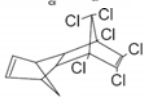	364.91	7.5×10^{-5} at 20°C	4.9×10^{-5}	6.50
dieldrin	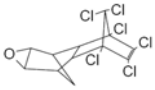	380.91	3.1×10^{-6} at 20°C	5.2×10^{-5}	6.2
Endrin	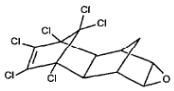	380.90	2.0×10^{-7} at 20°C	4.0×10^{-7}	5.6
Methoxychlor	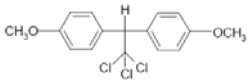	345.65	1.4×10^{-6} at 25°C (estimate)	1.6×10^{-5} (estimate)	4.68-5.08

[1] Data is obtained from Agency for Toxic Substances and Disease Registry. www.atsdr.cdc.gov/toxprofiles/

Table DS2. Fit parameters for pesticide concentrations in precipitation at Brule River

Pesticides	Half-life (years), (ln2)/365*a_1	Peak-to-valley ratio, e^{2a_2}	Maximum date (± days)	No. of detects	Average conc. (pg/L)	r^2
α-HCH	NS	NS	NS	39	710 ± 60	NS
β-HCH	–2.8 ± 1.2*	**3.8 ± 1.3**	**Feb 8 ± 12**	34	170 ± 24	0.50
γ-HCH	3.2 ± 1.6	**6.5 ± 1.3**	**Jun 24 ± 9**	39	860 ± 150	0.56
α-Endosulfan	NS	*2.1 ± 1.2*	**Jun 24 ± 16**	39	380 ± 31	0.28
β-Endosulfan	2.7 ± 1.2	**3.8 ± 1.3**	**Jul 13 ± 12**	39	450 ± 53	0.47
α-Chlordane	NS	**5.1 ± 1.4**	**Jan 21 ± 15**	63	180 ± 41	0.31
γ-Chlordane	NS	**3.9 ± 1.3**	*Feb 10 ± 13*	56	33 ± 5.5	0.31
trans-Nonachlor	NS	NS	NS	49	16 ± 2.2	NS
Dieldrin	NS	**2.4 ± 1.2**	NS	65	270 ± 20	0.30
Hexachlorobenzene	–6.3 ± 2.1*	**4.8 ± 1.4**	*Feb 3 ± 10*	65	21 ± 1.9	0.30
p,p'-DDT	NS	*4.9 ± 1.8*	NS	50	77 ± 21	0.15
p,p'-DDD	NS	NS	NS	22	20 ± 4.6	NS
p,p'-DDE	4.7 ± 2.4	**4.1 ± 1.3**	NS	61	36 ± 5.7	0.52
o,p'-DDT	Limited data	NS	NS	13	12 ± 3.7	NS
Heptachlor epoxide	NS	**2.3 ± 1.2**	NS	50	82 ± 7.0	0.35
Aldrin	Not available					
Endrin	1.1 ± 0.4	NS	NS	24	180 ± 45	0.49
Methoxychlor	NS	NS	NS	24	150 ± 35	NS

*A negative half-life indicates that the concentrations are increasing and the listed value is the doubling time.

Table DS3. Fit parameters for pesticide concentrations in precipitation at Eagle Harbor

Pesticides	Half-life (years), (ln2)/365*a_1	Peak-to-valley ratio, e^{2a_2}	Maximum date (± days)	No. of detects	Average conc. (pg/L)	r^2
α-HCH	NS	NS	NS	56	890 ± 84	NS
β-HCH	*–3.2 ± 1.0**	**2.8 ± 1.2**	**Feb 8 ± 8**	64	160 ± 14	0.54
γ-HCH	*3.8 ± 1.5*	**5.2 ± 1.3**	**Jun 24 ± 8**	56	810 ± 130	0.54
α-Endosulfan	NS	1.5 ± 1.2	**Jun 14 ± 25**	56	400 ± 27	0.10
β-Endosulfan	4.7 ± 2.4	**5.1 ± 1.3**	**Jun 12 ± 8**	54	370 ± 40	0.52
α-Chlordane	NS	**8.3 ± 1.3**	**Feb 14 ± 9**	74	110 ± 14	0.52
γ-Chlordane	NS	**3.3 ± 1.3**	**Feb 4 ± 11**	64	22 ± 2.3	0.30
trans-Nonachlor	NS	*2.2 ± 1.3*	*Feb 1 ± 16*	53	12 ± 1.2	0.20
Dieldrin	NS	**2.6 ± 1.2**	*Jan 24 ± 7*	83	250 ± 19	0.32
Hexachlorobenzene	NS	**2.9 ± 1.2**	**Feb 12 ± 8**	82	21 ± 1.5	0.41
p,p'-DDT	NS	**5.1 ± 1.4**	NS	69	49 ± 7.4	0.25
p,p'-DDD	NS	NS	NS	19	36 ± 12	NS
p,p'-DDE	*4.7 ± 1.2*	**3.3 ± 1.2**	NS	78	27 ± 3.6	0.38
o,p'-DDT	NS	NS	NS	24	16 ± 5.9	NS
Heptachlor epoxide	NS	*1.8 ± 1.2*	*Feb 13 ± 17*	67	78 ± 4.8	0.14
Aldrin	Limited data	NS	NS	6	3.5 ± 2.8	NS
Endrin	NS	**5.2 ± 1.5**	**Jan 16 ± 12**	43	200 ± 37	0.33
Methoxychlor	Limited data	NS	NS	24	75 ± 11	NS

*A negative half-life indicates that the concentrations are increasing and the listed value is the doubling time.

Table DS4. Fit parameters for pesticide concentrations in precipitation at Sleeping Bear Dunes

Pesticides	Half-life (years), (ln2)/365*a_1	Peak-to-valley ratio, e^{2a_2}	Maximum date (± days)	No. of detects	Average conc. (pg/L)	r^2
α-HCH	NS	1.8 ± 1.2	Feb 4 ± 22	54	670 ± 60	0.13
β-HCH	*–2.8 ± 1.0**	*3.0 ± 1.4*	NS	51	270 ± 27	0.29
γ-HCH	NS	**4.4 ± 1.3**	**Jun 9 ± 11**	56	720 ± 110	0.39
α-Endosulfan	NS	**2.5 ± 1.2**	**Jun 30 ± 14**	56	590 ± 64	0.27
β-Endosulfan	NS	**5.4 ± 1.3**	**Jul 18 ± 9**	55	600 ± 70	0.49
α-Chlordane	NS	**5.4 ± 1.3**	**Jan 23 ± 8**	81	250 ± 31	0.39
γ-Chlordane	NS	**2.7 ± 1.2**	*Feb 28 ± 9*	73	26 ± 1.8	0.37
trans-Nonachlor	NS	**3.7 ± 1.2**	**Feb 22 ± 9**	78	22 ± 2.0	0.36
Dieldrin	9.5 ± 4.7	**2.7 ± 1.1**	Mar 14 ± 8	85	420 ± 24	0.46
Hexachlorobenzene	NS	**2.6 ± 1.1**	**Feb 25 ± 7**	84	18 ± 1.0	0.46
p,p'-DDT	NS	NS	NS	77	79 ± 6.9	NS
p,p'-DDD	3.8 ± 1.5	**7.3± 1.5**	Mar 1 ± 12	41	24 ± 4.2	0.46
p,p'-DDE	4.7 ± 1.2	**2.8 ± 1.2**	NS	83	42 ± 8.4	0.40
o,p'-DDT	NS	**3.8 ± 1.3**	NS	35	13 ± 1.8	0.42
Heptachlor epoxide	NS	**2.4 ± 1.1**	NS	45	32 ± 3.3	0.33
Aldrin	Limited Data			5	2.7 ± 1.2	NS
Endrin	2.8 ± 1.4	2.9 ± 1.5	*Feb 3 ± 20*	48	160 ± 34	0.39
Methoxychlor	NS	NS	NS	41	250 ± 50	NS

*A negative half-life indicates that the concentrations are increasing and the listed value is the doubling time.

Table DS5. Fit parameters for pesticide concentrations in precipitation at Sturgeon Point

Pesticides	Half-life (years), (ln2)/365*a_1	Peak-to-valley ratio, e^{2a_2}	Maximum date (± days)	No. of detects	Average conc. (pg/L)	r^2
α-HCH	NS	NS	NS	58	580 ± 62	NS
β-HCH	NS	NS	NS	44	380 ± 38	NS
γ-HCH	NS	**3.7 ± 1.3**	**Jun 19 ± 13**	60	690 ± 96	0.28
α-Endosulfan	NS	**4.5 ± 1.2**	**Jul 24 ± 7**	59	710 ± 62	0.56
β-Endosulfan	–3.8 ± 1.5*	**6.6 ± 1.3**	**Aug 4 ± 9**	60	960 ± 110	0.46
α-Chlordane	NS	*3.0 ± 1.4*	**Jan 14 ± 15**	68	540 ± 62	0.20
γ-Chlordane	NS	**2.2 ± 1.2**	NS	79	34 ± 2.5	0.19
trans-Nonachlor	NS	NS	NS	84	24 ± 1.8	0.16
dieldrin	NS	*1.8 ± 1.2*	NS	87	310 ± 17	0.17
Hexachlorobenzene	NS	**2.3 ± 1.2**	Mar 7 ± 11	87	19 ± 1.2	0.25
p,p'-DDT	NS	NS	NS	85	130 ± 13	NS
p,p'-DDD	4.7 ± 2.4	*3.5 ± 1.4*	*Feb 5 ± 15*	61	31 ± 4.0	0.23
p,p'-DDE	6.3 ± 2.1	*2.0 ± 1.2*	**May 3 ± 18**	86	67 ± 9.1	0.19
o,p'-DDT	NS	NS	NS	48	29 ± 4.9	NS
Heptachlor epoxide	NS	*1.7 ± 1.2*	NS	62	77 ± 4.5	0.33
Aldrin	Limited Data			7	1.4 ± 0.4	NS
Endrin	NS	NS	NS	47	180 ± 24	NS
Methoxychlor	2.2 ± 0.7	NS	NS	52	370 ± 66	0.17

*A negative half-life indicates that the concentrations are increasing and the listed value is the doubling time.

Table DS6. Fit parameters for pesticide concentrations in precipitation at Chicago

Pesticides	Half-life (years), (ln2)/365*a_1	Peak-to-valley ratio, e^{2a_2}	Maximum date (± days)	No. of detects	Average conc. (pg/L)	r^2
α-HCH	NS	NS	NS	50	470 ± 48	NS
β-HCH	NS	NS	NS	34	650 ± 82	NS
γ-HCH	6.3 ± 4.2	**4.1 ± 1.4**	**Jun 1 ± 13**	50	1100 ± 270	0.37
α-Endosulfan	NS	*3.0 ± 1.3*	**Jul 7 ± 14**	50	700 ± 82	0.26
β-Endosulfan	NS	2.3 ± 1.4	*Jul 17 ± 19*	47	680 ± 94	0.21
α-Chlordane	NS	NS	NS	36	1100 ± 230	NS
γ-Chlordane	NS	*2.7 ± 1.3*	NS	69	150 ± 17	0.23
trans-Nonachlor	NS	*2.9 ± 1.3*	NS	67	100 ± 12	0.22
Dieldrin	NS	*2.6 ± 1.3*	NS	69	1400 ± 180	0.24
Hexachlorobenzene	6.3 ± 2.1	*2.8 ± 1.3*	NS	67	32 ± 3.9	0.25
p,p'-DDT	NS	*3.2 ± 1.4*	NS	68	570 ± 93	0.21
p,p'-DDD	**2.1 ± 0.2**	*3.0 ± 1.3*	NS	64	110 ± 17	0.52
p,p'-DDE	*3.8 ± 1.5*	**4.3 ± 1.4**	**May 3 ± 18**	67	210 ± 37	0.34
o,p'-DDT	NS	NS	NS	44	130 ± 24	NS
Heptachlor epoxide	NS	**3.0 ± 1.3**	NS	58	290 ± 33	0.29
Aldrin	NS	NS	NS	29	16 ± 5.8	NS
Endrin	NS	NS	NS	34	180 ± 25	NS
Methoxychlor	NS	NS	NS	52	370 ± 56	NS

Table DS7. Fit parameters for pesticide concentrations in precipitation at Brunt Island

Pesticides	Half-life (years), (ln2)/365*a_1	Peak-to-valley ratio, e^{2a_2}	Maximum date (± days)	No. of detects	Average conc. (pg/L)	r^2
α-HCH	**3.2 ± 0.5**	NS	NS	58	660 ± 56	0.38
β-HCH	NS	NS	NS	32	340 ± 76	NS
γ-HCH	**2.9 ± 0.5**	**4.0 ± 1.2**	Apr 28 ± 11	80	1400 ± 220	0.50
α-Endosulfan	NS	**2.9 ± 1.2**	**Jul 3 ± 12**	80	600 ± 93	0.26
β-Endosulfan	NS	**6.4 ± 1.3**	**Jul 10 ± 8**	80	760 ± 85	0.36
α-Chlordane	3.2 ± 1.6	NS	NS	68	540 ± 62	0.20
γ-Chlordane	NS	NS	NS	47	86 ± 19	NS
trans-Nonachlor	**–1.6 ± 0.3***	*4.2 ± 1.6*	*Feb 5 ± 16*	51	110 ± 42	0.39
Dieldrin	NS	NS	NS	80	300 ± 26	NS
Hexachlorobenzene	*2.9 ± 0.8*	*3.5 ± 1.4*	*Feb 15 ± 14*	59	82 ± 16	0.34
p,p'-DDT	2.0 ± 0.8	4.8 ± 2.0	NS	32	92 ± 21	0.31
p,p'-DDD	**0.9 ± 0.1**	NS	NS	32	29 ± 6.9	0.62
p,p'-DDE	**2.6 ± 0.6**	*2.8 ± 1.4*	*Feb 8 ± 17*	71	130 ± 36	0.32
o,p'-DDT	*1.5 ± 0.4*	NS	NS	38	100 ± 27	0.33
Heptachlor epoxide	NS	NS	NS	65	100 ± 11	NS
Aldrin	Limited Data			3	470 ± 230	NS
Endrin	NS	NS	NS	18	230 ± 88	NS
Methoxychlor	*2.0 ± 0.7*	*5.5 ± 1.8*	**Jun 8 ± 23**	42	280 ± 80	0.33

*A negative half-life indicates that the concentrations are increasing and the listed value is the doubling time.

Table DS8. Fit parameters for pesticide concentrations in precipitation at Point Petre

Pesticides	Half-life (years), (ln2)/365*a_1	Peak-to-valley ratio, e^{2a_2}	Maximum date (± days)	No. of detects	Average conc. (pg/L)	r^2
α-HCH	**2.2 ± 0.3**	1.7 ± 1.2	**Dec 3 ± 26**	81	630 ± 68	0.48
β-HCH	NS	NS	NS	36	390 ± 88	NS
γ-HCH	**2.5 ± 0.3**	**2.9 ± 1.2**	NS	79	1400 ± 170	0.58
α-Endosulfan	*5.3 ± 2.0*	**6.4 ± 1.3**	**Jun 17 ± 8**	80	600 ± 93	0.44
β-Endosulfan	5.8 ± 2.6	**14 ± 1.4**	**Jun 17 ± 7**	80	760 ± 85	0.52
α-Chlordane	NS	NS	NS	46	50 ± 13	NS
γ-Chlordane	NS	NS	NS	36	110 ± 58	NS
trans-Nonachlor	**–1.6 ± 0.3***	NS	NS	29	110 ± 42	0.39
Dieldrin	7.3 ± 2.8	*2.0 ± 1.2*	*Feb 1 ± 18*	77	300 ± 35	0.19
Hexachlorobenzene	NS	*2.4 ± 1.3*	*Jan 29 ± 17*	65	55 ± 9.3	0.34
P,p'-DDT	3.2 ± 1.0	NS	NS	59	200 ± 40	0.12
p,p'-DDD	**1.5 ± 0.3**	NS	NS	45	57 ± 14	0.30
p,p'-DDE	*6.3 ± 2.1*	NS	NS	77	180 ± 23	0.16
o,p'-DDT	*2.7 ± 0.8*	2.6 ± 1.5	NS	42	71 ± 14	0.38
Heptachlor epoxide	NS	NS	NS	52	78 ± 7.4	NS
Aldrin	Limited Data			3	470 ± 230	NS
Endrin	1.8 ± 0.7	NS	NS	20	180 ± 52	0.25
Methoxychlor	3.8 ± 2.3	3.6 ± 1.7	**Jun 20 ± 22**	46	420 ± 92	0.33

*A negative half-life indicates that the concentrations are increasing and the listed value is the doubling time.

Table DS9. Range and Annual Mean Concentration (ng/L) of Selected Organochlorine Pesticides in Precipitation from Various Studies

Pesticide	Sample Location	Site type	Sample time	Conc. Range	Mean Conc.	Ref.
α-HCH	Gdansk region, Poland	Urban[1]	1998-2000	1-12		(42)
	Paris, France	urban	Oct. 99-Oct. 00	0.6-7.4	2.8	(37)
	Chicago, U.S.	urban	Jun 99-Dec 03	0.066-1.6	0.47	this study
	Quessant, France	rural	Oct. 99-Oct. 00	0.3-0.9	0.48	(37)
	Senga Bay, South Africa	rural	Feb 97-May 98	0.06-0.3	0.13	(17)
	Sleeping Bear Dunes, U.S.	rural	Jun 99-Dec 03	0.2-2.4	0.67	this study
	Burnt Island, Canada	rural	Mar 97-Dec 03	0.04-2.5	0.66	this study
β-HCH	Senga Bay, South Africa	rural	Feb 97-May 98	<0.06	0.024	(17)
	Chicago, U.S.	urban	Jun 99-Dec 03	0.018-1.8	0.64	this study
	Sleeping Bear Dunes, U.S.	rural	Jun 99-Dec 03	0.013-0.93	0.27	this study
	Burnt Island, Canada	rural	Mar 97-Dec 03	0.009-1.5	0.34	this study
γ-HCH	Paris, France	urban	Oct. 99-Oct. 00	5.2-28.6	15.9	(37)
	Chicago, U.S.	urban	Jun 99-Dec 03	0.031-13.6	1.1	this study
	Quessant, France	rural	Oct. 99-Oct. 00	0.5-2.6	1.7	(37)
	Senga Bay, South Africa	rural	Feb 97-May 98	0.04-0.5	0.15	(17)
	Sleeping Bear Dunes, U.S.	rural	Jun 99-Dec 03	0.072-4.1	0.72	this study
	Burnt Island, Canada	rural	Mar 97-Dec 03	0.074-33.7	1.84	this study
α-Endosulfan	Cuiaba, Brazil	urban	Nov. 99- Mar 00	4-14	9	(16)
	Jersey City. U.S.	urban	Jan 00-May 01	0.025-0.067	0.046	(14)
	Chicago, U.S.	urban	Jun 99-Dec 03	0.038-3.0	0.70	this study
	Pineland, U.S.	rural	Jan 00-May 01	0.071-0.24	0.15	(14)
	Sleeping Bear Dunes, U.S.	rural	Jun 99-Dec 03	0.037-3.3	0.58	this study
	Burnt Island, Canada	rural	Mar 97-Dec 03	0.020-7.0	0.60	this study
β-Endosulfan	Cuiaba, Brazil	urban	Nov. 99-Mar 00	8-57	20	(16)
	Jersey City. U.S.	urban	Jan 00-May 01	0.16-0.42	0.29	(14)
	Chicago, U.S.	urban	Jun 99-Dec 03	0.10-3.4	0.68	this study
	Pineland, U.S.	rural	Jan 00-May 01	0.20-0.36	0.28	(14)
	Sleeping Bear Dunes, U.S.	rural	Jun 99-Dec 03	0.050-2.6	0.60	this study
	Burnt Island, Canada	rural	Mar 97-Dec 03	0.006-4.9	0.76	this study
ΣChlordane	Jersey City. U.S.	urban	Jan 00-May 01	0.13-0.14	0.18	(14)
	Chicago, U.S.	urban	Mar 97-Dec 03	0.057-41.3	1.8	this study
	Pineland, U.S.	rural	Jan 00-May 01	0.058-0.074	0.066	(14)
	Senga Bay, South Africa	rural	Feb 97-May 98	<0.23	0.029	(17)
	Sleeping Bear Dunes, U.S.	rural	Mar 97-Dec 03	0.004-1.7	0.026	this study
	Burnt Island, Canada	rural	Mar 97-Dec 03	0.002-4.6	0.22	this study
p,p'-DDT	Jersey City. U.S.	urban	Jan 00-May 01	0.18-0.55	0.37	(14)
	Gdansk region, N. Poland	urban	98-00	1-10		(37)
	Chicago, U.S.	urban	Mar 97-Dec 03	0.007-18.1	0.96	this study
	Senga Bay, South Africa	rural	Feb 97-May 98	<0.35	0.075	(17)
	Pineland, U.S.	rural	Jan 00-May 01	0.039-0.077	0.058	(14)
	Sleeping Bear Dunes, U.S.	rural	Mar 97-Dec 03	0.004-1.0	0.09	this study
	Burnt Island, Canada	rural	Mar 97-Dec 03	0.002-4.6	0.30	this study
p,p'-DDE	Senga Bay, South Africa	rural	Feb 97-May 98	<0.03	0.014	(17)
	Chicago, U.S.	urban	Mar 97-Dec 03	0.011-3.5	0.30	this study
	Sleeping Bear Dunes, U.S.	rural	Mar 97-Dec 03	0.0089-0.59	0.044	this study
	Burnt Island, Canada	rural	Mar 97-Dec 03	0.002-1.7	0.13	this study

[1].As defined by the census bureau in 1990, "urban" comprises all territory, population, and housing units in urbanized areas and in places of 2,500 or more persons outside urbanized areas. Territory, population, and housing units not classified as urban constitute "rural."

Appendix E. Trends in Polycyclic Aromatic Hydrocarbon Concentrations in the Great Lakes Atmosphere

Published in *Environmental Science & Technology*, **2006**, *40*, 6221-6227.

Trends in Polycyclic Aromatic Hydrocarbon Concentrations in the Great Lakes Atmosphere

Ping Sun,[1] Pierrette Blanchard,[2] Kenneth A. Brice[2] and Ronald A. Hites∗[1]

[1]School of Public and Environmental Affairs
Indiana University
Bloomington, Indiana, 47405 U.S.A.

and
[2]Environment Canada
4905 Dufferin Street
Toronto, ON M3H 5T4 Canada

∗Corresponding Author Email: hitesr@indiana.edu

Brief

Polycyclic aromatic hydrocarbons in the Great Lakes atmosphere are still an urban problem but a decline in their concentrations was observed with a decade of monitoring.

Abstract

Atmospheric polycyclic aromatic hydrocarbon (PAHs) concentrations were measured in both the vapor and particle phases at seven sites near the Great Lakes as a part of the Integrated Atmospheric Deposition Network. Lower molecular weight PAHs, including fluorene, phenanthrene, fluoranthrene, and pyrene, were dominant in the vapor phase, and higher molecular weight PAHs, including chrysene, benzo[*a*]pyrene, and coronene, were dominant in the particle phase. The highest PAH concentrations in both the vapor and particle phases were observed in Chicago followed by the semi-urban site at Sturgeon Point, NY. The spatial difference of PAH concentrations can be explained by the local population density. Long-term decreasing trends of most PAH concentrations were observed in both the vapor and particle phases at Chicago, with half-lives ranging from 3-10 years in the vapor phase and 5-15 years in the particle phase. At Eagle Harbor, Sleeping Bear Dunes, and Sturgeon Point, total PAH concentrations in the vapor phase showed significant, but slow, long-term decreasing trends. At the Sturgeon Point site, which was impacted by a nearby city, particle-phase PAH concentrations also declined. However, most particle-phase PAH concentrations did not show significant long-term decreasing trends at the remote sites. Seasonal trends were also observed for particle phase PAH concentrations, which were higher in the winter and lower in the summer.

Introduction

Atmospheric polycyclic aromatic hydrocarbons (PAH) concentrations have been measured by many researchers worldwide. Most of these studies were short-term measurements covering time periods ranging from a few months to a few years (*1*,*2*). Long-term measurements of PAH concentrations to determine temporal trends are still

limited (*3,4*). The Integrated Atmospheric Deposition Network (IADN) was begun in 1990 to measure PAHs and other persistent organic pollutant concentrations in air and precipitation around the Great Lakes (*5*). Previous IADN studies based on samples collected up to 1997 showed decreasing PAH concentrations in both the vapor and particle phases at several remote sites (*5,6,7*). Recently, we reported on the temporal trends of PAH concentrations from 1997 to 2003 in precipitation at the same sites discussed in this paper (*8*). However, long-term decreasing trends for PAH concentrations in precipitation were observed only at the urban site in Chicago (with half-lives of 2-5 years); there were few other significant temporal trends for PAH concentrations in precipitation at the remote IADN sites. Therefore, it was interesting to determine if PAH concentrations in the vapor and particle phases behave similarly to those in precipitation, or if these concentrations show long-term temporal trends that are different from the previously published results.

In this paper, the PAH concentrations in both the vapor and particle phases for samples collected up to December 2003 at seven IADN sites are reported. This paper not only extends the work of Cortes et al. (*6*) with an additional 6 years of data (1998-2003), but covers both U.S. and Canadian sites. In particular, we focused on the spatial and temporal trends of PAH concentrations to determine if they are responding to recent improvements in pollution control technology and to other pollution reduction efforts.

Experimental

Sampling and analytical methodology. Vapor and particle phase samples were collected at five U.S. IADN sites (Brule River and Eagle Harbor, near Lake Superior; Chicago and Sleeping Bear Dunes, near Lake Michigan; and Sturgeon Point, near Lake Erie) and at two Canadian sites (Burnt Island, near Lake Huron; and Point Petre, near Lake Ontario). The detailed site information is given at the IADN website (www.msc.ec.gc.ca/iadn).

Sampling procedures at the U.S. sites are described in detail by Basu and Lee (*9*). Briefly, 24-hour air samples were collected by modified Anderson high-volume air samplers (General Metal Works, model GS 2310) every 12 days. Particles were retained on quartz fiber filters (Whatman QM-A), and the vapor-phase organic compounds were retained on 40 g of XAD-2 resin (20-60 mesh). Prior to May 4, 1992, polyurethane foam (PUF) was used to collect vapor-phase samples. Temperature and other meteorological data were also recorded at each site concurrently with the sampling events.

After sampling, the XAD-2 sorbent and quartz fiber filters were Soxhlet extracted separately for 24 h using a 1:1 (v/v) mixture of hexane and acetone, concentrated by rotary evaporation and fractionated on 3.5% (w/w) water-deactivated silica gel. Hexane was first used to elute some pesticides. PAHs were then eluted with 1:1 hexane and dichloromethane. The extracts were further concentrated by N_2 blowdown to ~1 mL and spiked with d_{10}-anthracene, d_{12}-perylene, and d_{12}-benz[*a*]anthracene as internal standards. All PAHs were analyzed using gas chromatographic mass spectrometry with selected ion monitoring on DB-5 columns (J & W Scientific; 30 m × 250 μm i.d.; film thickness, 0.25 μm).

At the two Canadian sites, General Metal Works PS-1 high-volume samplers were used to collect air samples. The sampling head held a 10.2 cm diameter glass fiber filter (GFF, Gelman A/E Microfiber) for particle collection followed by a 7.5 cm high × 6.2 cm

diameter PUF plug (Levitt Safety) for vapor phase absorption. Sampling events occurred every 6 days through April 1994 and every 12 days since then. The PUF was Soxhlet extracted with hexane for 24 h. The extract was dried using anhydrous granular Na_2SO_4 (12-60 mesh), filtered through a small bed of anhydrous Na_2SO_4 supported by a Whatman glass fiber filter, and concentrated to 0.5 mL in isooctane. The volume was adjusted to 2 mL of isooctane and split into two equal portions. One portion was cleaned-up with a silica cartridge before analysis.

Prior to early 1999, the GFFs containing the particle phase PAHs were extracted with dichloromethane for 24 hr. After that time, an accelerated solvent extractor was used to extract the GFFs with a 30 mL of a 7:3 (v/v) mixture of hexane and acetone. Full details of the optimized extraction procedure were given by Alexandrou et al. (*10*). The PAHs were quantitated with a HP 1090 high performance liquid chromatograph (HPLC) with a 1046A programmable fluorescence detector using a 150 mm × 4.6 mm Vydac 202TP5415 C_{18} reverse phase column.

Sixteen PAHs were measured by both the U.S. and Canadian laboratories: fluorene, phenanthrene, anthracene, fluoranthene, pyrene, retene, benz[*a*]anthracene, triphenylene and chrysene (not resolved chromatographically at Indiana University and counted as one compound for both U.S. and Canadian sites), benzo[*b*]fluoranthene, benzo[*k*]fluoranthene, benzo[*e*]pyrene, benzo[*a*]pyrene, indeno[*1,2,3-cd*]pyrene, benzo[*ghi*]perylene, dibenz[*a,h*]-anthracene, and coronene. Measurements of PAHs in the vapor phase started at Eagle Harbor in November 1990, at Sturgeon Point in December 1991, at Sleeping Bear Dunes in January 1992, at Brule River and Chicago in January 1996. Although some vapor phase PAH measurements were available in the early 1990s at Point Petre and Burnt Island, the measurement of PAHs were stopped in 1992 and resumed in 1997. Therefore, only vapor phase data from January 1997 onward are reported at these two Canadian sites. For the particle-phase samples, data for all seven IADN sites from October 1996 to December 2003 were used because U.S. particle phase samples collected before October 1996 had been composited by month.

Strict quality assurance procedures were followed by both laboratories to ensure high data quality (*10,11*). Generally, field blanks account for at least 10% and laboratory blanks for at least 5% of the number of collected samples for both laboratories. The reported concentrations were not blank-corrected due to the low PAH concentrations in the blanks. At Indiana University, one matrix spike experiment was performed with every 20-24 samples. Surrogate standards (d_{10}-phenanthrene and d_{10}-pyrene) were also used in each sample to monitor recovery; the average percent recoveries were 83-89% (*11,12*). At Environment Canada, the extraction efficiencies, measured by matrix spike experiments, exceed 80% for the GFF and 70% for the PUF samples.

A split-sample, inter-laboratory comparison study was conducted in early 2001 to ensure data comparability (*12*). The results showed there was no bias in the PAH concentrations in the vapor and particle phase samples between the laboratories, except that unexpectedly high benzo[*e*]pyrene concentrations were reported in the vapor phase at Burnt Island and Point Petre. Therefore, in this paper, the total PAH (ΣPAH) concentration is the sum of the concentrations of the sixteen PAHs measured by both laboratories, except that benzo[*e*]pyrene was not included in the vapor phase concentrations at the two Canadian sites. Due to its small contribution to total vapor

phase PAH concentrations (usually less than 2%), omitting benzo[*e*]pyrene will not affect the spatial trend analysis of ΣPAH.

Trend analysis. In brief, the vapor-phase concentrations (in ng/m^3) of PAHs were first converted to partial pressures (P, in atm) using the ideal gas law. These partial pressures were then adjusted to a reference temperature of 288 K using equation 1 to remove the temperature effect on PAH gas-phase concentrations (*6*)

$$\ln P_{288} = \ln P - \frac{\Delta H}{R}\left(\frac{1}{288} - \frac{1}{T}\right) \tag{1}$$

where ΔH is a characteristic phase-transition energy of the compound (in kJ/mol), R is the gas constant, and T is the daily average atmospheric temperature at the sampling site (in Kelvin).In equation 1, the value of ΔH was determined by a preliminary regression of $\ln(P)$ vs. $1/T$. The values of $\ln(P_{288})$ were then regressed vs. time (t, in Julian days relative to January 1, 1990) to determine the rate of exponential decrease or increase of these partial pressures. If these rate constants were statistically significant, they were then converted to half-lives ($t_{1/2}$) by dividing the rates into ln(2) for each compound at each site. In this case, negative half-lives indicate that the concentrations were increasing over time.

The particle-phase PAH concentrations (C) were fitted by the following time-dependent function to study their temporal trends (*8*)

$$\ln C = a_0 + a_1 t + a_2 \sin\left(\frac{t}{a_3} + a_4\right) \tag{2}$$

where a_0 is the intercept (unitless), a_1 is a first-order rate constant (in days^{-1}) describing the rate of exponential decrease or increase over time, a_2 is the periodic amplitude (unitless), a_3 is the length of the period (in days), and a_4 is the periodic offset (in days). If a_1 values were significant ($p < 0.05$), either a decreasing ($a_1 < 0$) or increasing ($a_1 > 0$) trend in the PAH particle-phase concentrations could be determined for this sampling period, and these values were converted to half-lives by dividing the rate constants into ln(2) for each compound at each site. The anti-logarithm of $2a_2$ is the peak to valley amplitude of the seasonal variation, and a_4 indicates the time of the maximum concentration.

Results and Discussion

PAH concentrations and spatial trends. Concentration ranges of ΣPAH in the vapor and particle phases at the seven IADN sites are shown in Figure E1, sequenced by human population within a 25-km radius of the sampling site. The overall mean ΣPAH concentration in Chicago was 70 ± 5.2 ng/m^3 and 12 ± 0.7 ng/m^3 in the vapor and particle phases, respectively. These values are >10 times higher than those measured at the six other IADN sites. Sturgeon Point has the second highest ΣPAH concentration in both the vapor and particle phases with means of 6.3 ± 0.2 ng/m^3 and 1.1 ± 0.1 ng/m^3, respectively.

Student's *t*-tests ($\alpha = 0.05$) were conducted to compare the PAH concentrations in the vapor and particle phases at the other sites. Overall, for the ΣPAH concentrations in air (vapor plus particle phase), the spatial trend is: Burnt Island < Eagle Harbor < Brule

River ≈ Sleeping Bear Dunes ≈ Point Petre < Sturgeon Point << Chicago (Figure E1, top). However, the spatial trends of the PAH concentrations in the vapor and particle phases were different from the above trend. In the vapor phase, the spatial trend of PAH concentrations is: Burnt Island < Eagle Harbor ≈ Brule River ≈ Point Petre < Sleeping Bear Dunes < Sturgeon Point << Chicago. Brule River and Eagle Harbor, both near Lake Superior, had vapor phase PAH concentrations similar to those at Point Petre near Lake Ontario. Because atmospheric temperature will affect the vapor-phase PAH concentrations, especially for the low molecular weight PAHs, this effect was reduced by adjusting each concentration at each site to a reference temperature of 288 K using equation 1. These temperature-corrected, average vapor phase ΣPAH concentrations are given in Tables ES1-ES7. Using the corrected values, Sleeping Bear Dunes showed ΣPAH vapor-phase concentrations similar to those at Eagle Harbor, Brule River, and Point Petre. In the particle phase, the spatial trend of ΣPAH concentrations is: Eagle Harbor < Burnt Island ≈ Brule River ≈ Sleeping Bear Dunes < Point Petre <Sturgeon Point << Chicago. In all cases, the ΣPAH concentrations in the particle phase were generally much lower compared to those in the vapor phase, an observation which agrees with other studies (*1*,*4*).

Previous studies have suggested that there is a relationship between population density and atmospheric PAH concentrations (*13*,*14*). In particular, Hafner et al. showed a strong correlation between the population within a 25-km radius of the sampling site and the atmospheric PAH concentration measured at that site (*15*). Using the population data provided by Hafner et al. (*15*), we also observed that the atmospheric PAH concentrations at the seven IADN sites showed a strong correlation with local population (Figure E2), which suggests that spatial variations in atmospheric PAH concentrations can be explained by variations in population density.

As a large urban center, the very high ΣPAH concentrations in Chicago (e.g. averaging 70 ± 5.2 ng/m^3 and 12 ± 0.7 ng/m^3 in the vapor and particle phases, respectively) are not surprising. The major sources of PAHs in and around Chicago are vehicle emissions, coal and natural gas combustion, and coke production (*16*). Similarly, high atmospheric PAH concentrations in urban areas were also observed in other studies (*14*,*17*). Gigliotti et al. measured the atmospheric PAH concentrations in the Mid-Atlantic east coast region of the U.S. and reported higher PAH concentrations at the more urban and industrial sites (*4*). The highest PAH concentrations such as phenanthrene (15 ng/m^3) and pyrene (2.1 ng/m^3) measured by Gigliotti et al. in Jersey City, NJ, were still lower than those measured at our Chicago site (e.g. around 40 ng/m^3 and 5.5 ng/m^3 for phenanthrene and pyrene, respectively).

Atmospheric PAH concentrations at the IADN Chicago site have been reported before by other studies. Pirrone et al. reported an average concentration of 150 ± 48 ng/m^3 from July 8 to August 9, 1991, for total PAH concentrations in the vapor plus particle phases (*18*). Simcik et al. reported the mean ΣPAH concentrations (the sum of 19 PAHs) of 120 ± 14 ng/m^3 and 44 ± 17 ng/m^3 for the vapor and particle phase, respectively, during May and July 1994 and January 1995 (*19*). Average ΣPAH concentrations of 230 and 40 ng/m^3 were also reported by Vardar et al. for the vapor and particle phases, respectively, from August to September 1997 (*20*). In 1997, the average PAH atmospheric concentrations we report here were 150 ± 40 ng/m^3 in the vapor phase and 10 ± 1.4 ng/m^3 in the particle phase from August to September, which were similar to

those reported by Pirrone et al. (*18*) and Simcik et al. (*19*) but lower than those reported by Vardar et al. However, acenaphthene (approximately 80 ng/m^3) was included in the reported total vapor-phase PAH concentration by Vardar et al., and this compound was not measured in IADN samples. Therefore, the PAH concentrations reported by IADN agreed well with these previously reported data.

The second highest PAH concentrations we observed were at Sturgeon Point, which is located 25 km south of the city of Buffalo, NY, and about 110,000 people live within a 25-km radius of this sampling site. Due to the lower population, atmospheric PAH concentrations were lower at Sturgeon Point compared to Chicago (Figure E2). At the other five sites, the generally low atmospheric PAH concentrations may represent a background level in the Great Lakes basin of about 1.4 ng/m^3. The most remote site, Burnt Island, has by far the lowest population density (500 people within a 25-km radius) and by far the lowest ΣPAH concentration (0.6 ng/m^3). PAH sources to these remote regions include small cities such as Duluth, MN (*5*) and ship traffic along the St. Lawrence River and through the Great Lakes (*21*).

The atmospheric PAH concentrations at these sites are also comparable to data reported by previous studies. At rural sites in New Jersey, such as Delaware Bay, Alloway Creek, and the Pinelands measured by NJADN, the atmospheric PAH concentrations from October 1997 to May 2001 were similar to the concentrations reported here (*4*). A recent paper by Mandalakis et al. reported atmospheric ΣPAH concentrations ranging from 0.6 to 10 ng/m^3 at three European background sites (*22*). The average atmospheric ΣPAH concentration measured at Finokalia, Crete, a coastal site in the eastern Mediterranean Sea, was 19 ng/m^3 during 2000-2001 (*23*), which is comparable to the concentration at Sturgeon Point.

Several previous studies on the effects of wind and air trajectory directions on atmospheric concentrations of persistent organic pollutants were conducted to help locate the sources of these compounds (*19*,*24*). The results showed that PAHs have an urban source at Chicago – not surprisingly. At Sleeping Bear Dunes, air from the south was suggested to be the major source of PAHs. At Sturgeon Point, Cortes et al. investigated the hourly local wind directions and found that PAH concentrations were a factor of 3-5 times higher when the wind was coming to the sampling site from 30º to 89º (*6*); Buffalo, NY is located within this angle. At Brule River and Eagle Harbor, air trajectories originating from the southwest could transport PAHs to these two sites (*24*).

PAH Profiles. The concentration of each measured PAH was divided by the total concentration of the 16 PAHs in that sample to obtain a PAH profile in either the vapor or particle phase at a given site. These profiles are usually expressed in percent, and each profile consists of 16 percentages (one for each compound). The profiles for a given phase at a given site were then averaged, and standard errors were calculated. As examples, the profiles for the vapor phase in Chicago and at Point Petre are shown in Figure E3, top, and those for the particle phase at these two sites are shown in Figure E3, bottom. The agreement of these profiles with one another was measured by Pearson's correlation coefficients (r^2), which for 14 degrees of freedom has a critical value of 0.247 ($\alpha = 0.05$). These correlations were calculated for the 21 possible pairs of data in either the vapor or particle phases.

In general, the correlation coefficients for the vapor phase PAH profiles, taken pair-wise, were high ($0.81 < r^2 < 0.99$), which indicated a high similarity of PAH sources

at all seven sites. Similarly, the correlation coefficients for the particle phase profiles, taken pair-wise, were also high ($0.66 < r^2 < 0.97$), except between Point Petre and Chicago, where $r^2 = 0.40$ (see Figure D3, bottom). In this case, high relative amounts of phenanthrene, fluoranthene, and pyrene were observed in the particle phase at Chicago compared to Point Petre. The higher contributions of these three compounds in Chicago may indicate a coal combustion source (*25*). In both the vapor and particle phases, retene (RET) is relatively high at Point Petre as compared to Chicago; see Figure 3. Retene is usually considered a marker for wood burning, particularly of wood from coniferous trees (*26*). Our results suggest that wood burning may be more important at the rural site at Point Petre vs. the urban site at Chicago.

By comparing the average PAH profiles in the vapor phase vs. that in the particle phase (Figure E3 top vs. bottom), it is clear that the vapor phase is dominated by the lighter, more volatile compounds, such as phenanthrene, and that the particle phase is dominated by the heavier, less volatile compounds, such as the benzopyrenes. The PAH profiles in the vapor and particle phases in our study are similar to those observed in air samples collected by NJADN and by other studies (*4*,*16*,*19*,*27*). This distribution is primarily the result of vapor-particle partitioning driven by the individual compounds' vapor pressures (*28*). In addition, higher molecular weight PAHs are largely formed with soot particles (*29*); thus, the partitioning of PAHs between the vapor and particle phases is also dependent on the aerosol type (*30*).

Temporal trends. Figure E4 shows the long-term trends of ΣPAH concentrations in the vapor and particle phases at Chicago (top) and at Sleeping Bear Dunes (bottom). The detailed temporal trends of the other PAHs at the seven IADN sites are given in the Supporting Information (Figures ES1 and ES2). Concentrations of ΣPAH in both the vapor and particle phases showed significant decreases at Chicago. However, at Sleeping Bear Dunes, the particle-phase ΣPAH concentrations did not change over time while the vapor-phase ΣPAH concentrations showed a significant but slow decline. The calculated half-lives of PAHs in both the vapor and particle phases at the seven sites are given in Table E1. The half-life of ΣPAH in Chicago was 8.7 ± 2.1 years in the vapor phase and 8.9 ± 2.6 years in the particle phase. At two sites, Sturgeon Point and Point Petre, the ΣPAH concentrations showed faster declines in the particle phase ($t_{1/2} \approx 6$ years) compared to the rate of decline in the vapor phase. At the rural sites Eagle Harbor, Sleeping Bear Dunes, and Burnt Island, the ΣPAH concentrations either showed very slow declines (e.g. half-lives >15 years) or no significant temporal trends.

This is the first time that a long-term decreasing trend of PAH concentrations in Chicago's atmosphere has been reported. Demashki et al. showed atmospheric PAH concentrations have decreased appreciably between 1992 and 1997 at an urban site in Birmingham, U.K. (*31*), and they suggested that this decrease could have been due to legislation that required mandatory catalytic converters on new vehicles in 1993. Schauer et al. compared particle phase PAH concentrations observed in Munich, Germany from 2001 to 2002 with historical data from 1980 to 1993 and reported decreasing PAH concentrations over time (*32*). Our observed decline of PAH concentrations in air agreed well with the decline of PAH concentrations in precipitation at Chicago (*8*). These declines are likely due to a commitment to cleaner air, including improved petroleum fuels, automobile engines, and industrial pollution control technology, as discussed in detail in our previous work (*8*).

Decreasing trends of vapor-phase PAH concentrations at Eagle Harbor, Sleeping Bear Dune, and Sturgeon Point (with half-lives of 2-9 years) had been reported by Cortes et al. based on samples collected from 1991 to 1997 (*6*). We note that these earlier reported vapor-phase half-lives are significantly faster than those reported in this study (average half-lives longer than 16 years). A slower rate of decline of PAHs in the atmosphere in recent years is reasonable if atmospheric PAH concentrations are approaching a non-zero steady state (*33*). In this study, the observed decline of particle phase PAH concentrations at Sturgeon Point is also different from that observed by Cortes et al. (*6*), who reported that, at Sturgeon Point from 1991 to 1997, most PAHs in the particle phase did not show significant temporal trends. Our results, however, suggest that most PAH concentrations in the particle phase significantly decreased from 1996 to 2003 at this site (see Table E1). Because decreasing PAH concentrations in the particle phase were also observed at Point Petre and Brule River and because these sites are likely impacted by nearby cities, it is possible that efforts to reduce pollution in these cities have led to decreased PAH concentrations in the particle phase at these locations. Indeed, the Toxic Release Inventory of PAHs showed decreasing emissions around the U.S. Great Lakes from 1987 to 2003, particularly near Lakes Superior and Michigan (*34*).

The half-lives of each PAH in the vapor and particle phases at the 7 IADN sites are listed in Table E1. Retene, a marker for biomass burning (*26*), showed a slower rate of decline at the more rural sites compared to Chicago, perhaps indicating that biomass burning continues to be popular at the rural sites, while it is being eliminated in Chicago (*8*). Because the other PAHs have multiple sources, it is not possible to interpret their half-lives. In fact, some PAHs showed statistically *increasing* trends (e.g., benzopyrenes in the particle phase at Sleeping Bear Dunes and fluoranthene in the vapor phase at Point Petre and at Burnt Island). Generally, these increasing trends are slow, with doubling times of >10 years. It is not yet clear if these trends are real, and if so, what they mean.

Significant seasonal trends in particle phase PAH concentrations were also observed with higher concentrations in the winter (Figure E4, Figures ES1 and ES2). The ratios between the highest concentrations in the winter and the lowest concentration in the summer are given as the peak-to-valley ratio in Tables ES8 to ES14. These values are usually larger than 2 indicating the PAH concentrations in the winter were more than twice as high as those in the summer. There are many reasons that may lead to increased particle phase PAH concentrations in the winter; these include lower atmospheric mixing heights (*35*), decreased photolytic reactions in the atmosphere (*36*), and more emissions from space heating. This same effect was observed for PAH concentrations in the precipitation phase (*8*).

Acknowledgments

We thank Ilora Basu, Nick Alexandrou, and Team IADN for chemical measurements; Environment Canada's Meteorological Services for some data acquisition; Environment Canada and the U.S. Environmental Protection Agency's Great Lakes National Program Office for funding (Grant GL995656, Melissa Hulting, project monitor).

Literature cited

1 Poor, N.; Tremblay, R.; Kay, H.; Bhethanabotla, V.; Swartz, E.; Luther, M.; Campbell, S. Atmospheric concentrations and dry deposition rates of polycyclic aromatic hydrocarbons (PAHs) for Tampa Bay, Florida, U.S.A. *Atmos. Environ*. **2004**, *38*, 6005-6015.

2 Mastral, A. M.; Lopez, J. M.; Callen, M. S.; Garcia, T.; Murillo, R.; Navarro, M. V. Spatial and Temporal PAH concentration in Zaragoza, Spain. *Sci. Total Environ*. **2003**, *307*, 111-124.

3 Hung, H.; Blanchard, P.; Halsall, C. J.; Bidleman, T. F.; Stern, G. A.; Fellin, P.; Muir, D. C. G.; Barrie, L. A.; Jantunen, L. M.; Helm, P. A.; Ma, J.; Konoplev, A. Temporal and spatial variabilities of atmospheric polychlorinated biphenyls (PCBs), organochlorine (OC) pesticides and polycyclic aromatic hydrocarbons (PAHs) in the Canadian Arctic: Results from a decade of monitoring. *Sci. Total Environ*. **2005**, *342*, 119-144.

4 Gigliotti, C. L.; Totten, L. A.; Offenberg, J. H.; Dachs, J.; Reinfelder, J. R.; Nelson, E. D.; Glenn IV, T. R.; Eisenreich, S. J. Atmospheric concentrations and deposition of polycyclic aromatic hydrocarbons to the Mid-Atlantic east coast region *Environ. Sci. Technol.* **2005**, *39*, 5550-5559.

5 Buehler, S. S.; Basu, I.; Hites, R. A. A comparison of PAH, PCB, and pesticide concentration in air at two rural sites on Lake Superior. *Environ. Sci. Technol.* **2001**, *35*, 2417-2422.

6 Cortes, D. R.; Basu, I.; Sweet, C. W.; Hites, R. A. Temporal trends in and influence of wind on PAH concentrations measured near the Great Lakes. *Environ. Sci. Technol.* **2000**, *34*, 356-360.

7 Simcik, M. F.; Hoff, R. M.; Strachan, W. M.; Sweet, C. W.; Basu, I.; Hites, R. A. Temporal trends of semi-volatile organic contaminants in Great Lakes precipitation. *Environ. Sci. Technol.* **2000**, *34*, 361-367.

8 Sun, P.; Backus, S.; Blanchard, P.; Hites, R. A. Annual variation of PAH concentrations in precipitation collected near the Great Lakes. *Environ. Sci. Technol.* **2006**, 696-701.

9 Basu, I.; Lee, A. D. *Collection of Air and Precipitation Samples: IADN Project Standard Operating Procedure*; Indiana University: Bloomington, IN, 2003.

10 Alexandrou, N.; Smith, M.; Park, R.; Lumb K.; Brice K. A. The extraction of polycyclic aromatic hydrocarbons from atmospheric particulate matter samples by accelerated solvent extraction (ASE). *Int. J. Environ. An. Ch.* **2001**, *81*, 257-280.

11 Basu, I.; Arnold, K. *Quality Control Report 2002*; Indiana University: Bloomington, IN, 2003.

12 Fowlie, P. *Integrated Atmospheric Deposition Network (IADN) Interlaboratory Comparison for Pesticides, Polychlorinated Biphenyls and Polynuclear Aromatic Hydrocarbons in air and particulate samples, revision 2*; Cornerstone Science: Burlington, Ontario, 2002.

13 Garban. N.; Blanchard, H.; Motelay-Massei, A.; Chevreuil, M.; Ollivon, D. Atmospheric bulk deposition of PAHs onto France: trends from urban to remote sites. *Atmos. Environ.* **2002**, *36*, 5395-5403.

14 Eiguren-Fernandez, A.; Miguel, A. H.; Froines, J. R.; Thurairatnam, S.; Avol, E. L. Seasonal and spatial variation of polycyclic aromatic hydrocarbons in vapor-phase and PM 2.5 in Southern California urban and rural communities. *Aerosol Sci. Technol.* **2004**, *38*, 447-455.

15 Hafner, W. D.; Carlson, D. L.; Hites, R. A. Influence of local human population on atmospheric polycyclic aromatic hydrocarbon concentrations. *Environ. Sci. Technol.* **2005**, *39*, 7374-7379.

16 Simcik, M. F.; Eisenreich, S. J.; Lioy, P. J. Source apportionment and source/sink relationships of PAHs in the coastal atmosphere of Chicago and Lake Michigan. *Atmos. Environ*. **1999**, *33*, 5071-5079.

17 Panther, B.C.; Hooper, M. A.; Tapper, N. J. A comparison of air particulate matter and associated polycyclic aromatic hydrocarbons in some tropical and temperate urban environment. *Atmos. Environ*. **1999**, *33*, 4087-4099.

18 Pirrone, N.; Keeler, G. J.; Holsen, T. M. Dry deposition of semi-volatile organic compounds to Lake Michigan. *Environ. Sci. Technol.* **1995**, *29*, 2123-2132.

19 Simcik, M. F.; Zhang, H.; Eisenreich, S. J.; Franz, T. P. Urban contamination of the Chicago/coastal Lake Michigan atmosphere by PCBs and PAHs during AEOLOS. *Environ. Sci. Technol.* **1997**, *31*, 2141-2147.

20 Vardar, N.; Tasdemir, Y.; Odabasi, M.; Noll, K. E. Characterization of atmospheric concentrations and partitioning of PAHs in the Chicago atmosphere. *Sci. Total Environ*. **2004**, *327*, 163-174.

21 Brice, K. A. *The U.S./Canada Integrated Atmospheric Deposition Network (IADN): measurements of semi-volatile organics (PCBs, OCs, PAHs) and trace elements in the atmosphere of the Great Lakes basin.* WMO/EMEP/UNEP Workshop on Modeling of Atmospheric Transport and Deposition of Persistent Organic Pollutants and Heavy Metals, 16-19 Nov. 1999, Geneva, Switzerland, Vol 2, 67-84.

22 Mandalakis, M.; Gustafsson, O.; Alsberg, T.; Egeback, A.; Reddy, C. M.; Xu, L.; Klanova, J.; Holoubek, I.; Stephanou, E. G. Contribution of biomass burning to atmospheric polycyclic aromatic hydrocarbons at three European background sites. *Environ. Sci. Technol.* **2005**, *39*, 2976-2982.

23 Tsapakis, M.; Stephanou, E. G. Polycyclic aromatic hydrocarbons in the atmosphere of the Eastern Mediterranean. *Environ. Sci. Technol.* **2005**, *39*, 6584-6590.

24 Hafner, W. D.; Hites, R. A. Effects of wind and air trajectory directions on atmospheric concentrations of persistent organic pollutants near the Great Lakes. *Environ. Sci. Technol.* **2005**, *39*, 7817-7825.

25 Mastral, A. M.; Callen, M.; Murillo, R. Assessment of PAH emissions as a function of coal combustion variables. *Fuel* **1996**, *75*, 1533-1536.

26 Ramdahl, T. Retene-a molecular marker of wood combustion in ambient air. *Nature* **1983**, *306*, 580-582.

27 Ngabe, B.; Poissant, L. Polycyclic aromatic hydrocarbons in the air in the St. Lawrence Basin (Quebec). *Environ. Sci. Technol.* **2003**, *37*, 2094-2099.

28 Gustafson, K. E.; Dickhut, R. M. Particle/gas concentrations and distributions of PAHs in the atmosphere of Southern Chesapeake Bay. *Environ. Sci. Technol*. **1997**, *31*, 140-147.

29 Buckley, D. R.; Rockne, K. J.; Li, A.; Mills, W. J. Soot deposition in the Great Lakes: Implications for semi-volatile hydrophobic pollutant deposition. *Environ. Sci. Technol*. **2004**, *38*, 1732-1739.
30 Harner, T.; Bidleman, T. F. Octanol-air partition coefficient for describing particle/gas partitioning of aromatic compounds in urban air. *Environ. Sci. Technol*. **1998**, *32*, 1494-1502.
31 Dimashki, M.; Lim, L. H.; Harrison, R. M.; Harrad, S. Temporal Trends, temperature dependence, and relative reactivity of atmospheric polycyclic aromatic hydrocarbons. *Environ. Sci. Technol.* **2001**, *35*, 2264-2267.
32 Schauer, C.; Niessner, R.; Poschl, U. Polycyclic aromatic hydrocarbons in urban air particulate matter: decadal and seasonal trends, chemical degradation and sampling artifacts. *Environ. Sci. Technol.* **2003**, *37*, 2861-2868.
33 Schneider, A. R.; Stapleton, H. M.; Cornwell, J.; Baker J. E. Recent declines in PAH, PCB, and toxaphene levels in the northern Great Lakes as determined from high resolution sediment cores. *Environ. Sci. Technol.* **2001**, *35*, 3809-3815.
34 http://toxmap.nlm.nih.gov/toxmap/trends/, accessed on March 19, 2006.
35 Bidleman, T.; Billings, W. N.; Foreman, W. T. Vapor-particle partitioning of semi-volatile organic compounds: estimates from field collections. *Environ. Sci. Technol.* **1986**, *20*, 1038-1043.
36 Baek, S. O.; Field, R. A.; Goldstone, M. E.; Kirk, P. W.; Lester, J. N.; Perry, R. A review of atmospheric polycyclic aromatic hydrocarbons: sources, fate and behavior. *Water, Air, Soil Poll*. **1991**, *60*, 279-300.

Table E1. Half-lives (in years) of PAH concentrations in the vapor and particle phases at seven sites near the Great Lakes[1].

	Brule River		*Eagle Harbor*		*Chicago*		*Sleeping Bear*		*Sturgeon Point*		*Burnt Island*		Point Petre	
	Vapor	*Particle*	Vapor	*Particle*	Vapor	*Particle*	Vapor	*Particle*	Vapor	*Particle*	Vapor	*Particle*	Vapor	*Particle*
Fluo[2]	*7.0 ± 2.0*	NS	NS	NS	9.4 ± 2.5	**5.6 ± 1.1**	*17 ± 5.0*	NS	*21 ± 6.3*	**5.2 ± 0.8**	NS	*1.9 ± 0.3*	*-12 ± 4.0*	*2.2 ± 0.3*
Phen	NS	6.3 ± 2.1	**9.4 ± 2.5**	NS	8.8 ± 2.2	*9.5 ± 4.8*	**13 ± 2.9**	NS	**12 ± 2.1**	**4.8 ± 1.2**	NS	*9.4 ± 2.8*	NS	**7.0 ± 1.5**
Anth	NS	LD	17 ± 7.8	LD	**6.2 ± 1.5**	**5.5 ± 1.2**	NS	NS	NS	*7.9 ± 2.6*	**4.2 ± 0.6**	**5.2 ± 1.1**	*6.1 ± 1.6*	**5.3 ± 1.0**
Flan	NS	4.4 ± 1.1	*16 ± 4.7*	12 ± 4.8	10 ± 2.6	*9.8 ± 3.1*	*16 ± 5.3*	NS	**15 ± 3.7**	**4.7 ± 0.7**	-11 ± 5.1	*7.4 ± 1.9*	-19 ± 11	**5.1 ± 0.9**
Pyrn	NS	NS	**7.7 ± 1.3**	NS	**6.7 ± 1.2**	**8.3 ± 2.5**	**8.7 ± 1.6**	NS	**7.8 ± 1.2**	**4.5 ± 0.7**	*9.2 ± 2.4*	*7.9 ± 2.2*	NS	**6.5 ± 1.6**
Ret	7.1 ± 3.1	NS	10 ± 3.1	NS	**2.6 ± 0.2**	*7.9 ± 2.7*	*12 ± 4.0*	NS	NS	NS	NS	**6.0 ± 1.4**	8.3 ± 3.6	*5.5 ± 1.9*
B[a]A	NS	NS	LD	NS	**3.7 ± 0.6**	*6.8 ± 1.8*	LD	NS	12 ± 5.2	**5.0 ± 0.9**	2.5 ± 1.0	**5.0 ± 0.9**	*4.2 ± 1.2*	**5.7 ± 1.1**
Chry	NS	NS	**6.3 ± 0.9**	11 ± 4.5	**3.9 ± 0.5**	**7.4 ± 1.8**	**6.2 ± 1.0**	NS	**7.2 ± 1.1**	**4.5 ± 0.7**	6.2 ± 2.4	*8.8 ± 2.7*	NS	**5.9 ± 1.4**
B[b]F	*-3.2 ± 1.0*	NS	LD	NS	6.3 ± 2.0	14 ± 5.9	LD	NS	NS	*8.1 ± 2.4*	LD	*8.7 ± 2.6*	*2.1 ± 0.5*	**5.8 ± 1.3**
B[k]F	LD	NS	LD	NS	NS	*8.1 ± 2.2*	LD	-9.5 ± 4.8	NS	**6.6 ± 1.5**	LD	*8.4 ± 2.4*	**2.1 ± 0.5**	**7.1 ± 1.8**
B[e]P	LD	NS	LD	NS	NS	*15 ± 7.0*	LD	-11 ± 5.4	NS	*9.1 ± 2.9*	N/A	**5.0 ± 0.9**	N/A	**5.6 ± 1.2**
B[a]P	LD	NS	LD	NS	NS	9.6 ± 3.9	LD	-11 ± 5.6	NS	**4.8 ± 1.2**	LD	*11 ± 4.5*	LD	*11 ± 4.1*
I123P	LD	NS	LD	NS	NS	NS	LD	NS	LD	*8.6 ± 2.7*	LD	**6.6 ± 1.4**	LD	**6.2 ± 1.4**
BgP	LD	NS	LD	NS	NS	*10 ± 3.5*	LD	NS	LD	*8.4 ± 2.4*	LD	*7.9 ± 2.1*	LD	**6.5 ± 1.4**
DaA	LD	NS	LD	LD	NS	*8.8 ± 2.8*	LD	LD	LD	NS	LD	*7.3 ± 2.1*	LD	**6.6 ± 1.6**
Cor	LD	NS	LD	NS	NS	**7.0 ± 1.6**	LD	NS	LD	*9.2 ± 2.8*	N/A	LD	N/A	LD
ΣPAHs[3]	NS	4.0 ± 1.0	*19 ± 5.5*	*6.8 ± 1.9*	**8.7 ± 2.1**	*8.9 ± 2.6*	*15 ± 4.3*	NS	**15 ± 3.3**	*5.6 ± 1.1*	NS	NS	NS	**6.7 ± 1.6**

[1] The results are listed as mean ± standard error. Normal font numbers are significant for $0.01 < p < 0.05$; italic font numbers are significant for $0.001 < p < 0.01$, bold font numbers are significant at level of $p < 0.001$. "NS" means "not significant" at $p > 0.05$. "LD" means "Limited data" and no regression analysis was conducted. "N/A" means "no data are available". A negative half-life is actually a doubling time.

[2] Fluo: fluorene; Phen: phenanthrene; Anth: anthracene; Flan: fluoranthene; Pyrn: pyrene; Ret: retene; B[a]A: benz[*a*]anthracene; Chry: triphenylene and chrysene; B[b]F: benzo[*b*]fluoranthene; B[k]F: benzo[*k*]fluoranthene; B[e]P: benzo[*e*]pyrene; B[a]P: benzo[*a*]pyrene; I123P: indeno[*1,2,3-cd*]pyrene; BgP: benzo[*ghi*]perylene; DaA: dibenz[*a,h*]anthracene; Cor: coronene.

[3] ΣPAH is the total concentration of the 16 compounds listed here in note 2.

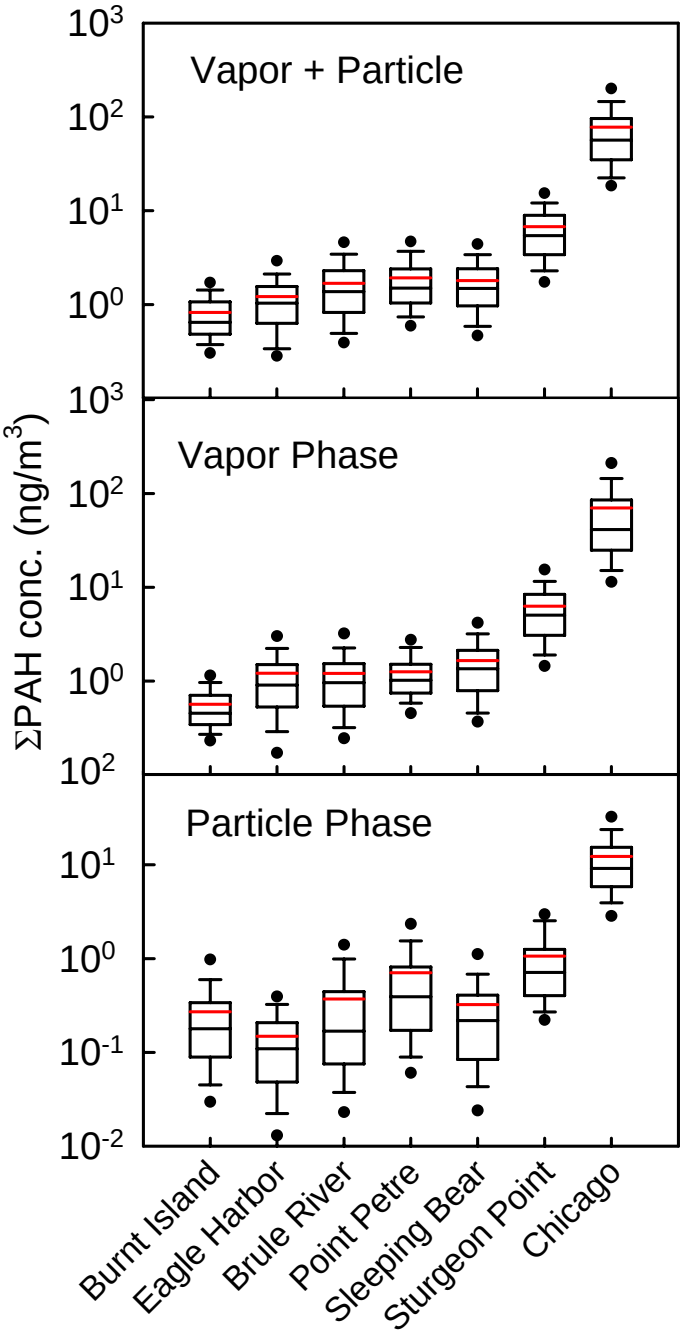

Figure E1. Total PAH concentrations in air (vapor plus particle) (top), vapor (middle) and particle (bottom) phases at seven IADN sites sequenced by the population living within a 25-km radius of the sampling site (*15*). The horizontal lines represent the 10th, 50th, and 90th percentiles; the red lines are the means; the boxes represent the 25th to 75th percentiles; and outliers are shown as the 5th and 95th percentiles.

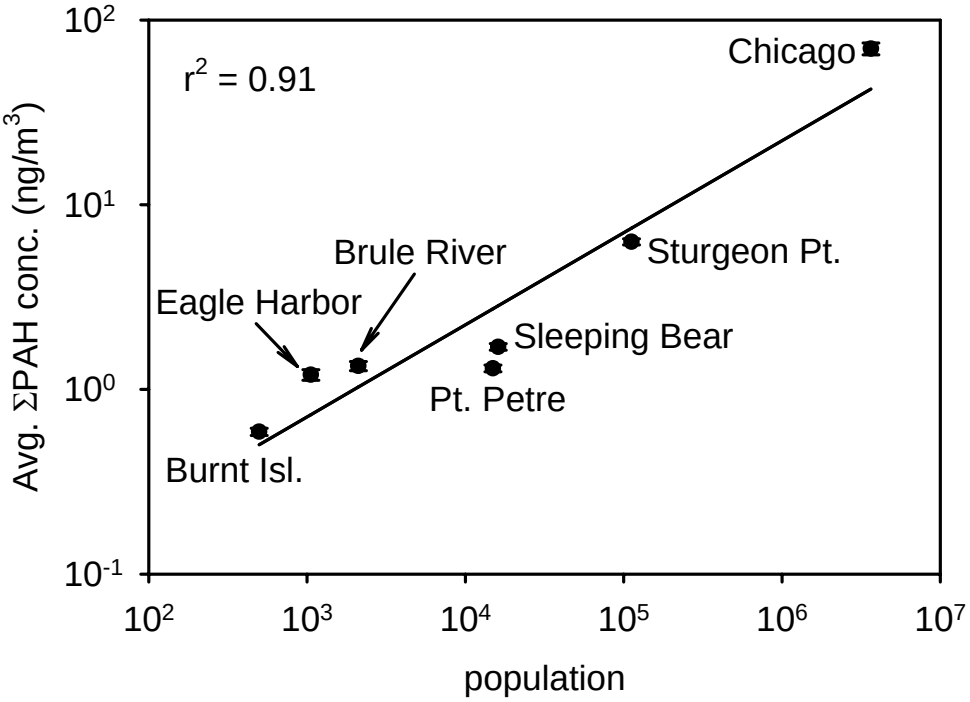

Figure E2. Average ΣPAH concentration at the seven IADN sampling sites as a function of the population living within a 25-km radius of the sampling site. The error bars are standard errors.

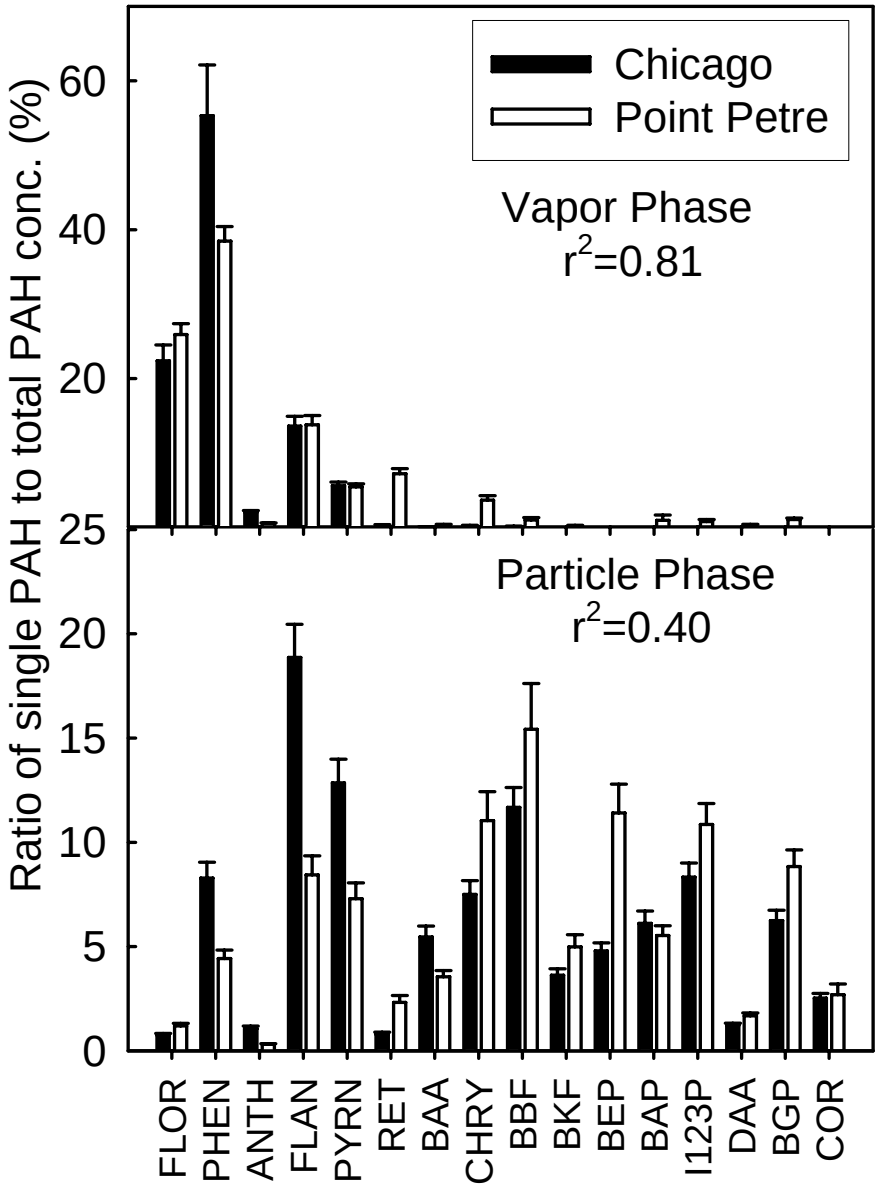

Figure E3. Average PAH profiles for the vapor (top) and particle (bottom) phases at Chicago and at Point Petre. The error bars represents one standard error. The compound abbreviations are given in Table D1.

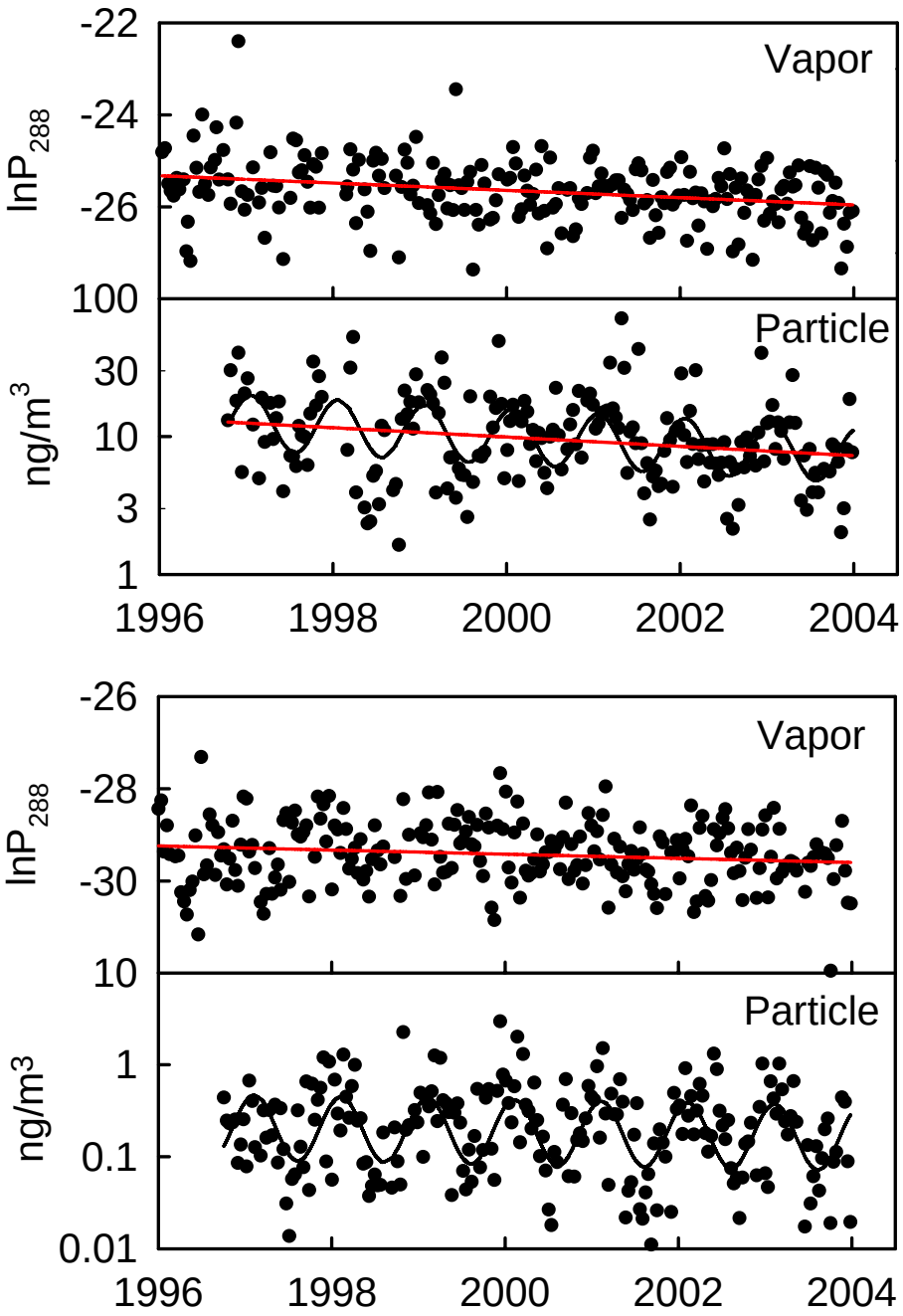

Figure E4. Temporal trends of vapor and particle phase ΣPAH concentrations at Chicago (top) and at Sleeping Bear Dunes (bottom). Only data from 1996 through 2003 are shown for the vapor phase at Sleeping Bear Dunes. The completed data set is shown in Figure DS1. The black curves are the fitting lines of the sinusoidal model (equation 2) with the period length (a_3) set to one year; the red lines indicate long-term, significant decreasing trends.

Supporting Information for:

Trends in Polycyclic Aromatic Hydrocarbons Concentrations in the Great Lakes Atmosphere

P. Sun, P. Blanchard, K. A. Brice, and R. A. Hites

This Supporting Information contains 14 tables of values derived from modeled parameters for PAH concentrations in the vapor and particle phases at seven IADN sites; and two figures showing temporal trends of PAH concentrations in the vapor and particle phases. Plots for PAH larger than benzo[*b*]fluoranthrene in the vapor phase are not shown because of the very limited data. ΣPAH is the sum of the 16 PAHs measured by both Indiana University and Environment Canada. These PAH are fluorene, phenanthrene, anthracene, fluoranthene, pyrene, retene, benz[*a*]anthracene, triphenylene plus chrysene (which are not resolvable by gas chromatography at Indiana University and thus count as one compound), benzo[*b*]fluoranthrene, benzo[*k*]fluoranthrene, benzo[*e*]pyrene, benzo[*a*]pyrene, indeno[1,2,3-*cd*]pyrene, benzo[*ghi*]-perylene, and dibenz[*a,h*]anthracene, and coronene.

The vapor phase PAH concentrations (in pg/m^3) were first converted to partial pressures (P, in atm) using the ideal gas law. These partial pressures were then adjusted to the reference temperature of 288 K using equation 1, where ΔH is a characteristic phase-transition energy of the compound (in kJ/mol), R is the gas constant, and T is the daily average atmospheric temperature at the sampling site (in Kelvin). The value of ΔH was determined by a preliminary regression of ln(P) vs. 1/T (see equation 2). The values of ln(P_{288}) were then regressed vs. time (t, in Julian days relative to January 1, 1990) using equation 3 to determine the rate (b_1, in days^{-1}) of exponential increase ($b_1 > 0$) or decrease ($b_1 < 0$) of these partial pressures. If this rate was statistically significant ($p < 0.05$), these rates were then converted to half-lives ($t_{1/2,}$ in years) by dividing the values into the ln(2)/365 for each compound at each site.

$$\ln P_{288} = \ln P - \frac{\Delta H}{R}\left(\frac{1}{288} - \frac{1}{T}\right) \tag{1}$$

$$\ln P = -\frac{\Delta H}{R}\left(\frac{1}{T}\right) + \text{const} \tag{2}$$

$$\ln P_{288} = b_0 + b_1 t \tag{3}$$

Tables ES1 to ES7 show the values of ΔH and the calculated half-lives from the b_1 values in equation 3. The results are listed as mean ± standard error. Normal font numbers are significant for $0.01 < p < 0.05$; italic font numbers are significant for $0.001 < p < 0.01$, bold font numbers are significant for $p < 0.001$. "NS" means "not significant" at $p > 0.05$. "LD" means "limited data", and no regression was calculated. "N/A" means "not available". A negative half-life is actually a doubling time.

Equation 4 was used to fit the PAH concentrations (C) in the particle phase:

$$\ln C = a_0 + a_1 t + a_2 \sin\left(\frac{t}{a_3} + a_4\right) \tag{4}$$

where t is the time in Julian Days relative to January 1 1990, a_0 is the intercept (unitless), a_1 is a first-order rate constant (in days^{-1}) describing the rate of exponential decrease or increase over time, a_2 is the periodic amplitude (unitless), a_3 is the length of the period (in days), and a_4 is the periodic offset (in days).

The ratio between the highest PAH concentration during winter time and the lowest concentration during summer time can be calculated from the fitted a_2 parameter by taking its anti-logarithm (e^{2a_2}, the factor of 2 in the exponent is needed to calculate the peak-to-valley amplitude). The sine wave would have a maximum at day 91 in a year. Therefore, the dates of the maximum of PAH concentrations were calculated by first converting the fitted a_4 values from radians to days (multiplying by 365/2π) and then subtracting these values from 91.

Tables ES8 to ES14 show results of the fit using equation 4 with a_3 set to 365 days. The results are listed as mean ± standard error. Normal font numbers are significant for $0.01 < p < 0.05$; italic font numbers are significant for $0.001 < p < 0.01$, bold font numbers are significant at $p < 0.001$. "NS" means "not significant at $p > 0.05$. A negative half-life is actually a doubling time.

Figure ES1 shows the temporal trends of vapor phase total PAH concentrations at the seven IADN sites. The concentrations were converted to P_{288} by equation (1). The values of $\ln(P_{288})$ were then plotted vs. time based on equation (3). The red lines indicate long-term significant decreasing or increasing trends.

Figure ES2 shows the temporal trends of particle phase total PAH concentrations at the seven IADN sites. The black curves are the fitting lines using the sinusoidal model with the period length (a_3) set to one year (equation 4); the red lines indicate long-term significant decreasing trends ($a_1 < 0$).

Table ES1. Fit parameters for PAHs in vapor phase at Brule River

PAHs	Average conc. (pg/m^3)	Half-life (years)	ΔH (kJ/mol)	No. of detects	r^2
Fluorene	560 ± 30	*7.0 ± 2.0*	NS	188	0.06
Phenanthrene	610 ± 40	NS	NS	188	NS
Anthracene	32 ± 8.7	NS	*20 ± 6.7*	74	0.12
Fluoranthene	95 ± 6.2	NS	8.2 ± 3.5	188	0.03
Pyrene	37 ± 2.5	NS	**17 ± 3.6**	172	0.12
Retene	34 ± 8.7	7.1 ± 3.1	**21 ± 4.7**	147	0.16
Benz[*a*]anthracene	5.5 ± 1.0	NS	15 ± 6.6	47	0.11
Triphenylene + Chrysene	8.0 ± 0.8	NS	NS	107	NS
Benzo[*b*]fluoranthrene	13 ± 1.7	*-3.2 ± 1.0**	NS	48	0.19
Benzo[*k*]fluoranthrene	6.2 ± 0.9	LD	LD	22	N/A
Benzo[*e*]pyrene	7.8 ± 1.0	LD	LD	26	N/A
Benzo[*a*]pyrene	7.8 ± 1.3	LD	LD	20	N/A
Indeno[1,2,3-*cd*]pyrene	8.6 ± 1.4	LD	LD	21	N/A
Benzo[*ghi*]perylene	7.9 ± 1.2	LD	LD	21	N/A
Dibenz[*a,h*]anthracene	4.1 ± 0.8	LD	LD	9	N/A
Coronene	6.3 ± 0.8	LD	LD	10	N/A
ΣPAH	1340 ± 75	NS	NS	188	NS
Temperature-corrected ΣPAH conc. (288 K)	1480 ± 83				

*A negative half-life indicates that the concentrations are increasing and the listed value is the doubling time.

Table ES2. Fit parameters for PAHs in vapor phase at Eagle Harbor

PAHs	Average conc. (pg/m^3)	Half-life (years)	ΔH (kJ/mol)	No. of detects	r^2
Fluorene	390 ± 18	NS	**17 ± 2.5**	367	0.12
Phenanthrene	600 ± 50	**9.4 ± 2.5**	**33 ± 2.5**	368	0.34
Anthracene	44 ± 14	17 ± 7.8	**42 ± 5.5**	168	0.27
Fluoranthene	100 ± 5.7	*16 ± 4.7*	**29 ± 2.8**	366	0.24
Pyrene	60 ± 5.3	**7.7 ± 1.3**	**17 ± 3.6**	325	0.12
Retene	48 ± 6.5	10 ± 3.1	**32 ± 5.4**	230	0.16
Benz[*a*]anthracene	15 ± 6.8	LD	LD	62	N/A
Triphenylene + Chrysene	15 ± 5.2	**6.3 ± 0.9**	12 ± 4.0	188	0.02
Benzo[*b*]fluoranthrene	14 ± 3.8	LD	LD	43	N/A
Benzo[*k*]fluoranthrene	11 ± 2.2	LD	LD	22	N/A
Benzo[*e*]pyrene	10 ± 2.5	LD	LD	17	N/A
Benzo[*a*]pyrene	18 ± 3.4	LD	LD	20	N/A
Indeno[1,2,3-*cd*]pyrene	10 ± 3.0	LD	LD	9	N/A
Benzo[*ghi*]perylene	12 ± 2.7	LD	LD	16	N/A
Dibenz[*a,h*]anthracene	4.7 ± 3.2	LD	LD	4	N/A
Coronene	2.4 ± 0.8	LD	LD	3	N/A
ΣPAH	1210 ± 80	*19 ± 5.5*	**27 ± 2.5**	368	0.25
Temperature-corrected ΣPAH conc. (288 K)	1740 ± 140				

Table ES3. Fit parameters for PAHs in vapor phase at Sleeping Bear Dunes

PAHs	Average conc. (pg/m^3)	Half-life (years)	ΔH (kJ/mol)	No. of detects	R^2
Fluorene	620 ± 25	*17 ± 5.0*	*11 ± 3.0*	331	0.06
Phenanthrene	780 ± 36	**13 ± 2.9**	*9.1 ± 2.6*	332	0.09
Anthracene	38 ± 8.3	NS	15 ± 6.7	112	0.05
Fluoranthene	150 ± 7.7	*16 ± 5.3*	NS	332	0.04
Pyrene	62 ± 3.6	**8.7 ± 1.6**	**21 ± 3.5**	313	0.16
Retene	31 ± 3.0	*12 ± 4.0*	**31 ± 4.6**	232	0.18
Benz[*a*]anthracene	6.8 ± 0.9	LD	LD	50	N/A
Triphenylene + Chrysene	11 ± 1.0	**6.2 ± 1.0**	NS	176	0.20
Benzo[*b*]fluoranthrene	11 ± 1.5	LD	LD	46	N/A
Benzo[*k*]fluoranthrene	6.0 ± 1.4	LD	LD	20	N/A
Benzo[*e*]pyrene	7.0 ± 1.1	LD	LD	28	N/A
Benzo[*a*]pyrene	6.4 ± 1.2	LD	LD	19	N/A
Indeno[1,2,3-*cd*]pyrene	9.1 ± 3.2	LD	LD	13	N/A
Benzo[*ghi*]perylene	7.0 ± 1.7	LD	LD	17	N/A
Dibenz[*a,h*]anthracene	2.4 ± 1.4	LD	LD	4	N/A
Coronene	5.6 ± 2.3	LD	LD	8	N/A
ΣPAH	1700 ± 70	*15± 4.3*	*11 ± 2.9*	332	0.07
Temperature-corrected ΣPAH conc. (288 K)	1800 ± 79				

Table ES4. Fit parameters for PAHs in vapor phase at Sturgeon Point

PAHs	Average conc. (pg/m^3)	Half-life (years)	ΔH (kJ/mol)	No. of detects	R^2
Fluorene	1900 ± 75	*21 ± 6.3*	**20 ± 2.3**	342	0.19
Phenanthrene	3100 ± 120	**12 ± 2.1**	**18 ± 2.5**	342	0.19
Anthracene	90 ± 13	NS	NS	169	NS
Fluoranthene	730 ± 31	**15 ± 3.7**	**19 ± 2.6**	342	0.16
Pyrene	280 ± 15	**7.8 ± 1.2**	**22 ± 3.2**	341	0.19
Retene	180 ± 44	NS	**50 ± 5.4**	293	0.23
Benz[*a*]anthracene	15 ± 1.9	12 ± 5.2	NS	149	0.23
Triphenylene + Chrysene	34 ± 2.4	**7.2 ± 1.1**	**15 ± 3.6**	307	0.16
Benzo[*b*]fluoranthrene	27 ± 3.1	NS	NS	143	NS
Benzo[*k*]fluoranthrene	17 ± 2.1	NS	NS	60	NS
Benzo[*e*]pyrene	17 ± 2.0	NS	NS	83	NS
Benzo[*a*]pyrene	16 ± 1.9	NS	NS	61	NS
Indeno[1,2,3-*cd*]pyrene	19 ± 2.9	LD	LD	49	N/A
Benzo[*ghi*]perylene	15 ± 2.2	LD	LD	50	N/A
Dibenz[*a,h*]anthracene	6.0 ± 2.1	LD	LD	7	N/A
Coronene	11 ± 2.6	LD	LD	13	N/A
ΣPAH	6300 ± 240	**15 ± 3.3**	**20 ± 2.5**	342	0.19
Temperature-corrected ΣPAH conc. (288 K)	7200 ± 280				

Table ES5. Fit parameters for PAHs in vapor phase at Chicago

PAHs	Average conc. (pg/m^3)	Half-life (years)	ΔH (kJ/mol)	No. of detects	r^2
Fluorene	16000 ± 930	9.4 ± 2.5	**40 ± 3.0**	218	0.47
Phenanthrene	39000 ± 3800	8.8 ± 2.2	**40 ± 3.1**	218	0.45
Anthracene	1500 ± 92	**6.2 ± 1.5**	**32 ± 4.3**	209	0.27
Fluoranthene	9500 ± 600	10 ± 2.6	**45 ± 2.6**	218	0.60
Pyrene	3900 ± 220	**6.7 ± 1.2**	**32 ± 2.9**	218	0.43
Retene	250 ± 18	**2.6 ± 0.2**	**45 ± 3.2**	204	0.66
Benz[*a*]anthracene	76 ± 7.0	**3.7 ± 0.6**	**12 ± 4.9**	168	0.20
Triphenylene + Chrysene	200 ± 14	**3.9 ± 0.5**	**46 ± 3.4**	217	0.54
Benzo[*b*]fluoranthrene	120 ± 11	6.3 ± 2.0	NS	168	0.06
Benzo[*k*]fluoranthrene	51 ± 5.5	NS	NS	132	NS
Benzo[*e*]pyrene	50 ± 4.4	NS	NS	141	NS
Benzo[*a*]pyrene	54 ± 7.0	NS	NS	122	NS
Indeno[1,2,3-*cd*]pyrene	58 ± 6.5	NS	NS	114	NS
Benzo[*ghi*]perylene	48 ± 4.9	NS	NS	116	NS
Dibenz[*a,h*]anthracene	16 ± 2.1	NS	NS	58	NS
Coronene	23 ± 2.4	NS	NS	61	NS
ΣPAH	70000 ± 5200	**8.7 ± 2.1**	**40 ± 2.9**	218	0.50
Temperature-corrected ΣPAH conc. (288 K)	73400 ± 3100				

Table ES6. Fit parameters for PAHs in vapor phase at Burnt Island

PAHs	Average conc. (pg/m^3)	Half-life (years)	ΔH (kJ/mol)	No. of detects	r^2
Fluorene	180 ± 9.6	NS	**15 ± 2.4**	200	0.18
Phenanthrene	230 ± 8.9	NS	NS	201	NS
Anthracene	3.5 ± 0.3	**4.2 ± 0.6**	NS	198	0.20
Fluoranthene	78 ± 13	-11 ± 5.1*	NS	199	0.03
Pyrene	31 ± 1.6	*9.2 ± 2.4*	**15 ± 2.5**	200	0.21
Retene	67 ± 7.1	NS	**23 ± 6.1**	113	0.13
Benz[*a*]anthracene	3.8 ± 1.6	2.5 ± 1.0	NS	54	0.13
Triphenylene + Chrysene	22 ± 1.6	6.2 ± 2.4	*18 ± 4.8*	145	0.14
Benzo[*b*]fluoranthrene	4.9 ± 1.3	LD	LD	15	N/A
Benzo[*k*]fluoranthrene	1.9 ± 0.5	LD	LD	11	N/A
Benzo[*e*]pyrene	N/A	N/A	N/A	N/A	N/A
Benzo[*a*]pyrene	1.7 ± 0.7	LD	LD	3	N/A
Indeno[1,2,3-*cd*]pyrene	15.3	LD	LD	1	N/A
Benzo[*ghi*]perylene	10 ± 1.8	LD	LD	35	N/A
Dibenz[*a,h*]anthracene	3.3 ± 0.5	LD	LD	33	N/A
Coronene	N/A	N/A	N/A	N/A	N/A
ΣPAH	590 ± 27	NS	NS	201	NS
Temperature-corrected ΣPAH conc. (288 K)	560 ± 26				

*A negative half-life indicates that the concentrations are increasing and the listed value is the doubling time.

Table ES7. Fit parameters for PAHs in vapor phase at Point Petre

PAHs	Average conc. (pg/m^3)	Half-life (years)	ΔH (kJ/mol)	No. of detects	r^2
Fluorene	350 ± 17	*-12 ± 4.0**	**24 ± 2.7**	207	0.31
Phenanthrene	520 ± 22	NS	NS	208	NS
Anthracene	7.6 ± 0.8	*6.1 ± 1.6*	*13 ± 4.2*	203	0.12
Fluoranthene	190 ± 16	-19 ± 11*	NS	207	0.06
Pyrene	74 ± 5.0	NS	NS	208	NS
Retene	97 ± 9.0	8.3 ± 3.6	13 ± 5.4	149	0.07
Benz[*a*]anthracene	4.8 ± 0.8	*4.2 ± 1.2*	NS	98	0.12
Triphenylene + Chrysene	50 ± 8.0	NS	*21 ± 6.5*	173	0.05
Benzo[*b*]fluoranthrene	14 ± 4.5	*2.1 ± 0.5*	NS	48	0.24
Benzo[*k*]fluoranthrene	3.1 ± 0.8	**2.1 ± 0.5**	NS	48	0.33
Benzo[*e*]pyrene	N/A	N/A	N/A	N/A	N/A
Benzo[*a*]pyrene	13 ± 9.6	LD	LD	10	N/A
Indeno[1,2,3-*cd*]pyrene	11 ± 3.8	LD	LD	2	N/A
Benzo[*ghi*]perylene	14 ± 2.4	LD	LD	30	N/A
Dibenz[*a,h*]anthracene	4.9 ± 0.9	LD	LD	29	N/A
Coronene	N/A	N/A	N/A	N/A	N/A
ΣPAH	1300 ± 55	NS	*11 ± 3.1*	208	0.06
Temperature-corrected ΣPAH conc. (288 K)	1200 ± 45				

*A negative half-life indicates that the concentrations are increasing and the listed value is the doubling time.

Table ES8. Fit parameters for PAHs in particle phase at Brule River

PAHs	Average conc. (pg/m^3)	Half-life (years)	Peak-to-valley ratio	Maximum date (± days)	No. of detects	r^2
Fluorene	10 ± 2.0	NS	**3.0 ± 1.2**	**Feb 3 ± 11**	98	0.22
Phenanthrene	45 ± 5.8	6.3 ± 2.1	**5.1 ± 1.2**	**Jan 25 ± 5**	163	0.42
Anthracene	7.4 ± 1.8	LD			36	N/A
Fluoranthene	58 ± 7.5	4.4 ± 1.1	**10.4 ± 1.2**	**Jan 26 ± 5**	166	0.52
Pyrene	43 ± 5.0	NS	**9.6 ± 1.2**	**Jan 24 ± 5**	132	0.50
Retene	25 ± 3.1	NS	*2.4 ± 1.2*	**Jan 6 ± 13**	160	0.14
Benz[*a*]anthracene	14 ± 1.6	NS	**8.1 ± 1.2**	**Jan 17± 6**	117	0.45
Triphenylene + Chrysene	37 ± 4.0	NS	**11.3 ± 1.2**	**Jan 18 ± 5**	152	0.49
Benzo[*b*]fluoranthrene	57 ± 6.2	NS	**7.8 ± 1.2**	**Jan 21 ± 5**	147	0.39
Benzo[*k*]fluoranthrene	23 ± 2.1	NS	**4.6 ± 1.3**	**Jan 14 ± 8**	107	0.26
Benzo[*e*]pyrene	26 ± 2.3	NS	**4.7 ± 1.2**	**Jan 28 ± 7**	116	0.32
Benzo[*a*]pyrene	21 ± 2.0	NS	**4.3 ± 1.3**	**Jan 28 ± 8**	104	0.27
Indeno[1,2,3-*cd*]pyrene	37 ± 3.9	NS	**4.4 ± 1.2**	**Jan 24 ± 8**	125	0.27
Benzo[*ghi*]perylene	27 ± 2.4	NS	**4.1 ± 1.2**	**Jan 27 ± 7**	126	0.29
Dibenz[*a,h*]anthracene	6.4 ± 0.7	LD			38	N/A
Coronene	18 ± 1.8	NS	**4.1 ± 1.3**	**Jan 26 ± 7**	87	0.29
ΣPAH	370 ± 39	4.0 ± 1.0	**9.2 ± 1.2**	**Jan 20 ± 5**	167	0.46

Table ES9. Fit parameters for PAHs in particle phase at Eagle Harbor

PAHs	Average conc. (pg/m^3)	Half-life (years)	Peak-to-valley ratio	Maximum date (± days)	No. of detects	r^2
Fluorene	3.6 ± 0.7	NS	**1.9 ± 1.1**	Feb 3 ± 11	85	0.20
Phenanthrene	17 ± 1.0	NS	**2.8 ± 1.1**	**Feb 15 ± 6**	210	0.32
Anthracene	4.2 ± 1.1	LD			22	N/A
Fluoranthene	5.1 ± 0.5	11.9 ± 4.8	**5.6 ± 1.2**	**Feb 4 ± 6**	82	0.24
Pyrene	23 ± 1.4	NS	**3.0 ± 1.2**	Feb 7 ± 7	215	0.13
Retene	8.4 ± 1.0	NS	**2.5 ± 1.2**	**Dec 31 ± 12**	151	0.13
Benz[*a*]anthracene	6.6 ± 0.6	NS	NS	NS	111	NS
Triphenylene + Chrysene	15 ± 0.9	11.3 ± 4.5	**3.1 ± 1.2**	**Jan 26 ± 7**	197	0.25
Benzo[*b*]fluoranthrene	27 ± 1.6	NS	**1.9 ± 1.1**	**Jan 16 ± 13**	179	0.10
Benzo[*k*]fluoranthrene	12 ± 1.2	NS	NS	NS	108	NS
Benzo[*e*]pyrene	13 ± 0.7	NS	NS	NS	145	NS
Benzo[*a*]pyrene	10 ± 0.7	NS	NS	NS	104	NS
Indeno[1,2,3-*cd*]pyrene	18 ± 1.0	NS	NS	NS	152	NS
Benzo[*ghi*]perylene	14 ± 0.8	NS	NS	NS	149	NS
Dibenz[*a*,*h*]anthracene	4.0 ± 0.8	LD			27	N/A
Coronene	12 ± 1.0	NS	NS	NS	88	NS
ΣPAH	150 ± 9.4	*6.8 ± 1.9*	**3.3 ± 1.2**	**Jan 30± 8**	215	0.23

Table ES10. Fit parameters for PAHs in particle phase at Sleeping Bear Dunes

PAHs	Average conc. (pg/m^3)	Half-life (years)	Peak-to-valley ratio	Maximum date (± days)	No. of detects	r^2
Fluorene	4.4 ± 0.3	NS	**2.1 ± 1.2**	**Feb 1 ± 12**	120	0.16
Phenanthrene	32 ± 2.3	NS	**3.6 ± 1.1**	**Feb 16 ± 6**	208	0.30
Anthracene	3.5 ± 0.3	NS	NS	NS	61	NS
Fluoranthene	53 ± 4.5	NS	**4.2 ± 1.2**	**Feb 13 ± 7**	213	0.25
Pyrene	37 ± 3.1	NS	**3.4 ± 1.2**	**Feb 17 ± 9**	186	0.19
Retene	7.2 ± 0.5	NS	**2.3 ± 1.2**	**Jan 29 ± 10**	147	0.15
Benz[*a*]anthracene	13 ± 1.4	NS	**2.8 ± 1.2**	**Feb 2 ± 11**	147	0.16
Triphenylene + Chrysene	29 ± 2.5	NS	**4.7 ± 1.2**	**Feb 7 ± 7**	200	0.27
Benzo[*b*]fluoranthrene	50 ± 4.0	NS	**4.2 ± 1.2**	**Feb 5 ± 7**	204	0.26
Benzo[*k*]fluoranthrene	19 ± 1.6	-9.5 ± 4.8*	1.6 ± 1.2	*Jan 23 ± 21*	150	0.08
Benzo[*e*]pyrene	24 ± 1.8	-11.4 ± 5.4*	**2.6 ± 1.2**	**Feb 9 ± 10**	167	0.16
Benzo[*a*]pyrene	20 ± 1.8	-11.0 ± 5.6*	*1.8 ± 1.2*	*Feb 10 ± 18*	152	0.08
Indeno[1,2,3-*cd*]pyrene	33 ± 2.8	NS	**2.9 ± 1.2**	**Feb 5 ± 9**	185	0.18
Benzo[*ghi*]perylene	26 ± 2.0	NS	**2.6 ± 1.2**	**Feb 5 ± 10**	185	0.16
Dibenz[*a*,*h*]anthracene	7.4 ± 0.8	LD			44	N/A
Coronene	17 ± 1.3	NS	**2.1 ± 1.2**	**Jan 16 ± 12**	128	0.14
ΣPAH	320 ± 26	NS	**5.0 ± 1.2**	**Feb 7 ± 7**	214	0.26

*A negative half-life indicates that the concentrations are increasing and the listed value is the doubling time.

Table ES11. Fit parameters for PAHs in particle phase at Sturgeon Point

PAHs	Average Conc. (pg/m^3)	Half-life (years)	Peak-to-valley ratio	Maximum date (± days)	No. of detects	r^2
Fluorene	8.8 ± 0.5	**5.2 ± 0.8**	**2.6 ± 1.1**	**Feb 17 ± 7**	174	0.39
Phenanthrene	78 ± 5.8	**4.8 ± 1.2**	**3.3 ± 1.1**	**Feb 17 ± 6**	219	0.43
Anthracene	6.4 ± 0.4	*7.9 ± 2.6*	*1.8 ± 1.2*	*Feb 8 ± 16*	140	0.13
Fluoranthene	170 ± 14	**4.7 ± 0.7**	**3.3 ± 1.1**	**Feb 12 ± 6**	219	0.38
Pyrene	98 ± 8.0	**4.5 ± 0.7**	**2.7 ± 1.2**	**Feb 17 ± 8**	215	0.31
Retene	16 ± 3.0	NS	NS	NS	188	NS
Benz[*a*]anthracene	34 ± 2.4	**5.0 ± 0.9**	**2.8 ± 1.2**	**Feb 5 ± 9**	202	0.31
Triphenylene + Chrysene	96 ± 7.6	**4.5 ± 0.7**	**3.6 ± 1.2**	**Feb 4 ± 6**	219	0.39
Benzo[*b*]fluoranthrene	180 ±12	*8.1 ± 2.4*	**3.0 ± 1.2**	**Feb 3 ± 8**	219	0.24
Benzo[*k*]fluoranthrene	50 ± 3.1	**6.6 ± 1.5**	**2.0 ± 1.2**	**Feb 5 ± 11**	216	0.18
Benzo[*e*]pyrene	69 ± 4.4	*9.1 ± 2.9*	**2.4 ± 1.2**	**Feb 7 ± 9**	217	0.19
Benzo[*a*]pyrene	50 ± 3.8	**4.8 ± 1.2**	**1.8 ± 1.2**	*Feb 12 ± 14*	217	0.20
Indeno[1,2,3-*cd*]pyrene	100 ± 6.8	*8.6 ± 2.7*	**2.2 ± 1.2**	**Feb 1 ± 11**	218	0.15
Benzo[*ghi*]perylene	74 ± 4.5	*8.4 ± 2.4*	**2.1 ± 1.1**	**Feb 1 ± 11**	218	0.16
Dibenz[*a,h*]anthracene	16 ± 1.1	NS	**1.8 ± 1.1**	*Feb 16 ±16*	131	0.16
Coronene	37 ± 2.5	*9.2 ± 2.8*	**2.4 ± 1.1**	**Feb 2 ± 9**	203	0.20
ΣPAH	1100 ±72	**5.6 ± 1.1**	**3.5 ± 1.2**	**Feb 10 ± 8**	219	0.29

Table ES12. Fit parameters for PAHs in particle phase at Chicago

PAHs	Average conc. (pg/m^3)	Half-life (years)	Peak-to-valley ratio	Maximum date (± days)	No. of detects	r^2
Fluorene	92 ± 7.8	**5.6 ± 1.1**	**3.0 ± 1.2**	**Jan 31 ± 7**	193	0.31
Phenanthrene	1000 ± 72	*9.5 ± 4.8*	**2.8 ± 1.1**	**Jan 31 ± 7**	193	0.27
Anthracene	130 ± 14	**5.5 ± 1.2**	**2.7 ± 1.2**	**Jan 17 ± 9**	193	0.23
Fluoranthene	2300 ± 140	*9.8 ± 3.1*	**2.7 ± 1.1**	**Jan 27 ± 7**	193	0.26
Pyrene	1600 ± 100	**8.3 ± 2.5**	**2.9 ± 1.2**	**Jan 21 ± 8**	193	0.25
Retene	97 ± 12	*7.9 ± 2.7*	**8.0 ± 1.2**	**Jan 7 ± 5**	183	0.46
Benz[*a*]anthracene	670 ± 50	*6.8 ± 1.8*	**2.4 ± 1.2**	**Jan 15 ± 10**	193	0.20
Triphenylene + Chrysene	920 ± 59	**7.4 ± 1.8**	**2.6 ± 1.1**	**Jan 23 ± 8**	192	0.25
Benzo[*b*]fluoranthrene	1400 ± 80	13.6 ± 5.9	**2.2 ± 1.1**	**Jan 25 ± 9**	193	0.18
Benzo[*k*]fluoranthrene	450 ± 27	*8.1 ± 2.2*	**2.2 ± 1.1**	**Jan 20 ± 10**	193	0.20
Benzo[*e*]pyrene	590 ± 32	14.7 ± 7.0	**2.3 ± 1.1**	**Jan 24 ± 9**	193	0.18
Benzo[*a*]pyrene	750 ± 58	9.6 ± 3.9	*1.9 ± 1.2*	**Jan 6 ± 15**	193	0.10
Indeno[1,2,3-*cd*]pyrene	1000 ± 58	NS	**2.1 ± 1.1**	**Jan 14 ± 10**	193	0.16
Benzo[*ghi*]perylene	770 ± 41	*10.5 ± 3.5*	**2.4 ± 1.1**	**Jan 12 ± 8**	193	0.22
Dibenz[*a,h*]anthracene	150 ± 11	*8.8 ± 2.8*	**1.8 ± 1.1**	**Jan 19 ± 14**	192	0.12
Coronene	310 ± 21	**7.0 ± 1.6**	**2.7 ± 1.1**	**Jan 8 ± 8**	193	0.28
ΣPAH	12000 ± 720	*8.9 ± 2.6*	**2.5 ± 1.1**	**Jan 21± 8**	193	0.24

Table ES13. Fit parameters for PAHs in particle phase at Burnt Island

PAHs	Average conc. (pg/m^3)	Half-life (years)	Peak-to-valley ratio	Maximum date (± days)	No. of detects	r^2
Fluorene	8.4 ± 1.1	*1.9 ± 0.3*	NS	NS	68	0.42
Phenanthrene	19 ± 1.7	*9.4 ±2.8*	**3.8 ± 1.2**	**Feb 3 ± 6**	232	0.32
Anthracene	3.5 ± 0.3	**5.2 ±1.1**	**2.2 ± 1.1**	**Feb 13 ± 12**	196	0.20
Fluoranthene	30 ± 2.5	*7.4 ± 1.9*	**3.6 ± 1.2**	**Feb 10 ± 7**	228	0.26
Pyrene	24 ± 1.8	*7.9 ± 2.2*	**3.1 ± 1.2**	**Feb 7 ± 8**	233	0.22
Retene	13 ± 1.5	**6.0 ± 1.4**	**2.9 ± 1.3**	**Jan 19 ± 12**	115	0.26
Benz[*a*]anthracene	13 ± 1.0	**5.0 ± 0.9**	**2.8 ± 1.2**	**Feb 5 ± 9**	214	0.27
Triphenylene + Chrysene	27 ± 1.8	*8.8 ± 2.7*	**3.4 ± 1.2**	**Feb 10 ± 7**	227	0.25
Benzo[*b*]fluoranthrene	31 ± 2.1	*8.7 ± 2.6*	**3.2 ± 1.2**	**Feb 6 ± 8**	226	0.24
Benzo[*k*]fluoranthrene	14 ± 0.9	*8.4 ± 2.4*	**2.6 ± 1.4**	**Feb 10 ± 9**	225	0.20
Benzo[*e*]pyrene	30 ± 2.0	**5.0 ± 0.9**	**2.6 ± 1.4**	**Feb 14 ± 10**	184	0.29
Benzo[*a*]pyrene	19 ± 1.2	11.2 ± 4.5	**2.3 ± 1.2**	**Feb 9 ± 11**	224	0.14
Indeno[1,2,3-*cd*]pyrene	31 ± 2.1	**6.6 ± 1.4**	**3.0 ± 1.1**	**Jan 27 ± 8**	205	0.28
Benzo[*ghi*]perylene	25 ± 1.6	*7.9 ± 2.1*	**3.0 ± 1.2**	**Feb 4 ± 8**	223	0.25
Dibenz[*a,h*]anthracene	6.2 ± 0.5	*7.3 ± 2.1*	**2.4 ± 1.2**	**Jan 18 ± 7**	191	0.16
Coronene	8.2 ± 1.6	LD			30	N/A
ΣPAH	270 ± 18	NS	**4.2 ± 1.2**	**Jan 23 ± 7**	233	0.24

Table ES14. Fit parameters for PAHs in particle phase at Point Petre

PAHs	Average conc. (pg/m^3)	Half-life (years)	Peak-to-valley ratio	Maximum date (± days)	No. of detects	r^2
Fluorene	9.0 ± 0.9	*2.2 ± 0.3*	1.8 ± 1.3	NS	62	0.60
Phenanthrene	33 ± 2.9	**7.0 ±1.5**	**5.4 ± 1.1**	**Feb 4 ± 5**	238	0.45
Anthracene	2.4 ± 0.2	**5.3 ±1.0**	**4.2 ±1.1**	**Feb 1 ± 4**	218	0.41
Fluoranthene	63 ± 6.6	**5.1 ± 0.9**	**5.8 ± 1.2**	**Feb 4 ± 5**	236	0.39
Pyrene	54 ± 5.5	**6.5 ± 1.6**	**6.5 ± 1.2**	**Feb 1 ± 5**	238	0.39
Retene	17 ± 2.4	*5.5 ± 1.9*	**4.4 ± 1.4**	**Feb 13 ± 10**	76	0.32
Benz[*a*]anthracene	26 ± 2.2	**5.7 ± 1.1**	**6.0 ± 1.2**	**Jan 27 ± 5**	228	0.42
Triphenylene + Chrysene	82 ± 10	**5.9 ± 1.4**	**7.8 ± 1.2**	**Jan 28 ± 5**	238	0.40
Benzo[*b*]fluoranthrene	110 ± 16	**5.8 ± 1.3**	**7.2 ± 1.2**	**Jan 24 ± 5**	237	0.39
Benzo[*k*]fluoranthrene	37 ± 4.2	**7.1 ± 1.8**	**6.2 ± 1.2**	**Jan 25 ± 5**	237	0.38
Benzo[*e*]pyrene	85 ± 10	**5.6 ± 1.2**	**4.7 ± 1.2**	**Jan 19 ± 7**	217	0.33
Benzo[*a*]pyrene	41 ± 3.3	*10.7 ± 4.1*	**5.7 ± 1.2**	**Jan 25 ± 5**	238	0.35
Indeno[1,2,3-*cd*]pyrene	80 ± 7.2	**6.2 ± 1.4**	**5.6 ± 1.2**	**Jan 21 ± 5**	227	0.38
Benzo[*ghi*]perylene	20 ± 2.2	**6.5 ± 1.4**	**5.9 ± 1.1**	**Jan 22 ± 5**	137	0.42
Dibenz[*a,h*]anthracene	12 ± 1.0	**6.6 ± 1.6**	**4.0 ± 1.1**	**Jan 18 ± 7**	220	0.29
Coronene	20 ± 3.8	LD			29	N/A
ΣPAH	710 ± 71	**6.7 ± 1.6**	**6.9 ± 1.2**	**Jan 27 ± 5**	238	0.42

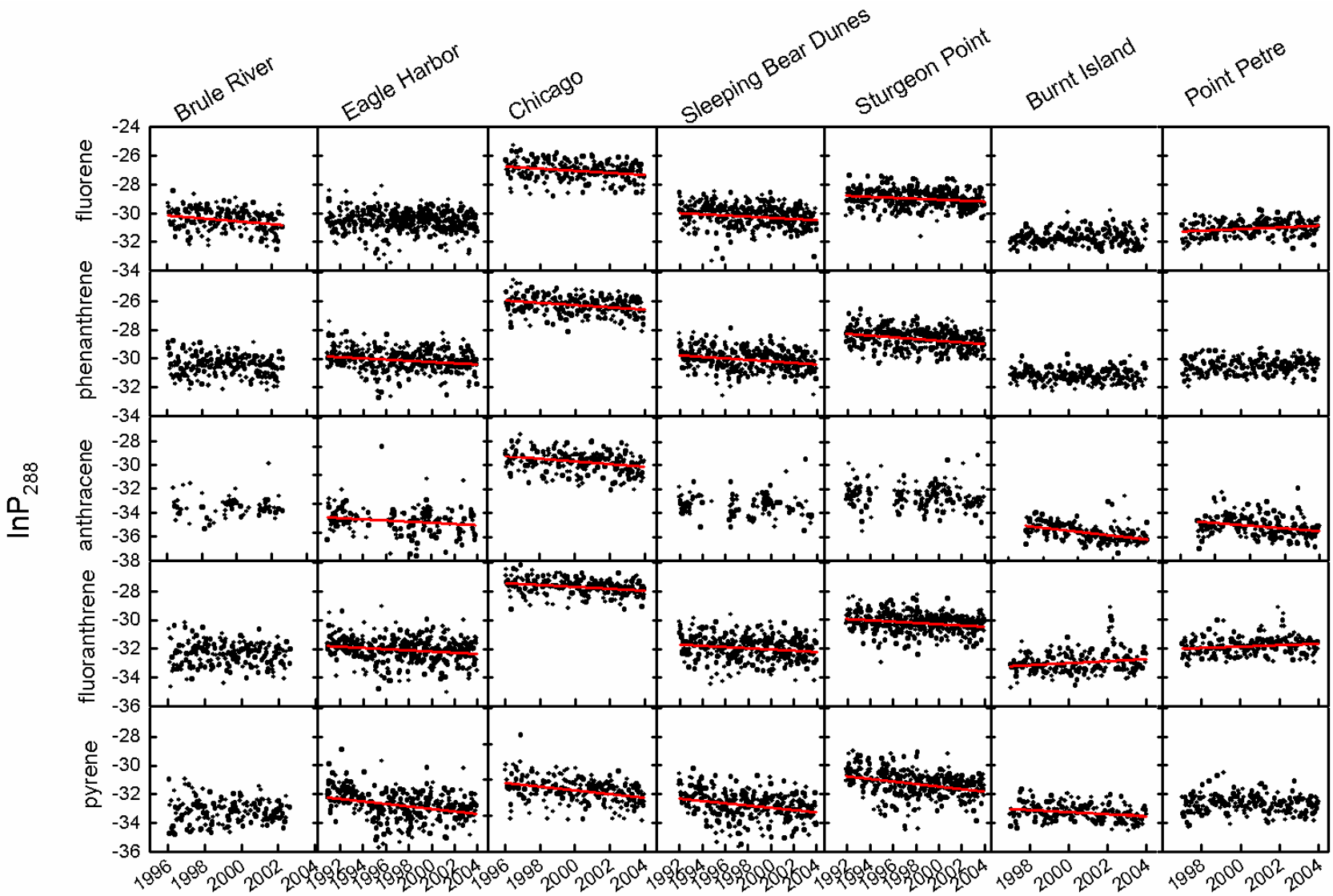

Figure ES1. Temporal trends of vapor-phase PAH concentrations at seven IADN sites. The red lines indicate long-term significant decreasing or increasing trends. Detailed information on the fitted parameters is in Tables DS1 to DS7.

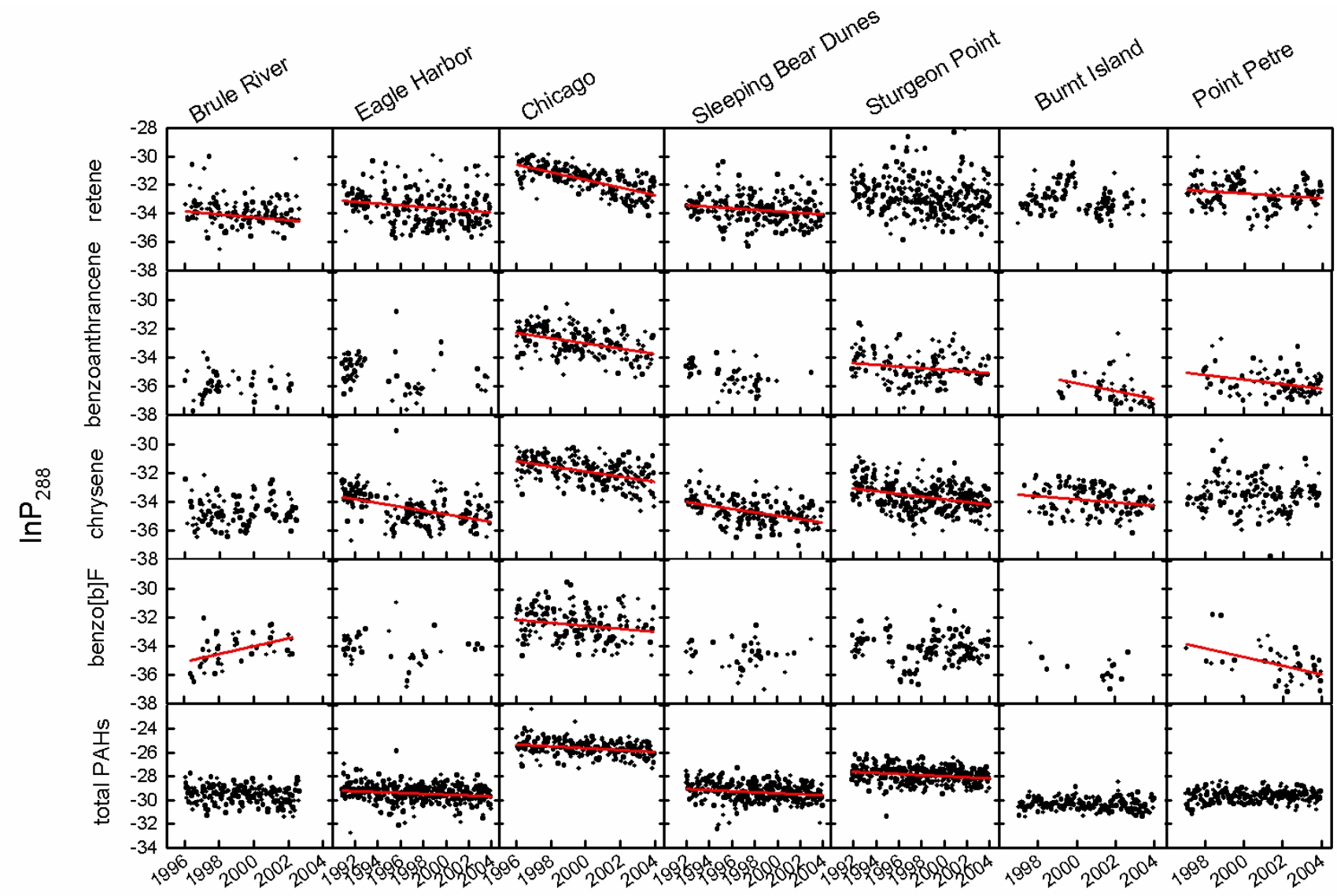

Figure ES1 (continued). Temporal trends of vapor-phase PAH concentrations at seven IADN sites.

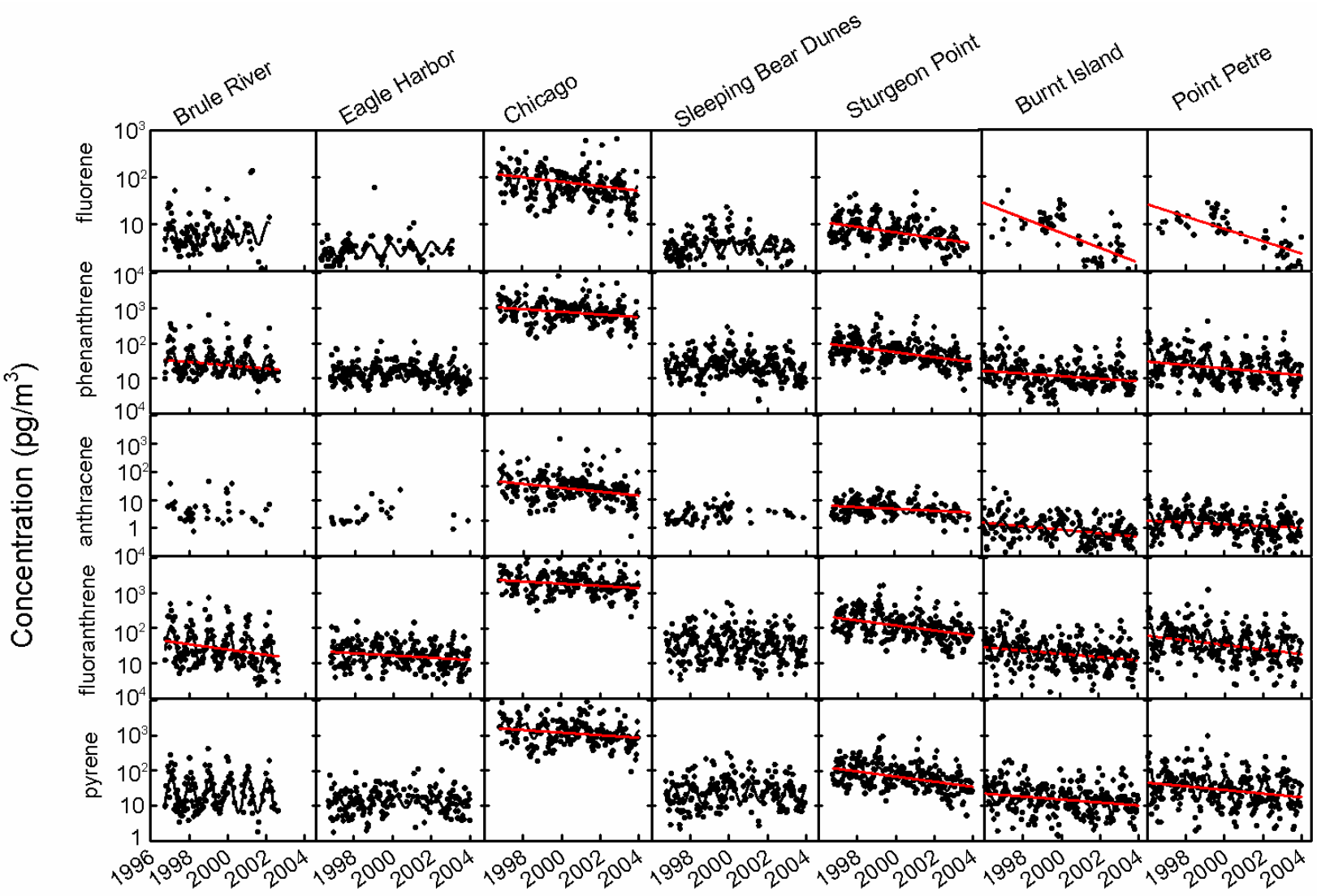

Figure ES2. Temporal trends of particle-phase PAH concentrations at seven IADN sites. The black curve is the fitted line using the sinusoidal model with a period length (a_3) set to one year. The red lines indicate long-term significant decreasing or increasing trends. Detailed information on the fitted parameters is in Tables DS8 to DS14.

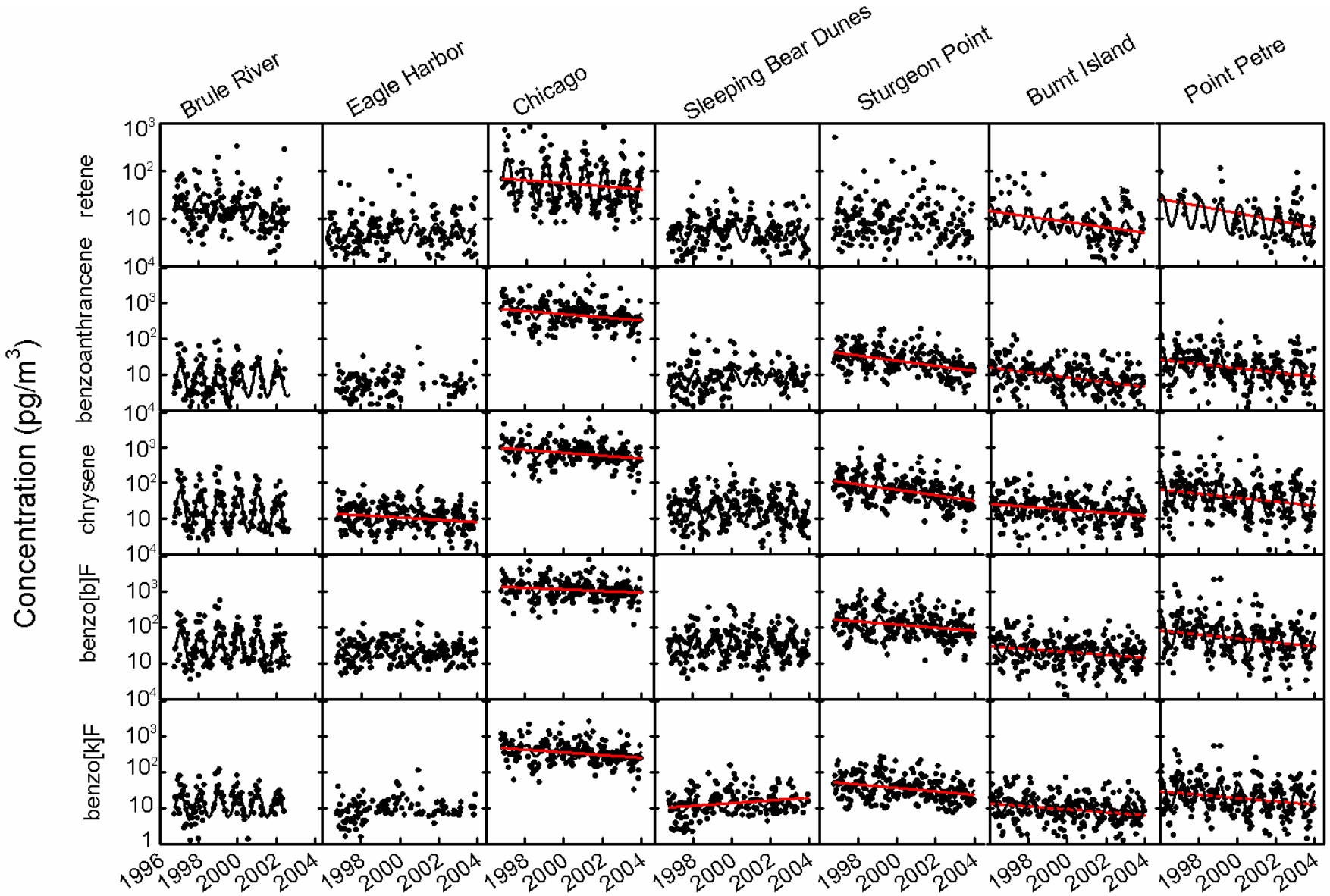

Figure ES2 (continued). Temporal trends of particle-phase PAH concentrations at seven IADN sites.

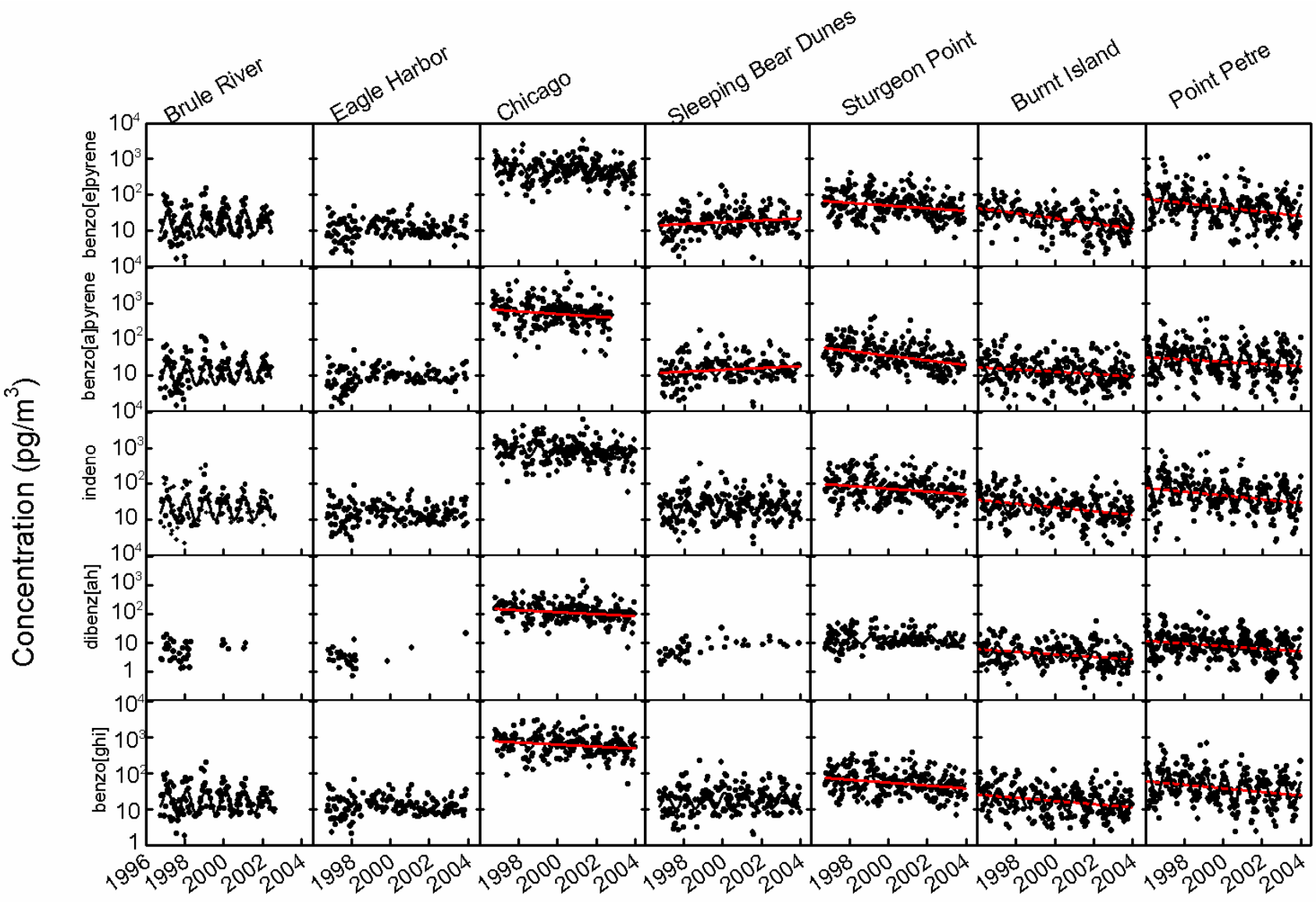

Figure ES2 (continued). Temporal trends of particle-phase PAH concentrations at seven IADN sites.

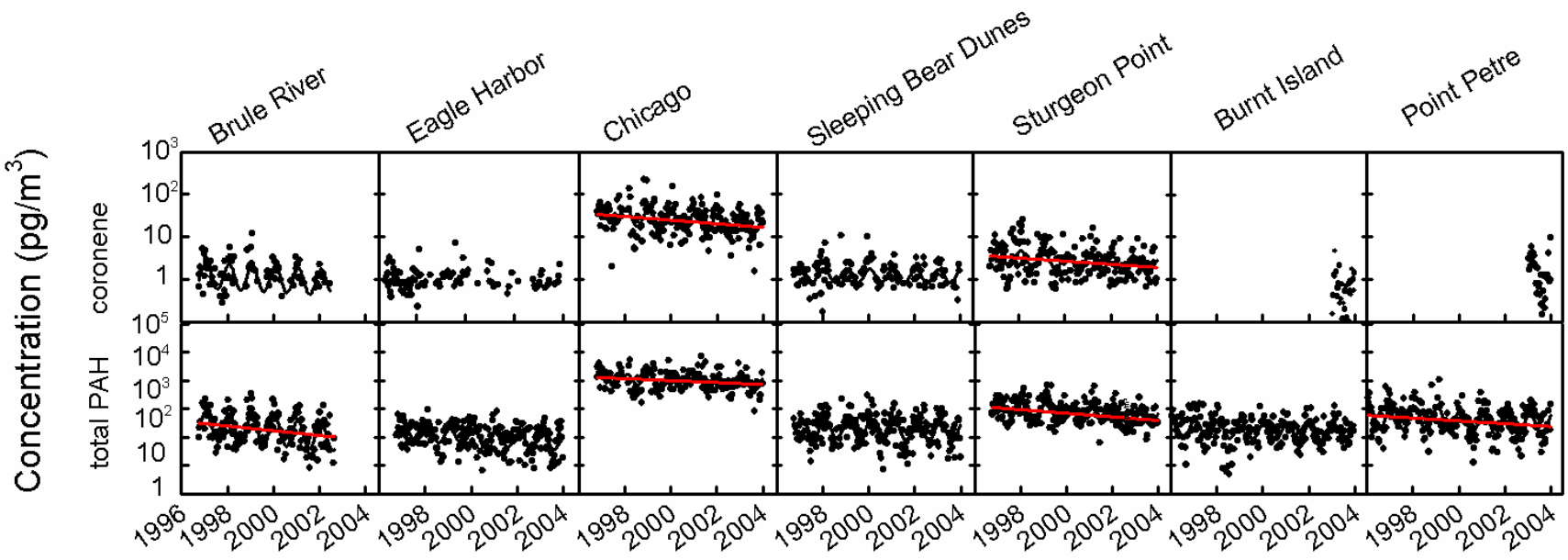

Figure ES2 (continued). Temporal trends of particle-phase PAH concentrations at seven IADN sites.

Appendix F. Atmospheric Organochlorine Pesticide Concentrations near the Great Lakes: Temporal and Spatial Trends

Published in *Environmental Science & Technology*, **2006**, *40*, 6587-6593.

Atmospheric Organochlorine Pesticide Concentrations near the Great Lakes: Temporal and Spatial Trends

Ping Sun,[1] Pierrette Blanchard,[2] Kenneth, Brice[2], and Ronald A Hites∗[1]

[1]School of Public and Environmental Affairs
Indiana University
Bloomington, Indiana, 47405 USA

and
[2]Environment Canada
4905 Dufferin Street
Toronto, ON M3H 5T4 Canada

∗Corresponding Author Email: hitesr@indiana.edu

Brief

Concentrations of most OC pesticides are decreasing with half-lives of 5-10 years based on data acquired by the Integrated Atmospheric Deposition Network during the period ~1990 through 2003.

Abstract

As a part of the Integrated Atmospheric Deposition Network, atmospheric organochlorine pesticide concentrations were measured in both the gas and particle phases at seven sites near the Great Lakes. Much higher organochlorine pesticide concentrations were found in the gas phase compared to that in the particle phase. Long-term decreasing trends were observed for most pesticides in both phases. Two different seasonal trends were observed in the particle phase: (a) In-use pesticides, such as endosulfan, showed higher concentrations in the summer, a time corresponding to their agriculture use. (b) Restricted organochlorine pesticides, such as lindane, showed higher particle-phase concentrations in the winter, presumably due to their enhanced partitioning from the gas phase to particles. Generally, Chicago had the highest concentrations of chlordanes, dieldrin, and ΣDDT, suggesting that urban areas could be sources of these compounds to atmosphere. Point Petre had the highest concentrations of endosulfan, likely due to its agricultural application in Southern Ontario.

Introduction

Organochlorine (OC) pesticides were widely used in North America before the 1970s, and some of these compounds are still present in the environment 20-30 years after their use was restricted. Several studies have shown that OC pesticides are re-volatilized from agricultural soils in the southern United States, Mexico, and the Canadian prairies and atmospherically transported to the Great Lakes (*1,2*). To study this transport, the Integrated Atmospheric Deposition Network (IADN) was founded in 1990. The network monitors OC pesticides in air, atmospheric particles, and precipitation around the Great Lakes, and IADN scientists have

published several studies on OC pesticides in air, reporting on their concentrations (*3,4*), their spatial variations (*5*), and their sources (*6*).

Only a few studies have examined long-term temporal trends of OC pesticides in air. Hung et al. reported a long-term decline of atmospheric OC pesticide concentrations from 1993 to 1997 in the Canadian Arctic (*7*). Cortes et al. (*8*), reported decreasing concentrations, with half-lives of <10 years for most gas-phase OC pesticides at five remote sites around the Great Lakes covering the period from November, 1990 to January, 1996. In this paper, we continue the work of Cortes et al. (*8*) by adding eight years of gas-phase results (from January 1996 to December 2003). The gas-phase OC pesticide concentrations at two additional sites (Brule River, near Lake Superior, and Chicago, near Lake Michigan) and particle-phase OC pesticide concentrations at five United States sites were also added. Using this extended database, the temporal and spatial trends of OC pesticide atmospheric concentrations around the Great Lakes have been investigated.

Experimental

Sampling and Analytical Methodology. The OC pesticides measured by IADN are aldrin, α- and γ-chlordane, *p,p'*- and *o,p'*-DDT, *p,p'*- and *o,p'*-DDD, *p,p'*-DDE, dieldrin, α- and β-endosulfan, endrin, heptachlor epoxide, hexachlorobenzene, α-, β-, and γ-hexachlorocyclohexane (HCH), methoxychlor, and *trans*-nonachlor.

Seven IADN sampling sites were chosen in this study, and a map of these locations is given elsewhere (*9*). Chicago is the only site located in an urban area, while Sturgeon Point is a semi-urban site located about 25 km south of Buffalo, NY. The other five sites (Eagle Harbor and Brule River, near Lake Superior; Sleeping Bear Dunes, near Lake Michigan; Burnt Island, near Lake Huron; and Point Petre, near Lake Ontario) are located in unpopulated areas near the Great Lakes. Detailed site information can be found at the IADN website (www.msc.ec.gc.ca/iadn).

Measurements of OC pesticides in the gas phase started at Eagle Harbor, MI in November 1990, at Sleeping Bear Dunes, MI and Sturgeon Point, NY in December 1991, at Point Petre, ONT in January 1992, at Burnt Island, ONT in January 1993, and at Brule River, WI and Chicago, IL in January 1996. The particle phase samples at the two Canadian sites (Burnt Island and Point Petre) are not discussed in this paper due to the limited data available. At the five U.S. sites, particle-phase data reported here started in October 1996 because prior to that time, two or three particle-phase samples had been combined into monthly samples. In all cases, the database ends with samples collected through December 2003 except at Brule River, which was closed in August 2002.

The methodologies employed for collection and analysis of samples up to January 1996 have been previously summarized in detail by Cortes et al. (*8*) and so will not be repeated here. There have been minimal modifications to these methodologies since January 1996 for samples collected up to December 2003 at all sites considered here. The detailed comparison of sampling and analytical procedures between the U.S. and Canadian sites is listed in Table FS1 of the Supporting Information.

Quality control and assurance procedures were followed to ensure data quality (*10,11*). For the OC pesticides that are the focus of this paper, the results of the QA activities have confirmed that the data from the U.S. and Canadian sites can be regarded, with a few possible exceptions (e.g. the HCHs), as generally equivalent so that spatial differences in ambient

concentrations can be considered to be real and not caused by artifacts or biases arising from differences in the sampling or analytical methodologies. The Canadian sampling method used one PUF plug to sample the gas phase. To evaluate the potential for breakthrough, two such PUF plugs were placed in series for several experiments during the summer of 2003. The results indicated breakthrough of the HCHs of the order of 10-20% (*11*). The Canadian HCH concentrations were not corrected in this paper, but the spatial distributions of HCHs are only discussed for the five U.S. sites.

Temporal Trend Analysis. A temporal trend analysis procedure adopted by Cortes et al. (*8*) will be used here. Briefly, the gas-phase pesticide concentrations are first converted to partial pressures (P) using the ideal gas law. The atmospheric temperature effect on the pesticide concentration was then corrected by adjusting the partial pressures to a reference temperature of 288 K. This corrected partial pressure, P_{288}, was calculated from

$$\ln P_{288} = -\frac{\Delta H}{R}\left(\frac{1}{288} - \frac{1}{T}\right) + \ln P \tag{1}$$

where P is the partial pressure converted from concentration (in atm), ΔH is a characteristic phase-transition energy of the compound (in kJ/mol), T is the average temperature at the sampling site during the day the sample was collected (in K), and R is the gas constant. The coefficient, $\Delta H/R$, was determined by a preliminary regression of ln(P) vs. 1/T. These temperature- corrected partial pressures were then regressed vs. sampling date in Julian days relative to January 1, 1990 (t) to find a first-order rate constant (a_1 in days^{-1}) for the rate of decrease (or increase) of the atmospheric concentrations:

$$\ln(P_{288}) = a_0 - a_1 t \tag{2}$$

The particle-phase concentrations (C_p) of the pesticides at the five U.S. sites were fitted by the following time-dependent function to study their temporal trends (*9*)

$$\ln C_p = b_0 + b_1 t + b_2 \sin\left(\frac{t}{b_3} + b_4\right) \tag{3}$$

where b_2 is the periodic amplitude (unitless), b_3 is the length of the period (in days), and b_4 is the periodic offset (in days). If b_1 was significant ($p < 0.05$), either a decreasing ($b_1 < 0$) or increasing ($b_1 > 0$) trend in the pesticide concentrations could be determined for this sampling period.

Results and Discussion

The average concentrations of the OC pesticides in the gas and particle phases as measured by IADN are listed in Table FS2-FS13 of the Supporting Information. Generally, pesticide concentrations in the particle phase are much lower (usually less than 10%) than those in the gas phase. For example, the average γ-HCH concentration in the particle phase at Chicago was 0.96 ± 0.07 pg/m^3, which is about 3% of this compound's concentration in the gas phase (35 ± 2.5 pg/m^3), and the total α- and γ-chlordane concentrations in the particle phase were less than ~10% of those in the gas phase. Similar results have been reported by the New Jersey Atmospheric Deposition Network (NJADN) (*12*). The preferred partitioning of OC pesticides toward the gas phase is consistent with what would be expected from their relatively high vapor pressures.

Comparisons of selected OC pesticide concentrations in the gas phase with measurements made by IADN and by other studies over the same time period are given in Table FS14. In

general, the IADN results are similar to other gas-phase OC pesticide concentrations reported for North America. The average concentration of gas-phase α- and γ-HCH at Jersey City, NJ were 23 and 22 pg/m^3, respectively, which are lower than those measured by IADN at Chicago (52 ± 2.5 pg/m^3 and 35 ± 2.5 pg/m^3 for α- and γ-HCH). The gas phase concentrations of α- and γ-chlordane were similar at Jersey City and at Chicago, while these concentrations were higher at Pineland, NJ, a rural site compared to Sleeping Bear Dunes, MI, a background site. One study showed higher chlordane concentrations at Rohwer, Arkansas compared to IADN, but this result could be attributed to the historically heavy use of chlordane near that Arkansas collection site (*13*).

Shen et al. measured α-endosulfan, *p,p'*-DDT, and *p,p'*-DDE at two IADN sites, Point Petre and Burnt Island, from May 2000 to May 2001 using passive samplers (*14*). A comparison of the concentrations of these three pesticides at Burnt Island (Table FS14) suggests that the results matched well between these two studies. Other studies reported selected OC pesticide concentrations in the gas phase in Birmingham, U.K.; Seoul, Korea; and Senga Bay, South Africa (*15,16,17*). Generally, the γ-HCH concentrations were higher in the U.K. than in North America, presumably due to heavier applications of purified γ-HCH (lindane) in Europe (*18*). The α-HCH concentrations were an order of magnitude higher in Seoul, Korea compared to Chicago and Jersey City, suggesting that technical HCH was more widely or more recently used in Korea than in North America. Pesticides measured at Senga Bay, South Africa showed lower atmospheric concentrations compared to the U.S. and the U.K., indicating less pesticide usage in this economically developing region (*17*).

Temporal trends. Most of the OC pesticide concentrations showed significant decreases over time either in the vapor or particle phase. The calculated half-lives of these OC pesticides in the gas and particle phases are listed in Table F1. Although different half-lives between the gas and particle phase were observed for some OC pesticides, most of the half-lives ranged from 4 to 9 years. For example, similar half-lives were observed in both the vapor and particle phases for γ-HCH (lindane) at Chicago and at Sturgeon Point and for dieldrin at all five U.S. sites. Figure E1 shows the temporal trends of γ-HCH and α-endosulfan in the vapor and particle phases, respectively while the long-term trends of the restricted OC pesticides are shown in Figures FS1 and FS2. Significant *increasing* trends were observed for some restricted pesticides. For example, in the gas phase, the *o,p'*-DDT concentration increased at Sleeping Bear Dunes and Sturgeon Point, and endrin increased at Chicago. However, for these cases, only data from 1999 to 2003 were available.

Although γ-HCH was still in-use in Canada until 2003, long-term decreasing trends were observed in both the gas and particle phases at all the sites except for the particle phase for at Brule River (Figure F1). Technical HCH contained 60-70% α-HCH, 2-12% β-HCH, 10-15% γ-HCH, and 3-28% other minor isomers and had been widely used in North America until it was phased out in the 1970s and replaced by lindane, which is the purified γ isomer (*19*). Long-term decreasing trends of atmospheric HCH concentrations have been observed by other researchers (*7,8,20*). Garmouma and Poissant reported a longer half-life of atmospheric α-HCH (>10 years) compared to γ-HCH (~5 years) in Quebec, Canada (*21*). Hung et al. observed a slow decrease of α-HCH concentrations (average half-life of 17 years) in Arctic air based on data collected from 1993 to 1997. After adding two more years-worth of data, Hung et al. estimated that the half-life α-HCH concentrations in Arctic air had significantly decreased to 9 years (*7*). However, the half-life of γ-HCH did not change using the extended the data set. Although we observed similar

half-lives for HCHs, our results showed that γ-HCH had a longer half-life (5 to 10 years) compared to a 4-year half-life for α-HCH at most IADN sites (Table F1). The only exception was at Sleeping Bear Dunes, where these two pesticides showed similar half-lives of ~4 years. Similar results were reported by Buhler et al. for Eagle Harbor and Sturgeon Point based on IADN samples collected from 1990 to 2001 (*4*). The slower decline of γ-HCH measured by IADN in the Great Lakes region is likely due to the continuing usage of lindane in Canada. In fact, ~8660 t of lindane have been applied during the same period in the Canadian prairies, and there is evidence that atmospheric transport of this pesticide to the Great Lakes region was occurring (*22*).

Unlike α- and γ-HCH, β-HCH concentrations did not show significant trends at most sites (Figure FS1). This difference may be the result of the various properties of the HCH isomers. Compared to α- and γ-HCH, β-HCH has the highest physical and metabolic stability because of its relatively planar structure (*23*). As a result, β-HCH's environmental concentrations seem to decrease more slowly than those of α- and γ-HCH. Thus, it is possible that we will need samples over a longer time period before we are able to observe a decreasing trend of β-HCH concentrations at these sites.

α-Endosulfan, a current-use pesticide, showed no long-term decreasing trends in the vapor phase at Eagle Harbor, Sleeping Bear Dunes, or Sturgeon Point (Figure F1). However, α-endosulfan's concentrations in the particle phase declined at all five U.S. sites. The National Center for Food and Agriculture Policy provides an endosulfan usage database for the period 1992-97 (*24*). Although endosulfan usage in Michigan significantly decreased from 29 tons to 19 tons between 1992 and 1997, increasing usage was also observed in the surrounding states, including New York, Indiana, Kentucky, and Minnesota. Because of the lack of updated usage data, we are reluctant to correlate the decreasing α-endosulfan concentrations in the particle phase with its usage pattern.

Chlordane concentrations in the gas phase declined at all seven sites (Figure FS1). Overall, α-chlordane concentrations in the gas phase had half-lives greater than 10 years and slightly less than 10 years in the particle phase (Table F1). Gas phase γ-chlordane concentrations decreased with half-lives of ~7 years at most sites except Burnt Island. *trans*-nonachlor concentrations showed similar decreasing trends as α-chlordane with half-lives of ~10 years. Technical chlordane was a mixture containing γ-chlordane (13%), α-chlordane (11%), *trans*-nonachlor (5%), and more than 140 other compounds with six to nine chlorine atoms (*25*). Of these components, γ-chlordane is generally regarded as the most susceptible to degradation by microorganisms in soil (*26,27*). This observation generally agreed with our results, which showed a faster rate of decline of γ-chlordane compared to α-chlordane and *trans*-nonachlor. The half-lives of chlordane in this study were slightly longer than in other studies. For example, Bidleman et al. observed a decline of α- and γ-chlordane and *trans*-nonachlor concentrations in Arctic air with half-lives ranging from 4.9 to 9.7 years over the time period 1984 to 1998 (*28*). Hung et al. reported the half-lives of 6.1, 5.5, and 6.2 years for α-, γ-chlordane and *trans*-nonachlor, respectively, at Alert, Canada from 1993 to 1999 (*7*). A previous publication by IADN also reported shorter half-lives for chlordane concentrations at Sleeping Bear Dunes, Sturgeon Point, and Point Petre based on samples collected from 1990 to 1996 (*8*). Technical chlordane was introduced in 1947 and phased out in the United Sates in 1988, thus, the faster decline reported previously could have been a response to its restriction. The slower decline rate

of chlordane that we now observe may be a result of these concentrations approaching a steady state in recent years (*29*).

Technical DDT consisted of *p,p´*-DDT (65-80%), *o,p´*-DDT (15-21%), *p,p´*-DDD (<4%) and small amounts of other compounds. *p,p´*-DDT can dehydrochlorinate in the environment to form *p,p'*-DDE (*30*). IADN measures the gas phase concentrations of several DDT-related compounds, including *p,p'*-DDT, *p,p'*-DDD, *p,p'*-DDE, *o,p'*-DDT, and *o,p'*-DDD in the gas phase, but in the particle phase, *p,p'*-DDE and *o,p'*-DDT are not measured. As shown in Figures ES1 and ES2, no long-term trends were observed for DDT-related compounds in the particle phase with two exceptions: *p,p'*-DDD concentrations decreased at Chicago, and *o,p'*-DDD concentrations decreased at Sleeping Bear Dunes. In the gas phase, *p,p'*-DDT, *p,p'*-DDD, *p,p'*-DDE, and *o,p'*-DDD concentrations showed decreasing trends at most sites, although shorter datasets resulted in a significant *increasing* trend of *o,p´*-DDT concentrations at Sleeping Bear Dunes and Sturgeon Point. Hung et al. also found an increasing trend for *o,p´*-DDT at Alert, Canada from 1993 to 1997 (*20*). Given that DDT was banned in 1970s in the North America, no newly manufactured or applied DDT is now entering the North American environment; thus, the cause of these increasing trends is not clear.

In general, most of the OC pesticide half-lives listed in Table F1 are longer than those reported by Cortes and co-workers (*8*). For example, α-chlordane has a half-life of 10 ±1.3 years at Sturgeon Point compared to a previously reported 4.1 ±1.4 years. At Sleeping Bear Dunes, the half-life of *p,p'*-DDT increased from 2.3 ± 0.6 years to 11 ± 3.1 years. With the additional eight years of data, the longer half-lives of OC pesticides that we now observe suggest that these concentrations are now approaching a steady state. In addition, with a longer sampling period, the calculated half-lives in our study showed lower relative standard errors compared to the previously reported results (*8*).

We also compared the decline of OC pesticide concentrations in the vapor and particle phase with those measured in different environmental compartments including precipitation, lake surface water, and biota in the Great Lakes (*9,31,32,33*). Some similarities were observed for selected pesticides. For example, γ-HCH had a half-life of 4 to 6 years in precipitation at Eagle Harbor and Chicago (*9*), which is similar to those in the vapor and particle phases. Trends of chlorinated organic contaminants in rainbow smelt from Lake Huron, Michigan, and Superior from 1983 to 1999 have recently been reported (*31*). The half-lives of chlordane (7-11 years) and *p,p'*-DDE (7-9 years) in biota in these three lakes agree with the half-lives measured in our study. We note that, although the reported half-lives for OC pesticides in different compartments had a wide range (e.g. 2 to 35 years in lake trout, *33*), most of them are around 6 to 10 years, similar to the values we measured in the atmosphere. These similarities suggested that those pesticides are at a long-term equilibrium among these environmental compartments (*34*).

Two different seasonal trends were observed for OC pesticide concentrations measured by IADN in the particle phase: First, the concentrations peak in the summer for current in-use pesticides, such as endosulfan, a time which corresponds well to their agricultural use (*4,35)*. For example, the highest β-endosulfan concentration was ~30 times higher than the lowest concentration (Table FS8-FS12) at Sleeping Bear Dunes, indicating substantial seasonal variations. Second, the concentrations peak in the winter (in January or February) for restricted pesticides, such as chlordane. These restricted pesticides enter the atmosphere from re-volatilization from lake and terrestrial surfaces (*33*), and their concentrations in the atmospheric

particle phase tend to increase during the winter due to enhanced partitioning from the gas phase to the particle phase.

Spatial Trends. The spatially resolved concentrations of the three major technical HCH isomers in the gas phase are summarized in Figure F2. Among these five U.S. sites, the α-HCH concentrations were slightly higher (average 100 ± 5.3 pg/m^3) at Eagle Harbor [F = 24.9, p < 0.001]. These concentrations were similar (average 82 ± 1.8 pg/m^3) at Sleeping Bear Dunes and Sturgeon Point [F = 2.56, p = 0.06]. Chicago and Brule River showed similar but lower α-HCH concentrations (average 54 ± 2.2 pg/m^3 [F = 1.54, p= 0.21]. β-HCH concentrations were highest in Chicago, followed by Sturgeon Point and Sleeping Bear Dunes. Similar and the lower β-HCH concentrations were observed at Brule River and Eagle Harbor. [F = 2.39, p = 0.07]. Chicago, Sleeping Bear Dunes, and Sturgeon Point had similar γ-HCH concentrations [F = 1.0, p = 0.39], but these were significantly higher than γ-HCH gas-phase concentrations at Brule River and Eagle Harbor [F = 12, p < 0.001].

The different spatial trends of the three HCH isomers could be related to their different physical and chemical properties. α-HCH is more volatile than β-HCH and γ-HCH, and α-HCH is slower to react with hydroxyl radicals (*23*). Therefore, α-HCH is more readily transported through the atmosphere, and it tends to have a relatively uniform global atmospheric concentration. The higher β-HCH concentrations at Chicago and Sturgeon Point suggests past use of technical HCH in urban areas (*36*).

Since α- and γ-HCH have different vapor pressures, we corrected the atmospheric temperature effect on their concentrations (see eq 1) and calculated the corrected ratio between α- and γ-HCH at 288 K in the gas phase. This ratio was around 5 at Brule River and Eagle harbor, the two sites closest to Lake Superior; around 4 at Sturgeon Point and Point Petre; and around 2 at Chicago and Burnt Island. A slightly higher value of 7 was calculated at Sleeping Bear Dunes. In the technical HCH mixture, the ratio between α- and γ-HCH is expected to be between 4 and 7 (*19*). The lower values at Burnt Island, Point Petre, and Sturgeon Point could be due to the relatively high concentrations of γ-HCH recently used in Canada. The low ratio of 2 at Chicago may indicate historically heavy use of γ-HCH at that location. At Brule River, Eagle Harbor and Sleeping Bear Dunes, this ratio is similar to that of technical HCH, perhaps indicating past use of technical HCH in the northern Great Lakes region.

As shown in Figure F3, the spatial trend of the gas-phase concentrations of chlordanes (presented as the sum of α- and γ-chlordane and *trans*-nonachlor concentrations) is: Chicago> Sturgeon Point > Sleeping Bear Dunes > Point Petre > Brule River≈ Eagle Harbor ≈ Burnt Island. Chlordane's most common use in the U.S. was for termite control near homes, suggesting that urban areas could be emission sources (*37,38*). Indeed, NJADN also reported higher gas-phase chlordane concentrations at urban as compared to rural sites (*12*). Although most abundant in the south and southeastern United States, subterranean termites are found in every state except Alaska, with moderate to heavy structural infestations in Chicago. It has been suggested that volatilization of chlordane from soil in the southern United States was the predominant source of chlordane to the Great lakes (*6*). Thus, *both* historical local applications used to control termites *and* the influence of long-range transport from areas of high chlordane use could contribute to the relatively high chlordane concentrations at Chicago.

In the technical product, the ratio between γ- to α-chlordane is 1.2. Considering the slightly higher volatility of γ-chlordane, this ratio is expected to be 1.4 at 20 ºC in the atmosphere (*14*). Since γ-chlordane is more susceptible to degradation by microorganisms in soil (*26*), a

ratio of <1.4 indicates a weathered chlordane source. In this study, the ratio of γ- to α-chlordane concentrations in the gas phase was similar at all the seven sites, ranging from 0.88 to 0.95. In the particle phase at the five U.S. sites, the ratio was also similar but lower, at around 0.7, which could be due to the lower vapor pressure of α-chlordane, leading to more sorption of α-chlordane on atmospheric particles. The relatively low ratios we observed in air collected near the Great Lakes suggests that the chlordane is from historically usage – as opposed to the technical product.

The endosulfan concentrations (shown as the sum of α- and γ-endosulfan) showed a clear increasing trend from the west to east (Figure F3, bottom), except for the remote site at Burnt Island. At each site, the average concentration was affected by high concentration outliers that usually occurred in the summer and were likely due to the current agricultural use of endosulfan. Higher endosulfan concentrations were observed at Point Petre, Sturgeon Point and Sleeping Bear Dunes, which could be explained by its heavily use in the surrounding areas (*13*). For example, endosulfan is still widely used in Michigan and New York states and in the southern and western portions of Ontario, Canada (*6, 39*).

The highest concentrations of DDT (presented as the sum of *p,p'*-DDT, *p,p'*-DDE and *p,p'*-DDD) were also observed in Chicago. Similarly, DDT concentrations in air measured by NJADN also showed higher concentrations in urban areas compared to rural areas (*12*). Among the DDT isomers measured by IADN, the gas-phase concentrations of *p,p'*-DDE were the highest, which is not surprising given its relatively high vapor pressure among the DDT-related compounds. Similarly, a study of pesticides showed higher DDE concentrations in the air in Quebec (*40*), and Shen et al. reported higher *p,p'*-DDE concentration in air samples collected in North America (*14*).

Although the spatial distributions of the other pesticides in the gas and particle phases varied (Tables FS2-FS13), most restricted pesticides had higher concentration in Chicago's atmosphere. For example, dieldrin concentrations were an order of magnitude higher in Chicago than at the other sites. Hexachlorobenzene and heptachlor epoxide also had relatively high concentrations at Chicago. This re-iterates the importance of urban areas as sources of atmospheric contaminants, including restricted pesticides, to the Great Lakes.

Acknowledgments

We thank Ilora Basu and Team IADN at Indiana University and staff at the Organic analysis Laboratory of Environment Canada for data acquisition; the U. S. Environmental Protection Agency's Great Lakes National Program Office for funding (Grant GL995656, Melissa Hulting, project monitor); and Frank Froude and his staff for sample collection at the Canadian sites.

Supporting Information

Tables of sampling and analytical method comparisons between U.S. and Canadian sites (Table FS1), average organochlorine (OC) pesticide concentrations and values derived from modeled parameters for pesticide concentrations in the vapor and particle phases at seven IADN sites (Tables FS2-FS13), and comparisons between the results in this study and previous studies conducted by other researchers (Table FS14) and figures of temporal trends of OC pesticide concentrations in the vapor and particle phases (Figures FS1 and FS2). This material is available free of charge via the Internet at http://pubs.acs.org.

Literature Cited

1 Hoff, R. M.; Muir, D. C. G.; Grift, N. P. Annual cycle of polychlorinated biphenyls and organohalogen pesticides in air in southern Ontario. 2. Atmospheric transport and sources. *Environ. Sci. Technol.* **1992**, *26*, 276-283.

2 Ma, J. M.; Hung, H.; Blanchard, P. How do climate fluctuations affect persistent organic pollutant distribution in North America? Evidence of decade monitoring. *Environ. Sci. Technol.* **2004**, *38*, 2538-2543.

3 Buehler, S. S.; Basu, I.; Hites, R. A. A comparison of PAH, PCB, and pesticide concentration in air at two rural sites on Lake Superior. *Environ. Sci. Technol.* **2001**, *35*, 2417-2422.

4 Buehler, S. S.; Basu, I.; Hites, R. A. Causes of variability in pesticide and PCB concentrations in air near the Great Lakes. *Environ. Sci. Technol.* **2004**, *38*, 414-422.

5 Strandberg, B.; Dodder, N. G.; Basu, I.; Hites, R. A. Concentrations and spatial variations of polybrominated diphenyl ethers and other organohalogen compounds in Great Lakes air. *Environ. Sci. Technol.* **2001**, *35*, 1078-1083.

6 Hafner, W. D.; Hites, R. A. Potential sources of pesticides, PCBs, and PAHs to the atmosphere of the Great Lakes. *Environ. Sci. Technol.* **2003**, *37*, 3764-3773.

7 Hung, H.; Blanchard, P.; Halsall, C. J.; Bidleman, T. F.; Stern, G. A.; Fellin, P.; Muir, D. C. G.; Barrie, L. A.; Jantunen, L. M.; Helm, P. A.; Ma, J.; Konoplev, A. Temporal and spatial variabilities of atmospheric polychlorinated biphenyls (PCBs), organochlorine (OC) pesticides and polycyclic aromatic hydrocarbons (PAHs) in the Canadian Arctic: Results from a decade of monitoring. *Sci. Total Environ*. **2005**, *342*, 119-144.

8 Cortes, D. R.; Basu, I.; Sweet, C. W.; Brice, K. A.; Hoff, R. Am.; Hites, R. A. Temporal trends in gas-phase concentrations of chlorinated pesticides measured at the shores of the Great Lakes. *Environ. Sci. Technol.* **1998**, *32*, 1920-1927.

9 Sun, P.; Backus, S.; Blanchard, P.; Hites, R. A. Temporal and spatial trends of organochlorine pesticides in Great Lakes precipitation. *Environ. Sci. Technol.* **2006**, *40*, 2135-2141.

10 Basu, I.; Arnold, K. *Quality Control Report 2002*; Indiana University: Bloomington, IN, 2003.

11 Fowlie, P. *IADN air sampling breakthrough tests for PCB congeners and pesticides from polyurethane foam*. Cornerstone Science, Burlington, Canada, 2005.

12 Gioia, R.; Offenberg, J. H.; Gigliotti, C. L.; Totten, L. A.; Du, S. Y.; Eisenreich, S. J. Atmospheric concentrations and deposition of organochlorine pesticides in the US mid-Atlantic region. *Atmos. Environ*. **2005**, *39*, 2309-2322.

13 Hoh, E.; Hites, R. A. Sources of toxaphene and other organochlorine pesticides in North America as determined by air measurements and potential source contribution function analyses. *Environ. Sci. Technol.* **2004**, *38*, 4187-4194.

14 Shen, L.; Wania, F.; Lei, Y. D.; Teixeira, C.; Muir, D. C. G.; Bidleman, G. F. Atmospheric distribution and long-range transport behavior of organochlorine pesticides in North America. *Environ. Sci. Technol.* **2005**, *39*, 409-420.

15 Harrad, S.; Mao, H. J. Atmospheric PCBs and organochlorine pesticides in Birmingham, UK: concentrations, sources, temporal and seasonal trends. *Atmos. Environ*. **2004**, *38*, 1437-1445.

16 Yeo, H-G.; Choi, M.; Sunwoo, Y. Seasonal variations in atmospheric concentrations of organochlorine pesticides in urban and rural areas of Korea. *Atmos. Environ*. **2004**, *38*, 4779-4788.
17 Karlsson, H.; Muir, D. C. G.; Teixiera, C. F.; Burniston, D. A.; Strachan, W. M. J.; Hecky, R. E.; Mwita, J.; Bootsma, H. A.; Grift, N. P.; Kidd, K. A.; Rosenberg, B. Persistent chlorinated pesticides in air, water and precipitation form the Lake Malawi Area, Southern Africa. *Environ. Sci. Technol.* **2000**, *34*, 4490-4495.
18 Sang, S.; Petrovic, S.; Cuddeford, V. *Lindane A Review of Toxicity and Environmental Fate*; World Wildlife Fund Canada: Toronto, ON, 1999.
19 Iwata, H.; Tanabe, S.; Sakai, N.; Tatsukawa, R. Distribution of persistent organochlorines in the oceanic air and surface seawater and the role of ocean on their global transport and fate. *Environ. Sci. Technol.* **1993**, *27*, 1080-1098.
20 Hung, H.; Halsall, C. J.; Blanchard, P.; Li, H. H.; Fellin, P.; Stern, G.; Rosenberg, B. Temporal trends of organochlorine pesticides in the Canadian Arctic atmosphere. *Environ. Sci. Technol.* **2002**, *36*, 862-868.
21 Garmouma, M.; Poissant, L. Occurrence, temperature and seasonal trends of α- and γ-HCH in air (Quebec, Canada). *Atmos. Environ*. **2004**, *38*, 369-382.
22 Ma, J.; Daggupaty, S.; Harner, T.; Blanchard, P.; Waite, D. Impacts of lindane usage in the Canadian prairies on the Great Lakes ecosystem. 2. Modeled fluxes and loadings to the Great Lakes. *Environ. Sci. Technol.* **2004**, *38*, 984-990.
23 Willett, K. L.; Ulrich, E. M.; Hites, R. A. Differential toxicity and environmental fates of hexachlorocyclohexane isomers. *Environ. Sci. Technol.* **1998**, *32*, 2197-2207.
24 http://www.ncfap.org accessed on March 23, 2006.
25 Dearth, M. A.; Hites, R. A. Complete analysis of technical chlordane using negative ionization mass spectrometry. *Environ. Sci. Technol.* **1991**, *25*, 245-254.
26 Beeman, R. W.; Matsumura, F. Metabolism of cis- and trans-chlordane by a soil microorganism. *J. Agric. Food Chem.* **1981**, *29*, 84-89.
27 Kurt-Karakus, P.; Bidleman, T.; Jones, K. C. Chiral organochlorine pesticide signatures in global background soils. *Environ. Sci. Technol.* **2005**, *39*, 8671-8677.
28 Bidleman, T. F.; Jantunen, L. M. M.; Helm P. A.; Brorstrom-Lunden, E.; Juntto, S. Chlordane enantiomers and temporal trends of chlordane isomers in Arctic air. *Environ. Sci. Technol.* **2002**, *36*, 539-544.
29 Schneider, A. R.; Stapleton, H. M.; Cornwell, J.; Baker J. E. Recent declines in PAH, PCB, and toxaphene levels in the northern Great Lakes as determined from high resolution sediment cores. *Environ. Sci. Technol.* **2001**, *35*, 3809-3815.
30 Ranson, H.; Jensen, B.; Wang, X.; Prapanthadara, L.; Hemingway, J.; Collins, F. H. Genetic mapping of two loci affecting DDT resistance in the malaria vector anopheles gambiae. *Insect Mole. Biol*. **2000**, *9*, 499–507.
31 Chernyak, S. M.; Rice, C. P.; Quintal, R. T.' Begnoche, L, J.; Hickey, J. P.; Vinyard, B. T. Time Trends (1983-1999) for organochlorines and polybrominated diphenyl ethers in rainbow smelt (*Osmerus Mordax*) from Lake Michigan, Huron, and Superior, USA. *Environ. Toxicol. Chem.* **2005**, *24*, 1632-1641.
32 Marvin, C. H.; Painter, S.; Charlton, M. N.; Fox, M. E.; Thiessen, P. A. Trends in spatial and temporal levels of persistent organic pollutants in Lake Erie sediments. *Chemosphere* **2004**, *54*, 33-40.

33 Hickey, J. P.; Batterman, S. A.; Chernyak, S. M. Trends of chlorinated organic contaminants in Great Lakes Trout and Walleye from 1970 to 1998. *Arch. Environ. Contam. Toxicol*. **2006**, *50*, 97-110.
34 Simcik, M. F.; Hoff, R. A.; Strachan, W. M.; Sweet, C. W.; Basu, I.; Hites, R. A. Temporal trends of semi-volatile organic contaminants in Great Lakes precipitation. *Environ. Sci. Technol.* **2000**, *34*, 361-367.
35 Waite, D. T.; Gurprasad, N. P.; Sproull, J. F.; Quiring, D. V.; Kotylak, M. W. Atmospheric movements of Lindane (γ-hexachlorocyclohexane) from canola fields planted with treated seeds. *J. Environ. Qual*. **2001**, *30*, 768-775.
36 Li, Y.-F.; Scholtz, M. T.; Van Heyst, B. J. Global gridded emission inventories of β-hexachlorocyclohexane. *Environ. Sci. Technol.* **2003**, *37*, 3493-3498.
37 Persistent Bioaccumulative and Toxic (PBT) Chemical Program: Chlordane; U.S. Environmental Protection Agency: Washington, DC, 2002; http://www.epa.gov/opptintr/pbt/chlordane.htm, accessed in March, 2006.
38 Harner, T.; Shoeib, M.; Diamond, M.; Stern, G.; Rosenberg, B. Using passive air samplers to assess urban-rural trends for persistent organic pollutants. 1. polychlorinated biphenyls and Organochlorine pesticides. *Environ. Sci. Technol.* **2004**, *38*, 4474-4483.
39 Takacs, P. *Pesticides in Ontario: A Critical Assessment of Potential Toxicity of Agricultural Products to Wildlife, with Consideration for Endocrine Disruption. Volume 1: Endosulfan, EBDC fungicides, Dinitroaniline herbicides, 1,3-Dichloropropene, Azinphos-methyl, and pesticide mixtures*. Technical Report Series No. 340. Canadian Wildlife Service, Ontario Region. 2000.
40 Aulagnier, F.; and Poissant, L. Some pesticides occurrence in air and precipitation in Quebec, Canada. *Environ. Sci. Technol.* **2005**, *39*, 2960-2967.

Table F1. Half-lives (in years) of Selected OC Pesticides in the Gas and Particle Phases at Seven IADN Sites[1].

	Brule River		*Eagle Harbor*		*Chicago*		*Sleeping Bear*		*Sturgeon Pt.*		*Burnt Island*		Point Petre	
	Gas	*Part.*	Gas	*Part.*	Gas	*Part.*	Gas	*Part.*	Gas	*Part.*	Gas	*Part.*	Gas	*Part.*
α-HCH[2]	**3.1 ± 0.3**	1.6 ± 0.5	**4.2 ± 0.1**	**1.9 ± 0.4**	**4.1 ± 0.4**	NS	**4.0 ± 0.2**	**1.7 ± 0.3**	**3.8 ± 0.2**	*2.3 ± 0.7*	**4.0 ± 0.1**	N/A	**4.1 ± 0.1**	N/A
β-HCH	NS	2.1 ± 0.9	4.5 ± 1.8	4.9 ± 2.3	NS	NS	NS	1.5 ± 0.6	2.7 ± 1.1	LD	NS	N/A	*–14 ± 5.0*	N/A
γ-HCH	10 ± 4.5	NS	**5.9 ± 0.4**	**3.5 ± 0.5**	**5.6 ± 0.9**	**5.1 ± 1.0**	**4.2 ± 0.3**	**3.1 ± 0.5**	**5.0 ± 0.4**	**4.1 ± 0.9**	**7.7 ± 0.8**	N/A	**7.8 ± 0.7**	N/A
α-Endo	7.6 ± 3.1	*5.2 ± 1.5*	NS	**5.4 ± 1.0**	*8.4 ± 2.7*	*8.1 ± 2.3*	NS	**3.4 ± 0.5**	NS	*7.7 ± 2.2*	*19 ± 6.9*	N/A	**8.2 ± 1.4**	N/A
β-Endo	5.2 ± 2.4	*4.6 ± 1.6*	*5.8 ± 1.9*	5.9 ± 2.5	**3.2 ± 0.7**	8.0 ± 3.8	*5.2 ± 1.5*	**3.0 ± 0.5**	**5.7 ± 1.3**	*7.1 ± 2.3*	*9.7 ± 2.6*	N/A	**4.1 ± 0.4**	N/A
α-chlor	*8.8 ± 2.5*	10 ± 5.1	**13 ± 2.6**	**6.6 ± 1.5**	**11 ± 2.7**	**4.7 ± 1.1**	**11 ± 1.7**	*9.2 ± 3.2*	**10 ± 1.3**	7.7 ± 2.7	**11 ± 1.8**	N/A	**9.3 ± 1.0**	N/A
γ-chlor	NS	7.3 ± 2.2	**6.5 ± 0.9**	*8.4 ± 2.6*	**6.7 ± 1.2**	*11 ± 3.0*	**6.1 ± 0.8**	7.0 ± 1.6	**7.4 ± 0.8**	*8.5 ± 2.4*	**11 ± 1.9**	N/A	**8.6 ± 1.0**	N/A
t-nona	NS	NS	**13 ± 2.9**	NS	*13 ± 4.5*	NS	**12 ± 2.7**	*7.7 ± 2.4*	**9.6 ± 1.4**	NS	**7.7 ± 1.0**	N/A	**7.0 ± 0.6**	N/A
dieldrin	9.6 ± 4.7	9.5 ± 4.7	**4.9 ± 0.5**	**3.9 ± 0.5**	**6.1 ± 1.2**	**6.2 ± 1.2**	**5.3 ± 0.7**	4.3 ± 0.7	**5.7 ± 0.6**	4.0 ± 0.5	**8.9 ± 1.4**	N/A	**8.1 ± 0.9**	N/A
HCB	*9.5 ± 2.8*	N/A	**18 ± 2.7**	N/A	**8.3 ± 0.9**	N/A	**12 ± 1.0**	N/A	**15 ± 1.4**	N/A	**32 ± 7.2**	N/A	**30 ± 5.6**	N/A
DDT	NS	NS	*16 ± 5.8*	NS	14 ± 6.1	NS	*11 ± 3.1*	NS	**9.1 ± 1.8**	NS	**5.2 ± 0.6**	N/A	**5.4 ± 0.5**	N/A
DDD	NS	NS	*14 ± 5.2*	LD	*5.8 ± 2.1*	**3.8 ± 0.8**	*9.2 ± 2.7*	NS	**5.0 ± 0.8**	NS	**5.1 ± 0.6**	N/A	**6.0 ± 0.6**	N/A
DDE	*7.9 ± 2.5*	N/A	**6.0 ± 0.5**	N/A	**6.3 ± 0.8**	N/A	**5.9 ± 0.5**	N/A	**7.0 ± 0.6**	N/A	**6.5 ± 0.7**	N/A	**6.3 ± 0.5**	N/A
HPED	NS	–4.8 ± 1.9	**–2.5 ± 0.4**	NS	7.7 ± 3.3	NS	*7.3 ± 2.7*	*6.3 ± 1.9*	7.6 ± 3.8	NS	**6.8 ± 1.6**	N/A	**5.8 ± 0.7**	N/A

1. The results are listed as mean ± standard error. Normal font numbers are significant for $0.01 < p < 0.05$; italic font numbers are significant for $0.001 < p < 0.01$, bold font numbers are significant at level of $p < 0.001$. "NS" means "not significant" at $p > 0.05$. "LD" means "Limited data" and no regression analysis was conducted. "N/A" means "no data is available". A negative half-life is actually a doubling time.
2. α-Endo: α-endosulfan; β-Endo: β-Endosulfan; α-chlor: α-chlordane; γ-chlor: γ-chlordane; *t*-nona: *trans*-nonachlor; DDT: *p,p'*-DDT; DDD: *p,p'*-DDD; DDE: *p,p'*-DDE; HPED: heptachlor epoxide.

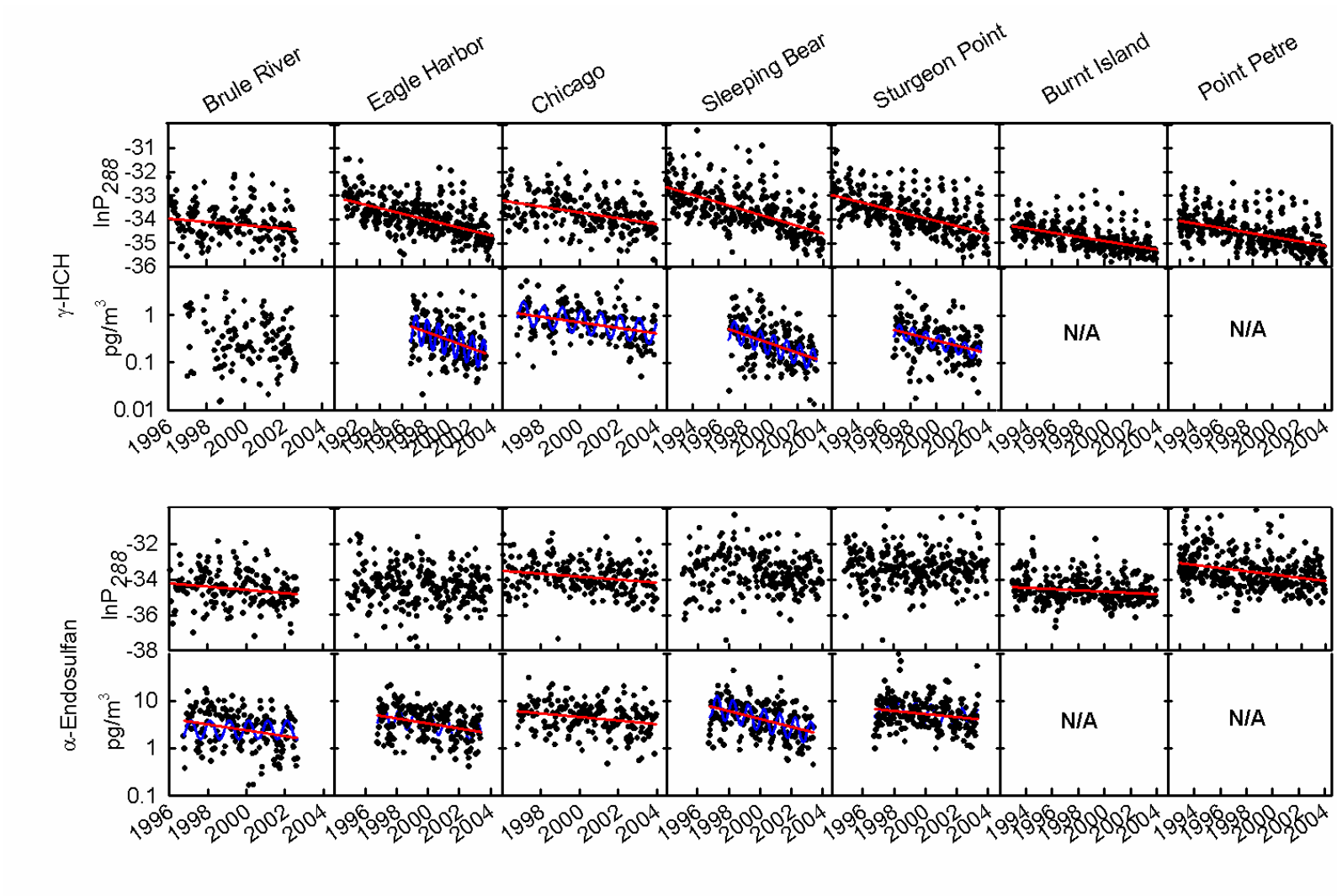

Figure F1. Concentrations of γ-HCH and α-endosulfan in the gas-phase (upper) and particle-phase (lower) at the seven IADN sites. The red lines indicate long-term significant decreasing trends; the blue curve is the fitting line of the sinusoidal model with the period length (b_3) set to one year.

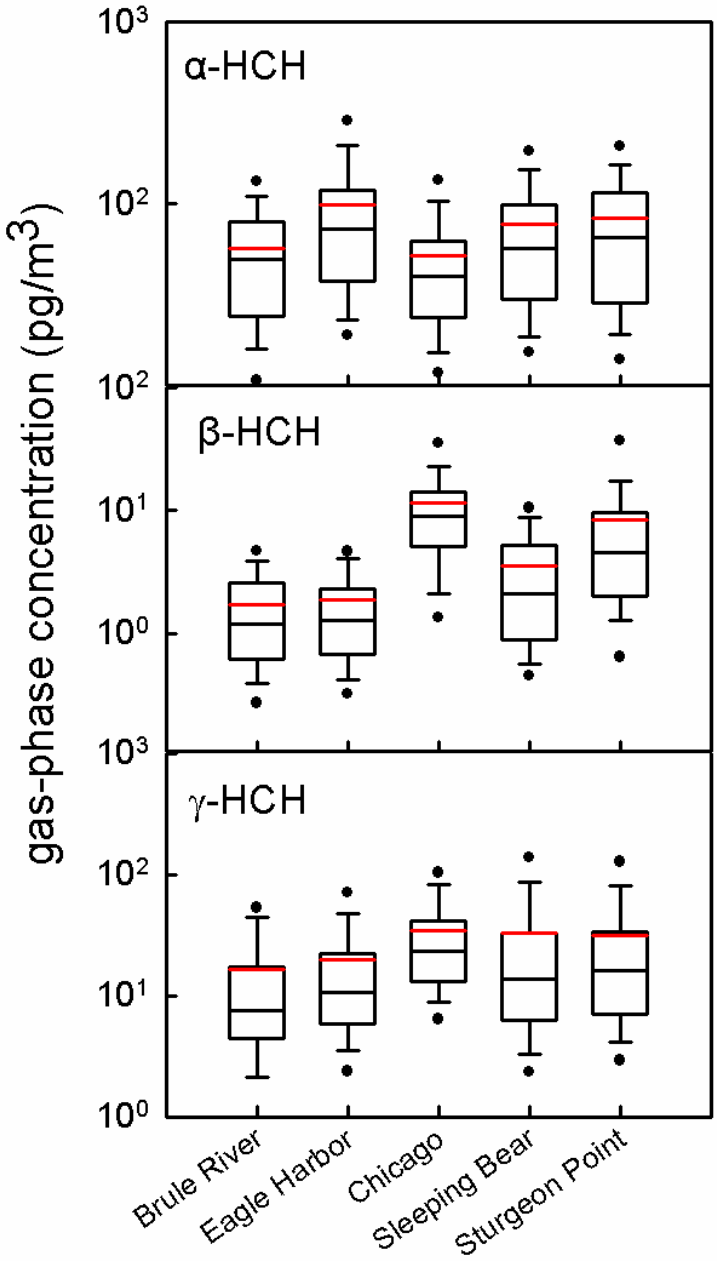

Figure F2. Concentrations of α-HCH (top), β-HCH (middle), and γ-HCH (bottom) in the gas-phase at the five U.S. IADN sites. The boxes represent the 25th to 75th percentiles, the black lines in the boxes are the medians and the red lines are the means. The two vertical lines outside each box extend to the outliers representing the 10th and 90th percentiles; and outliers are shown at 5th and 95th percentile.

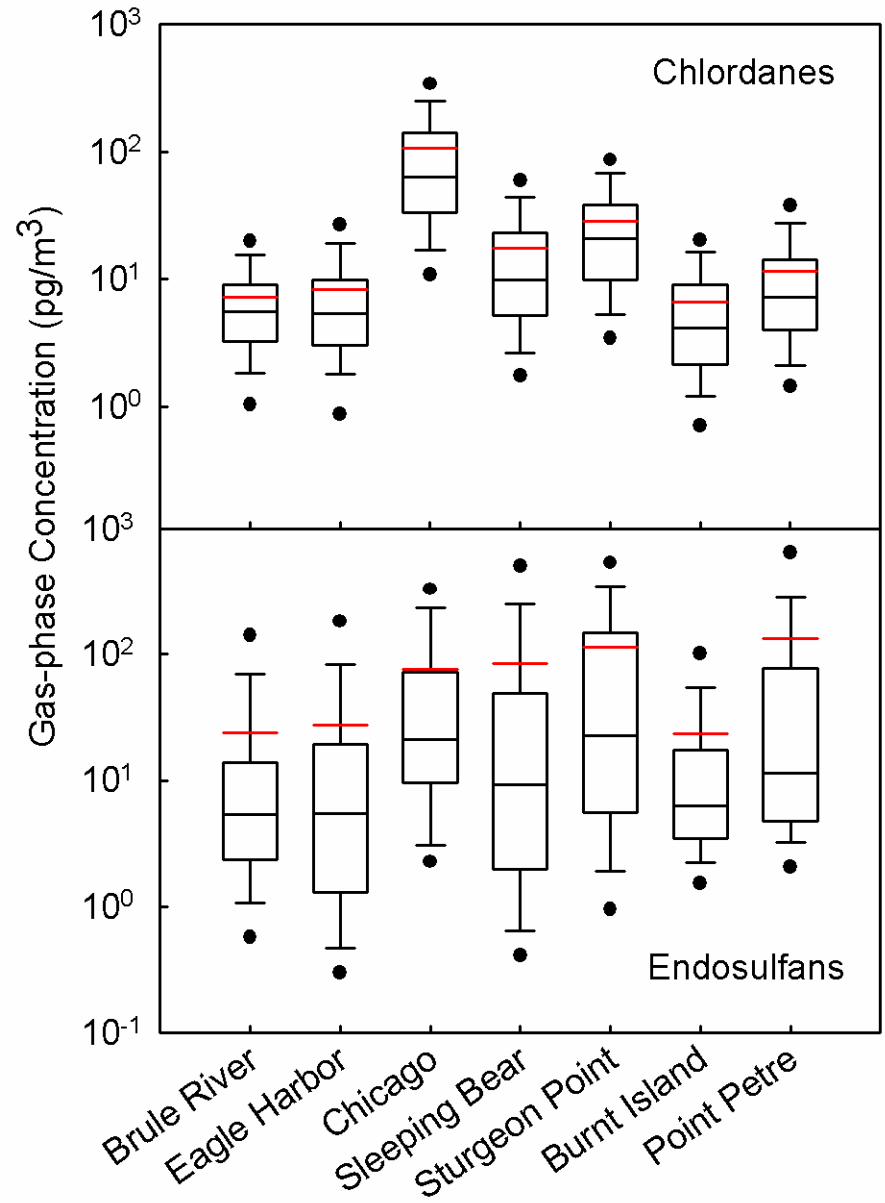

Figure F3. Concentrations of chlordanes (sum of α-, β-chlordane, and *trans*-nonachlor, top) and endosulfans (α- plus β-endosulfan, bottom) in the gas-phase at the seven IADN sites. See Figure F2 for the description of the box-plots.

Supporting Information for:

Atmospheric Organochlorine Pesticide Concentrations near the Great Lakes: Temporal and Spatial Trends

Ping Sun,[1] Pierrette Blanchard,[2] Kenneth, Brice[2], and Ronald A Hites∗[1]

[1]School of Public and Environmental Affairs
Indiana University
Bloomington, Indiana, 47405 USA

and
[2]Environment Canada
4905 Dufferin Street
Toronto, ON M3H 5T4 Canada

∗Corresponding Author Email: hitesr@indiana.edu

This Supporting Information contains 14 tables and 2 figures. Table FS1 is the sampling and analytical method comparison between U.S. and Canadian sites. Table FS2 to FS13 show the average organochlorine (OC) pesticide concentrations and values derived from modeled parameters for pesticide concentrations in the vapor and particle phases at seven IADN sites. Table FS14 is a comparison between the results in this study and previous studies conducted by other researchers. Figures FS1 and FS2 show temporal trends of OC pesticide concentrations in the vapor and particle phases. Eighteen pesticides were measured. These pesticides are aldrin, α-chlordane, γ-chlordane, *p,p'*-DDT, *p,p'*-DDD, *p,p'*-DDE, *o,p'*-DDT, dieldrin, α-endosulfan, β-endosulfan, endrin, heptachlor epoxide, HCB, α-HCH, β-HCH, γ-HCH, methoxychlor, and *trans*-nonachlor.

The vapor phase pesticide concentrations (in pg/m^3) were first converted to partial pressures (P, in atm) using the ideal gas law. These partial pressures were then adjusted to the reference temperature of 288 K using equation 1, where ΔH is a characteristic phase-transition energy of the compound (in kJ/mol), R is the gas constant, and T is the daily average atmospheric temperature at the sampling site (in Kelvin). The value of ΔH was determined by a preliminary regression of ln(P) vs. 1/T, which is the Clausius-Clapeyron equation (see equation 2). The values of ln(P_{288}) were then regressed vs. time (t, in Julian days relative to January 1, 1990) using equation 3 to determine the rate (a_1, in days^{-1}) of exponential increase ($a_1 > 0$) or decrease ($a_1 < 0$) of these partial pressures. If this rate was statistically significant ($p < 0.05$), these rates were then converted to half-lives ($t_{1/2,}$ in years) by dividing the values into the ln(2)/365 for each compound at each site.

$$\ln P_{288} = \ln P - \frac{\Delta H}{R}\left(\frac{1}{288} - \frac{1}{T}\right) \tag{1}$$

$$\ln P = -\frac{\Delta H}{R}\left(\frac{1}{T}\right) + const \tag{2}$$

$$\ln P_{288} = a_0 + a_1 t \tag{3}$$

Tables FS1 to FS7 show the values of ΔH and the calculated half-lives from the a_1 values in equation 3. The results are listed as mean ± standard error. Normal font numbers are significant for $0.01 < p < 0.05$; italic font numbers are significant for $0.001 < p < 0.01$, bold font numbers are significant for $p < 0.001$. "NS" means "not significant" at $p > 0.05$. "LD" means "limited data", and no regression was calculated. "N/A" means "not available". A negative half-life is actually a doubling time.

Equation 4 was used to fit the pesticide concentrations (C) in the particle phase:

$$\ln C = b_0 + b_1 t + b_2 \sin\left(\frac{t}{b_3} + b_4\right) \tag{4}$$

where t is the time in Julian Days relative to January 1 1990, b_0 is the intercept (unitless), b_1 is a first-order rate constant (in days^{-1}) describing the rate of exponential decrease or increase over time, b_2 is the periodic amplitude (unitless), b_3 is the length of the period (in days), and b_4 is the periodic offset (in days).

To establish the dates of maximum pesticides concentrations, the ratio between the highest pesticide concentration and the lowest concentration can be calculated from the fitted b_2 parameter (equation 4) by taking its anti-logarithm (e^{2b_2}, the factor of 2 in the exponent is needed to calculate the peak-to-valley amplitude). The sine wave would have a maximum at day 91 in a year. Therefore, the dates of the maximum of pesticide concentrations were calculated by first converting the fitted b_4 values from radians to days (multiplying by $365/2\pi$) and then subtracting these values from 91.

Tables FS8 to FS12 show results of the fit using equation 4 with b_3 set to 365 days. The results are listed as mean ± standard error. Normal font numbers are significant for $0.01 < p < 0.05$; italic font numbers are significant for $0.001 < p < 0.01$, bold font numbers are significant at $p < 0.001$. "NS" means not significant at $p > 0.05$. A negative half-life is a doubling time.

Figure FS1 shows the temporal trends of vapor phase OC pesticide concentrations at the seven IADN sites. The concentrations were converted to P_{288} by equation (1). The values of $\ln(P_{288})$ were then plotted vs. time based on equation (3). The red lines indicate long-term significant decreasing or increasing trends.

Figure FS2 shows the temporal trends of particle phase OC pesticide concentrations at the five IADN sites. The black curves are the fitting lines using the sinusoidal model with the period length (b_3) set to one year (equation 4); the red lines indicate long-term significant decreasing trends ($b_1 < 0$) or increasing trends ($b_1 > 0$).

The complete monitoring results (e.g. concentrations of pesticides, PCBs, and PAHs) can be downloaded from the IADN website: www.msc.ec.gc.ca/iadn. In addition, the meteorological data such as temperature can also be found at this website.

Table FS1. Method comparison between U.S. and Canadian sites

	U.S. SITES	*CANADIAN SITES*
Sampling time/frequency	24 hours /every 12 days	24 hours /every 12 days
Sampler Type	General Metal Works GS310	General Metal Works PS-1
Typical Air Volume	816 m^3	350 m^3
Sampler Media	QFF + XAD-2	GFF + PUF
Sample Extraction	XAD-2 Soxhlet (24 hours) with 1:1 hexane: acetone GFF same as for XAD-2	PUF Soxhlet (24 hours) w. hexane GFF not analyzed routinely for OC pesticides
Cleanup/Fractionation	Silica gel (3.5% w/w water-deactivated) column chromatography: Fraction 1: hexane elution of HCB, p,p'-DDE, o,p'-DDT; Fraction 2: 50% hexane / 50% dichloromethane elution of other target OC pesticides.	Florisil (~3% water-deactivated) column chromatography: Fraction 1: hexane elution of PCBs, HCB, heptachlor, aldrin, p,p'-DDE, o,p'-DDT, t-nonachlor (partial), p,p'-DDT (partial); Fraction 2: 15% DCM / 85% hexane elution of HCHs, o,p'-DDD, p,p'-DDD, chlordanes, t-nonachlor (partial), p,p'-DDT (partial) + coplanar PCBs; Fraction 3: DCM elution of polar OC pesticides (dieldrin, endosulfans, methoxychlor, endrin, heptachlor epoxide).
Instrumental Measurement	GC-ECD (HP5890): heated splitless/split injector, 60-m DB-5 capillary column	GC-ECD (HP5890 Series II): dual heated splitless/split injectors, dual capillary columns (60-m DB-5 and 30-m DB-17)
Instrument Calibration	Internal standardization	External standardization

Table FS2. Average Concentrations and Fit parameters for Pesticides in the Gas Phase at Brule River

OC Pesticide	Average conc. (pg/m^3)	Half-life (years), (ln2)/365a	ΔH	No. of detects	r^2
α-HCH	57 ± 3.3	**3.1 ± 0.3**	**30 ± 2.0**	191	0.64
β-HCH	1.7 ± 0.19	NS	16 ± 6.8	66	0.09
γ-HCH	16 ± 1.8	10 ± 4.5	**54 ± 3.7**	182	0.56
α-Endosulfan	23 ± 3.8	7.6 ± 3.1	**80 ± 4.4**	177	0.64
β-Endosulfan	2.1 ± 0.4	5.2 ± 2.4	**36 ± 6.7**	113	0.22
α-Chlordane	3.2 ± 0.18	*8.8 ± 2.5*	**33 ± 2.6**	182	0.50
γ-Chlordane	2.4 ± 0.17	NS	**27 ± 4.1**	171	0.22
trans-Nonachlor	2.0 ± 0.15	NS	**40 ± 3.1**	180	0.48
Dieldrin	8.0 ± 0.81	9.6 ± 4.7	**73 ± 4.0**	174	0.67
Hexachlorobenzene	66 ± 1.4	*9.5 ± 2.8*	**11 ± 2.4**	190	0.14
p,p'-DDT	1.6 ± 0.18	NS	*25 ± 6.2*	135	0.11
p,p'-DDD	1.4 ± 0.13	NS	NS	117	N/A
p,p'-DDE	1.2 ± 0.10	*7.9 ± 2.5*	**53 ± 3.3**	180	0.59
o,p'-DDT	0.53 ± 0.09	NS	**71 ± 7.8**	51	0.64
o,p'-DDD	3.7 ± 0.58	LD	LD	71	N/A
Heptachlor epoxide	5.4 ± 0.53	NS	**66 ± 4.0**	118	0.71
Aldrin	0.17 ± 0.02	NS	NS	51	N/A
Endrin	3.4 ± 0.30	LD	LD	66	N/A
Methoxychlor	1.6 ± 0.41	LD	LD	20	N/A

Table FS3. Average Concentrations and Fit Parameters for Pesticides in the Gas Phase at Eagle Harbor

OC Pesticide	Average conc. (pg/m^3)	Half-life (years), (ln2)/365a	ΔH	No. of detects	r^2
α-HCH	100 ± 5.3	**4.2 ± 0.1**	**26 ± 1.4**	363	0.75
β-HCH	1.9 ± 0.21	4.5 ± 1.8	**24 ± 4.7**	107	0.24
γ-HCH	20 ± 1.4	**5.9 ± 0.4**	**48 ± 2.1**	362	0.66
α-Endosulfan	27 ± 3.6	NS	**100 ± 4.5**	250	0.67
β-Endosulfan	2.2 ± 0.32	*5.8 ± 1.9*	**61 ± 6.6**	153	0.38
α-Chlordane	3.3 ± 0.16	**13 ± 2.6**	**40 ± 2.1**	309	0.55
γ-Chlordane	2.9 ± 0.24	**6.5 ± 0.9**	**42 ± 3.3**	301	0.41
trans-Nonachlor	2.5 ± 0.15	**13 ± 2.9**	**52 ± 2.6**	301	0.58
Dieldrin	10 ± 0.78	**4.9 ± 0.5**	**84 ± 3.5**	341	0.66
Hexachlorobenzene	68 ± 1.4	**18 ± 2.7**	**10 ± 1.4**	357	0.2
p,p'-DDT	2.7 ± 0.20	*16 ± 5.8*	**41 ± 3.9**	280	0.31
p,p'-DDD	1.2 ± 0.09	*14 ± 5.2*	9.7 ± 4.6	217	0.06
p,p'-DDE	1.9 ± 0.12	**6.0 ± 0.5**	**49 ± 2.4**	353	0.60
o,p'-DDT	0.47 ± 0.05	NS	**54 ± 4.8**	81	0.62
o,p'-DDD	2.4 ± 0.30	**1.8 ± 0.3**	*12 ± 4.6*	99	0.29
Heptachlor epoxide	5.5 ± 0.46	7.7 ± 3.3	**70 ± 4.4**	165	0.64
Aldrin	0.07 ± 0.01	**2.4 ± 0.3**	*13 ± 3.7*	68	0.50
Endrin	3.0 ± 0.33	NS	NS	112	N/A
Methoxychlor	0.94 ± 0.21	LD	LD	26	N/A

Table FS4. Average Concentrations and Fit Parameters for Pesticides in the Gas Phase at Sleeping Bear Dunes

OC Pesticide	Average conc. (pg/m^3)	Half-life (years), (ln2)/365a	ΔH	No. of detects	r^2
α-HCH	78 ± 4.0	**4.0 ± 0.2**	**22 ± 1.8**	341	0.65
β-HCH	3.5 ± 0.40	NS	**32 ± 6.3**	103	0.20
γ-HCH	47 ± 8.2	**4.2 ± 0.3**	**61 ± 2.8**	336	0.65
α-Endosulfan	86 ± 14	NS	**130 ± 5.0**	223	0.74
β-Endosulfan	8.9 ± 1.3	*5.2 ± 1.5*	**92 ± 6.8**	193	0.50
α-Chlordane	6.5 ± 0.37	**11 ± 1.7**	**48 ± 2.3**	323	0.60
γ-Chlordane	6.1 ± 0.39	**6.1 ± 0.8**	**53 ± 3.4**	312	0.49
trans-Nonachlor	5.3 ± 0.36	**12 ± 2.7**	**64 ± 2.7**	322	0.64
Dieldrin	24 ± 2.1	**5.3 ± 0.7**	**92 ± 3.8**	336	0.65
Hexachlorobenzene	74 ± 1.6	**12 ± 1.0**	**13 ± 1.2**	339	0.42
p,p'-DDT	4.9 ± 0.45	*11 ± 3.1*	**60 ± 4.0**	295	0.45
p,p'-DDD	1.8 ± 0.17	*9.2 ± 2.7*	*18 ± 5.0*	231	0.10
p,p'-DDE	8.1 ± 0.51	**5.9 ± 0.5**	**72 ± 2.3**	339	0.76
o,p'-DDT	1.2 ± 0.13	-6.3 ± 2.1*	**73 ± 4.5**	113	0.71
o,p'-DDD	2.6 ± 0.21	**3.3 ± 0.7**	NS	111	0.17
Heptachlor epoxide	9.8 ± 1.0	*7.3 ± 2.7*	**75 ± 3.8**	167	0.71
Aldrin	0.08 ± 0.01	*3.7 ± 1.0*	**25 ± 4.6**	78	0.32
Endrin	3.6 ± 0.32	NS	NS	96	N/A
Methoxychlor	2.1 ± 0.41	LD	LD	34	N/A

*A negative half-life indicates that the concentrations are increasing and the listed value is the doubling time.

Table FS5. Average Concentrations and Fit Parameters for Pesticides in the Gas Phase at Sturgeon Point

OC Pesticide	Average conc. (pg/m^3)	Half-life (years), (ln2)/365a	ΔH	No. of detects	r^2
α-HCH	84 ± 4.2	**3.8 ± 0.2**	**27 ± 1.8**	354	0.67
β-HCH	8.5 ± 1.3	2.7 ± 1.1	*26 ± 8.8*	81	0.20
γ-HCH	31 ± 2.2	**5.0 ± 0.4**	**56 ± 2.5**	348	0.65
α-Endosulfan	110 ± 11	NS	**130 ± 4.3**	272	0.76
β-Endosulfan	9.5 ± 1.0	**5.7 ± 1.3**	**86 ± 5.4**	213	0.55
α-Chlordane	11 ± 0.56	**10 ± 1.3**	**57 ± 1.8**	331	0.76
γ-Chlordane	10 ± 0.51	**7.4 ± 0.8**	**57 ± 2.5**	323	0.65
trans-Nonachlor	7.7 ± 0.42	**9.6 ± 1.4**	**67 ± 2.3**	331	0.73
Dieldrin	26 ± 1.9	**5.7 ± 0.6**	**85 ± 3.2**	340	0.69
Hexachlorobenzene	77 ± 1.5	**15 ± 1.4**	**16 ± 1.0**	349	0.52
p,p'-DDT	9.0 ± 0.61	**9.1 ± 1.8**	**68 ± 3.5**	336	0.54
p,p'-DDD	3.5 ± 0.36	**5.0 ± 0.8**	NS	259	0.13
p,p'-DDE	17 ± 0.92	**7.0 ± 0.6**	**76 ± 2.0**	353	0.81
o,p'-DDT	2.1 ± 0.20	*-3.0 ± 0.8**	**71 ± 5.3**	110	0.64
o,p'-DDD	5.4 ± 0.61	*3.3 ± 0.9*	12 ± 5.2	87	0.18
Heptachlor epoxide	7.9 ± 0.65	7.6 ± 3.8	**58 ± 4.1**	115	0.65
Aldrin	0.14 ± 0.03	LD	LD	48	N/A
Endrin	4.6 ± 0.33	NS	NS	96	N/A
Methoxychlor	1.7 ± 0.21	LD	LD	72	N/A

*A negative half-life indicates that the concentrations are increasing and the listed value is the doubling time.

Table FS6. Average Concentrations and Fit Parameters for Pesticides in the Gas Phase at Chicago

OC Pesticide	Average conc. (pg/m^3)	Half-life (years), (ln2)/365a	ΔH	No. of detects	r^2
α-HCH	52 ± 2.9	**4.1 ± 0.4**	**21 ± 2.5**	215	0.46
β-HCH	12 ± 1.2	NS	**28 ± 6.5**	87	0.18
γ-HCH	35 ± 2.5	**5.6 ± 0.9**	**32 ± 3.2**	210	0.41
α-Endosulfan	72 ± 9.2	*8.4 ± 2.7*	**88 ± 4.1**	211	0.69
β-Endosulfan	6.0 ± 0.75	**3.2 ± 0.7**	**48 ± 7.3**	143	0.34
α-Chlordane	39 ± 2.8	**11 ± 2.7**	**59 ± 2.4**	215	0.74
γ-Chlordane	46 ± 3.8	**6.7 ± 1.2**	**55 ± 2.8**	215	0.66
Trans-Nonachlor	23 ± 1.6	*13 ± 4.5*	**62 ± 2.8**	215	0.71
Dieldrin	110 ± 11	**6.1 ± 1.2**	**68 ± 3.5**	215	0.65
Hexachlorobenzene	90 ± 3.0	**8.3 ± 0.9**	**20 ± 1.3**	216	0.60
p,p'-DDT	23 ± 1.9	14 ± 6.1	**66 ± 3.3**	211	0.66
p,p'-DDD	4.2 ± 0.46	*5.8 ± 2.1*	NS	144	0.05
p,p'-DDE	29 ± 1.9	**6.3 ± 0.8**	**60 ± 2.1**	216	0.80
o,p'-DDT	7.2 ± 0.63	NS	**60 ± 3.6**	132	0.68
o,p'-DDD	8.8 ± 1.4	LD	LD	23	N/A
Heptachlor epoxide	28 ± 2.8	7.7 ± 3.3	**70 ± 4.4**	163	0.63
Aldrin	16 ± 2.2	NS	*34 ± 9.1*	135	0.11
Endrin	9.4 ± 1.2	*-2.4 ± 0.9**	*18 ± 6.2*	90	0.15
Methoxychlor	4.0 ± 0.76	LD	LD	76	N/A

*A negative half-life indicates that the concentrations are increasing and the listed value is the doubling time.

Table FS7. Average Concentrations and Fit Parameters for Pesticides in the Gas Phase at Burnt Island

OC Pesticide	Average conc. (pg/m^3)	Half-life (years), (ln2)/365a	ΔH	No. of detects	r^2
α-HCH	26 ± 0.9	**4.0 ± 0.1**	**22 ± 0.87**	286	0.86
β-HCH	0.65 ± 0.12	NS	55 ± 22	166	0.08
γ-HCH	9.2 ± 0.6	**7.7 ± 0.8**	**39 ± 1.6**	315	0.68
α-Endosulfan	21 ± 2.8	*19 ± 6.9*	**60 ± 2.4**	312	0.67
β-Endosulfan	2.6 ± 0.41	*9.7 ± 2.6*	**75 ± 3.6**	276	0.63
α-Chlordane	2.4 ± 0.14	**16 ± 3.4**	**51 ± 1.8**	313	0.73
γ-Chlordane	1.9 ± 0.12	**11 ± 1.9**	**46 ± 2.1**	313	0.61
trans-Nonachlor	2.4 ± 0.15	**7.7 ± 1.0**	**53 ± 2.2**	314	0.67
Dieldrin	9.2 ± 0.59	**8.9 ± 1.4**	**61 ± 2.4**	309	0.69
Hexachlorobenzene	29 ± 0.52	**32 ± 7.2**	NS	316	0.20
p,p'-DDT	0.68 ± 0.04	**5.2 ± 0.6**	**42 ± 2.7**	300	0.51
p,p'-DDD	0.17 ± 0.01	**5.1 ± 0.6**	**27 ± 3.0**	200	0.42
p,p'-DDE	2.2 ± 0.11	**6.5 ± 0.7**	**38 ± 2.1**	313	0.57
o,p'-DDT	0.98 ± 0.06	**7.6 ± 1.4**	**40 ± 3.0**	298	0.41
o,p'-DDD	0.31 ± 0.03	**8.8 ± 2.1**	**32 ± 3.3**	178	0.37
Heptachlor epoxide	1.7 ± 0.13	**6.8 ± 1.6**	**29 ± 4.5**	239	0.21
Aldrin	0.91 ± 0.06	11 ± 5.2	**40 ± 3.9**	189	0.39
Endrin	0.78 ± 0.07	**5.7 ± 1.0**	**38 ± 3.8**	195	0.42
Methoxychlor	3.0 ± 0.79	LD	LD	63	N/A

Table FS8. Average Concentrations and Fit Parameters for Pesticides in the Gas Phase at Point Petre

OC Pesticide	Average conc. (pg/m^3)	Half-life (years), (ln2)/365a	ΔH	No. of detects	r^2
α-HCH	28 ± 0.9	**4.1 ± 0.1**	**21 ± 1.1**	388	0.82
β-HCH	0.54 ± 0.02	NS	**20 ± 3.4**	213	0.15
γ-HCH	12 ± 0.7	**7.8 ± 0.7**	**47 ± 2.1**	388	0.60
α-Endosulfan	110 ± 22	**8.2 ± 1.4**	**100 ± 3.6**	385	0.69
β-Endosulfan	24 ± 4.3	**4.1 ± 0.4**	**140 ± 4.3**	347	0.76
α-Chlordane	3.9 ± 0.20	**9.3 ± 1.0**	**60 ± 2.0**	388	0.72
γ-Chlordane	3.6 ± 0.18	**8.6 ± 1.0**	**52 ± 2.4**	384	0.58
trans-Nonachlor	4.0 ± 0.21	**7.0 ± 0.6**	**61 ± 2.3**	387	0.24
Dieldrin	13 ± 0.86	**8.1 ± 0.9**	**72 ± 2.5**	382	0.70
Hexachlorobenzene	32 ± 0.63	**30 ± 5.6**	NS	387	0.46
p,p'-DDT	2.8 ± 0.19	**5.4 ± 0.5**	**25 ± 6.2**	385	0.66
p,p'-DDD	0.43 ± 0.02	**6.0 ± 0.6**	**0.3 ± 0.01**	290	0.52
p,p'-DDE	11 ± 0.69	**6.3 ± 0.5**	**53 ± 3.3**	386	0.72
o,p'-DDT	2.9 ± 0.18	**19 ± 4.7**	NS	383	0.34
o,p'-DDD	0.76 ± 0.05	**4.5 ± 0.3**	**46 ± 3.2**	250	0.55
Heptachlor epoxide	2.9 ± 0.13	**5.8 ± 0.7**	**28 ± 3.7**	339	0.27
Aldrin	0.97 ± 0.06	NS	**24 ± 5.0**	191	0.14
Endrin	1.3 ± 0.12	**4.0 ± 0.3**	**41 ± 4.0**	256	0.44
Methoxychlor	3.4 ± 0.78	NS	NS	112	N/A

Table FS9. Average Concentrations and Fit Parameters for Pesticides in the Particle Phase at Brule River

OC Pesticide	Average conc. (pg/m^3)	Half-life (years), (ln2)/365b_1	Peak-to-valley ratio, e^{2b_2}	Maximum date (± days)	No. of detects	r^2
α-HCH	1.6 ± 0.38	1.6 ± 0.5	NS	NS	55	N/A
β-HCH	1.2 ± 0.23	2.1 ± 0.9	NS	NS	44	0.10
γ-HCH	0.47 ± 0.05	NS	NS	NS	118	NS
α-Endosulfan	3.6 ± 0.24	*5.2 ± 1.5*	**2.4 ± 1.2**	*Aug 4 ± 12*	171	0.18
β-Endosulfan	1.1 ± 0.19	*4.6 ± 1.6*	**7.5 ± 1.3**	**Sep 19 ± 43**	120	0.33
α-Chlordane	0.61 ± 0.05	10 ± 5.1	**2.3 ± 1.2**	**Jan 19 ± 11**	163	0.17
γ-Chlordane	0.36 ± 0.03	7.3 ± 2.2	**2.4 ± 1.2**	NS	153	0.27
trans-Nonachlor	0.27 ± 0.02	NS	**2.9 ± 1.2**	**Jan 10 ± 12**	135	0.14
Dieldrin	2.2 ± 0.16	9.5 ± 4.7	**2.0 ± 1.2**	Mar 1 ± 15	171	0.12
Hexachlorobenzene	N/A	N/A	N/A	N/A	N/A	N/A
p,p'-DDT	0.95 ± 0.18	NS	NS	NS	50	NS
p,p'-DDD	0.57 ± 0.06	NS	**4.6 ± 1.3**	**Aug 31 ± 56**	106	0.23
p,p'-DDE	N/A	N/A	N/A	N/A	N/A	N/A
o,p'-DDD	1.6 ± 0.24	NS	NS	NS	61	N/A
Heptachlor epoxide	0.90 ± 0.10	-4.8 ± 1.9*	**2.0 ± 1.2**	Mar 1 ± 15	110	0.36
Aldrin	N/A	N/A	N/A	N/A	N/A	N/A
Endrin	0.30 ± 0.04	LD	N/A	N/A	43	N/A
Methoxychlor	0.87 ± 0.21	LD	N/A	N/A	9	N/A

*A negative half-life indicates that the concentrations are increasing and the listed value is the doubling time.

Table FS10. Average Concentrations and Fit Parameters for Pesticides in the Particle Phase at Eagle Harbor

OC Pesticide	Average conc. (pg/m^3)	Half-life (years), (ln2)/365b_1	Peak-to-valley ratio, e^{2b_2}	Maximum date (± days)	No. of detects	r^2
α-HCH	0.93 ± 0.14	**1.9 ± 0.4**	NS	NS	79	0.26
β-HCH	0.53 ± 0.06	NS	**4.0 ± 1.2**	**Feb 8 ± 8**	86	0.37
γ-HCH	0.49 ± 0.04	**3.5 ± 0.5**	**4.0 ± 1.2**	**March 12 ± 7**	176	0.40
α-Endosulfan	4.2 ± 0.22	**5.4 ± 1.0**	**2.4 ± 1.1**	**Aug 16 ± 8**	201	0.29
β-Endosulfan	1.1 ± 0.16	5.9 ± 2.5	**18 ± 1.3**	**Sep 13 ± 26**	134	0.46
α-Chlordane	0.4 ± 0.03	**6.6 ± 1.5**	**2.2 ± 1.1**	**Jan 26 ± 10**	172	0.25
γ-Chlordane	0.28 ± 0.02	*8.4 ± 2.6*	**2.4 ± 1.2**	**Feb 7 ± 9**	175	0.23
trans-Nonachlor	0.23 ± 0.01	NS	**2.9 ± 1.2**	**Feb 3 ± 9**	141	0.24
Dieldrin	2.7 ± 0.19	**3.9 ± 0.5**	**2.8 ± 1.1**	**Feb 18 ± 7**	200	0.37
Hexachlorobenzene	N/A	N/A	N/A	N/A	N/A	N/A
p,p'-DDT	0.41 ± 0.04	NS	**1.8 ± 1.2**	**Jan 28 ± 22**	90	0.19
p,p'-DDD	0.43 ± 0.09	LD	N/A	N/A	27	N/A
p,p'-DDE	N/A	N/A	N/A	N/A	N/A	N/A
o,p'-DDD	0.76 ± 0.12	NS	3.8 ± 1.5	*Jan 22 ± 16*	59	0.18
Heptachlor epoxide	0.84 ± 0.07	NS	**2.5 ± 1.2**	**Feb 11 ± 10**	137	0.28
Aldrin	N/A	N/A	N/A	N/A	N/A	N/A
Endrin	0.26 ± 0.02	LD	N/A	N/A	48	N/A
Methoxychlor	1.1 ± 0.21	LD	N/A	N/A	10	N/A

Table FS11. Average Concentrations and Fit Parameters for Pesticides in the Particle Phase at Sleeping Bear Dunes

OC Pesticide	Average conc. (pg/m^3)	Half-life (years), (ln2)/365b_1	Peak-to-valley ratio, e^{2b_2}	Maximum date (± days)	No. of detects	r^2
α-HCH	0.91 ± 0.25	**1.7 ± 0.32**	NS	NS	77	0.28
β-HCH	0.92 ± 0.25	**1.5 ± 0.57**	NS	NS	34	0.13
γ-HCH	0.42 ± 0.04	**3.1 ± 0.51**	**2.8 ± 1.2**	NS	171	0.26
α-Endosulfan	11 ± 3.6	**3.4 ± 0.49**	**3.0 ± 1.2**	NS	201	0.31
β-Endosulfan	4.0 ± 1.0	**3.0 ± 0.50**	**29 ± 1.2**	**Jun 26 ± 19**	169	0.61
α-Chlordane	0.61 ± 0.06	**9.2 ± 3.2**	**2.9 ± 1.2**	**Jan 25 ± 8**	187	0.26
γ-Chlordane	0.42 ± 0.02	**7.0 ± 1.6**	**3.0 ± 1.1**	**Feb 14 ± 7**	183	0.34
trans-Nonachlor	0.30 ± 0.02	7.3 ± 2.4	**3.1 ± 1.2**	**Feb 3 ± 7**	158	0.31
Dieldrin	4.1 ± 0.28	**4.3 ± 0.67**	**4.3 ± 1.1**	**Feb 17 ± 5**	201	0.44
Hexachlorobenzene	N/A	N/A	N/A	N/A	N/A	N/A
p,p'-DDT	0.69 ± 0.11	NS	NS	NS	101	N/A
p,p'-DDD	0.40 ± 0.03	NS	**4.1 ± 1.2**	Sep 3 ± 49	107	0.28
p,p'-DDE	N/A	N/A	N/A	N/A	N/A	N/A
o,p'-DDD	0.55 ± 0.11	**2.6 ± 0.95**	NS	NS	55	0.28
Heptachlor epoxide	0.86 ± 0.05	6.3 ± 1.9	**4.0 ± 1.2**	**Feb 14 ± 6**	144	0.50
Aldrin	N/A	N/A	N/A	N/A	N/A	N/A
Endrin	0.46 ± 0.04	NS	NS	NS	63	N/A
Methoxychlor	1.0 ± 0.16	LD	LD	LD	35	N/A

Table FS12. Average Concentrations and Fit Parameters for Pesticides in the Particle Phase at Sturgeon Point

OC Pesticide	Average conc. (pg/m^3)	Half-life (years), (ln2)/365b$_1$	Peak-to-valley ratio, e^{2b_2}	Maximum date (± days)	No. of detects	r^2
α-HCH	0.77 ± 0.23	2.3 ± 0.57	NS	NS	60	0.31
β-HCH	0.79 ± 0.14	LD	NS	NS	26	N/A
γ-HCH	0.46 ± 0.04	**4.1 ± 0.86**	**2.0 ± 1.2**	NS	160	0.16
α-Endosulfan	7.8 ± 0.83	*7.8 ± 2.1*	**2.6 ± 1.1**	**Jun 24 ± 16**	209	0.24
β-Endosulfan	3.7 ± 0.47	*7.0 ± 2.3*	**19 ± 1.2**	**Jul 18 ± 18**	195	0.59
α-Chlordane	1.5 ± 0.11	7.7 ± 2.7	*1.8 ± 1.2*	**Jan 15 ± 17**	203	0.10
γ-Chlordane	0.60 ± 0.03	*8.5 ± 2.4*	**3.3 ± 1.1**	**Feb 15 ± 6**	201	0.33
trans-Nonachlor	0.36 ± 0.03	NS	**2.6 ± 1.2**	**Jan 19 ± 12**	174	0.14
Dieldrin	4.1 ± 0.24	**4.0 ± 0.53**	**3.2 ± 1.1**	**Feb 9 ± 6**	210	0.43
Hexachlorobenzene	N/A	N/A	N/A	N/A	N/A	N/A
p,p'-DDT	1.0 ± 0.09	NS	*4.9 ± 1.8*	NS	130	0.06
p,p'-DDD	0.60 ± 0.05	NS	**4.4 ± 1.8**	**Sep 14 ± 41**	128	0.26
p,p'-DDE	N/A	N/A	N/A	N/A	N/A	N/A
o,p'-DDD	0.99 ± 0.11	NS	NS	91	91	0.21
Heptachlor epoxide	0.94 ± 0.07	NS	**1.8 ± 1.2**	**Mar 13 ± 5**	133	0.09
Aldrin	N/A	N/A	N/A	N/A	N/A	N/A
Endrin	0.69 ± 0.08	NS	NS	NS	53	NS
Methoxychlor	1.2 ± 0.13	NS	NS	NS	53	NS

Table FS13. Average Concentrations and Fit Parameters for Pesticides in the Particle Phase at Chicago

OC Pesticide	Average conc. (pg/m^3)	Half-life (years), (ln2)/365b$_1$	Peak-to-valley ratio, e^{2b_2}	Maximum date (± days)	No. of detects	r^2
α-HCH	0.56 ± 0.11	NS	NS	NS	62	NS
β-HCH	1.3 ± 0.09	NS	**3.6 ± 1.2**	**Jan 20 ± 9**	123	NS
γ-HCH	0.96 ± 0.07	**5.1 ± 1.0**	**3.2 ± 1.2**	**Feb 7 ± 8**	158	0.35
α-Endosulfan	5.6 ± 0.31	*8.1 ± 2.3*	**1.5 ± 1.1**	**Sep 9 ± 18**	199	0.11
β-Endosulfan	3.3 ± 0.40	8.0 ± 3.8	**18 ± 1.3**	**Jul 16 ± 25**	161	0.46
α-Chlordane	9.3 ± 0.9	**4.7 ± 1.1**	*2.0 ± 1.2*	**Dec 14 ± 17**	158	0.16
γ-Chlordane	3.4 ± 0.17	*11 ± 3.0*	**3.4 ± 1.1**	**Jan 28 ± 5**	201	0.46
trans-Nonachlor	1.4 ± 0.08	NS	**4.0 ± 1.2**	**Jan 9 ± 6**	196	0.32
Dieldrin	22 ± 1.3	**6.2 ± 1.2**	**3.6 ± 1.1**	**Feb 8 ± 6**	201	0.37
Hexachlorobenzene	N/A	N/A	N/A	N/A	N/A	N/A
p,p'-DDT	7.6 ± 0.44	NS	*1.8 ± 1.2*	**Jan 25 ± 15**	188	0.09
p,p'-DDD	1.4 ± 0.13	**3.8 ± 0.8**	*2.1 ± 1.2*	NS	158	0.18
p,p'-DDE	N/A	N/A	N/A	N/A	N/A	N/A
o,p'-DDD	3.1 ± 0.20	NS	*2.0 ± 1.2*	NS	121	0.09
Heptachlor epoxide	2.3 ± 0.14	NS	**2.8 ± 1.2**	**Feb 1 ± 9**	163	0.24
Aldrin	N/A	N/A	N/A	N/A	N/A	N/A
Endrin	1.0 ± 0.10	NS	NS	NS	86	NS
Methoxychlor	3.6 ± 0.3	NS	NS	NS	113	NS

Table FS14. Range and Mean Concentration (pg/m^3) of Selected Organochlorine Pesticides in the Gas Phase from Various Studies

Pesticide	Sample location	Site type	Sample time	Concentration Range	Mean Con. ± Std Err	Ref.
α-HCH	Birmingham, UK*	urban	April 1999-July 2000		30	(15)
	Seoul, Korea*	urban	July 1999-May 2000	34-2000	230 ± 22	(16)
	Chicago, U.S.	urban	Jan 1996-Dec 2003	3.6-290	52 ± 2.9	this study
	Jersey City. U.S.	urban	Jan 2000-May 2001		23	(12)
	Pinelands, NJ	rural	Jan 2000-May 2001		55	(12)
	Sleeping Bear Dunes, U.S.	rural	Jan 1992-Dec 2003	8.2-700	78 ± 4.0	this study
	Burnt Island, Canada	rural	Jan 1993-Dec 2003	8.7-250	74 ± 2.7	this study
	Senga Bay, South Africa	rural	Feb 1997-May 1998	1.8-10	9.4 ± 0.57	(17)
β-HCH	Senga Bay, South Africa	rural	Feb 1997-May 1998	0-34	5.3 ± 0.72	(17)
	Chicago, U.S.	urban	Jan 1999-Dec 2003	1.0-73	12 ± 1.2	this study
	Sleeping Bear Dunes, U.S.	rural	Jan 2000-Dec 2003	0.27-23	3.5 ± 0.4	this study
	Burnt Island, Canada	rural	Jan 1993-Dec 2003	0.06-26	1.9 ± 0.4	this study
γ-HCH	Birmingham, UK*	urban	April 1999-July 2000		453	(15)
	Seoul, Korea*	urban	July 1999-May 2000	5.1-310	39 ± 22	(16)
	Chicago, U.S.	urban	Jan 1996-Dec 2003	1.4-300	35 ± 2.5	this study
	Jersey City. U.S.	urban	Jan 2000-May 2001		22	(12)
	Pinelands, NJ	rural	Jan 2000-May 2001		48	(12)
	Senga Bay, South Africa	rural	Feb 1997-May 1998	0-176	25 ± 3.1	(17)
	Sleeping Bear Dunes, U.S.	rural	Jan 1992-Dec 2003	0.30-1900	47 ± 8.2	this study
	Burnt Island, Canada	rural	Jan 1993-Dec 2003	2.5-260	26 ± 1.7	this study
α-Endosulfan	Seoul, Korea*	urban	July 1999-May 2000	34-2000	230 ± 22	(16)
	Camden, NJ, U.S.	urban	Jan 2000-Jan 2001		102	(12)
	Chicago, U.S.	urban	Jan 1996-Dec 2003	0.20-1200	72 ± 9.2	this study
	Pineland, U.S.	rural	Jan 2000-May 2001		59	(12)
	Sleeping Bear Dunes, U.S.	rural	Jun 1995-Dec 2003	0.12-1600	84 ± 4.2	this study
	Burnt Island, Canada	rural	Jan 1993-Dec 2003	0.50-580	21 ± 2.8	this study
	Burnt Island, Canada*	rural	May 2000-May 2001		18	(14)
	Senga Bay, South Africa	rural	Feb 1997-May 1998	0-61	24 ± 1.2	(17)
β-Endosulfan	Seoul, Korea*	urban	July 1999-May 2000	8.9-1100	330 ± 22	(16)
	Camden, NJ, U.S.	urban	Jan 2000-May 2001		1.8	(12)
	Chicago, IL, U.S.	urban	Jan 1996-Dec 2003	0.048-65	6.0 ± 0.75	this study
	Pineland, NJ, U.S.	rural	Jan 2000-May 2001		10	(12)
	Sleeping Bear Dunes, NI, U.S.	rural	Jan 1995-Dec 2003	0.013-120	8.9 ± 1.3	this study
	Burnt Island, Canada	rural	Jan 1993-Dec 2003	0.018-77	2.6 ± 0.41	this study

Table FS14 (continued). Range and Mean Concentration (pg/m^3) of Selected Organochlorine Pesticides in the Gas Phase from Various Studies

Pesticide	Sample location	Site type	Sample time	Concentration Range	Mean Con. ± Std Err	Ref.
ΣChlordane	Jersey City. NJ, U.S.	urban	Jan 2000-May 2001		114	(12)
	Chicago, IL, U.S.	urban	Jan 1996-Dec 2003	2.4-860	110 ± 8.1	this study
	Rohwer, AR, U.S	rural	Feb 2002-Sep 2003	15-600	200 ± 20	(13)
	Pineland, NJ, U.S.	rural	Jan 2000- Jan 2001		127	(12)
	Senga Bay, South Africa	rural	Feb 1997-May 1998	ND-298	51 ± 4.4	(17)
	Sleeping Bear Dunes, MI, U.S.	rural	Jul 1992-Dec 2003	0.36-130	18 ± 1.0	this study
	Burnt Island, Canada	rural	Mar 1997-Dec 2003	0.21-48	6.6 ± 0.38	this study
p,p'-DDT	Birmingham, UK*	urban	April 1999-July 2000		3.1	(15)
	Seoul, Korea*	urban	July 1999-May 2000	34-2000	25 ± 8.4	(16)
	Chicago, IL, U.S.	urban	Jan 1996-Dec 2003	0.34-160	23 ± 1.9	this study
	Senga Bay, South Africa	rural	Feb 1997-May 1998	ND-140	12 ± 3.4	(17)
	Sleeping Bear Dunes, MI, U.S.	rural	Jan 1992-Dec 2003	0.0049-74	4.9 ± 0.45	this study
	Burnt Island, Canada	rural	Jan 1993-Dec 2003	0.0014-4.9	0.68 ± 0.04	this study
	Burnt Island, Canada*	rural	May 2000-May 2001		0.59	(14)
p,p'-DDE	Seoul, Korea*	urban	July 1999-May 2000	ND-29	8.6 ± 3.6	(16)
	Birmingham, UK*	urban	April 1999-July 2000		8.4	(15)
	Chicago, IL, U.S.	urban	Jan 1996-Dec 2003	0.58-160	29 ± 1.9	this study
	Bloomington, IN, U.S.	urban	Feb 2002-Sep 2003	0.66-35	6.4 ± 0.9	(13)
	Sleeping Bear Dunes, MI, U.S.	rural	Jan 1992-Dec 2003	0.12-74	8.1 ± 0.51	this study
	Burnt Island, Canada	rural	Jan 1993-Dec 2003	0.054-16	2.2 ± 0.11	this study
	Burnt Island, Canada*	rural	May 2000-May 2001		2.7	(14)

*gas + particle phase

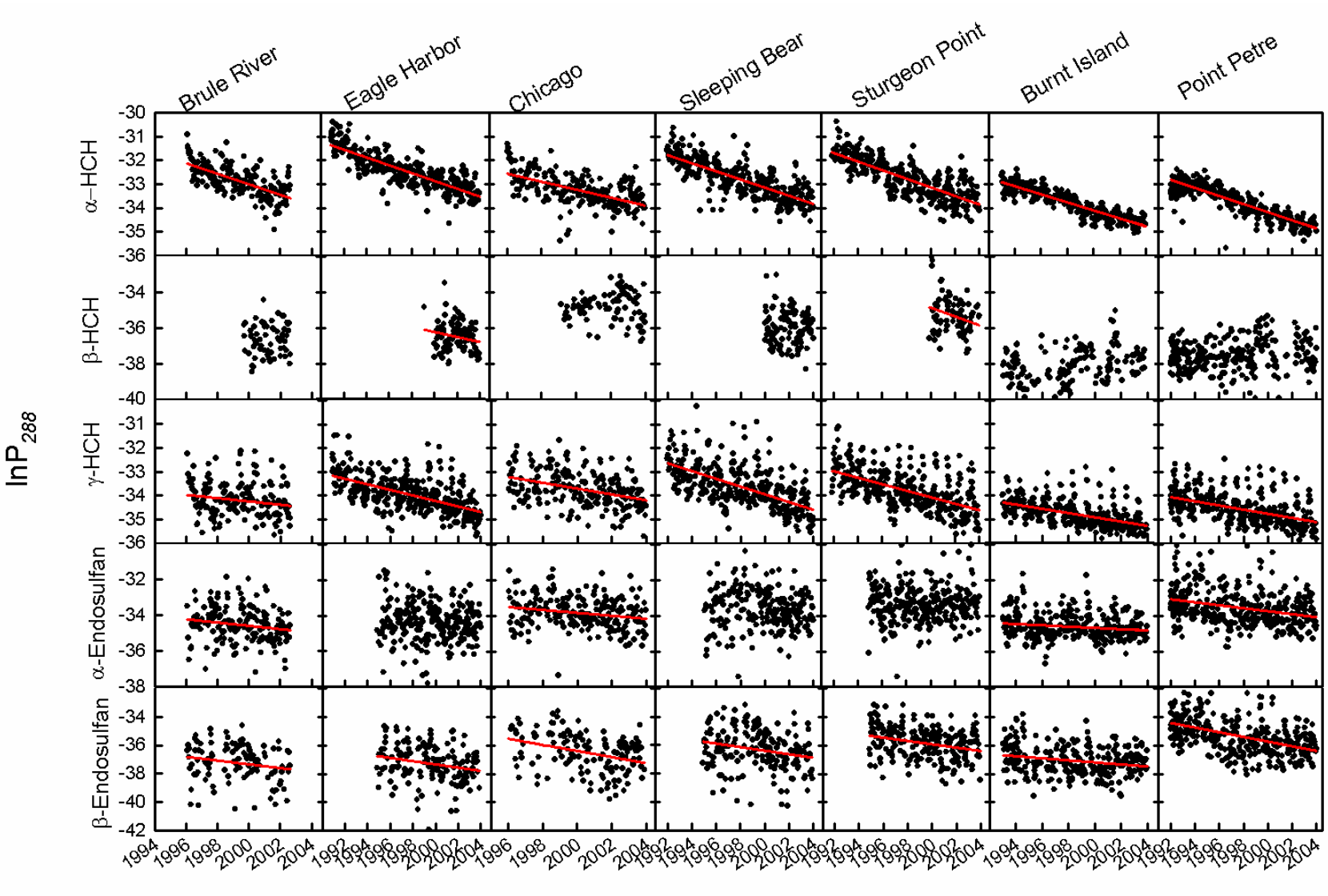

Figure FS1. Temporal trends of gas-phase OC pesticide concentrations at seven IADN sites. The red lines indicate long-term significant decreasing or increasing trends. Detailed information ion the fitted parameters is in Tables FS1 to FS7.

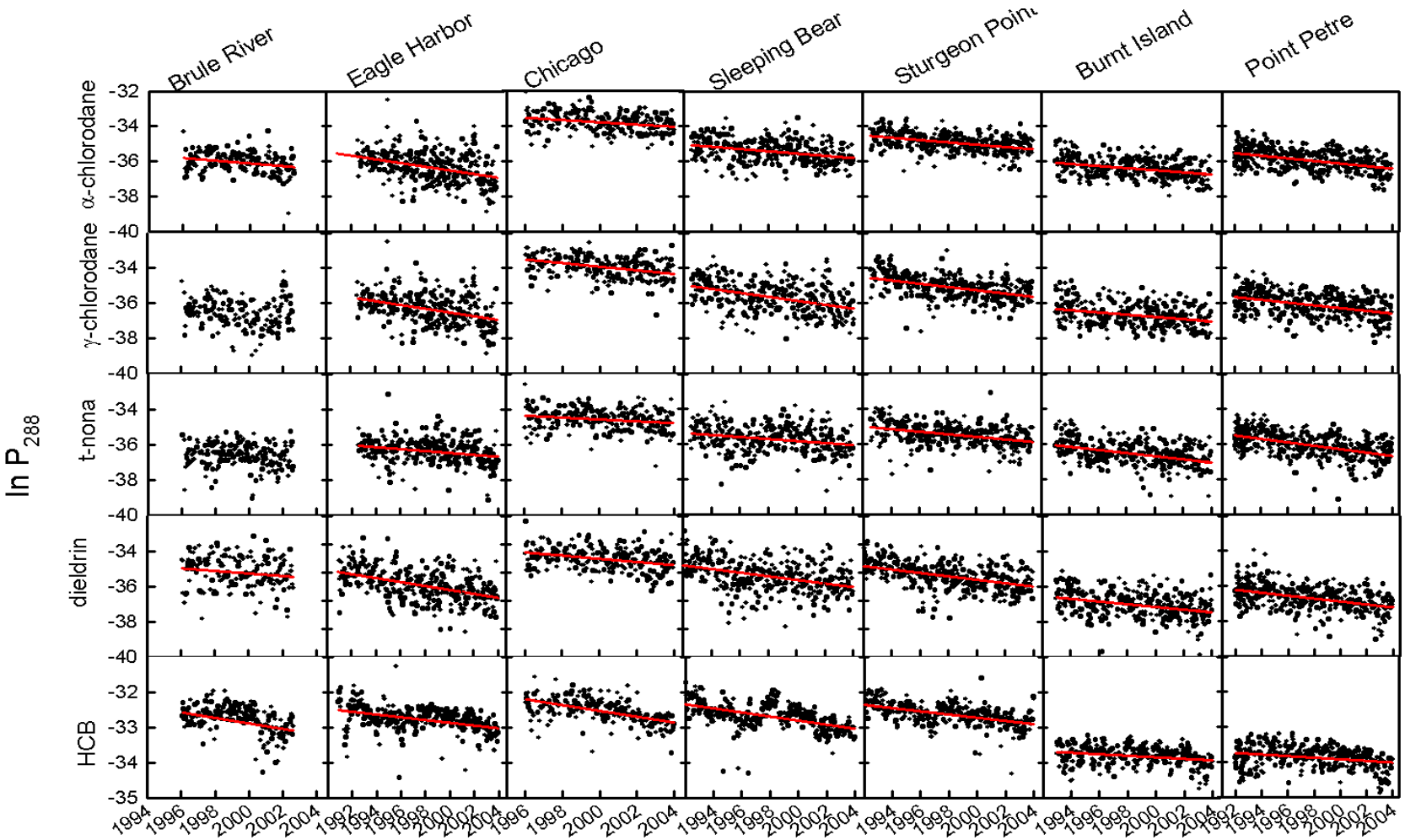

Figure FS1. (Continued)

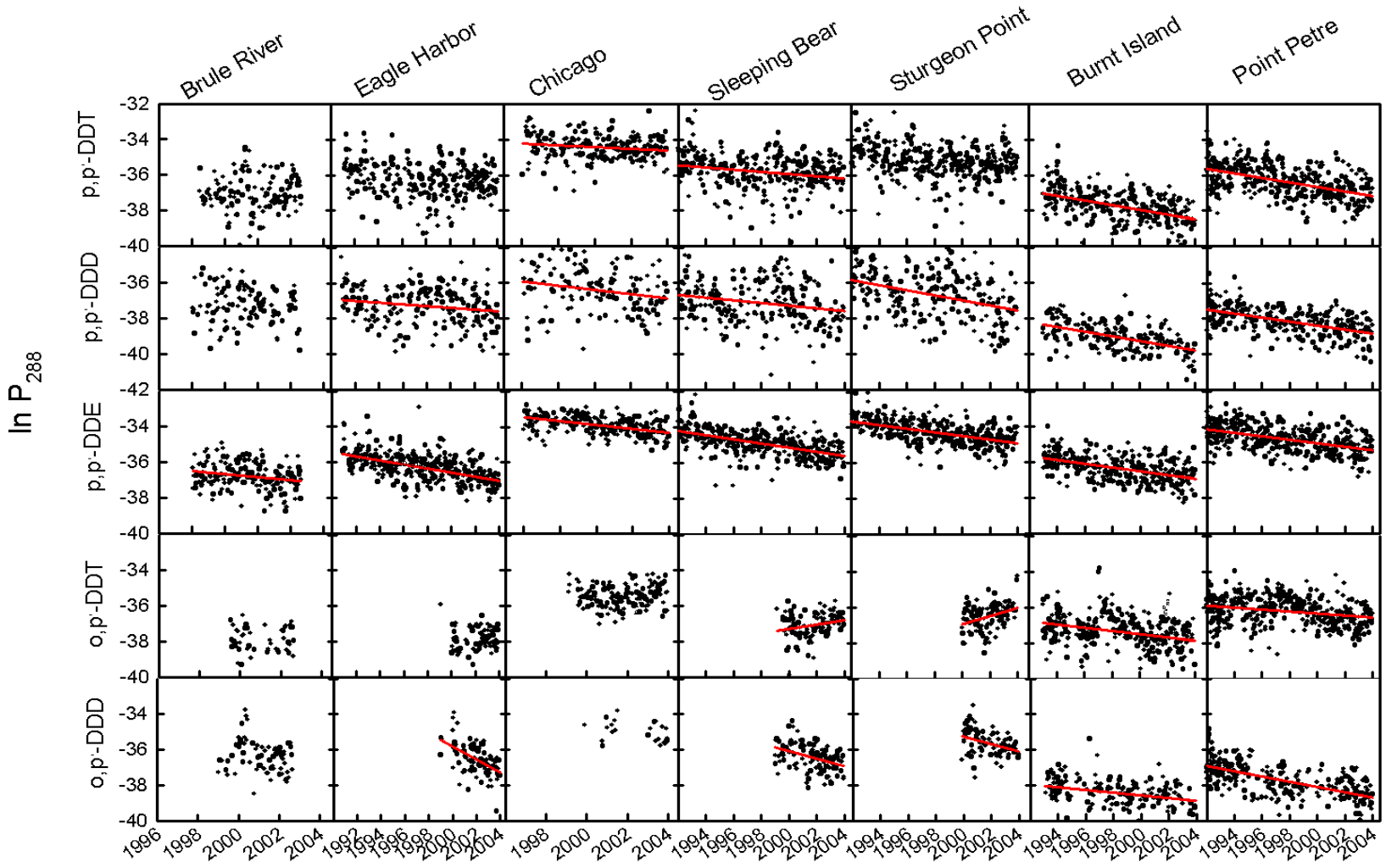

Figure FS1. (Continued)

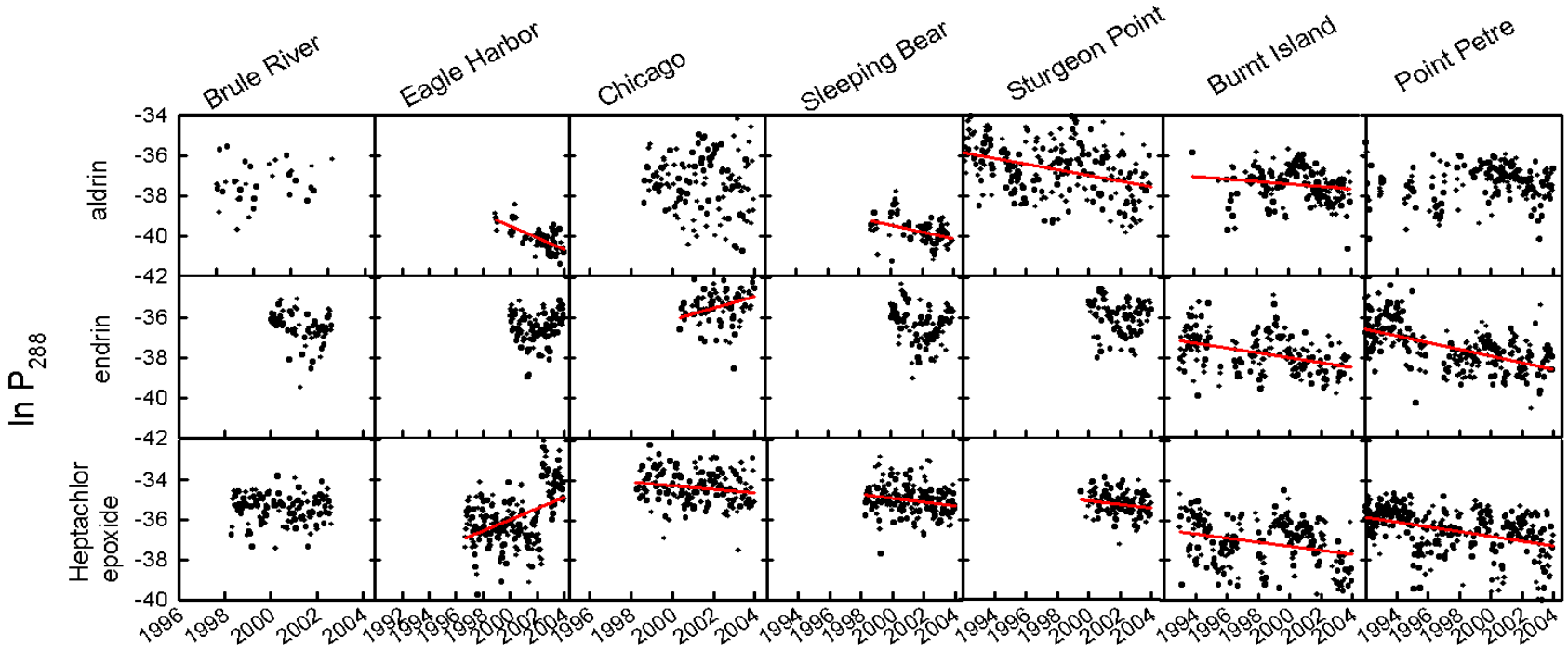

Figure FS1. (Continued)

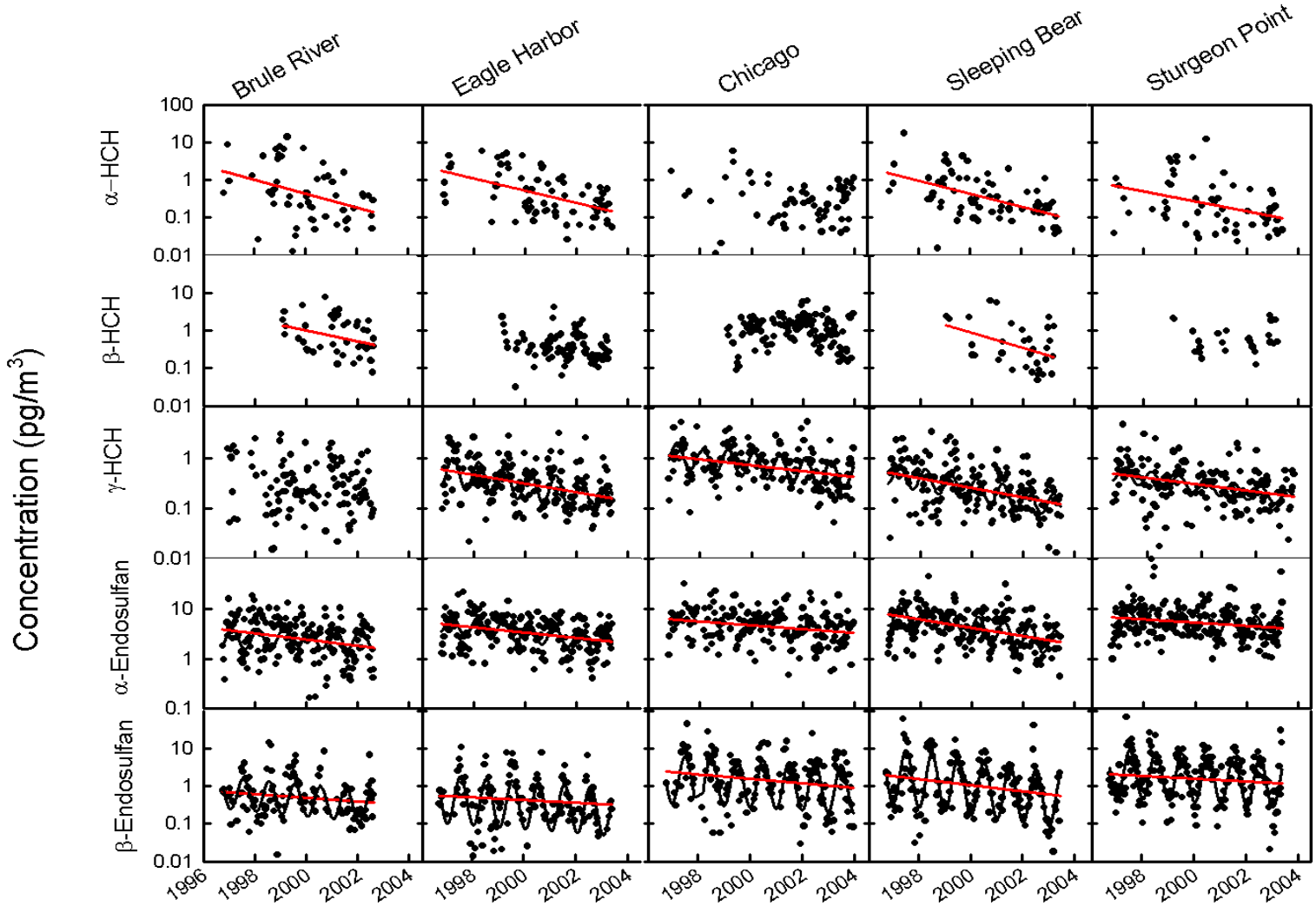

Figure FS2. Temporal trends of particle-phase OC pesticide concentrations at five U.S. IADN sites. The black curve is the fitted line using the sinusoidal model with a period length (b_3) set to one year. The red lines indicate long-term significant decreasing or increasing trends. Detailed information on the fitted parameters is in Tables ES8 to ES12.

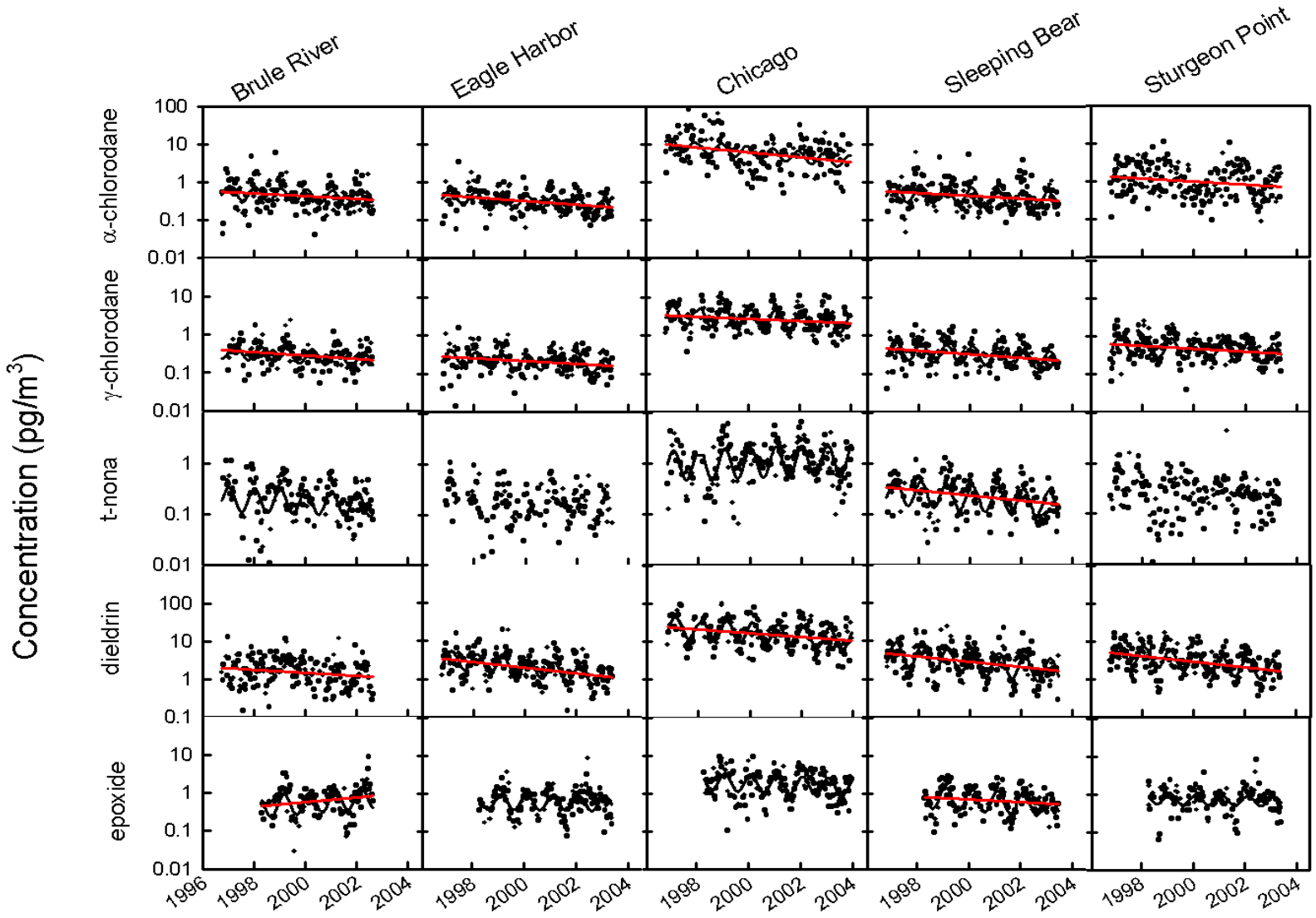

Figure FS2 (Continued).

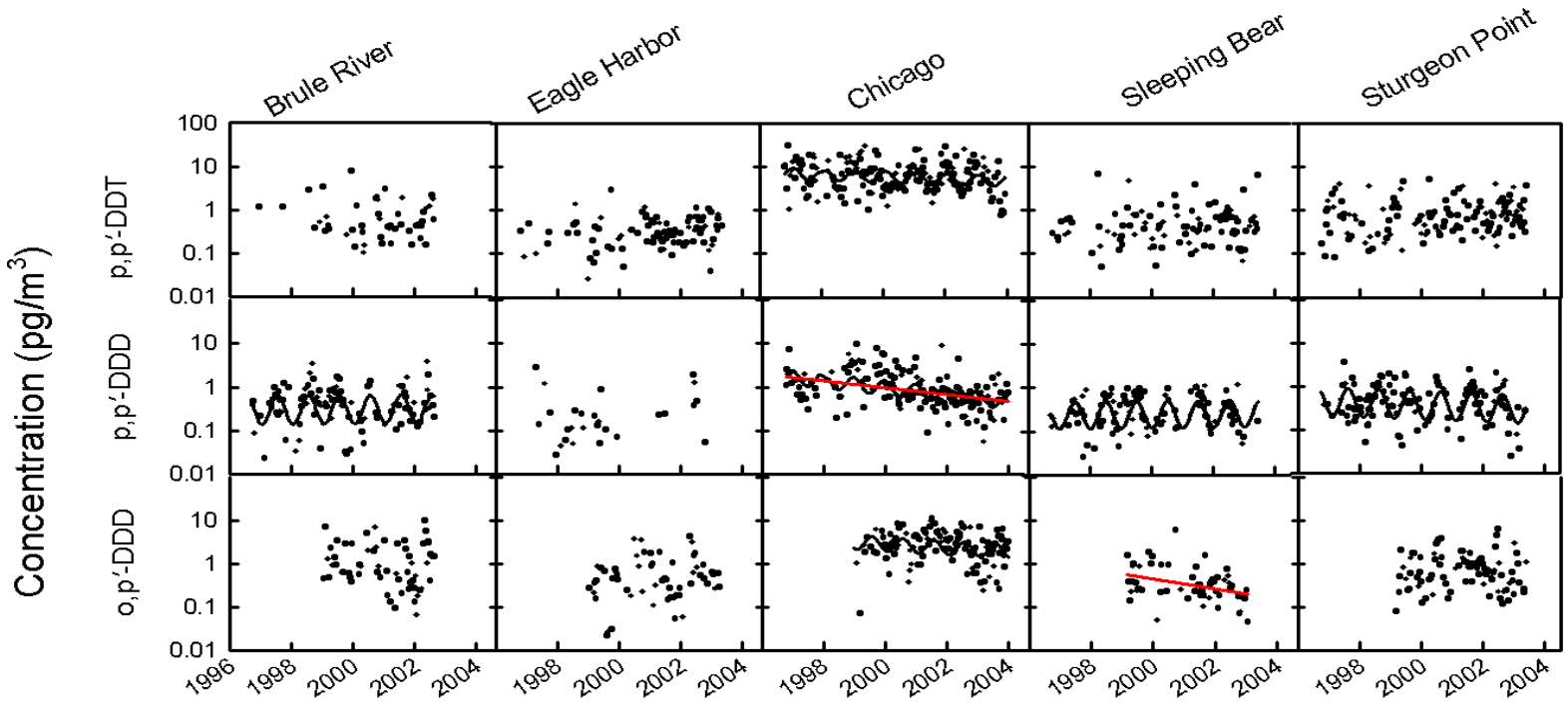

Figure FS2 (Continued).

Appendix G. Temporal and Spatial Trends of Atmospheric Polychlorinated Biphenyl Concentrations near the Great Lakes

Environmental Science & Technology, **2007**, *41*, 1131-1136.

Temporal and Spatial Trends of Atmospheric Polychlorinated Biphenyl Concentrations near the Great Lakes

Ping Sun,[1] Ilora, Basu[1], Pierrette Blanchard,[2] Kenneth A. Brice[2] and Ronald A. Hites∗[1]

[1]School of Public and Environmental Affairs
Indiana University
Bloomington, Indiana 47405
U.S.A.

and
[2]Environment Canada
4905 Dufferin Street
Toronto ON M3H 5T4
Canada

∗Corresponding Author Email: hitesr@indiana.edu

Brief

Atmospheric PCB concentrations are decreasing relatively rapidly near Lakes Michigan and Ontario and correlate with local population, observations which indicate controllable, urban, PCB sources.

Abstract

Polychlorinated biphenyl (PCB) concentrations were measured in the atmosphere at six regionally representative sites near the five Great Lakes from 1990 to 2003 as part of the Integrated Atmospheric Deposition Network (IADN). Concentration data for several individual PCB congeners and for total PCBs were analyzed for temporal and spatial trends after correcting for the temperature dependency of the partial pressures. Atmospheric PCB concentrations are decreasing relatively slowly for tetra- and pentachlorinated congeners, an observation that is in agreement with primary emissions modeling. Relatively rapid decreases in PCB concentrations at the sites near Lakes Michigan and Ontario may reflect successful reduction efforts in Chicago and Toronto, respectively. Atmospheric PCB concentrations near Lakes Superior and Huron are now so low that the air and water concentrations may be close to equilibrium. Atmospheric PCB concentrations at sites near Lakes Michigan, Erie, and Ontario are relatively higher than those measured at sites near Lakes Superior and Huron. The highest PCB level was observed at the site near Lake Erie, most likely due to nearby urban activity. However, this relatively higher concentration is still 6-10 times lower than that previously reported at the Chicago site. A correlation between average gas-phase PCB concentrations with local population indicates a

strong urban source of PCBs. The temperature dependence of gas-phase PCB concentrations is similar at most sites except at Burnt Island on Lake Huron, where very low concentrations, approaching virtual elimination, prevent reliable temperature correlation calculations.

Introduction

The use and sale of polychlorinated biphenyls (PCBs) have been banned in industrialized countries since the 1970s; for example, PCBs have not been sold in the United States since 1976 (*1*). Nevertheless, even after 30 years, PCBs are still being detected in various environmental compartments such as air, water, sediment, and biota (2-4), and PCBs are still being emitted into the atmosphere through primary sources (e.g. vaporization from products containing PCBs) or through secondary sources (e.g., vaporization from the Great Lakes). Once in the atmosphere, PCBs are transported from sources to remote areas of the globe through advective and depositional processes (*5,6*).

The Integrated Atmospheric Deposition Network (IADN) is a long-term monitoring program that has measured the atmospheric concentrations of PCBs and many other contaminants in air near the Great Lakes since 1990 (*7*). Several previously published studies by IADN have shown long-term decreasing concentrations of PCBs in air at regionally representative sites near the Great Lakes, such as Eagle Harbor, Sleeping Bear Dunes, Sturgeon Point, and Point Petre (*8,9*). Half-lives of 10 years at Sleeping Bear Dunes and 6 years at Eagle Harbor for gas-phase PCB concentrations were reported based on IADN data up to the year 2000 and supplemental historical data going back to 1977 (*8*). More recently, we reported on the temporal trends of PCB concentrations in precipitation (from 1997 to 2003) and in air (from 1996 to 2003) at Chicago. A decline of PCB concentrations in both phases with half-lives of ~7 years was reported, suggesting that reduction efforts are working at this location (*10*). In general, these reported rates of decline for PCB concentrations in air and precipitation agreed well with trend data previously reported for aquatic biota (*11,12*).

In this paper, we have extended the previous IADN trend study (*13*) on gas-phase PCB concentrations with an additional three year's of data (up to 2003) at the U.S. IADN sites. For the first time, congener-specific PCB concentrations measured at *all* IADN sites (including the Canadian sites near Lakes Ontario and Huron from 1990 to 2003) have been used to determine temporal trends. The PCB concentrations measured at all regionally representative sites were compared to those previously reported for Chicago to study the spatial distribution of PCBs at these sites.

Experimental

Sampling and Analytical Methodology. The locations of the six regionally representative IADN sites (and Chicago) are shown in Figure G1. Detailed information about these sites is given at the IADN website (www.msc.ec.gc.ca/iadn). Collection and measurement of gas phase samples started at Eagle Harbor (near Lake Superior) in November 1990, at Sturgeon Point (near Lake Erie) in December 1991, at Sleeping Bear Dunes (near Lake Michigan) and Point Petre (near Lake Ontario) in January 1992, at Burnt Island (near Lake Huron) in January 1993, and at Brule River (near Lake Superior) in January 1996. Measurements stopped at Brule River in August, 2002 because most pollutant concentrations measured there were similar to those measured at Eagle Harbor. Data through December 2003

are presented in this study for the other five sites. In addition, PCB data from January 1996 to December 2003 measured at the urban site in Chicago are presented in this paper for comparison.

Indiana University is responsible for collecting and measuring samples at the U.S. sites: Brule River, Eagle Harbor, Sleeping Bear Dunes, Sturgeon Point, and Chicago, while the Meteorological Service at Environmental Canada handles samples collected at the two Canadian sites: Burnt Island and Point Petre. For both the U.S. and Canadian operations, it is significant that there have been minimal fundamental modifications to the sampling and analytical methodologies since the inception of IADN. Such adherence to established procedures over such an extended time period has been a deliberate decision taken in the quest for measurement consistency and continuity, which are crucial and which allow us to interpret long-term trends in the data.

The detailed sampling and analytical procedures have been described elsewhere (*14-17*). The sampling and analytical methodologies for the U.S. and Canadian sites differ in some significant aspects. Sun et al. have summarized these differences with specific regard to atmospheric organochlorine pesticides, but the comparison is also applicable to PCBs (*18*). In summary, both research groups used hi-volume air samplers; however, at the U.S. sites, gas-phase PCBs were retained on 40 g of XAD-2 resin (Sigma, Amberlite, 20-60 mesh) with a total air sample volume of approximately 820 m^3. After fractionation, PCBs were analyzed using a DB-5 column (J & W Scientific; 60 m × 250 μm i.d.; film thickness, 0.10 μm) on a Hewlett-Packard (HP) 6890 gas chromatograph with a ^{63}Ni electron capture detector. At the Canadian sites, vapor-phase PCBs were retained on a polyurethane foam plug, 7.5 cm high × 6.2 cm diameter (PUF, Levitt Safety) with a total air sample volume of approximately 350 m^3. After fractionation, PCBs were analyzed using a DB-5 (60 m × 250 μm i.d.; film thickness, 0.25 μm) and a DB-17 column (30 m × 250 μm i.d.; film thickness, 0.25 μm) on a Hewlett-Packard 5890 gas chromatograph with dual ^{63}Ni electron capture detectors.

These differences in sampling and analytical procedures required comprehensive quality control (QC) and quality assurance (QA) procedures, which are documented in detail in the IADN Quality Assurance Program Plan and in the IADN Quality Control Project Plan (*19*). Surrogate standards (e.g. PCB congeners 14, 65, and 166 for the U.S. samples and PCB 30 and 204 for the Canadian samples) were spiked into the samples prior to extraction to monitor PCB recovery. The average percent recoveries for these surrogates were 83-100%. While laboratory blanks for PCBs were generally satisfactory (*19)*, field blanks have proved to be of concern, particularly as ambient PCB levels have decreased. At the U.S. sites, the field blank levels were usually less then 10% of actual sample values. At the Canadian sites, field blanks were about 40% of the average PCB concentrations at Burnt Island and 12-15% at Point Petre. This resulted in PCB concentrations at or near the method detection limit (defined as the average blank value plus 3 times the standard deviation of this average) for the Burnt Island site. None of the concentrations reported here have been blank corrected.

Considerable QA effort has been expanded over the years to ensure data compatibility between the U.S. and Canadian laboratories. A common reference standard was distributed in 2001 to determine the level of analytical agreement between the two laboratories. For the PCB congeners chosen for this study, the agreement was between 65 and 140% of the standard value, which was considered acceptable. In early 2001, a split-sample inter-laboratory comparison was conducted to evaluate possible systematic biases between the participating laboratories from the extraction, fractionation, and analytical procedures (*20*). U.S. laboratory values were 20-60%

higher than Canadian laboratory values for PCB congeners 18, 37+42, 45, 49, 52, 95, 101, 132+105+153, 123+149, and 180, congeners selected to represent tri- to heptachlorinated homologues. (The notation "xxx + yyy" is used to indicate chromatographically unresolvable congeners that are quantitated together.)

In 1998, a co-located sampler study was initiated at the Point Petre site to determine if and how sampling practices contributed to potential biases between the two research laboratories. This co-location experiment gave PCB concentrations that sometimes differed by up to a factor of 2.5 between the two laboratories during the summertime. In order to quantify the sources of these differences, an intensive inter-laboratory study was conducted in 2003, in which 8 samples were collected under winter and summer conditions. For these samples, four co-located samplers were used, and media (PUF and XAD) were exchanged between the two laboratories to investigate variables such as analytical methodology, sampling media, and sampler. A separate breakthrough study was also conducted in the summer of 2004 using two PUF plugs in series; this latter special study revealed appreciable breakthrough of some of the mono- and dichlorinated PCB congeners but showed that for trichlorinated congeners (e.g. PCB 18) the potential errors resulting from the use of a single PUF plug were acceptable. For congeners with four or more chlorines, breakthrough on PUF was found to be essentially insignificant. The 2003 study suggested that PCB 18 in the U.S. data may have been over-reported by a factor of 2.2; the source of this discrepancy has not yet been determined.

Temporal Trend Analysis. Atmospheric temperature variations affect the gas phase PCB concentrations, and these variations must be removed before a temporal trend can be determined. The temperature correction procedure was given by Cortes et al. in detail (*17*). Briefly, the gas phase concentrations of each PCB congener were first converted to a partial pressure (P) using the ideal gas law. These partial pressures were then corrected to a reference temperature of 288 K by application of the Clausius-Clapeyron equation:

$$P_{288} = P \exp\left[\frac{\Delta H}{R}\left(\frac{1}{T} - \frac{1}{288}\right)\right] \tag{1}$$

where *exp* is the exponential function, ΔH is a characteristic phase-transition energy (in kJ/mol), R is the gas constant, and T is the mean atmospheric temperature during the 24-hour sampling period (in K). The value of ΔH was determined by a linear regression of the natural logarithm of the partial pressure (P) versus the reciprocal of T.

$$\ln P = -\left(\frac{\Delta H}{R}\right)\left(\frac{1}{T}\right) + \text{const} \tag{2}$$

The natural logarithms of the corrected partial pressures at 288 K (called here P_{288}) of individual PCB congeners and total PCBs (see the Supporting Information for the list of congeners included in this total) were then regressed against time (in Julian days relative to January 1, 1990) to determine if a temporal trend was present.

Results and Discussion

Temporal trends. The calculated half-lives of several PCB congeners are listed in Table GS1 of the Supporting Information, and the half-lives of total PCB are listed in Table G1. Figure G2 shows the significant long-term trend of total PCB concentrations in the gas phase at the six regionally representative IADN sites. Brule River individual PCB congener half-lives were generally not statistically significant or negative, indicating an increase as a function of

time. The total PCB concentrations at Brule River also showed a significant increasing trend over time. Given that the data for the Brule River site covered only 6 years, we do not consider these trends reliable; thus, PCB trends at this site will not be discussed further. For all remaining IADN sites, average PCB half-lives were 7-8 years for the trichlorinated congeners (PCB 18 and 37), 8-13 years for the tetra- and pentachlorinated congeners (PCB 45, 49, 52, 95, and 101), 7-8 years for the hexachlorinated congeners (PCB 132, 149, and 153), and 4-6 years for the heptachlorinated congener (PCB 180). Similar trend behavior, as a function of PCB chlorination, has been observed by Hung et al. (*21*), who suggested that the decline of atmospheric PCB concentrations during the 1990s was mostly driven by declines in primary emissions. Indeed, the half-lives of primary emissions mirrored the half-lives obtained for the Great Lakes region.

For many congeners (e.g. PCB 45, 52, 95, and 101) and total PCBs, half-lives at Sturgeon Point were on the order of ~20 years. This slower rate of decrease for PCB concentrations in recent years at Sturgeon Point may indicate that atmospheric PCB concentrations are now approaching a steady state in Lake Erie after a more rapid decline from 1975 to 1995 (*13*). This suggestion agrees with the study by Hickey et al., who suggested that PCB concentrations in Great Lakes' lake trout have declined rapidly with relatively short half-lives of 5-10 years after PCBs were banned, but these concentrations have not changed much since 1990 (*22*). Congeners representing tri- and tetrachlorinated PCBs had faster rates of decline at Sleeping Bear Dunes and Point Petre, while much slower rates of decrease were observed at Eagle Harbor and Burnt Island. For PCB 52, there is no statistically significant decline over the sampling period at these two sites. The overall slower decline of PCB concentrations near Lakes Superior and Huron may be due to the colder water temperatures and larger volumes of these lakes. On the other hand, the relatively faster decline of gas-phase PCB concentrations around Lakes Michigan and Ontario may be due to effective reduction efforts, aimed at eliminating PCB point sources that have occurred in the areas surrounding these two lakes.

PCBs are among the pollutants that were targeted for reduction in the "Canada-United States Strategy for the Virtual Elimination of Persistent Toxic Substances in the Great Lakes Basin" (the so-called Binational Toxics Strategy). Based on the 2004 Great Lakes Binational toxics strategy report, approximately 88% of Ontario's high-level PCB-containing wastes had been destroyed (*23*). In addition, many successful PCB reduction efforts have been reported. For example, Canada's Niagara Power, located in Fort Erie, ON, had removed all their PCB-containing transformers and capacitors by 2003. These efforts may have led to a faster rate of decline of PCB concentrations around Lakes Erie and Ontario.

In general, the decreasing trends of gas-phase PCB concentrations found in this study agree with the declining PCB concentrations in other environmental compartments near the Great Lakes. A study on PCB concentrations in Lake Michigan water showed a decline from 1980 to 1991 with a half-life of 9 ± 2 years (*24*), which is statistically the same as those measured in the gas phase at Sleeping Bear Dunes and Chicago, the two sites located near Lake Michigan (see Table G1). Marvin et al. studied the temporal trends of PCB concentrations in Lake Erie sediments and reported a ~70% decline of PCB concentrations from 1971 to 1997, which gives a half-life of 15 years (*25*). At our Lake Erie site, Sturgeon Point, the gas-phase total PCB half-life was 20 ± 4 years, which agrees with that observed in sediments. Another study conducted by Marvin et al. showed that surficial sediment PCB concentrations declined by about six-fold in Lake Ontario from 1981 to 1998, giving a half-life of ~7 years (*26*). Our

measured decreasing trend of gas phase PCB concentrations at our Lake Ontario site, Point Petre, showed a half-life of 7 ± 0.4 years.

Correlation of gas-phase total PCB concentrations with local population. The average concentrations of selected PCB congeners in the gas phase at each IADN site are listed in Table GS1, and the total PCB concentrations are shown in Table G1. Among the six regionally representative sites, the highest concentrations of PCB congeners and total PCB are usually observed at Sturgeon Point, and the other five sites have concentrations similar to one another. However, the relatively higher PCB concentrations at Sturgeon Point are still approximately 6-10 times lower than PCB's gas-phase concentrations at Chicago (*10*).

A strong positive correlation between the average total PCB concentration and the human population within a 25 km radius of each sampling site was observed; see Figure G3. Clearly, higher total PCB concentrations are associated with larger populations. The watersheds of Lake Michigan, Erie, and Ontario are more populated compared to the watersheds of Lakes Superior and Huron, and this larger population could provide more PCB sources, resulting in higher PCB concentrations (*27*). Previous studies have shown that industrial or urban centers are PCB sources (*27,28*). One example is the higher concentrations of PCBs in air and precipitation in Chicago (*28,29*), indicating a strong source of PCBs in this urban area (*10*). Similarly, the relatively higher PCB concentrations observed at Sturgeon Point compared to other regionally representative sites could be attributed to an urban effect of Buffalo, New York, which is located approximately 25 km northeast of the Sturgeon Point sampling site.

Interestingly, Hafner and Hites (*30*) studied the potential sources of PCBs to the atmosphere at Sturgeon Point, Sleeping Bear Dunes, and Eagle Harbor. Based on their analyses, the sources of PCBs at Sturgeon Point were predominantly the east coast of the United States. The historically heavy-usage of PCBs in the Boston-Washington area and substantial PCB discharge into the local waterways (including the Hudson River) could have contributed to the higher atmospheric PCB concentrations measured at Sturgeon Point (*31*). A recent study on the wind and air trajectory directions predicted that the PCB source direction is nearly 120º south of Buffalo (*32*). Thus, it is still not clear whether Buffalo is the source of PCBs or whether there are additional sources at Sturgeon Point.

The other five IADN sites (i.e. Brule River, Eagle Harbor, Sleeping Bear Dunes, Burnt Island, and Point Petre) are all located more than 40 km from areas of more than 10,000 inhabitants, heavy industry, or other major sources of air pollutants. The lower PCB concentrations at Eagle Harbor, Brule River and Burnt Island indicate that there are few nearby PCB sources. Indeed, Hafner and Hites suggested the source of PCBs around Eagle Harbor could be long-range atmospheric transport from the greater Chicago area (*30*). The slightly higher PCB concentrations at Sleeping Bear Dunes and Point Petre may be due to their relative proximity to PCB sources (e.g. Chicago and Toronto) as compared to Eagle Harbor and Burnt Island.

We expected lower PCB concentrations at the Canadian sites not only because less population at these sites but also became the historical consumption of PCB was much less in Canada than in the U.S. According to Breivik et al., nearly 46% of the global production and consumption of PCBs occurred in the U.S., but only 3% occurred in Canada from 1930 to 1993 (*27*). Our results, however, demonstrated that the average gas-phase PCB concentrations for several congeners at Point Petre were similar to those at Sleeping Bear Dunes. Point Petre is located about 160 km east of Toronto and approximately 85 km north of Rochester, NY. These

urban areas could be sources of gas phase PCBs at Point Petre. In addition, Lake Ontario itself could be a source of PCBs to Point Petre. Lake Ontario consistently has large PCB volatilization fluxes, and volatilization of all PCB congeners were observed from this Lake (*33*). The primary sources of PCBs into Lake Ontario were the Niagara River and the Niagara River watershed in western New York (*34,35*).

The gas phase concentrations of PCB measured at these IADN sites are comparable with other studies. For example, in this study, average concentrations of PCB congeners 18, 52, and 101 are 31 ± 1.6, 19 ± 0.9, and 12 ± 0.6 pg/m^3, respectively, at the Sturgeon Point site. Similar average gas-phase concentrations for PCB congeners 18, 52, and 101 of 34, 31, and 14 pg/m^3 were observed at Sandy Hook, New Jersey, near the Atlantic Ocean from February 1998 to 1999 (*36*). Manodori et al. reported PCB concentrations at two sites in the Venice Lagoon not directly influenced by urban/industrialized influences (*37*). Their concentrations for selected PCB congeners were 6-25 pg/m^3 for PCB 18, 4-6 pg/m^3 for PCB 49, 7-12 pg/m^3 for PCB 52, 5-7 pg/m^3 for PCB 95, 6-9 pg/m^3 for PCB 105+132+153, and 3-5 pg/m^3 for PCB 149. These reported values are similar to those measured at the five remote IADN sites (see Table GS1), especially for the lighter congeners. Similarly, gas-phase PCB concentrations for congener 18 (3.1 pg/m^3), 49 (1.1 pg/m^3), 52 (7.7 pg/m^3), 95 (4.1 pg/m^3), and 101 (4.4 pg/m^3) were reported for the islands of the Chagos Archipelago, which is near Jakarta, Indonesia, and Singapore (*38*), and these values are also similar to those measured at the five remote IADN sites.

Temperature effects on PCB concentrations. The regression slopes and the calculated phase transition energy ΔH values of several PCB congeners are reported in Table GS1, and this information for total PCBs is given in Table G1. The slopes for the trichlorinated PCBs (PCB 18 and 37) are shallower at the Canadian sites than at the U.S. sites. This may be the result of sampling artifacts rather than different processes influencing the PCB behavior of the lighter congeners. For example, breakthrough of PCB 18 from PUF at the Canadian sites and over-reporting of PCB 18 at US sites (as mentioned in the experimental section) may lead to some of the discrepancy observed. Both these sampling artifacts occur in the summer and thus would bias the temperature dependency of lighter PCBs. For all other congeners, the slopes observed between all IADN sites are similar, except at Burnt Island where slopes are somewhat shallower.

Several studies have discussed the effect of temperature on the atmospheric concentrations of semi-volatile organic pollutants. Wania et al. (*39*) and Hoff et al. (*40*) suggested that long-distance transport of organic pollutants could lead to shallower regression slopes between ln(P) and 1/T, while a local source could result in steeper slopes. Burnt Island is a very remote site with only ~500 people living within a 25-km radius of the sampling site, and there are no nearby PCB sources. Therefore, the shallower slope at Burnt Island could be due to the long-range transport of PCBs according to Wania et al. (*39*) and Hoff et al. (*40*). However, Carlson and Hites studied the temperature dependence of atmospheric PCB concentrations, and they argued that the magnitude of the slope was not due to local vs. long-range PCB sources, but it was due to other factors including the size of the data set, the temperature range, low measured concentrations, and the PCB congener profiles (*41*). The slope tends to be shallower as more low temperature data are included in the data set and when PCB concentrations are just above field blank levels. Winter temperatures at Burnt Island were 7 to 10 ºC lower than at Eagle Harbor during the sampling period and ambient PCB levels, having dropped considerably over the last 10 years, are now at or near the method detection limit. These two factors likely contributed to the shallower slopes at Burnt Island. Thus, it seems that at the remote Canadian

site of Burnt Island, PCB concentrations are now approaching "virtual elimination" from the atmosphere.

Acknowledgments

We thank Team IADN (including Karen Arnold and Jennifer Kelley) and Environment Canada's Organic Analysis Laboratory for chemical measurements; Environment Canada's Science and Technology Branch for data acquisition: IADN QA officer, Rosa Wu; and Environment Canada and the U.S. Environmental Protection Agency's Great Lakes National Program Office for funding (Grant GL995656, Melissa Hulting, project monitor).

Supporting Information

This Supporting Information contains one table of average concentrations of PCB congener 18, 37, 45, 49, 52, 95, 101, 105+132+153, 123+149, and 180, and the values derived from modeled parameters at the seven IADN sites and one figure for temporal trends of the temperature corrected PCB congener partial pressures in the gas phase at the seven sites. This material is available free of charge via the Internet at http://pubs.acs.org

Literature cited

1. http://www.epa.gov/pcb/, accessed on April 13, 2006.
2. Jeremasion, J. D.; Hornbuckle, K. C.; Eisenreich, S. J. PCBs in Lake Superior, 1978-1992; decrease in water concentrations reflect loss by volatilization. *Environ. Sci. Technol.* **1994**, *28*, 903-914.
3. Metre, V.; Peter, C.; Mahler, B. J. Trends in hydrophobic organic contaminants in urban and reference lake sediments across the United States: 1970-2001. *Environ. Sci. Technol.* **2005**, *39*, 5567-5574.
4. Tanabe, S.; Niimi, S.; Minh, T. B.; Miyazaki, N.; Petrov, E. A. Temporal trends of persistent organochlorine contamination in Russia: A case study of Baikal and Caspian Seal. *Arch. Environ. Con. Tox.* **2003**, *44*, 533-545.
5. Mandalakis, M.; Stephanou, E. G. Wet deposition of polychlorinated biphenyls in the eastern Mediterranean. *Environ. Sci. Technol.* **2004**, *38*, 3011-3018.
6. Swackhamer, D. L.; McVeety, B. D.; Hites, R. A. Deposition and Evaporation of Polychlorobiphenyl Congeners to and from Siskiwit Lake, Isle Royale, Lake Superior. *Environ. Sci. Technol.* **1988**, *22*, 664-672.
7. Buehler, S. S.; Hites, R. A. The Great Lakes' Integrated Atmospheric Deposition Network. *Environ. Sci. Technol.* **2002**, *36*, 355A-359A.
8. Buehler, S. S.; Basu, I.; Hites, R. A. Gas-phase polychlorinated biphenyl and hexachlorocyclohexane concentrations near the Great Lakes: a historical perspective. *Environ. Sci. Technol.* **2002**, *36*, 5051-5056.
9. Hillery, B. R.; Basu, I.; Sweet, C. W.; Hites, R. A. Temporal and spatial trends in a long-term study of gas-phase PCB concentrations near the Great Lakes. *Environ. Sci. Technol.* **1997**, *31*, 1811-1816.
10. Sun, P.; Basu, I.; Hites, R. A. Temporal trends of polychlorinated biphenyls in precipitation and air at Chicago. *Environ. Sci. Technol.* **2006**, *40*, 1178-1183.

11. Ryckman, D. P.; Weseloh, D. V.; Hamr, P.; Fox, G. A.; Collins, B.; Ewins, P. J.; Norstrom, R. J. Spatial and temporal trends in organochlorine contamination and bill deformities in double-crested cormorants (*Phalacrocoraxauritus*) from the Canadian Great Lakes. *Environ. Monit. Assess*. **1998**, *53*, 169-195.
12. Ashpole, S. L.; Bishop, C. A.; Brooks, R. J. Contaminant residues in snapping turtle (Chelydra s. serpentine) eggs from the Great Lakes-St. Lawrence River basin (1999 to 2000). *Arch. Environ. Con. Tox*. **2004**, *47*, 240-252.
13. Buehler, S. S.; Basu, I.; Hites, R. A. Causes of variability in pesticide and PCB concentrations in air near the Great Lakes. *Environ. Sci. Technol.* **2004**, *38*, 414-422.
14. Basu, I.; Lee, A. D. *Collection of Air and Precipitation Samples: IADN Project Standard Operating Procedure*; Indiana University: Bloomington, IN, 2003.
15. Basu, I. Analysis of PCBs, Pesticides, and PAHs in Air and Precipitation Samples, IADN Project Sample Preparation Procedure; Indiana University: Bloomington, IN, 1999.
16. Fowlie, P. *Integrated Atmospheric Deposition Network (IADN) Report on Laboratory Audit, revision 2*; Cornerstone Science: Burlington, Ontario, 2001.
17. Cortes, D. R.; Basu, I.; Sweet, C. W.; Brice, K. A.; Hoff, R. Am.; Hites, R. A. Temporal trends in gas-phase concentrations of chlorinated pesticides measured at the shores of the Great Lakes. *Environ. Sci. Technol.* **1998**, *32*, 1920-1927.
18. Sun, P.; Blanchard, P.; Brice, K.; Hites, R. A. Organochlorine pesticide in the Great Lakes atmosphere: temporal and spatial trends, *Environ. Sci. Technol.* **2006**, 6587-6593.
19. Fowlie, P. *Integrated Atmospheric Deposition Network Quality Assurance Program Plan (Revision 1.1)*; Environment Canada (Downsview, ON) and U.S. Environmental Protection Agency (Chicago, IL), 2001.
20. Fowlie, P. *Integrated Atmospheric Deposition Network (IADN) Interlaboratory Comparison for Pesticides, Polychlorinated Biphenyls and Polynuclear Aromatic Hydrocarbons in air and particulate samples, revision 2*; Cornerstone Science: Burlington, Ontario, 2002.
21. Hung, H.; Lee, S.C.; Wania, F.; Blanchard, P.: Brice, K. Measuring and simulating atmospheric concentration trends of polychlorinated biphenyls in the Northern Hemisphere. *Atmos. Environ.* **2005**, *39*, 6502-6512.
22. Hickey, J. P.; Batterman, A.; Chernyak, S. M. Trends of chlorinated organic contaminants in Great Lakes trout and walleye from 1970 to 1998. *Arch. Environ. Contam. Toxicol*. **2006**, *50*, 97–110.
23. *Great Lakes Binational Toxic Strategy 2004 Progress Report*. http://www.binational.net.
24. Pearson, R. F.; Hornbuckle, K. C.; Eisenreich, S. J.; Swackhamer, D. L. PCBs in Lake Michigan water revisited, *Environ. Sci. Technol.* **1996**, *30*, 1429-1436.
25. Marvin, C. H.; Painter, S.; Charlton, M. N.; Fox, M. E.; Thiessen, P. A. L. Trends in spatial and temporal levels of persistent organic pollutants in Lake Erie sediments. *Chemosphere* **2004**, *54*, 33-40.
26. Marvin, C. H.; Painter, S.; Williams, D.; Richardson, V.; Rossmann, R.; Hoof, P. V. Spatial and temporal trends in surface water and sediment contamination in the Laurentian Great Lakes. *Environ. Pollut.* **2004**, *129*, 131-144.
27. Breivik, K.; Sweetman, A.; Pacyna, J. M.; Jones, K. C. Towards a global historical emission inventory for selected PCB congeners -- A mass balance approach. 2. Emissions. *Sci. Total Environ.* **2002**, *290*, 199-224.

28. Offenberg, J. H.; Baker, J. E. Polychlorinated biphenyls in Chicago precipitation: Enhanced wet deposition to near-shore Lake Michigan. *Environ. Sci. Technol.* **1997**, *31*, 1534-1538.
29. Tasdemir, Y.; Vardar, N.; Odabasi, M.; Holsen, T. M. Concentrations and gas/particle partitioning of PCBs in Chicago. *Environ. Pollut.* **2004**, *131*, 35-44.
30. Hafner, W. D.; Hites, R. A. Potential sources of pesticides, PCBs, and PAHs to the atmosphere of the Great Lakes. *Environ. Sci. Technol.* **2003**, *37*, 3764-3773.
31. Hudson River PCBs: Background and Site Information; U.S. Environmental Protection Agency: Washington, DC, 2002; http://www.epa.gov/hudson/background.htm
32. Hafner, W. D.; Hites, R. A. Effects of wind and air trajectory directions on atmospheric concentrations of persistent organic pollutants near the Great Lakes. *Environ. Sci. Technol.* **2005**, *39*, 7817-7825.
33. Blanchard P.; Audette, C.; Hulting, M.L.; Basu, I.; Brice, K. A.; Chan, C. H.; Dryfhout-Clark, H.; Hites, R. A.; Neilson, M. *Atmospheric Deposition of Toxic Substances to the Great Lakes: IADN Results through 2000*; United States Environmental Protection Agency and Environment Canada, Chicago, IL and Toronto, ON, 2003.
34. Marvin, C. H.; Charlton, M. N.; Stern, G. A.; Braekevelt, E.; Reiner, E. J.; Painter, S. Spatial and temporal trends in sediment contamination in Lake Ontario. *J. Great Lakes Res.* **2003**, *29*, 317-331.
35. Howdeshell, M J.; Hites, R. A. Is the Hyde Park Dump, near the Niagara River, still affecting the sediment of Lake Ontario? *Environ. Sci. Technol.* **1996**, *30*, 1429-1436.
36. Brunciak, P. A.; Dachs, J.; Gigliotti, C. L.; Nelson, E. D.; Eisenreich, S. J. Atmospheric polychlorinated biphenyl concentrations and apparent degradation in coastal New Jersey. *Atmos. Environ.* **2001**, *35*, 3325-3339.
37. Manodori, L.; Gambaro, A.; Moret, I.; Capodaglio, G.; Cairns, W. R. L.; Cescon, P. Seasonal evolution of gas-phase PCB concentrations in the Venice Lagoon area. *Chemosphere* **2005**, *62*, 449-458.
38. Wurl, O.; Potter, J. R.; Obbard, J. P.; Durville, C. Persistent organic pollutants in the equatorial atmosphere over the open Indian ocean. *Environ. Sci. Technol.* **2006**, *40*, 1454-1461.
39. Wania, F.; Haugen, J-E.; Lei, Y. D.; Mackay, D. Temperature dependence of atmospheric concentrations of semi-volatile organic compounds. *Environ. Sci. Technol.* **1998**, *32*, 1013-1021.
40. Hoff, R. M.; Brice, K. A.; Halsall, C. J. Nonlinearity in the slopes of Clausius-Clapeyron plots for SVOCs. *Environ. Sci. Technol.* **1998**, *32*, 1793-1798.
41. Carlson, D. L.; Hites, R. A. Temperature dependence of atmospheric PCB concentrations. *Environ. Sci. Technol.* **2005**, *39*, 740-747.

Table G1. Average Total PCB[a] Concentrations, Half-lives, Clausius-Clapeyron Slopes, and Phase-transition Energies at the Seven IADN Sites.

	C_{avg} ± std err (pg/m^3)	$t_{1/2}$ [b] (year)	Slope [c]	ΔH [d] (kJ/mol)	N [e]	r^2 [f]
Brule River	86 ± 6.9	**–10 ± 2.8**	**–5300 ± 280**	**43 ± 2.3**	187	0.67
Eagle Harbor	86 ± 5.4	*26 ± 9.5*	**–5200 ± 270**	**42 ± 2.2**	361	0.51
Sleeping Bear	110 ± 6.5	**7.7 ± 0.8**	**–5600 ± 270**	**46 ± 2.2**	332	0.60
Sturgeon Point	230 ± 11	**20 ± 4.3**	**–6200 ± 220**	**51 ± 1.7**	355	0.70
Burnt Island	60 ± 2.1	NS	**–1500 ± 220**	**12 ± 1.8**	345	0.12
Point Petre	80 ± 2.6	**7.1 ± 0.4**	**–4100 ± 190**	**34 ± 1.5**	392	0.64
Chicago (ref *10*)	1300 ± 74	**8.0 ± 1.1**	**–5400 ± 230**	**44 ± 1.9**	219	0.74

a. For the complete list of the PCB congeners that make up this total, see the Supporting Information.
b. The results of half-life, slope, and phase-transition energies are listed as mean ± standard error. Normal font numbers are significant for $0.01 < p < 0.05$; italic font numbers are significant for $0.001 < p < 0.01$, bold font numbers are significant at level of $p < 0.001$. NS means the result is not significant at $p < 0.05$ level. A negative half-life is actually a doubling time.
c. The slope value is from the linear regression of the natural logarithm of the partial pressure (P) vs. the reciprocal of T (see equation 2).
d. ΔH is the characteristic phase-transition energy.
e. N is the number of samples collected up to 2003 and used in the regressions.
f. r^2 is the Pearson's multi-regression coefficient between $\ln(P)$, $1/T$, and time.

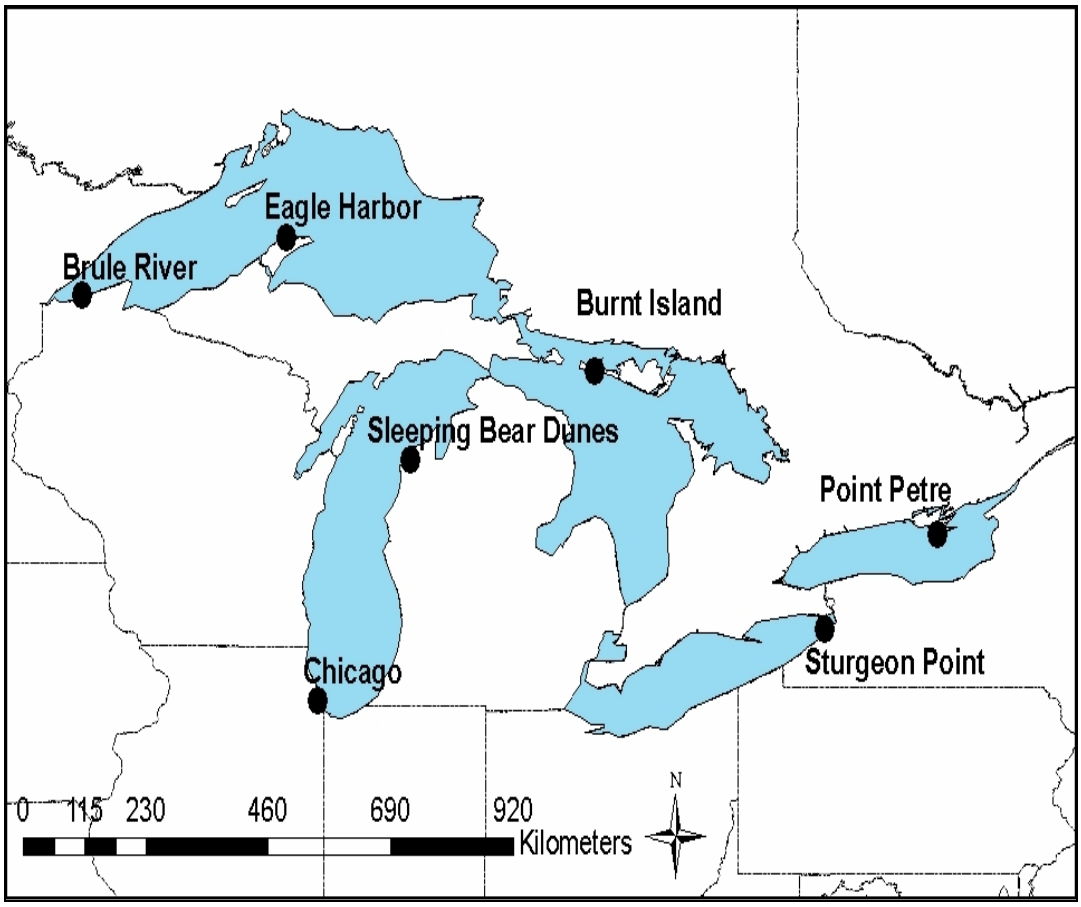

Figure G1. Map of the Great Lakes indicating the six regionally representative Integrated Atmospheric Deposition Network (IADN) sampling sites. The location of the urban site in Chicago is also given.

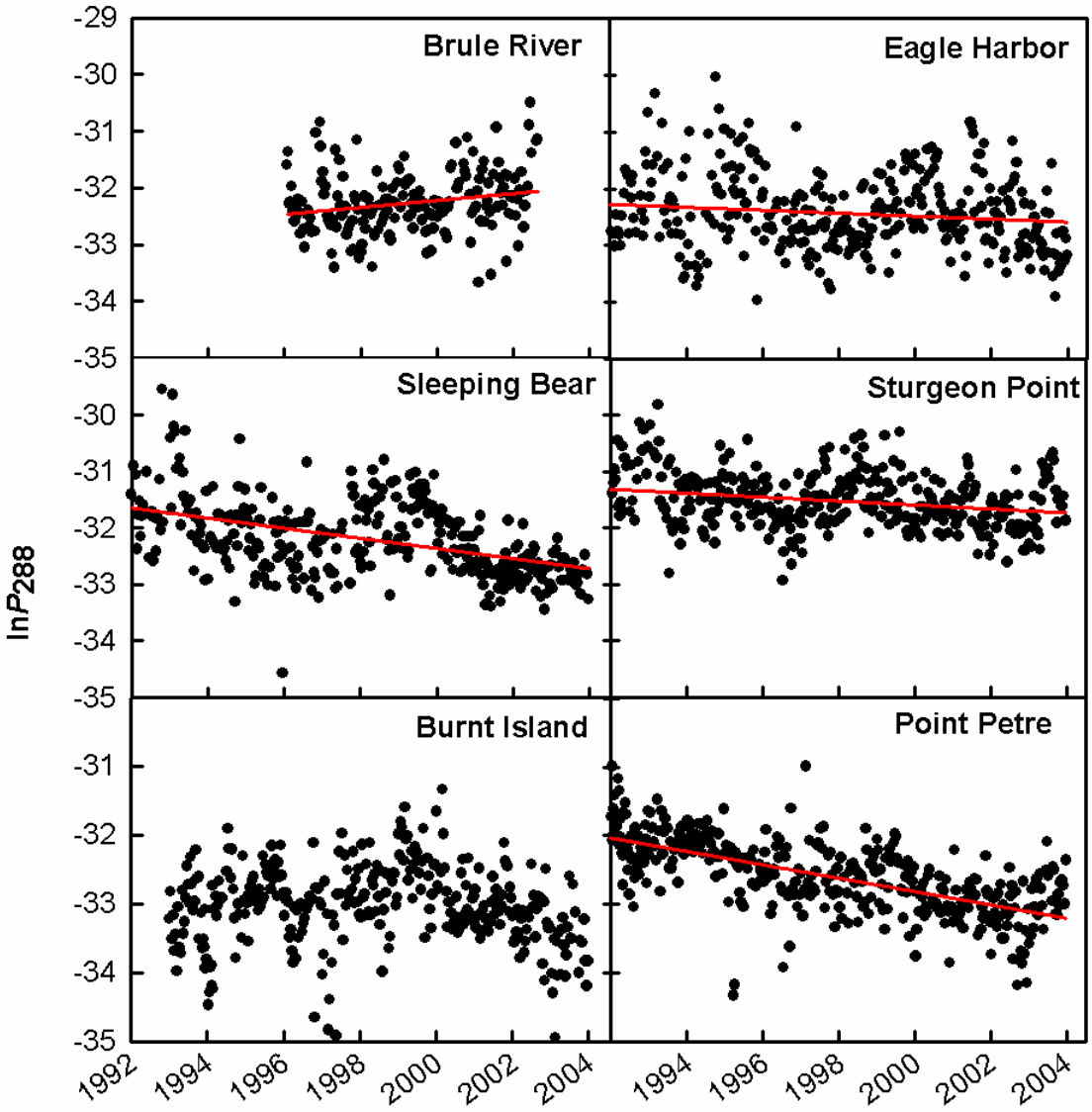

Figure G2. Long-term trend of temperature corrected total PCB partial pressures in the gas phase at the six regionally representative IADN sites. Red lines indicate statistically significant ($p < 0.05$) regressions of the data. A significant long-term *increasing* trend is observed at Brule River. Significant decreasing trends are observed at Eagle Harbor, Sleeping Bear Dunes, Sturgeon Point, and Point Petre.

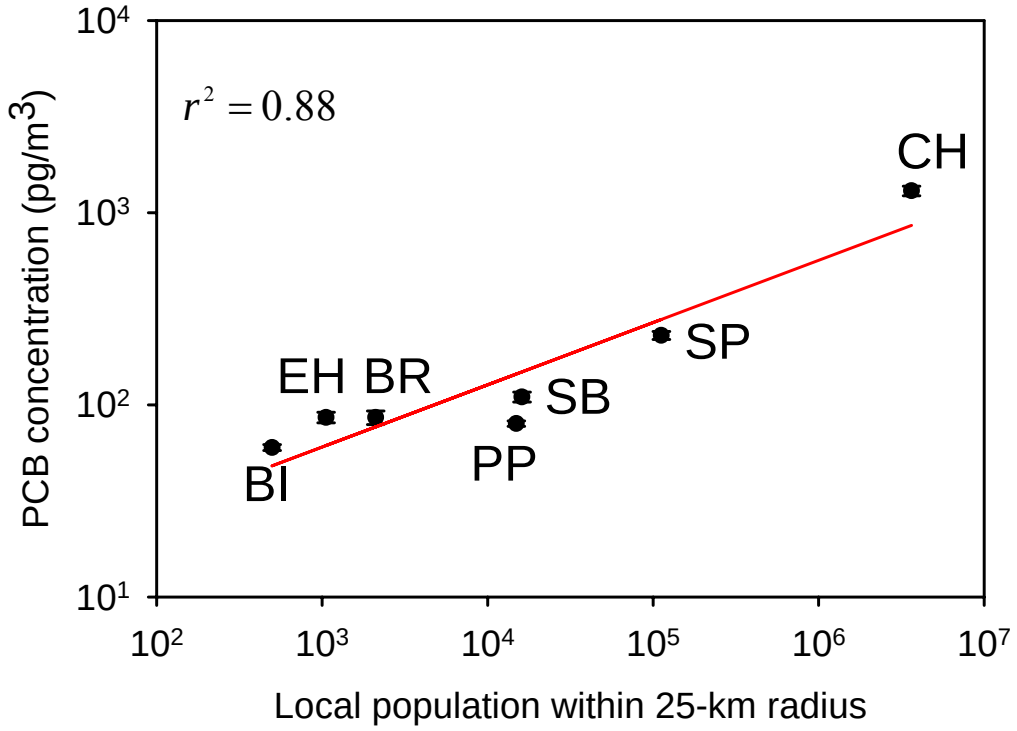

Figure G3. Correlation between average total PCB concentration and the local population within a 25 km radius of the sampling site. The error bars are standard errors. BI, Burnt Island; EH, Eagle Harbor; BR, Brule River; PP, Point Petre; SB, Sleeping Bear Dunes; SP, Sturgeon Point; and CH, Chicago.

Supporting Information

Temporal and Spatial Trends of Atmospheric Polychlorinated Biphenyl Concentrations near the Great Lakes

Ping Sun, Ilora, Basu, Pierrette Blanchard, Kenneth A. Brice and Ronald A. Hites*

Congeners included in the total PCB summation are: 15+17, 16+32, 18,19, 22, 26, 28, 31, 33+53, 37+42, 41+64+71, 45, 47+48, 49, 52, 56+60+84+92, 70+76, 74, 77+110, 83, 85, 87+81,89, 91, 95+66, 97, 99,100, 101, 105+132+153, 114+131, 118, 119, 123+149, 126, 128+167,135+144,138+163, 156+171+202, 169, 170+190, 172, 174, 180, 194+205, 199, 201, 206, and 207. (The notation "xxx + yyy" is used to indicate chromatographically unresolvable congeners that are quantitated together.) Each congener in this list either contributes more than 1% to the total PCB mass for at least one site within the network or is regarded to be toxicologically important (PCB 77, 105, 126, 128, 138, 156, 169 and 170). All results reported here are for PCBs in the vapor-phase, which is operationally-defined by the sampling procedures employed.

This supporting Information contains one table of average concentrations of PCB congener 18, 37, 45, 49, 52, 95, 101, 105+132+153, 123+149, and 180, and the values derived from modeled parameters at seven IADN sites; and one figure for temporal trends of these PCB congeners in gas phase.

The vapor-phase concentrations (in pg/m^3) of PCB congeners were first converted to partial pressure (P, in atm) using the ideal gas law. These partial pressures were then adjusted to the reference temperature of 288 K using equation 1, where ΔH is a characteristic phase-transition energy of the compound (in kJ/mol), R is the gas constant, and T is the daily average atmospheric temperature at the sampling site (in Kelvin). The value of ΔH was determined by a preliminary regression of ln(P) vs. 1/T, which is the Clausius-Clapeyron equation (equation 2). The values of ln(P_{288}) were then regressed vs. time (t, in Julian days relative to January 1, 1990) using equation 3 to determine the rate of exponential increase ($a > 0$) or decrease ($a < 0$) of these partial pressures. If this rate was statistically significant ($p < 0.05$), these rates were then converted to half-lives ($t_{1/2,}$ in years) by dividing the values of a into the ln(2)/365 for each compound at each site.

$$\ln P_{288} = \ln P - \frac{\Delta H}{R}\left(\frac{1}{288} - \frac{1}{T}\right) \tag{1}$$

$$\ln \mathrm{P} = -\frac{\Delta \mathrm{H}}{\mathrm{R}}\left(\frac{1}{\mathrm{T}}\right) + \text{constant} \tag{2}$$

$$\ln P_{288} = aT + b \tag{3}$$

Table GS1 lists all the values of ΔH and the calculated half-life times from the a values in equation 3. The results are listed as mean ± standard error. Normal font numbers are significant for $0.01 < p < 0.05$; italic font numbers are significant for $0.001 < p < 0.01$, bold font numbers are significant at level of $p < 0.001$. "NS" means "not significant" because $p > 0.05$. A negative half-life is actually a doubling time.

Table GS1. Selected PCB congener concentrations, half-lives, Clausius-Clapeyron slopes, and phase-transition energies at the six regionally representative IADN sites. Data at the Chicago site are also presented for comparison.

	C_{avg} ± std err (pg/m^3)	$t_{1/2}$ [a] (year)	Slope [b]	ΔH [c] (kJ/mol)	N[d]	r^2 [e]
PCB 18						
Brule River	8.3 ± 0.7	**–12 ± 4.4**	**–4400 ± 290**	**36 ± 2.4**	187	0.57
Eagle Harbor	8.1 ± 0.4	NS	**–4500 ± 240**	**37 ± 2.0**	361	0.51
Sleeping Bear	12 ± 0.7	**8.8 ± 1.1**	**–5100 ± 270**	**42 ± 2.2**	310	0.56
Sturgeon Point	31 ± 1.6	**13 ± 1.8**	**–5200 ± 220**	**43 ± 1.8**	353	0.63
Burnt Island	6.6 ± 0.2	**8.8 ± 0.8**	**–2100 ± 150**	**17 ± 1.2**	321	0.49
Point Petre	9.6 ± 0.3	**7.9 ± 0.6**	–2900 ± 190	**23 ± 1.5**	390	0.51
Chicago	97 ± 5.7	**7.8 ± 1.5**	**–4300 ± 320**	**35 ± 2.0**	218	0.51
PCB 37						
Brule River	5.7 ± 0.7	NS	**–8100 ± 490**	**67 ± 4.0**	170	0.62
Eagle Harbor	3.1 ± 0.3	**11 ± 2.7**	**–6100 ± 400**	**50 ± 3.3**	345	0.50
Sleeping Bear	3.2 ± 0.2	**5.2 ± 0.5**	**–6100 ± 340**	**50 ± 2.8**	320	0.57
Sturgeon Point	4.9 ± 0.3	**8.7 ± 1.1**	**–6100 ± 300**	**50 ± 2.4**	345	0.58
Burnt Island	1.0 ± 0.1	NS	**–3300 ± 250**	**27 ± 2.0**	319	0.37
Point Petre	2.1 ± 0.1	**8.2 ± 0.3**	**–4800 ± 240**	**39 ± 2.0**	388	0.56
Chicago	20 ± 1.2	**5.3 ± 0.6**	**–5500 ± 270**	**45 ± 2.2**	218	0.71
PCB 45						
Brule River	0.5 ± 0.1	*–7.1 ± 2.1*	**–4100 ± 410**	**34 ± 3.3**	168	0.43
Eagle Harbor	0.7 ± 0.1	*17 ± 5.2*	**–4900 ± 350**	**40 ± 2.8**	334	0.38
Sleeping Bear	0.8 ± 0.1	**8.8 ± 1.3**	**–5200 ± 310**	**42 ± 2.6**	322	0.49
Sturgeon Point	1.8 ± 0.1	32 ± 14	**–5300 ± 270**	**44 ± 2.2**	349	0.52
Burnt Island	1.3 ± 0.1	**18 ± 4.5**	**–4000 ± 210**	**33 ± 1.7**	279	0.58
Point Petre	1.8 ± 0.1	**10 ± 1.1**	**–3800 ± 240**	**31 ± 2.0**	375	0.47
Chicago	10 ± 0.6	**6.6 ± 0.9**	**–5200 ± 270**	**42 ± 2.2**	219	0.67
PCB 49						
Brule River	1.9 ± 0.2	**–6.2 ± 1.2**	**–5100 ± 300**	**42 ± 2.4**	187	0.65
Eagle Harbor	2.3 ± 0.2	**11 ± 1.7**	**–5400 ± 280**	**44 ± 2.3**	350	0.53
Sleeping Bear	2.7 ± 0.2	**7.0 ± 0.7**	**–5600 ± 270**	**46 ± 2.2**	330	0.62
Sturgeon Point	5.9 ± 0.3	**11 ± 1.4**	**–6100 ± 230**	**50 ± 1.9**	353	0.68
Burnt Island	1.6 ± 0.1	NS	**–3400 ± 170**	**28 ± 1.4**	319	0.56
Point Petre	2.9 ± 0.1	**16 ± 2.3**	**–4600 ± 200**	**38 ± 1.6**	390	0.59
Chicago	30 ± 1.6	**7.2 ± 0.9**	**–5500 ± 230**	**45 ± 1.9**	218	0.75
PCB 52						
Brule River	7.1 ± 0.6	**–7 ± 1.4**	**–5400 ± 270**	**44 ± 2.2**	187	0.71
Eagle Harbor	5.8 ± 0.4	NS	**–5100 ± 260**	**42 ± 2.1**	361	0.52
Sleeping Bear	6.9 ± 0.3	**11 ± 1.4**	**–5200 ± 230**	**43 ± 1.9**	332	0.63
Sturgeon Point	19 ± 0.9	**22 ± 5.6**	**–6500 ± 220**	**53 ± 1.8**	355	0.71
Burnt Island	2.3 ± 0.1	NS	**–3300 ± 160**	**27 ± 1.3**	317	0.57
Point Petre	5.6 ± 0.2	**9.0 ± 0.7**	**–4700 ± 190**	**38 ± 1.5**	384	0.67

Chicago	90 ± 4.6	**11 ± 2.0**	**–5500 ± 210**	**44 ± 1.7**	219	0.76
PCB 95						
Brule River	3.0 ± 0.2	**–6.3 ± 1.1**	**–5000 ± 260**	**41 ± 2.1**	187	0.69
Eagle Harbor	3.2 ± 0.3	*21 ± 5.7*	**–5300 ± 270**	**44 ± 2.2**	358	0.53
Sleeping Bear	3.3 ± 0.2	**10 ± 1.3**	**–5400 ± 240**	**44 ± 2.0**	330	0.63
Sturgeon Point	10 ± 0.5	**20 ± 4.8**	**–6800 ± 230**	**56 ± 1.9**	353	0.71
Burnt Island	2.0 ± 0.1	**7.4 ± 0.8**	**–4400 ± 220**	**36 ± 1.8**	321	0.58
Point Petre	4.6 ± 0.2	**6.8 ± 0.5**	**–5100 ± 240**	**42 ± 2.0**	390	0.60
Chicago	52 ± 2.9	**14 ± 3.4**	**–5800 ± 210**	**47 ± 1.8**	219	0.78
PCB 101						
Brule River	3.4 ± 0.2	*–11 ± 3.3*	**–5200 ± 250**	**42 ± 2.1**	187	0.71
Eagle Harbor	4.0 ± 0.3	*20 ± 6.0*	**–5500 ± 280**	**45 ± 2.3**	361	0.51
Sleeping Bear	4.4 ± 0.2	**10 ± 1.4**	**–5600 ± 250**	**45 ± 2.1**	332	0.62
Sturgeon Point	12 ± 0.6	**17 ± 3.2**	**–7000 ± 230**	**57 ± 1.9**	355	0.73
Burnt Island	1.0 ± 0.1	**8 ± 0.7**	**–4400 ± 180**	**36 ± 1.5**	319	0.67
Point Petre	2.8 ± 0.1	**5.9 ± 0.4**	**–5900 ± 230**	**46 ± 1.9**	388	0.67
Chicago	68 ± 3.6	**11 ± 2.1**	**–6000 ± 210**	**49 ± 1.8**	219	0.80
PCB 105+132+153						
Brule River	1.3 ± 0.1	NS	**–5200 ± 290**	**43 ± 2.3**	187	0.65
Eagle Harbor	2.5 ± 0.2	**4.7 ± 0.3**	**–5200 ± 290**	**43 ± 2.4**	347	0.57
Sleeping Bear	2.6 ± 0.2	**4.9 ± 0.4**	**–5500 ± 280**	**45 ± 2.3**	327	0.63
Sturgeon Point	5.7 ± 0.3	**7.5 ± 0.7**	**–7100 ± 250**	**58 ± 2.1**	349	0.71
Burnt Island	0.7 ± 0.1	**6.3 ± 0.7**	**–4300 ± 270**	**35 ± 2.2**	320	0.50
Point Petre	2.0 ± 0.1	**5.1 ± 0.3**	**–5600 ± 280**	**46 ± 2.3**	389	0.61
Chicago	41 ± 3.0	**7.4 ± 1.0**	**–7400 ± 250**	**61 ± 2.0**	219	0.82
PCB 123+149						
Brule River	1.0 ± 0.1	NS	**–5200 ± 270**	**43 ± 2.2**	187	0.68
Eagle Harbor	1.3 ± 0.1	**7.1 ± 0.9**	**–5500 ± 270**	**45 ± 2.2**	276	0.63
Sleeping Bear	1.6 ± 0.1	**6.7 ± 0.6**	**–5700 ± 260**	**46 ± 2.2**	327	0.63
Sturgeon Point	3.7 ± 0.2	**10 ± 1.1**	**–6500 ± 210**	**54 ± 1.7**	352	0.74
Burnt Island	0.5 ± 0.1	**9.2 ± 1.5**	**–4600 ± 270**	**38 ± 2.2**	303	0.52
Point Petre	1.2 ± 0.1	**7.1 ± 0.6**	**–5400 ± 260**	**44 ± 2.1**	386	0.58
Chicago	24 ± 1.5	**8.4 ± 1.2**	**–6700 ± 220**	**55 ± 1.8**	219	0.82
PCB 180						
Brule River	0.2 ± 0.1	NS	**–4900 ± 560**	**40 ± 4.6**	138	0.38
Eagle Harbor	0.3 ± 0.1	**4.4 ± 0.3**	**–4000 ± 320**	**32 ± 2.6**	300	0.52
Sleeping Bear	0.3 ± 0.1	**5.1 ± 0.5**	**–5400 ± 360**	**45 ± 3.0**	271	0.55
Sturgeon Point	0.7 ± 0.2	**5.6 ± 0.5**	**–6400 ± 320**	**53 ± 2.6**	337	0.61
Burnt Island	0.1 ± 0.0	**4.3 ± 0.4**	**–3000 ± 310**	**24 ± 2.5**	280	0.42
Point Petre	0.3 ± 0.1	**4.9 ± 0.4**	**–4300 ± 330**	**36 ± 2.7**	374	0.46
Chicago	3.6 ± 0.3	**6.1 ± 0.8**	**–9300 ± 280**	**76 ± 2.3**	215	0.84

Notes for Table GS1

a. The results of half-life, slope, and phase-transition energies are listed as mean ± standard error. Normal font numbers are significant for $0.01 < p < 0.05$; italic font numbers are significant for $0.001 < p < 0.01$, bold font numbers are significant at level of $p < 0.001$. NS means the result is not significant at $p < 0.05$ level. A negative half-life is actually a doubling time.

b. The slope value is the linear regression of the natural logarithm of the partial pressure (P) vs. the reciprocal of T (see equation 2).

c. ΔH is the characteristic phase-transition energy.

d. N is the number of samples collected up to 2003 and used in the regressions.

e. r^2 is the Pearson's multi-regression coefficient between ln(P), 1/T, and time.

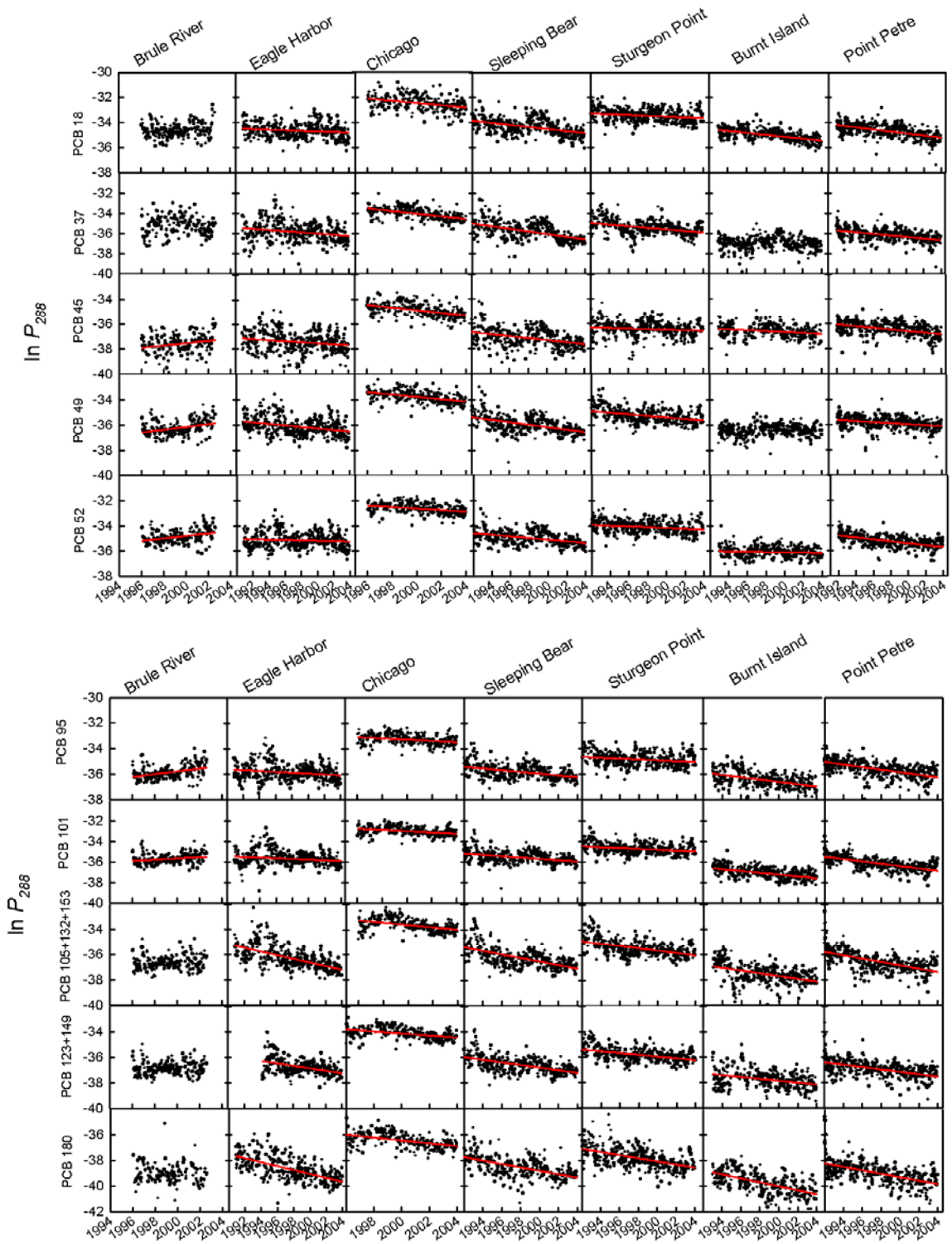

Figure GS1. Long-term trends of PCB congener partial pressures in the gas phase at seven IADN sites. Each dot is a measured partial pressure that has been adjusted to a standard temperature of 288 K. Red lines indicate statistically significant decreasing or increasing long-term trends where $p < 0.05$.

PUF Breakthrough Study, 2004

This sampling study was conducted in July and August 2004, using a glass fiber filter followed by two 7.5 cm diameter × 7.5 cm long PUF filters in series installed in a Meteorological Services of Canada PS-1 Hi-Vol air sampler at Point Petre. Samples of approximately 350 m^3 were taken over 24 hours. A blank and a co-located sample from another sampler were also collected using a single 7.5 × 7.5 cm PUF filter. The MSC Organic Analysis Laboratory carried out analysis of these PUF samples for PCB congeners and pesticides. Sampling dates and atmospheric temperatures were:

Date	Temperature (°C)
26-Jul-04	21.2
07-Aug-04	17.7
19-Aug-04	18.3
31-Aug-04	20.9

A breakthrough statistic (*BT%*) showing the percent analyte retained on the downstream or back PUF plug (*B*) after passing through the upstream or front PUF plug (*F*) was calculated as:

$$BT\% = \frac{(B*100)}{(F+B)}$$

Average *BT%* values determined were:

Congener	BT%
PCB 18	11%
PCB 37+42	1.5%
PCB 45	2.5%
PCB 49	2.5%
PCB 52	2.5%

For further details see: Fowlie, P. (2005). "Integrated Atmospheric Deposition Network (IADN). Air Sampling Breakthrough Test for PCB Congeners and Pesticides from Polyurethane Foam (PUF)". Cornerstone Scientific, May 19, 2005.